PERIPHERAL TOLERANCE IN ANTI-INSULIN B LYMPHOCYTES

By

Jonathan Murphy Williams

Dissertation
Submitted to the Faculty of the
Graduate School of Vanderbilt University
in partial fulfillment of the requirements
for the degree of

DOCTOR OF PHILOSOPHY
in

Microbiology and Immunology
December, 2015
Nashville, Tennessee

Approved:

Mark Boothby, M.D., Ph.D.

Luc Van Kaer, Ph.D.

Eric Sebzda, Ph.D.

Maureen Gannon, Ph.D.

James W. Thomas, M.D.

DEDICATION

"And the God of all grace, who called you to His eternal glory in Christ, after you have suffered a little while, will Himself restore you and make you strong, firm, and steadfast."

-- First Peter 5:10 --

To my Mother, Ann, my prayer warrior, my biggest supporter and number one fan,

To my wife and best friend, Megan, for loving and accepting me, for walking beside me,

To my brother, Jamion, the best man I know, for being there from the beginning,

To all of those who have encouraged, motivated, and supported me on this journey,

To all of those who suffer from type 1 diabetes and remain hopeful for a cure,

This work is dedicated to you.

ACKNOWLEDGEMENTS

I would not be where I am today without the leadership, encouragement, and support from by boss, Dr. James (Tom) W. Thomas. He was the best mentor I could have ever asked for, always there when I needed him, exhibiting the perfect balance between up close and personal training but also stepping back and letting me figure things out myself. Tom is the most brilliant scientist I have ever met and has taught me so much about what it takes to be successful student. He is kinder than he is brilliant, which is saying something. I will never forget our long conversations together, whether poring over data in his office, discussing big picture B cell immunology, or laughing over the taste of fish eyes in New Orleans. You made me want to finish school and pursue my dream, Tom, and for that I am forever grateful.

Thanks to my Thesis Advisory Committee members, Drs. Mark Boothby, Luc Van Kaer, Eric Sebzda, and Maureen Gannon, for constantly challenging me to be better; to improve my writing and communication skills; for being critical when I thought I did not need the criticism; for asking tough questions and expecting great things of me. You all were quick to realize that I was most productive when the pressure was turned up and the going got tough, and I appreciate you sticking with me.

Thank you to Dr. Klaus Rajewsky for providing the $pIV_HL2neoR$ targeting vector that made the generation of V_H125^{SD} mice possible, and to Dr. Richard Breyer for EIIA-Cre B6 mice. Thanks to the Vanderbilt Technologies for Advanced Genomics Sequencing Core, the Transgenic Mouse/Embryonic Stem Cell Shared Resource, the Vanderbilt Flow Cytometry Shared Resource, and the Translational Pathology Shared Resource. Thank you to the Division of Animal Care for their assistance in the maintenance of the mice.

Thanks to Rachel Henry-Bonami, Ph.D., and Chrys Hulbert, my colleagues in the Thomas Lab, for always being there for me when I needed to ask a question or know where various things were located in lab. Rachel was my second mentor and my day-to-day source of knowledge and information. I most definitely would not be here without her help and support.

I am eternally grateful to the never-ending support I received from my family during my time in graduate school. My mother, Ann, has always and forever will be my biggest fan. Her prayers are felt all the way from her home in Augusta, GA, and knowing I had her in my corner made things a lot easier to deal with when times were tough. Thanks to her for not letting me give up and for always loving me for who I am. Thanks to my older brother, Jamion, and his wife Randi, for their love and support and for always being just a phone call away.

Thanks to my beautiful wife, Megan, for being my best friend in the world and for standing by my side all the way through grad school. We started the same year, in 2009, and we were classmates for a few years until we finally realized we were meant to be together. I am so proud of her for finishing her Ph.D. earlier this year and accepting the position of Assistant Director of the Medical Scientist Training Program at Vanderbilt. She brings out the best in me, challenges me intellectually, makes me laugh, and loves watching sports. I cannot imagine being married to a better woman, and I am grateful to her for loving me. I am excited for our lives together, forever linked by the pursuit of a Ph.D. at Vanderbilt.

This work would not have been possible without financial support by National Institutes of Health Grants T32 AR059039 and AI051448, Juvenile Diabetes Research Foundation Grants 1-2005-167 and 3-2013-121, and by Vanderbilt Diabetes Research and Training Center Grant DK20593. In the world of research, money makes the world go ‘round, so I will always be grateful to the various institutions for providing funding to Tom and myself to perform research.

TABLE OF CONTENTS

LIST OF TABLES

Table Page

LIST OF FIGURES

Figure Page

LIST OF ABBREVIATIONS

AID ..... Activation-induced cytodine deaminase

AIRE ..... Autoimmune regulator

APC ..... Antigen presenting cell

B6 ..... C57Bl/6

BCR ..... B cell receptor

BRT ..... *Brucella abortus* ring test antigen

Ca^{2+} ..... Calcium^{2+}

CSR ..... Class switch recombination

FO ..... Follicular

GC ..... Germinal center

HEL ..... Hen egg lysozyme

IFN ..... Interferon

Ig ..... Immunoglobulin

IKK ..... I kappa B kinase

IRAK ..... IL-1 receptor-associated kinase

IRF ..... Interferon regulatory factor

LPS ..... Lipopolysaccharide

Mab ..... Monoclonal antibody

MFI ..... Mean fluorescence intensity

MHC ..... Major histocompatibility complex

MyD88 ..... Myeloid differentiation factor 88

MZ..... Marginal zone

NF-κB ..... Nuclear factor kappa B

NFAT ..... Nuclear factor of activated T cells

NOD ..... Non-obese diabetic

NP ..... Nitrophenol

PI3K ..... Phosphoinositide 3-kinase

PLCγ2 ..... Phospholipase Cγ2

RAG ..... Recombination activating gene

RSS ..... Recombination signal sequence

SAH..... Short arm homology

SAP ..... Signaling lymphocyte activation molecule-associated protein

T1 ..... Transitional 1

TCR..... T cell receptor

TD ..... T cell-dependent

Tg ..... Transgenic

TI..... T cell-independent

TLR ..... Toll-like receptor

TRAF ..... Tumor necrosis factor receptor-associated factor

Tregs ..... Regulatory T cells

TRIF ..... Toll/IL-1 receptor-domain-containing adapter-inducing interferon-β

V_H125^{SD} ..... Anti-insulin VDJ_H-125 site-directed to the native IgH locus

WT ..... Wild-type

CHAPTER I

INTRODUCTION

Thesis Overview

The overall goal of my thesis project was to gain a more thorough understanding of the critical events that mediate loss of B lymphocyte tolerance for the clinically relevant autoantigen (autoAg), insulin. Immune tolerance, defined as antigen-specific unresponsiveness, is absolutely essential to guard against autoimmunity. Regulatory systems are in place during B and T cell development and throughout life to help ensure tolerance to self, but the high rate of autoimmune disease both in this country and around the world demonstrates that immune tolerance is not perfect. The presence of IgG autoantibodies (autoAbs) in patients with autoimmune disease indicates a breach in tolerance in the B cell compartment and implicates B cells as critical players in autoimmunity.

Type 1 diabetes is an autoimmune disorder characterized by the destruction of insulin-producing beta cells in the pancreatic islets. The presence of IgG autoAbs to insulin in patients with type 1 diabetes correlates with a role for anti-insulin B cells in the breakdown in tolerance that mediates disease pathogenesis. However, little is known regarding the earliest stages of tolerance reversal in anti-insulin B cells and how, when, and where these cells become insulin autoAb-secreting cells. In my studies, I uncovered a new pathway to drive loss of anti-insulin B cell tolerance and the production of IgG antibodies utilizing a new site-directed transgenic (Tg) mouse model with a population of anti-insulin B cells competent to undergo isotype switch.

Innate Immunity

Protection against foreign pathogens results from the combined function and efficiency of the innate and adaptive branches of the immune system. Innate immunity is characterized by the speed and immediacy of the response and the lack of antigen specificity needed by the host to clear whatever pathogens are present. This includes physical barriers like the skin and mucous membranes, as well as certain immune cells that can detect and eliminate microbes within hours of exposure without the assistance of antigen-specific receptors. For example, natural killer cells are essential for clearance of cancer cells and virus-infected cells. Natural killer cells contain unique proteins in their granules, such as perforin, which forms pores in the target cell so that apoptosis may be induced by granzymes (1, 2). Neutrophils, macrophages, and dendritic cells are specialized phagocytes that recognize and engulf damaged or dead cells during an infection. In addition to their role in innate immunity, macrophages and dendritic cells also assist the adaptive immune response, as they can process and present peptides to $CD4^+$ T lymphocytes for further immune system activation and modulation.

The innate immune system also consists of blood or plasma proteins, together called complement, that work together to clear extracellular pathogens directly via the membrane attack complex (MAC), or indirectly through a process called opsonization. Complement activation is achieved utilizing one of three pathways. The MB-lectin pathway involves binding of complement proteins with mannose-binding proteins that have bound the pathogen. There is the alternative pathway to complement activation in which complement directly binds to the surface of the pathogen, usually a bacterium. Third, the classical pathway leads to indirect complement activation via binding of complement proteins to antibodies that have already bound antigen. Thus, the classical pathway of complement activation actually serves the effector phases of the

adaptive immune system. Regardless of the pathway, once complement is activated the MAC forms and introduces pores into the membranes of the targeted pathogen, ultimately leading to cell lysis (3, 4). Alternatively, complement that is bound either directly to bacteria or to antibodies that have bound antigen may opsonize the microbe. Opsonization improves phagocytosis through enhanced recognition of all of the newly available Fc on the pathogen-binding antibodies (5).

There is also the possibility for several negative outcomes of complement activation. Opsonization may occur with autoAbs binding to self-antigens, and phagocytosis of these immune complexes by antigen presenting cells (APC) like dendritic cells or macrophages could result in autoAg processing and loading onto major histocompatibility complex II (MHC) for inappropriate $CD4^+$ T cell activation. Additionally, autoimmune hemolytic anemia can arise when autoAbs against red blood cells promote lysis of those cells (6). The resulting circulating hemoglobin can be harmful to the liver and kidneys.

Fc recognition combines features of both the innate and adaptive immune systems. The Fc portion of an antibody dictates the isotype of the antibody, although it is not responsible for antigen binding. Regardless of the specificity or affinity of the antibody for antigen, the Fc portion remains constant. Phagocytes express various Fc receptors that bind the Fc regions on antibodies that arise during the immune response. Fc recognition by phagocytes is natural and non-discriminatory against the antibodies they bind, so the innate immune system has a way to always be able to clear pathogens that are bound by specific antibodies that arise during an immune response. Phagocytosis via Fc recognition is possible with or without complement, although the latter can dramatically enhance phagocytosis through opsonization.

While it is true that innate immune cells do not possess receptors specific for particular antigens, they do express pattern recognition receptors that recognize distinct pathogen-associated molecular patterns on microbes and other foreign invaders. These receptors equip the host with the ability to defend against both bacteria and viruses through recognition of the unique proteins and properties of the pathogen. For example, a specialized class of transmembrane receptors exist called toll-like receptors (TLR) that are expressed on intracellular organelles and the cell surface. TLR2 recognizes lipoproteins and peptidoglycans of Gram-positive and some Gram-negative bacteria (7, 8). TLR3 is expressed on endosomal compartments inside the cell and is activated by dsRNA derived from viruses (9). TLR7 and TLR8 are also expressed intracellularly and recognize viral ssRNA (10), although TLR8 is expressed only in humans. TLR9 on endosomal compartments is activated by hypomethylated CpG DNA (11), which is normally found in bacteria. TLR4 recognizes lipopolysaccharide (LPS) on Gram-negative bacterial membranes (12, 13), while TLR5 binds bacterial flagellin (14). Diversity in pattern recognition is further generated by the ability of TLRs to form heterodimers with one another. For example, TLR2/6 dimers are necessary for identification of diacylated lipoproteins (15), while TLR1/2 dimers identify triacylated lipoproteins (16, 17). TLRs are expressed in nearly every cell type, including B cells (18, 19), thus, innate immunity is essentially omnipresent throughout the host. Interestingly, TLRs in humans and mice are structurally and functionally similar to those from *Drosophila*, indicating their extreme evolutionary conservation.

One of the primary outcomes of TLR stimulation and signaling is activation of the transcription factor, nuclear factor-kappa B (NF-κB). NF-κB activation elicits a wide variety of pro- and some anti-inflammatory immune effector functions that are critical for protective immunity (20, 21). TLRs primarily signal through the adaptor protein, myeloid differentiation

factor 88 (MyD88). MyD88 activation promotes recruitment of IL-1 receptor-associated kinase 4 (IRAK), which subsequently phosphorylates IRAK1. IRAK1 associates with tumor necrosis factor receptor-associated factor 6 (TRAF) and activates the IκB kinase (IKK) complex. IKK consists of two kinases, IKKα and IKKβ, and a third regulatory subunit called the NF-κB essential modulator. Activated IKK phosphorylates IκB proteins that are bound to NF-κB/Rel subunits in the cytoplasm. Normally, IκB proteins function to restrict NF-κB access to the nucleus. However, phosphorylation of IκB releases NF-κB, allowing it to translocate to the nucleus where it regulates gene transcription. When TLR ligands are no longer present, IKK is not able to phosphorylate IκB, resulting in the termination of gene transcription and restriction of NF-κB subunits back to the cytoplasm. Of note, some TLR pathways can signal independently of MyD88 through the toll/IL-1 receptor-domain-containing adapter-inducing interferon-β (TRIF) (22, 23). TRIF can activate TRAF6 and the IKK complex without IRAK1/4, highlighting an alternative means to elicit NF-κB transcription and inflammatory cytokines like interferon-β. A summary of the TLR ligands and TLR signaling is shown in Fig. I-1.

TLR stimulation provides a means of B cell activation independent of B cell receptor (BCR) engagement by antigen. Autoreactive B cells that have been rendered tolerant, or functionally silenced, in the periphery exhibit impaired responses to TLR stimulation in addition to reduced BCR-mediated activation. Typically, stimulation through either receptor alone does not deliver a strong enough signal to break tolerance and promote normal B cell responses like proliferation, differentiation, and antibody production. However, it has been demonstrated that the potential for autoimmunity can arise following combined stimulation of both TLR and BCR (24), indicating the potential for improper interactions between innate and adaptive components of B cell signaling.

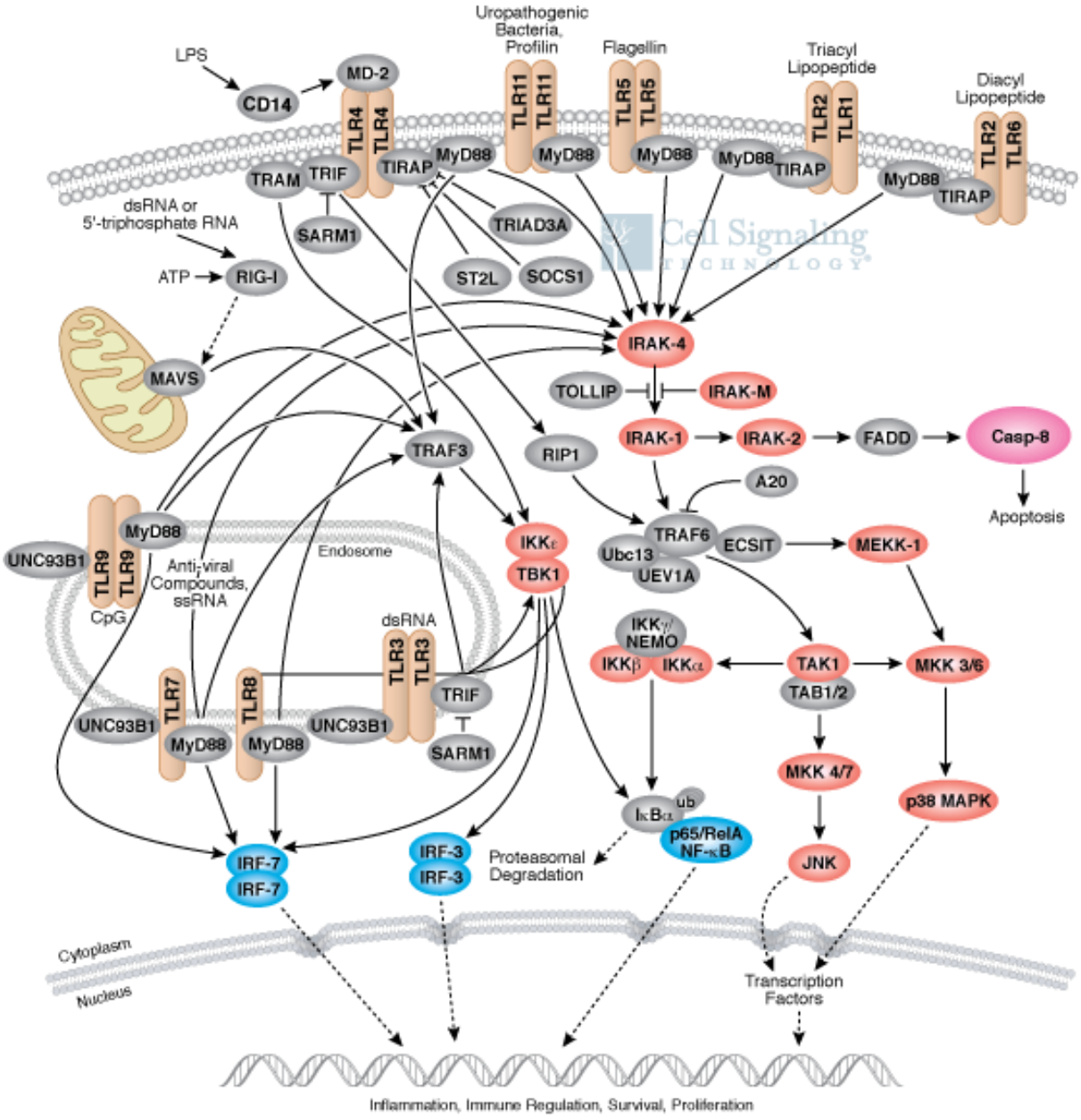

FIGURE I-1. Toll-like receptor agonists and signaling pathways. *Illustration reproduced courtesy of Cell Signaling Technology, Inc. (www.cellsignal.com).*

Adaptive Immunity

The adaptive immune system distinguishes itself from the innate immune system by the massively diverse repertoire of antigen receptors generated in T and B lymphocytes during their development via genetic recombination programs unique to these cell types. This permits recognition of a huge number of antigens by B cells and the processing and presentation of peptides via MHC to $CD4^+$ and $CD8^+$ T cells to drive T cell activation and eventual pathogen clearance. T cell activation requires two signals. The first signal is stimulation of the T cell receptor (TCR):CD3 complex by peptide-loaded MHC-I or MHC-II plus CD8 or CD4 binding of the MHC. The second signal is co-stimulatory and requires CD80/CD86 on APCs to interact with CD28 on the T cell. Activated T cells also express cytotoxic T lymphocyte-associated protein 4 that has a higher affinity than CD28 for CD80/CD86, and it serves as an immune checkpoint to downregulate T cell responses. B cells are one of three professional APCs, along with macrophages and dendritic cells, and upregulate CD80/CD86 upon activation, emphasizing the importance of B cells for T cell activation and regulation.

In addition to specificity and diversity, memory is also an important characteristic of the adaptive immune system, as both B and T cells possess the capacity to "remember" antigen upon reencounter. This equips the immune system with the ability to quickly clear pathogens that were once-present, on the basis of immunological memory of the antigen. An easy illustration of this is whenever we get a booster shot after a primary immunization. At the cellular level, memory B cells predominantly arise in germinal center (GC) reactions through interactions with follicular helper cells and cytokines that promote B cell differentiation. Memory B cells can be either IgM^+ or isotype switched (most commonly IgG^+) and can arise independently of a GC, although it has been shown that the memory B cell phenotype in these scenarios is incomplete,

likely the result of low levels of isotype switch or mutations that improve antigen affinity (25). Upon subsequent secondary antigen exposure, IgG^+ memory B cells may acquire Blimp-1 expression and quickly differentiate into antibody-secreting plasmablasts, providing another route for protective humoral immunity. Similarly, a low frequency of activated T cells at the end of their effector phase may persist as memory T cells (26). Memory B and T differentiation is not completely understood, yet memory B and T cells provide long-lived protection against foreign pathogens at the cellular level due to their capacity to revert back into effector cells.

Humoral immunity results from plasmablasts and plasma cells that circulate in the blood and lymph and secrete protective antibodies. Additionally, a large portion of plasma cells are concentrated in the bone marrow and non-circulating. Thus, the ability to communicate with and activate cognate T helper cells paired with their antibody secretion potential and capacity to form long-lived memory responses points to the B cell as one of the critically important cell types in the immune system. The fact that they also express nearly all of the TLRs further indicates the importance of the B cell and shows that they are capable of responding to foreign pathogens naturally, without specificity (innate) and with antigen training (adaptive).

There are five classes of immunoglobulins (Ig, antibodies) that can be induced during a humoral response: IgM, IgD, IgG, IgA, and IgE. These five antibody isotypes exist because they each elicit different effector functions from the immune system, based on the current isotype of the antigen-specific antibodies as well as the Fc receptors present on other cell types. For example, phagocytes express Fcγ, Fcα, and Fcε receptors for purposes of internalizing IgG, IgA, or IgE antibodies that have bound antigen in circulation. This is also how opsonized pathogens are cleared. All newly-developed B cells express IgM on their surface, and IgD is co-expressed along with IgM in mature B cells (27). Early antibody defenses against foreign pathogens are

predominantly of the IgM isotype, but the most predominant antibody isotype in circulation is IgG. There are subclasses of IgG in mice, including IgG1, IgG2a/c, IgG2b, and IgG3, each with a unique role and effector function. Humans express IgG1, IgG2, IgG3, and IgG4. When it becomes necessary for mature IgM^+ IgD^+ B cells to change their isotype, they do so through a process called Ig class switch recombination (CSR), also called isotype switch.

CSR occurs when mature B cells are stimulated with antigen plus co-stimulatory molecules, as well as cytokines that elicit specific antibody isotypes. Once stimulated, the genetic recombination is initiated by the unique B cell enzyme, activation-induced cytodine deaminase (AID). AID deaminates cytosines on DNA in switch regions that are located upstream from each of the H chain constant regions, one for each isotype. The deaminated cytosines are converted to uracils that are subsequently removed by uracil DNA-glycosylase. These now abasic sites have "nicks" introduced in the DNA strands by apurinic, apyrimidinic endonuclease. DNA breaks promote removal of the target genes from the switch regions, and then DNA is repaired or rejoined through non-homologous recombination, thus permitting transcription of new Ig isotypes (28). This process is irreversible, and after each round of recombination, only downstream switch regions and their corresponding isotypes can be induced. Importantly, the affinity of BCR for antigen remains unchanged during isotype switch, as CSR serves to change the effector function of antibodies and not their antigen-binding potential. In other words, the V_H portion of the BCR remains constant during CSR, hence their specificity for antigen does not change.

Antibody responses arise from plasmablasts and plasma cells that have undergone B cell differentiation. Plasmablast differentiation can occur independently of T cell help, for quick IgM antibody responses (29). However, T cells can dramatically help the B cells via CD40L:CD40

signaling and cytokines that serve to promote survival and further activation and differentiation of the B cell (30). These cognate interactions can occur in GCs, specialized structures within secondary lymphoid organs such as the spleen, lymph nodes, and Peyer's patches. Once inside the GC, cognate B and T cells receive help from each other and from localized cells like follicular dendritic cells to carry out normal, protective immunity. A normal B cell response to protein antigen is illustrated in Fig. I-2.

The GC provides a unique environment for cognate interactions between antigen-specific T and B cells. The primary function of the GC is to select the highest affinity B cell clones for long-lived immune responses like antibody-secretion via plasma cell differentiation, as well as formation of memory B cells for quick recall against foreign pathogens that have already been encountered. Affinity maturation of BCRs is achieved through somatic hypermutation, a process that largely occurs in the GC. Isotype switch can also occur in GC reactions and is the product of CD40 signaling/co-stimulation by CD40L expression from activated T follicular helper cells. Importantly, GC B cells upregulate expression of the death receptor, Fas, to guard against the potential generation of high-affinity autoAbs (31, 32). Effective peripheral tolerance serves to keep clonally expanding and maturing B cells at bay, as any non-tolerant B cell participating in an unbiased GC reaction has the potential to acquire mutations that result in high-affinity antibodies. Thus, the GC offers a unique environment for generation of productive, protective immunity, yet there is a downside that must be accounted for to guard against autoimmunity.

Recently, it was reported that affinity maturation through somatic hypermutation can occur completely independent of the GC reaction in extrafollicular spaces during *Salmonella* infection (33). The authors originally hypothesized that the massive plasmablast response was polyclonal and non-specific due to innate B cell activation. However, BCRs specific for

Salmonella were found to exist in a polyclonal repertoire at relatively high frequency but at very low affinity. These B cells acquired mutations necessary for affinity maturation in the extrafollicular space, thus highlighting a GC-independent mechanism for the response to a Gram-negative pathogen through "promiscuous" activation of *Salmonella*-specific B cells.

In my studies, anti-insulin B cells exist at relatively high frequency (1 in 250) in the polyclonal repertoire of V_H125^{SD} B6 mice, yet there is an obvious antigen-specific GC response that arises following immunization with insulin conjugated to a Gram-negative pathogen. There is strong evidence for somatic hypermutation in anti-insulin GC B cells during this response, thus, these data and the studies noted above indicate that there are both GC-dependent and GC-independent pathways for B cell responses specific for T cell-independent (TI) antigens.

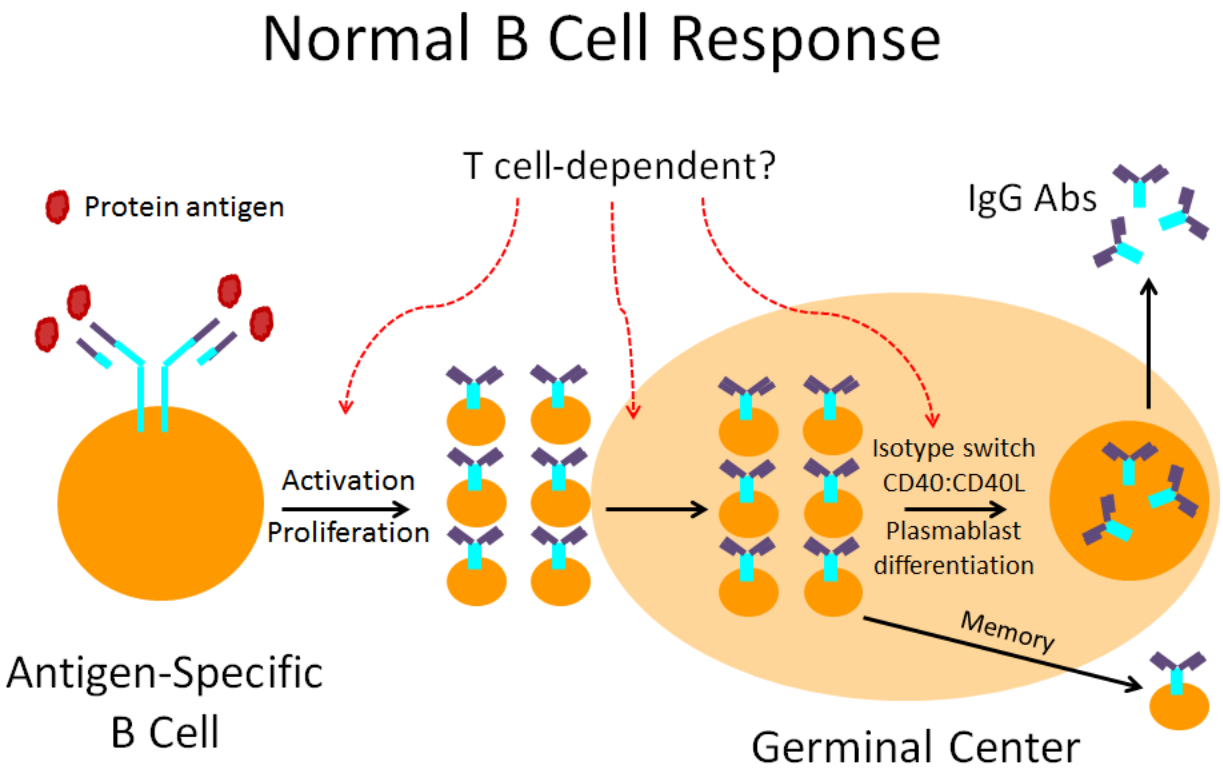

FIGURE I-2. Normal B cell response to protein antigen. When an antigen-specific B cell encounters its cognate antigen, it will activate and undergo clonal expansion. Somatic hypermutation predominantly occurs in the GC and serves to introduce mutations in the BCR to elicit higher affinity responses. Isotype switch also occurs in the GC. IgM and IgG antibodies are secreted by plasmablasts and plasma cells that have undergone B cell differentiation in the GC that is largely considered to be a T-dependent phenomenon. Memory responses also arise from GC reactions. T cell support via CD40L helps drive B cell differentiation in the GC.

B Cell Development and Central Tolerance

The random nature of genetic recombination in developing B lymphocytes plus the sheer numbers of receptors generated during the process (10^{14}) means that not all of the antigen receptors expressed on newly-developed B cells will be functional. Inevitably, receptors will be created that have the propensity to bind self. These cells, if not appropriately controlled, can promote autoimmunity and the induction of autoimmune disease. Fortunately, there are regulatory mechanisms in place to guard against autoimmunity, a process called tolerance. The objective of tolerance induction is to re-structure, paralyze, or eliminate autoreactive cells present in the host, while preserving the anti-microbial power and potential of the immune system as a whole.

The concept of tolerance was first established in the 1940s, when Ray Owen observed two different types of red blood cells in cattle twins. He deduced that the lack of immune reactivity to the foreign red blood cells must have resulted from an acquired tolerance in young cattle due to early exposure of the foreign antigen (34), an observation later validated by Burnet and Fenner (35). A few years later, Peter Medawar extended this observation and demonstrated that young mice receiving skin grafts from an entirely different strain of mice would tolerate the graft if they first received spleen cells from the donor (36). Years later, we know now that the cells responsible for tolerating or rejecting grafts are T and B cells, as the introduction of foreign antigens into the developing immune system of young mice serves to tolerize the cells against future skin grafts. This also points to an early window of time in a mammal's life where the host's immune system can be more easily tweaked or manipulated than that of an adult, when B and T cell repertoires are relatively established. The antigen-specific nature of tolerance is emphasized by the fact that a skin graft from a third party mouse is still rejected. To this day, a

primary yet elusive goal of immunologists is to achieve a more thorough understanding of the concepts of immunological tolerance to self-antigens. Breaches in self-tolerance are the underlying causes of autoimmunity.

B cells initially develop in the fetal liver and then in the bone marrow throughout life. B cells start out as stem cells or lymphoid progenitor cells before receiving signals from stromal cells to begin B cell development. The objective of B cell development essentially is to create productive, functional antigen receptors that are expressed on the surfaces of new B cells. This is achieved through genetic recombination of variable (V), diversity (D), and joining (J) gene segments in the heavy (H) chain locus first, followed by V-J recombination in the light (L) chain locus. Recombination is mediated by the lymphocyte-specific proteins, recombination activating genes (RAG) 1 and 2. The mechanism of gene segment assembly is achieved by recombination signal sequences (RSS) that flank each specific V, D, or J segment. RSSs consist of conserved nucleotide heptamer and nonamer sequences separated by a spacer of either 12 or 23 nucleotides in length. Recombination only occurs between RSSs of 12- and 23-nucleotide spacers, called the 12/23 rule, thus ensuring highly efficient gene assembly and avoiding unproductive arrangement. Once the segments are brought together, the DNA is cleaved and hairpin loops form at the end of the desired segments to be joined. Once the hairpins are cleaved, DNA ligase IV rejoins the broken DNA. The constant regions are joined to the newly formed V-D-J to form one cohesive immunoglobulin gene segment that is ready for transcription.

Successful V_H-DJ_H recombination of the H chain leads to emergence of the critical pre-B cell stage. Pre-BCRs are transiently expressed on developing B cells and are comprised of the new IgM H chain and temporary surrogate L chains, VpreB and lambda5, along with the Igα/Igβ signal transducer (37). Signaling through the pre-BCR terminates H chain rearrangement,

stimulates proliferation of pre-B cells, and induces V_L-J_L rearrangement in the L chain locus. There are two main L chain isotypes, kappa and lambda, and the frequency of which L chain is chosen depends on the species. Unproductive rearrangement at either the H chain or L chain loci results in additional attempts at rearrangement on the other allele. For L chains, both kappa alleles are attempted first, then the lambda alleles. If rearrangement remains unproductive after these attempts, apoptosis will be induced in the B cell due to a failure to establish a basal signaling profile from an assembled BCR. Eventually, after productive rearrangement occurs, pre-B cells emerge as immature B cells that express IgM^+ antigen receptors (H chain plus L chain) on their surface, and at this stage antigen is exposed to test the affinity between BCR and antigen, effectively initiating central tolerance. If the signal is satisfactorily low enough, the clone is permitted to survive and exits into the peripheral repertoire. However, if the newly developed BCR interacts with self-antigen, central tolerance will be induced and the clone may be negatively selected (38).

B cell central tolerance in the developing repertoire is characterized by receptor editing and clonal deletion (38-41). Clonal deletion is the complete removal or elimination of self-reactive B cells from the repertoire. Receptor editing is a last attempt at keeping the clone alive, as the potentially autoreactive BCR will have its L chains replaced to determine if the new BCR will suffice. If multiple iterations of BCR editing do not work, the clone may be eliminated altogether. The discovery of receptor editing is widely attributed to Nemazee and Weigert, who separately demonstrated that self-reactive B cells developing in the bone marrow would undergo L chain replacement (kappa to lambda) when the autoAg – either $H\text{-}2^k$ MHC-I or dsDNA – was ubiquitously expressed (42, 43). When expression of the autoAg was removed from the bone marrow, the self-reactive B cells were found in the peripheral repertoire.

These mechanisms of central tolerance play an absolutely essential role in the prevention of autoimmunity, as they represent the first line of defense against destructive, self-reactive B lymphocytes. Not all self-reactive B cells are removed by central tolerance, as BCRs with monovalent or weak interactions with autoAgs may avoid elimination or revision (43, 44). A downside of BCR revision through receptor editing is that the process allows for the possibility of allelic inclusion of the originally autoreactive BCR with the new BCR. Normally, only one type of BCR is generated and expressed on the B cell surface during Ig rearrangement. Allelic inclusion arises when two separate BCRs are expressed, permitting the escape of a potentially harmful BCR into the repertoire. This retains the B cell's potential to produce autoAbs, should subsequent mechanisms of tolerance fail (45).

The overall scope of immune tolerance is not complete without an understanding of how T cells develop and how tolerance is imposed on potentially autoreactive T cells. Stem cells in the bone marrow that commit to the T cell lineage enter the thymus to begin T cell development. Immature thymocytes that have just entered the thymus do not express any of the surface markers associated with T cells, including the TCR, CD3, CD4, or CD8, and they are referred to as "double negatives." The TCR beta chains are rearranged at this stage, and they pair with an invariant chain to form the pre-TCR that complexes with CD3 on the cell surface. CD3 is the signaling component of the TCR complex, consisting of two heterodimers of four invariant chains, εδ and εγ. A ζζ chain intracellular homodimer finalizes the signaling complex of the TCR. Without CD3 and the ζ chain homodimer, the TCR cannot signal that antigen has bound. After productive pre-TCR formation, thymocytes express CD4 and CD8 ("double positives"), and alpha chain rearrangement occurs. Successful generation of an alpha/beta TCR precedes differentiation into single positive mature $CD3^+$ $CD4^+$ $CD8^-$ or $CD3^+$ $CD4^-$ $CD8^+$ T cells that then

exit the thymus and enter the peripheral repertoire. Whether double positive thymocytes retain CD8 or CD4 positivity depends on the affinity of the TCR for either MHC-I or MHC-II on thymic epithelial cells and APCs.

TCR genes undergo rearrangement through a process very similar to immunoglobulin gene rearrangement during B cell development. V-D-J gene segments code the variable region of the TCR, and the process is mediated by RAG. The β chain locus rearranges first, analogous to the H chain of the BCR, followed by the α chain, analogous to the BCR L chain. Productive rearrangement of each chain blocks rearrangement on the other allele, termed allelic exclusion, to ensure only one type of TCR is expressed on each T cell surface. The diversity of the TCR repertoire is actually estimated to be larger than the BCR repertoire (10^{18}). Still, the T cell repertoire undergoes a rigid negative selection process to help prevent the generation of TCRs specific for self-antigens, an event that is inevitable given the massive diversity of the repertoire and the random nature of recombination.

Central tolerance in the thymus selects TCRs on the basis of peptide/MHC affinity. Thymocytes expressing low affinity TCRs die because they do not receive the necessary survival signal. TCRs with high affinity for peptide/MHC complexes receive a death signal and undergo negative selection. An important gene called autoimmune regulator (AIRE) has been implicated in the expression of self-antigens by medullary thymic epithelial cells in the thymus to assist in the negative selection of autoreactive T cells (46), and AIRE deficiency results in increased risk of autoimmunity due to defective negative selection (47). Insulin is one of the tissue-specific antigens that are expressed in the thymus, and a low level of insulin mRNA transcription has been implicated in an increased risk to develop type 1 diabetes (48). Reduced expression of these autoAgs results in impaired central tolerance and poor negative selection in the thymus.

TCRs that possess affinity for peptide/MHC that is neither too low nor too high will receive a survival signal at the immature "double positive" T cell stage and undergo positive selection and become $CD4^+$ or $CD8^+$ T cells. This process of selection is imperfect, however, and not all autoreactive T cells are removed by central tolerance in the thymus, similar to B cell central tolerance in the bone marrow. Thus, additional mechanisms of tolerance must be imposed on both the B cell and T cell repertoires in the periphery.

Peripheral Tolerance

Autoreactive B and T cells that escape central tolerance and mature are a liability, but mechanisms of peripheral tolerance are in place to protect against autoimmunity (49-52). B cells may be clonally ignorant and ignore or never bind self-antigens. Alternatively, B cells reactive to self-antigens may be rendered clonally anergic or functionally silent to immune stimuli in the periphery. Tolerant B cells exhibit decreased surface Ig expression, impaired Ca^{2+} mobilization, restricted competition for available survival factors and follicular niches, and impaired responses to both T cell help and B cell mitogens (50, 53). Tonic signaling through surface IgM and phosphoinositide 3-kinase (PI3K) is essential for survival of mature B cells (54). This is achieved in part through basal level BCR-mediated Ca^{2+} flux via the phospholipase Cγ2 (PLCγ2) pathway. Decreased surface IgM expression in tolerant B cells serves to reduce the basal signal delivered through the BCR, leading to impaired downstream responses and Ca^{2+} mobilization. Notably, newly developed B cells that were rendered tolerant in the bone marrow compete poorly for B cell activating factor (BAFF) as they emerge in the spleen (55, 56). Anergic B cells are not deleted in the periphery but allowed to survive, albeit in a quiescent state, and usually with a shorter lifespan. Such B cells are recognized in both normal and autoimmune repertoires (57-59). An anergic B cell response is illustrated in Fig. I-3.

The importance of BCR signaling for maintaining peripheral tolerance is emphasized by the reversal of anergy upon removal of chronic cognate Ag (53, 57). In this classic experiment, naïve B cells specific for the irrelevant antigen, hen egg lysozyme (HEL), were rendered anergic when crossed with a separate transgenic mouse expressing soluble HEL. These tolerant anti-HEL B cells were transferred into recipient mice that did not express soluble HEL, and anergy was reversed. If HEL antigen was reintroduced to the B cells, anergy was restored. Alterations in BCR signaling pathways and mediators like PI3K, protein kinase C theta, and the negative regulator protein tyrosine phosphatase non-receptor type 22 have been shown to impact tolerance (60-62). Comprehensive normal BCR signal transduction is illustrated in Fig. I-4.

Signaling via TLRs and MyD88 reverses anergy in some autoreactive B cells, suggesting that environmental factors that lead to infection and inflammation may also alter tolerance (63, 64). B cells deficient in MyD88 demonstrate impaired IgM responses to bacterial antigens, indicating that innate signaling through TLR pathways is critical for early TI immune defense (65). TLR4 stimulation by LPS unlocks alternate signaling pathways to ERK phosphorylation and NF-κB activation independent of conventional BCR-dependent signaling mediators (66) that may be impaired in anergic B cells.

TLR9 has been implicated in the loss of self-tolerance to DNA and supports development of systemic lupus erythematosus. Marshak-Rothstein's group has done extensive work showing that autoreactive B cells can be activated through engagement of both BCR and TLR9 with dsDNA autoAgs (24, 63). She identified that signals delivered by a TLR bound by microbial ligand paired with BCRs engaged by autoAgs can combine to break tolerance and promote the activation of autoreactive B cells, even if the two separate signals alone are sub-threshold. The constant availability of insulin in circulation paired with available TLRs on anti-insulin B cells

could point to a possible mechanism of tolerance reversal in these harmful B cells that are known to promote type 1 diabetes.

Cognate interactions with T cells may also drive loss of B cell tolerance and promote somatic hypermutation and isotype switch in GC reactions associated with ongoing autoimmune disorders (67, 68). The fact most pathogenic autoAbs are of the IgG isotype further implicates T cells as potential vectors for driving loss of B cell tolerance. Thus, the effectiveness of immune tolerance for B lymphocytes depends on the nature of BCR interaction with autoAgs, potential encounter with innate signals in the environment, and availability of epitopes that promote cognate T-B interactions.

Like B cells, T cells possess antigen-specific receptors that must distinguish between foreign and self. Unlike B cells, however, whose BCRs recognize intact antigens, TCRs recognize peptides that have been processed and loaded onto MHC. TCRs will only recognize peptides that are presented by APCs when the MHC is self, a phenomenon known as MHC restriction. Cytotoxic T cells isolated from a mouse with an H-2^b MHC haplotype that has been infected with virus will kill virus presented by APCs with H-2^b MHC (self) but not by APCs with H-2^k MHC (non-self).

Induction of peripheral tolerance in T cells depends on whether or not the cell receives the second signal required for activation in addition to TCR binding by peptide/MHC presented by APCs. This second signal is co-stimulatory and is mediated by CD28 binding on T cells by CD86 (B7.2) on APCs. Co-stimulatory signal alone in the absence of TCR ligation causes no effect on the T cell, whereas ligation of the TCR alone by peptide/MHC in the absence of the co-stimulatory signal results in the induction of an anergy program similar to that in B cells. T cells that have been rendered anergic are functionally inactivated, exhibiting impaired proliferation,

differentiation, and Ca^{2+} mobilization (69). Maintenance of peripheral tolerance is driven largely by the continuous presentation of self-antigens to T cells in the absence of co-stimulatory signal. This emphasizes the importance of tolerance in the B cell compartment, as anergic B cells display poor CD86 activation and thus, poor T cell co-stimulation.

A specialized subset of T cells exist called regulatory T cells (Tregs), whose primary function is the regulation and maintenance of peripheral tolerance in B and T cells. Severe autoimmunity results from a deficiency in Tregs. For example, patients with type 1 diabetes have dysfunctional Tregs, and re-establishing the function of Tregs, and thus the reinforcement of self-tolerance, has been an objective of many of the therapies attempted to date. Natural $CD4^+$ Tregs arise from T cell precursors in the thymus, characterized by expression of CD25 on the cell surface and *Foxp3* gene transcription. Tregs may also be induced in the periphery following stimulation with transforming growth factor beta in the presence of antigen, although inducible Tregs and natural Tregs have similar functional properties (70). *Foxp3* is considered the master control gene for both the development and function of Tregs (71). Conditional knockout of *Foxp3* in non-obese diabetic (NOD) mice leads to overt diabetes within three days, emphasizing the importance of Tregs in controlling disease progression (72). Tregs suppress immune responses through both direct cell contact and secretion of inhibitory cytokines.

The overall effectiveness of immune self-tolerance depends on efficient collaboration between the efforts of central tolerance in the developing thymus and bone marrow and peripheral tolerance in the B and T cell repertoire for those cells that escape central tolerance. Receptor editing, clonal deletion, anergy, and Tregs must all work together to maximally protect from autoimmunity. However, the incidence of autoimmune disease in this country and around the world indicates that these mechanisms of tolerance remain imperfect.

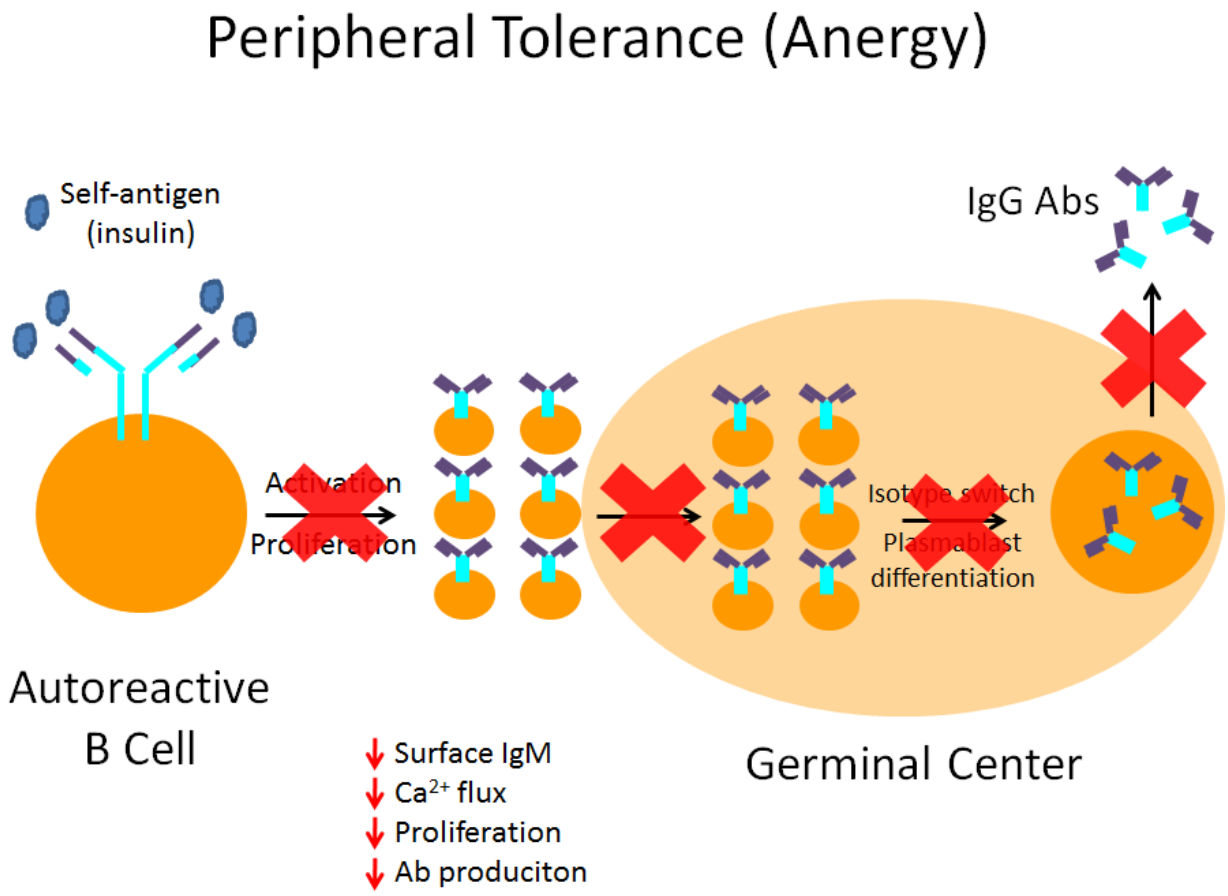

FIGURE I-3. Anergic B cell response. When an autoreactive B cell encounters its autoAg, peripheral tolerance is enforced through a process called anergy. Tolerant B cells exhibit impaired Ca^{2+} mobilization, proliferation, and antibody production, in part through a reduction in surface IgM expression. This serves to prevent immune activation and the possible entry into the GC, where isotype switch and affinity maturation take place. When tolerance is broken, any or all of these impairments may be lifted, and autoimmunity may arise.

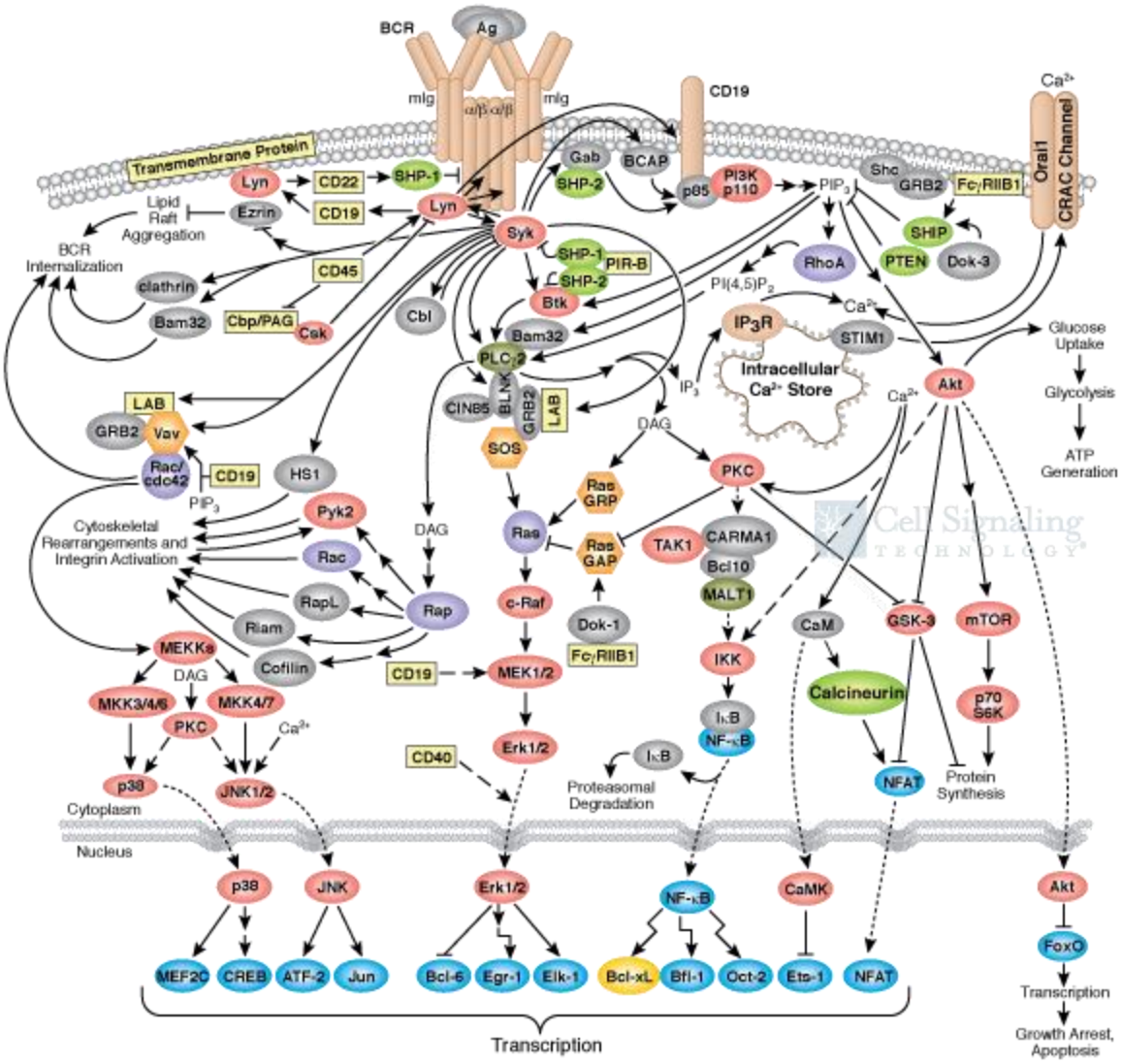

FIGURE I-4. Comprehensive B cell receptor signal transduction. *Illustration reproduced courtesy of Cell Signaling Technology, Inc. (www.cellsignal.com).*

Transgenic Mouse Models of B Cell Tolerance

Several mouse models generated in the 1980s established a basic framework for studies in B cell tolerance. The first seminal discovery came with the creation of the hen egg lysozyme (HEL) transgenic mouse. HEL is a clinically irrelevant autoAg, but even though it is not expressed in humans or rodents, it is still the model antigen in the field of B cell tolerance. A high-affinity anti-HEL antibody, MD4, was expressed as a $\mu^{+}\delta^{+}$ transgenic BCR in mice, with the resulting B cell progeny possessing naïve specificity for HEL antigen (53). HEL-specific B cells demonstrated robust responses upon activation with HEL *in vitro* and *in vivo*, similar to most naïve B cell responses when antigen is seen for the very first time. When anti-HEL MD4-Tg mice were crossed with another transgenic mouse with HEL permanently expressed as a soluble antigen, sHEL ML5-Tg, the HEL-specific B cells were found to be profoundly anergic (53, 57). When these cells were transferred into mice that did not express sHEL, B cell anergy was reversed, indicating a requirement for continuous antigen exposure to enforce tolerance. The paradigm of B cell anergy in the HEL model is still used to this day both in the designing of new experiments and in the instruction of new students on the concepts of tolerance.

As indicated earlier, receptor editing as a mode of central tolerance was discovered by Nemazee and Weigert in the early 1990s, who used separate BCR Tg models to show that autoAg expression during B cell development in the bone marrow drove L chain replacement. Nemazee's discovery utilized 3-83 Tg mice in which B cells possess specificity for the MHC haplotype H-2^{k} (38, 42). Weigert's group utilized a site-directed Tg model with B cell specificity against dsDNA (73). The resulting B cell repertoire in the periphery was almost entirely non-autoreactive, pointing to the efficiency of receptor editing in the initiation of central tolerance and defense against potentially harmful, self-reactive B cells.

While anergy is the predominant mechanism of peripheral tolerance, clonal deletion has also been demonstrated to occur in the periphery. A modified version of the 3-83 anti-MHC Tg mouse model was introduced several years after the original model and helped establish clonal deletion as a mode of peripheral tolerance. Expression of H-2^k was restricted to the liver, thus, B cells specific for MHC developed normally in the bone marrow but underwent rapid deletion when they encountered membrane-bound autoAg in the liver (74, 75). However, administration of a bacteriophage containing a 15 amino acid mimotope recognized by 3-83 B cells reversed tolerance and promoted their survival and robust Ig production (74). Thus, tolerant B cells that are normally deleted in the periphery were actually rescued when self-antigen was presented to the B cell in a TI fashion.

Clonal deletion was also observed in a modified HEL model, when anti-HEL MD4-Tg mice were crossed with a membrane-bound HEL-Tg mouse instead of the sHEL ML5-Tg (76). In both the 3-83 and anti-HEL x mHEL models, the anchoring of antigen to membrane delivered a stronger signal to the BCR that led to cell death, compared to the relatively weak signal delivered by soluble HEL for anergic anti-HEL B cells. Thus, the mechanism of peripheral tolerance elicited in autoreactive B cells depends not just on the interaction between BCR and autoAg, but rather the strength of signal delivered through the BCR as a result of antigen concentration, localization, or physical presentation.

About 15-20 years ago, a BALB/c mouse was immunized with human insulin in order to study immune response gene control of anti-insulin antibodies. Hybridomas were generated from monoclonal anti-insulin B cells that arose during this primary immunization. One of the monoclonal antibodies (mAb) that arose, mAb125, was cloned and sequenced because it was autoreactive and bound rodent insulin in a non-autoimmune strain of mice. To study mAb125 in

greater detail, the construct was engineered into an anti-insulin transgene and expressed in B cells. The resulting 125Tg (H chain + L chain) was backcrossed onto both the non-autoimmune C57Bl/6 (B6) background and into autoimmune, type 1 diabetes-prone NOD mice. Both B6 and NOD mice possess B cells whose BCR H chains are [b] allotype, whereas BALB/c mice' BCR H chains are all [a] allotype. This small important difference allows for quick identification and distinguishing between endogenous B cells and transgenic anti-insulin B cells ([b] vs [a]). Of note, the 125Tg line was generated as a conventional transgenic, meaning all of the anti-insulin B cells that develop in these mice are μ-only, IgM-restricted, and therefore cannot undergo isotype switch.

A separate transgenic mouse was generated where the anti-insulin H chain was expressed by itself. B cells in these "H chain only" V_H125Tg B6 mice use endogenous L chains to generate functional BCRs. Thus, only a very small fraction of the repertoire is anti-insulin (< 1%) due to the rare event of pairing an endogenous anti-insulin L chain with the transgenic H chain. Studies using these conventional IgM-restricted anti-insulin BCR transgenic mice revealed anti-insulin B cells enter the mature repertoire but are anergic and fail to produce anti-insulin antibodies following T cell-dependent (TD) immunization (77). Such functionally silenced B cells residing in the periphery retain cellular functions such as antigen presentation that enable them to promote autoimmunity in NOD mice (68, 78).

V_H125Tg was also bred onto the NOD background to study anti-insulin B cells in the context of a mouse genetically predisposed to develop type 1 diabetes. V_H125Tg NOD possess a small frequency of anti-insulin B cells (1-2%) that exacerbate disease incidence in comparison to WT NOD mice that do not have a detectable frequency of such B cells (79). This is an interesting observation considering that NOD mice spontaneously develop insulin autoAbs.

While this indicates that anti-insulin B cell tolerance is broken, the presence of insulin autoAbs themselves is not enough to promote disease. Indeed, there are patients with type 1 diabetes who do not possess detectable autoAbs to insulin, suggesting they are not required for disease pathogenesis. The frequency of anti-insulin B cell precursors appears to be the major contributing factor.

Insulin autoAbs associated with type 1 diabetes, as well as antibodies that arise in response to insulin therapy and complicate disease management, are predominantly of the IgG isotype (80-85). To assess peripheral tolerance in anti-insulin B cells competent to undergo somatic hypermutation and CSR, we generated B6 mice that harbor an anti-insulin H chain site-directed to its native locus (V_H125^{SD}). V_H125^{SD} pairs with endogenous L chains to generate a polyclonal B cell repertoire, where physiologically relevant CSR-competent anti-insulin B cells successfully compete and make up a small fraction of the repertoire. V_H125^{SD} B6 mice crossed with anti-insulin Vκ125Tg mice generates a monoclonal B cell repertoire in which > 95% of the B cells bind insulin (V_H125^{SD}/Vκ125Tg), a model utilized for *in vitro* experiments. These two models are used to assess the fate and function of anti-insulin B cells that are competent to undergo isotype switch in either a monoclonal or polyclonal repertoire. A summary of all of the anti-insulin transgenic mice used in these studies is shown in Table I-1, including the affinities of the anti-insulin BCR for various insulins – human, rodent, and bovine (86).

Mouse	Site-Directed?	Anti-Insulin?	
		H chain	*L chain*
V_H125^{SD}	H chain	yes	endogenous
V_H125^{SD}/Vκ125Tg	H chain	yes	yes
125^{SD}	H + L chain	yes	yes
V_H125Tg	no	yes	endogenous
125Tg	no	yes	yes

125Tg Insulin Reactivity	
Species	**Affinity (L/M)**
Human	$3x10^8$
Rodent	$7.9x10^6$
Bovine	$2.6x10^6$

TABLE I-1. Anti-insulin transgenic mice and insulin affinities. A summary of all of the anti-insulin transgenic mice used in these studies is shown, including H chain and L chain insulin-specificities and whether or not each chain was site-directed to the locus. Also shown are the original 125Tg affinities (L/M) for human, rodent, and bovine insulin.

Insulin

Autoimmunity arises when tolerance is ineffective at culling or dampening responses in autoreactive B and T cells. A highly relevant autoimmune disease in both society and for me personally is type 1 diabetes, an organ-specific autoimmune disorder characterized by infiltration of self-reactive B and T lymphocytes in the pancreatic islets, where insulin-producing beta cells and other surrounding antigens are attacked and destroyed. The resulting inability to control blood glucose eventually leads to clinical diagnosis, most commonly in juveniles. Type 1 diabetes affects over two million people in the United States alone, and 20,000 – 40,000 new diagnoses are reported every year in juveniles (http://diabetes.niddk.nih.gov/dm/pubs/statistics). Insulin therapy and well-controlled diet represent the most effective treatment regimen for type 1 diabetics, although a cure for the disease has remained elusive.

Transplantation of islets and whole pancreas has been performed with moderate results, but with serious risk of immune rejection and poor long-term efficacy. Thus, any true cure for the disease must include either the elimination or complete paralysis of such autoreactive B and T lymphocytes to avoid repetitive destruction of all new insulin produced by the host. Therapies like Rituximab, an anti-CD20-mediated B cell depletion, have been used with moderate success in patients with autoimmune diseases such as rheumatoid arthritis and type 1 diabetes, as well as other diseases like non-Hodgkin's lymphoma (87). This suggests that B cells are a viable target for autoimmune therapy, but this comes at the expense of losing the entire B cell repertoire. Given the importance of B cells in protective immunity, antigen-specific therapies are becoming more popular and desirable so that just the harmful, self-reactive B cells are targeted.

Insulin is a protein hormone that was first discovered in the early 1920s by Charles Best and Sir Frederick Banting (88). They experimented with diabetic dogs that they treated with

extract from ducts of pancreata removed from the same dogs, under Banting's presumption that some internal secretion machinery of the pancreas might be responsible for glucose regulation. Consistently, the treated animals showed lower blood glucose, and other disease symptoms were improved. The method for harvesting insulin from pancreas was dramatically improved when Banting and Best came up with the idea of prepping the organ in alcohol rather than saline, such that the alcohol in solution from tissue macerated for 48 h could be evaporated. The leftover powder/residue was dissolved in saline and administered to diabetic dogs with remarkable results. Before these monumental discoveries, a clinical diagnosis of type 1 diabetes was a death sentence; the chronic inability to regulate blood glucose leads to polyuria, neuropathy, organ failure, and eventually death without insulin intervention. Thus, Banting and Best's discovery nearly a century ago literally changed the world, offering newfound hope to those who suffered from a previously incurable disease.

Insulin's small size and low circulating concentration was previously thought to limit BCR interactions necessary for tolerance (89, 90). One of the earliest experiments that debunked this myth was performed by Rosalyn Yalow and Solomon Berson, who together discovered insulin-binding antibodies and designed the radioimmunoassay (RIA) (89). Early diabetic patients were treated with bovine insulin, so Yalow and Berson used Iodine-125 to radioactively label and track the fate of injected insulin. They noticed healthy controls passed the labelled insulin through their system much faster than diabetics who had been taking therapeutic insulin, leading Yalow and Berson to eventually conclude that antibodies arose to the foreign bovine insulin, and these antibodies must both slow down the passage of insulin through the body and limit the effectiveness of the insulin itself. This revolutionary discovery had two long-lasting implications. First, Yalow and Berson helped demonstrate that human insulin was a better

therapy than bovine insulin for treatment of human diabetics. Second, these were some of the first studies that showed anti-insulin antibodies actually existed. Years later, we now know that the numbers of different autoAbs that arise in type 1 diabetes significantly correlate with disease incidence in humans (91), and those autoAbs that bind insulin are the most abundant and usually the first to arise (Fig. I-5).

The presence of insulin autoAbs demonstrates that insulin is a tolerogenic molecule but also indicates that B cell tolerance to insulin is inherently flawed. IgG insulin autoAbs that arise in humans accurately predict type 1 diabetes outcome and complicate disease management by disrupting insulin therapies. The infiltration of pancreatic islets by anti-insulin B and T cells and the destruction of insulin-producing beta cells further prove that loss of tolerance in autoreactive B and T cells is an important event in the progression to type 1 diabetes. Since T cell activation largely depends on interaction with cognate B cells, loss of anti-insulin B cell tolerance represents one of the earliest stages in the initiation of autoimmunity. We need a more thorough understanding of the early events in the onset of disease, specifically those that preclude loss of tolerance in B cells specific for the autoAg, insulin.

Anti-insulin B cells cannot be tracked in WT mice due to their very low frequency in the repertoire, despite the fact that WT mice generate anti-insulin antibodies following immunization with insulin (77). This indicates that anti-insulin B cells must be present in order to generate an antibody response; however, they exist below the level of detection in a WT repertoire. Therefore, a transgenic mouse model with a trackable population of anti-insulin B cells was generated to gain necessary insight into the behavior and function of these autoreactive B cells using *in vitro* and *in vivo* experiments.

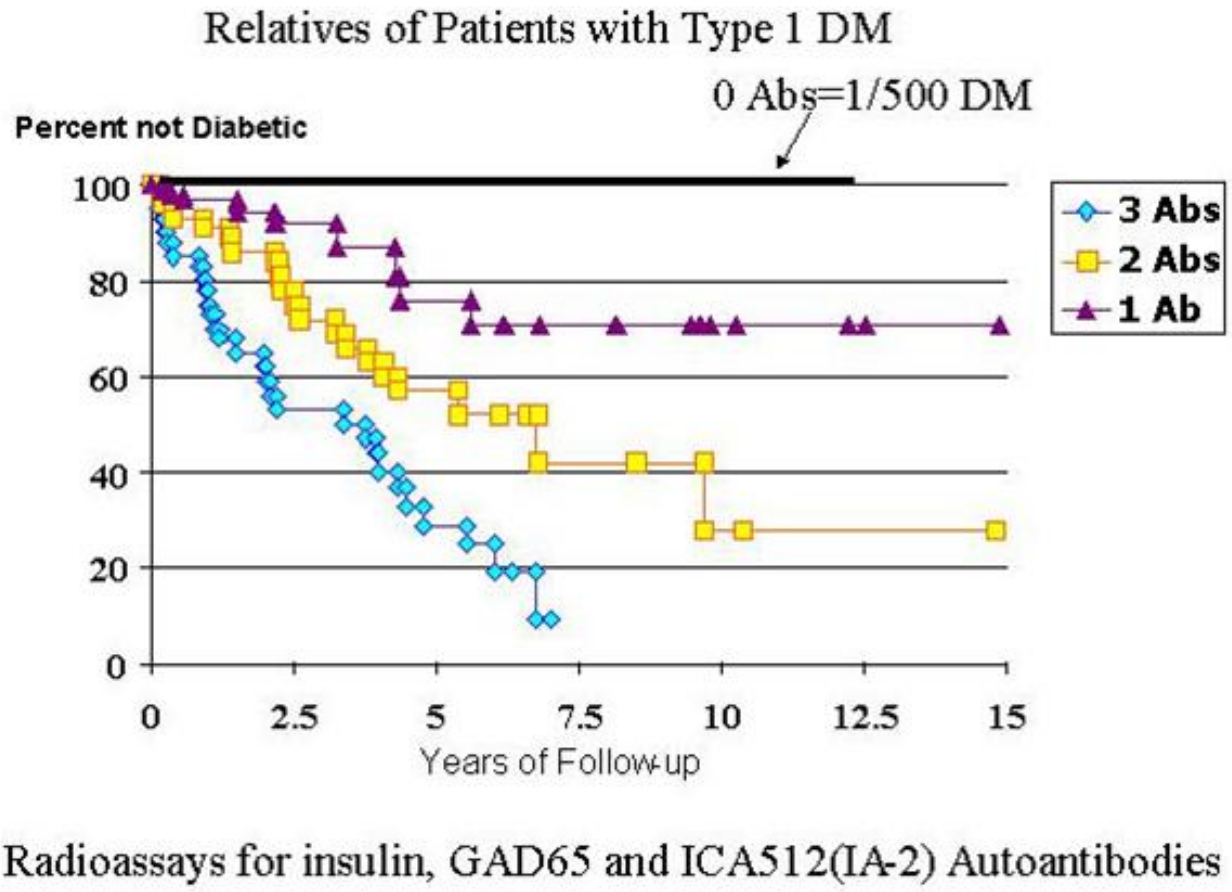

FIGURE I-5. Antibodies arise to multiple islet autoantigens in type 1 diabetes. The incidence of disease significantly correlates with number of autoAbs that arise in the onset of type 1 diabetes. There are multiple autoAgs that are targeted by B cells; however, the most common one is insulin. The majority of patients with only one autoAb have anti-insulin specificity.

Significance of the Research

Type 1 diabetes remains a worldwide health concern, and the incidence of the disease is increasing. Despite advances in modern medicine, a clinical diagnosis of type 1 diabetes, at minimum, guarantees health problems and risks later in life. These complications include kidney failure, retinopathy, neuropathy, and the definite possibility of a shortened lifespan. The contribution of anti-insulin B cells to the loss of self-tolerance to insulin and ultimate progression to type 1 diabetes emphasizes that more information is needed regarding the mechanisms behind how tolerance is broken in these B cells that are normally functionally silenced.

Anti-insulin B cells likely develop in most people due to the fact that as many as 75% of all newly formed B cells are autoreactive (92). However, only a fraction of the population suffers from autoimmunity. This indicates that the combined efforts of central and peripheral tolerance are remarkably effective at revising or removing harmful B cells from the repertoire. This also suggests that a genetic predisposition to develop autoimmune disease must exist, that there is some unidentified cue or trigger that improperly activates tolerant anti-insulin B cells, or both. T cells have the capacity to transfer disease in NOD mice (93, 94), while B cells by themselves cannot. However, NOD mice deficient in B cells or NOD mice treated with B cell-depleting anti-CD20 therapy exhibit remarkable protection from disease, implicating the B lymphocyte as one of the main culprits in both the initiation and continuation of autoimmunity through their function as APCs.

The current work reveals a new pathway to drive loss of tolerance for CSR-competent anti-insulin B cells. Antigen-specific GCs and IgG anti-insulin antibodies arise in V_H125^{SD} B6 mice immunized with insulin conjugated to a type 1 TI antigen (90, 95). This combined BCR/TLR4 engagement breaks tolerance, while stimulation of either receptor by itself does not.

These results support Marshak-Rothstein's concept of combined BCR/TLR engagement as a potentially important mechanism in eliciting autoimmunity in the B cell compartment. Infection and inflammation could play a pivotal role in the breach in tolerance in anti-insulin B cells.

CHAPTER II

PHENOTYPE AND FUNCTION OF A NEW SITE-DIRECTED ANTI-INSULIN TRANSGENIC MOUSE MODEL

Introduction

The previously-generated μ-only BCR transgenic mouse model does not address how native cellular functions like CSR impact the state of immune tolerance for anti-insulin B lymphocytes. Insulin autoAbs that arise in patients with type 1 diabetes and complicate insulin therapies are predominantly of the IgG isotype (81, 82), suggesting that CSR in B cells is an important biological process in the breakdown of self-tolerance to insulin. Thus, a new mouse model was needed to study the behavior of more physiologically relevant anti-insulin B cells. Accordingly, an anti-insulin H chain (VDJ_H125) was targeted to the H chain locus of B6 mice to generate anti-insulin B cells competent to undergo all native B cell functions, including isotype switch (V_H125^{SD} B6). These mice were crossed with anti-insulin Vκ125Tg mice to generate mice with a nearly monoclonal population of anti-insulin B cells, a tool I first used to phenotype and characterize these new B cells through *in vitro* experiments.

There are other isotype switch-competent BCR Tg mouse models that have been described, notably the SW_{HEL} model established in 2003 that permitted CSR to all isotypes in anti-HEL B cells (96). B cells in SW_{HEL} mice crossed with soluble HEL Tg mice became anergic similar to the original CSR-incompetent MD4 anti-HEL x soluble HEL double Tg mice, but when anergic SW_{HEL} B cells were stimulated *in vitro* with BCR-independent stimuli like LPS or anti-CD40 plus IL-4, the cells proliferated and produced IgG anti-HEL antibodies as capably

as naïve anti-HEL B cells from SW_{HEL} mice (96). The authors concluded that anergy by itself does not eliminate the ability of tolerant B cells to undergo CSR, but rather the production of IgG autoAbs must be prevented by some alternate mechanism that restricts BCR-independent stimulation through CD40, TLRs, and the IL-4 receptor. My goal was to determine how the capacity to undergo isotype switch impacts the function of anti-insulin B cells, and to identify the BCR-dependent or –independent stimuli that may reverse tolerance in such B cells.

Results

A site-directed BCR transgenic mouse model generates class switch-competent anti-insulin B lymphocytes

To examine peripheral tolerance for anti-insulin B cells competent to undergo isotype switch, B6 mice that harbor anti-insulin VDJ_H-125 site-directed to the Ig H chain locus were developed as described in Materials and Methods. Fig. II-1A summarizes the strategy for generating the targeting construct used to develop site-directed V_H125^{SD} B6 mice. Southern blot, PCR, and flow cytometry confirmed successful Ig H chain locus targeting, as $B220^+$ splenic B cells from V_H125^{SD} B6 mice co-express IgM^a and IgD^a while those from conventional μ-only V_H125Tg B6 mice express only IgM^a as expected (Fig. II-1B).

Flow cytometry with biotinylated insulin was used to investigate the contribution of different anti-insulin transgenes to insulin-binding B cells (Fig. II-1C). As shown on the left, mice that possess only an anti-insulin L chain (Vκ125Tg) show low numbers of insulin-binding B cells in the spleen (0.12 ± 0.01%, n = 3), but these weakly binding cells are not specific, as they are not inhibited with excess competitive insulin (not shown). V_H125^{SD} B6 mice (center) have B cells in which the targeted transgene pairs with endogenous L chains to generate a small

population of insulin-binding B cells (0.46 ± 0.05%, n = 9) (Fig. II-1C). Intercrosses that pair V_H125^{SD} with Vκ125Tg confers insulin-binding specificity to > 98% of the B cells (right). Unlike other site-directed mouse models, such as the SW_{HEL} model (96), V_H gene revision or editing is not prevalent for IgM^+ B cells in V_H125^{SD}, as > 95% are of the [a] allotype and retain their insulin-binding potential. HEL-binding B cells exist at a much lower frequency in the peripheral repertoire in SW_{HEL} mice due to revision of the H chain that generates non-HEL-specific B cells that compete with the HEL-specific B cells for entry and residence in mature compartments. This either does not occur in site-directed anti-insulin B cells or occurs at a significantly lower frequency that does not impair their ability to coexist with the endogenous B cells. These data demonstrate that a novel site-directed BCR transgenic model can be used to assess the fate and function of CSR-competent anti-insulin B lymphocytes within a monoclonal or polyclonal repertoire.

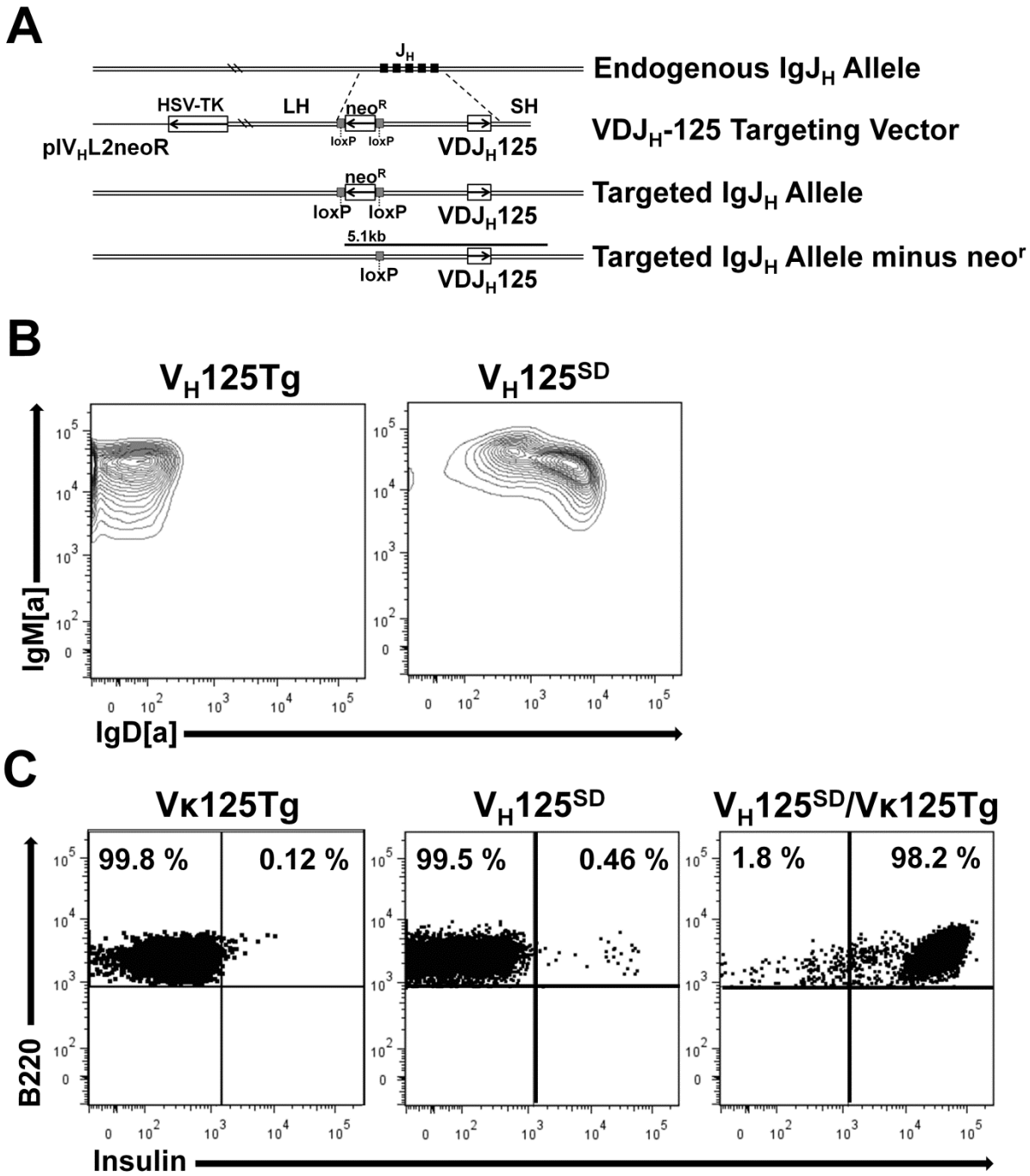

FIGURE II-1. A site-directed BCR transgenic mouse model generates class switch-competent anti-insulin B lymphocytes. **(A)** Strategy for targeting anti-insulin VDJ_H-125 to the Ig H chain locus (site-directed V_H125^{SD}). **(B)** Flow cytometry was used to assess IgM and IgD expression on B cells ($B220^+$ live lymphocytes) from spleens of V_H125^{SD} B6 mice (right) and conventional IgM-restricted, non-site-directed V_H125Tg B cells (left). **(C)** Insulin-binding B cells identified by flow cytometry in Vκ125Tg B6 mice (left), site-directed V_H125^{SD} B6 mice (middle), and in mice that harbor both V_H125^{SD} and Vκ125Tg (right).

Class switch-competent anti-insulin B cells populate the spleens in V_H125^{SD}/Vκ125Tg B6 mice

I first wished to determine whether anti-insulin B cells in V_H125^{SD}/Vκ125Tg B6 mice distribute into peripheral subsets in the spleen. One mechanism of B cell tolerance is the reduced access to important survival factors like BAFF as well as restricted entry into mature compartments (55, 97). I used flow cytometry to identify anti-insulin B cell distribution into transitional 1 (T1, $CD21^-$ $CD23^-$), follicular (FO, $CD21^{int}$ $CD23^{high}$), and marginal zone (MZ, $CD21^{high}$ $CD23^{low}$) compartments of the spleen (Fig. II-2A).

WT B6 mice demonstrated largely a FO B cell phenotype with moderate numbers of MZ B cells (73% FO, 9.6% MZ, 4.9% T1). Anti-insulin B cells in the monoclonal repertoire of V_H125^{SD}/Vκ125Tg B6 mice, however, exhibited a dramatic increase in the frequency of MZ B cells in the spleen, concomitant with a decrease in the percent of FO B cells (51% FO, 42.8% MZ, 2.7% T1). This high frequency of MZ B cells is likely due to one of two explanations. First, signaling through a BCR Tg could skew the repertoire toward a MZ phenotype, as reported for other BCR Tg models (98, 99). Alternatively, the presence of serum $IgMa^+$ anti-insulin antibodies likely causes an increase in concentration of circulating insulin in V_H125^{SD}/Vκ125Tg B6 mice, as observed in the original non-site-directed 125Tg (H + L chain) B6 mice (data not shown). Elevated levels of autoAg in these mice compared to WT mice could alter BCR signaling at the T1 stage and skew toward a MZ phenotype. The frequency of IgD^- MZ B cells in V_H125^{SD}/Vκ125Tg B6 mice is similar to that reported for 125Tg B6 mice (78), suggesting that the lack of IgD expression in non-site-directed 125Tg B6 mice is not the reason for the increase in MZ B cells.

Additionally, I assessed emergence of $B220^{low}CD5^{low}$ B1a anti-insulin B cells into the peritoneal cavity of V_H125^{SD}/Vκ125Tg B6 mice. B1a cells originate in the fetal liver and have

been implicated in autoAb production and other autoimmune responses, emphasized by the increased frequency of such B cells in humans and mice who suffer from autoimmune disease (100). The original non-site-directed 125Tg (H + L chain) and "H chain only" V_H125Tg B6 mice both had a profound lack of B1a B cells in their peritoneum, compared to WT mice (77). I used flow cytometry to assess the presence of this autoimmune-prone population of B1a B cells in site-directed, CSR-competent in V_H125^{SD}/Vκ125Tg B6 mice (Fig. II-2B). Whereas WT mice possessed a normal frequency of peritoneal B1a B cells (13.5%), anti-insulin B cells in V_H125^{SD}/Vκ125Tg mice demonstrated a reduced frequency of such cells (3.94%). B1a B cells were confirmed to be largely insulin-binding in V_H125^{SD}/Vκ125Tg mice, compared to WT B1a B cells that were not insulin-binding. These data validate earlier reports of a reduction in B1a anti-insulin B cells in 125Tg mice and suggest that acquiring the capacity to undergo isotype switch does not alter this phenotype.

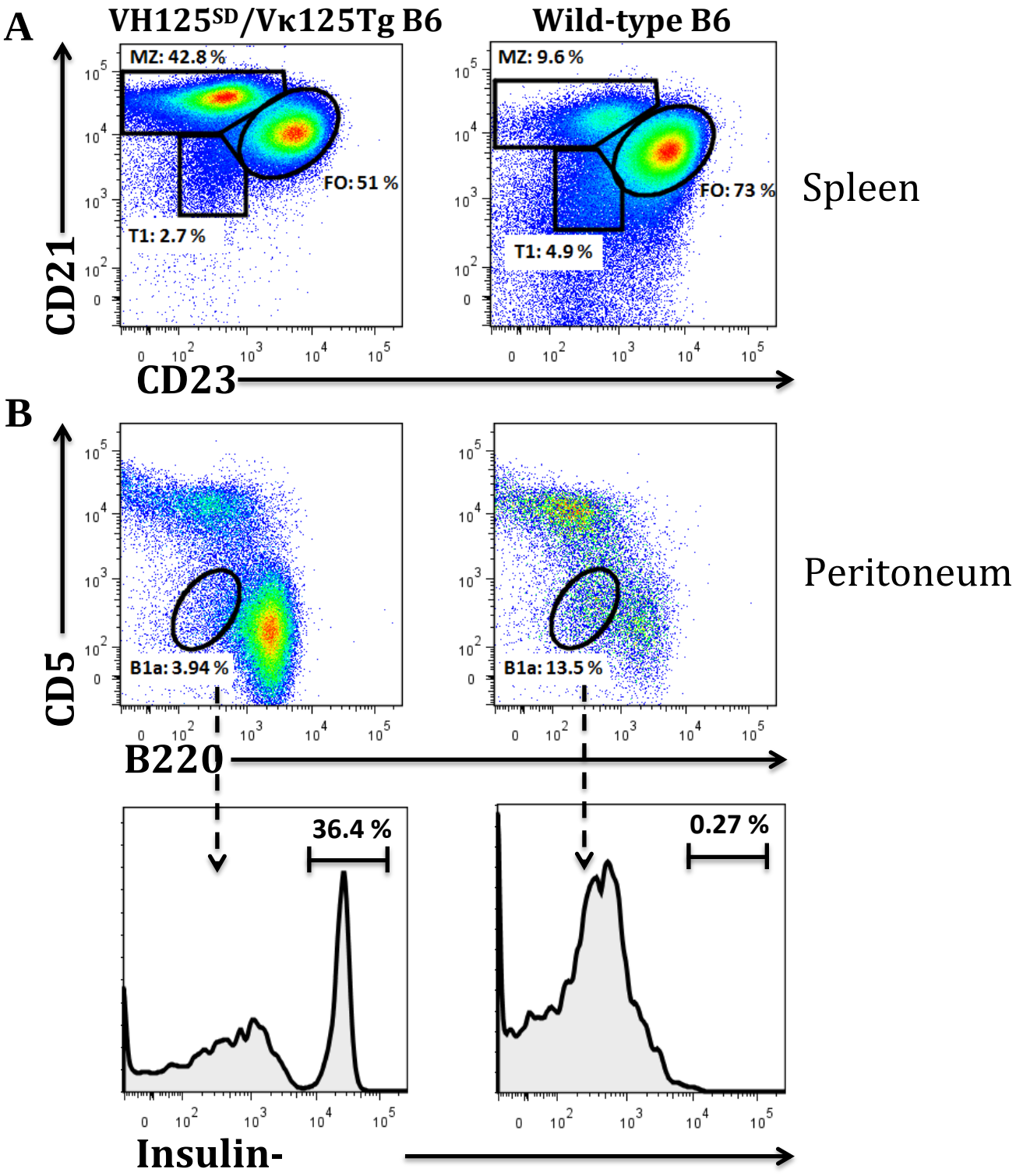

FIGURE II-2. Peripheral subset distribution of class switch-competent IgM^+ IgD^+ anti-insulin B cells. (**A**) Flow cytometry was used to identify $B220^+$ IgM^+ live lymphocytes that distributed into transitional 1 (T1), follicular (FO), and marginal zone (MZ) B cell populations in V_H125^{SD}/Vκ125Tg and WT B6 mice. (**B**) Live lymphocytes were assessed for B1a B cell formation, defined in flow cytometry as $CD5^{low}B220^{low}$, and insulin-binding potential.

Anti-insulin B cells can be identified in the spleens of WT recipients following adoptive transfer

Anti-insulin B cells in the monoclonal repertoire of V_H125^{SD}/Vκ125Tg B6 mice do not undergo developmental arrest and escape into peripheral subsets in the spleen. Given the fact one key feature of peripheral tolerance is the impaired ability to compete with non-tolerant B cells for survival factors and residence in the periphery, I wished to provide a setting for anti-insulin B cells that would allow them to compete with such B cells. Accordingly, I determined whether anti-insulin B cells could populate the spleens of non-irradiated WT B6 mice following adoptive transfer. Recipient WT mice were not irradiated to allow for maximum competition between endogenous WT B cells and donor anti-insulin B cells. One downside of this approach is that non-irradiated recipient mice already have populated peripheries that may significantly limit the ability for donor anti-insulin B cells to settle into niches. CD43- anti-insulin B cells were purified using MACS from site-directed 125^{SD} (H + L chain) B6 mice, and 20 x 10^6 cells were injected i.p. into WT B6 mice. Four days later, the presence of $IgMa^+$ anti-insulin B cells in the spleens of recipient mice was assessed by flow cytometry (Fig. II-3).

Four days after adoptive transfer, a small population of anti-insulin B cells was detected in the spleen of the recipient WT B6 mouse (0.103%). While the frequency was low and only a fraction of the number of cells injected, the presence of $IgMa^+$ anti-insulin B cells demonstrates that these tolerant B cells actually compete quite well with non-insulin-binding B cells for peripheral residence. They did so despite being injected into a mouse that already possessed a full B cell repertoire, in addition to all of the other endogenous immune and epithelial cells present in the mouse at the time of adoptive transfer. This experiment shows that anti-insulin B cells can compete for residence in the periphery of a WT mouse, revealing that the tolerant state of anti-insulin B does not restrict their entry into a competing polyclonal B cell repertoire.

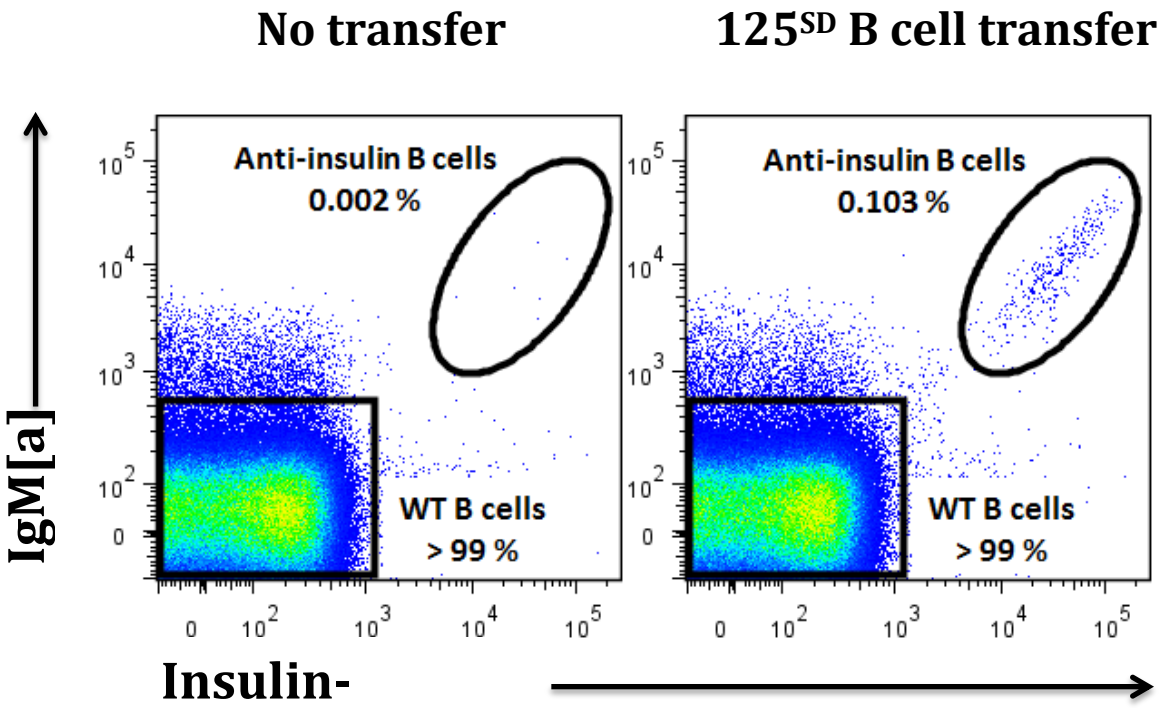

FIGURE II-3. Adoptive transfer of anti-insulin B cells into WT recipients. WT B6 mice were injected i.p. with 20 x 10^6 CD43- purified B cells from 125^{SD} (H + L chain) B6 mice. Four days later, spleens were removed from the WT recipients, and flow cytometry was used to identify the presence of $IgMa^+$ anti-insulin B cells.

Anergy in anti-insulin B cells is reversed by TLR4 but not CD40 co-stimulation in vitro

To determine whether CSR-competent anti-insulin B cells are functionally impaired, or anergic, CD43$^-$ B cells were purified from V_H125^{SD}/Vκ125Tg or wild-type (WT) B6 mice using MACS, and tritiated thymidine incorporation was used to assess B cell proliferation *in vitro* in response to anti-IgM, anti-CD40, or LPS stimulation (Fig. II-4). Anti-insulin B cells exhibit impaired proliferative responses to stimulation through BCR, CD40, and TLR4, compared to B cells from WT B6 mice (Fig. II-4A). Thus, anergy is maintained for CSR-competent IgM^{a+} IgD^{a+} anti-insulin B cells *in vitro*, similar to that reported for anti-insulin B cells in conventional μ-only 125Tg mice (H + L chain) (78).

Different co-stimulation pathways were assessed for their impact on proliferation in the context of BCR encounter with autoAg. B cells were purified from V_H125^{SD}/Vκ125Tg B6 mice or naïve anti-HEL MD4-Tg mice (53) and stimulated with anti-CD40 (Fig. II-4B) or LPS (Fig. II-4D) in the presence or absence of cognate antigen. B cells specific for hen egg lysozyme (HEL) were used as naïve control, and stimulation with HEL and anti-CD40 at low concentration (0.1 μg/mL) synergized to significantly augment proliferation (30x increase, Fig. II-4C). In contrast, stimulation of anti-insulin B cells with insulin plus anti-CD40 did not enhance their proliferation, but instead blunted the response (0.52x, Fig. II-4C). Synergy is defined here as the mathematical value representing the effect of B cell co-stimulation relative to the effect of the sum of each individual stimulus. Failure to demonstrate synergy between insulin and anti-CD40 was consistent across a wide range of antigen and antibody concentrations (data not shown). These data suggest that anergy is maintained for isotype switch-competent anti-insulin B cells co-stimulated with cognate antigen and anti-CD40, which mimics T cell help. Proliferation was readily observed in anergic anti-insulin B cells stimulated with anti-CD40 plus IL-4 (data not

shown), a combination that has been shown to drive proliferation and IgG antibody production in other models of anergy. This indicates that tolerance imposed through the CD40 pathway in anti-insulin B cells is not absolute but rather is enforced when the cell is co-stimulated with antigen via the BCR.

Using naïve anti-HEL B cells as control, co-stimulation with HEL and LPS at low concentration (0.1 µg/mL) only marginally boosted proliferation, with no evidence of synergy (1.2x, Fig. II-4E). Some mild synergy was observed at high concentration of LPS (10 µg/mL) plus HEL antigen (2.6x), suggesting that synergy is dose-specific. However, interpretation of synergy is most relevant at low stimulating concentrations, as this is more representative of a potential microbial or antigenic interaction *in vivo*. In contrast to anti-HEL B cells, anti-insulin B cells co-stimulated with insulin and LPS at low concentration synergized to enhance B cell proliferation (10x, Fig. II-4E). These data demonstrate that *in vitro* responses of anti-insulin B cells are altered by prior exposure of the monoclonal repertoire to antigen *in vivo*. Anti-insulin B cells are anergic, as they fail to proliferate to insulin alone or anti-CD40 with or without antigen. However, this anergy is reversed by simultaneous engagement of BCR and TLR4 *in vitro*.

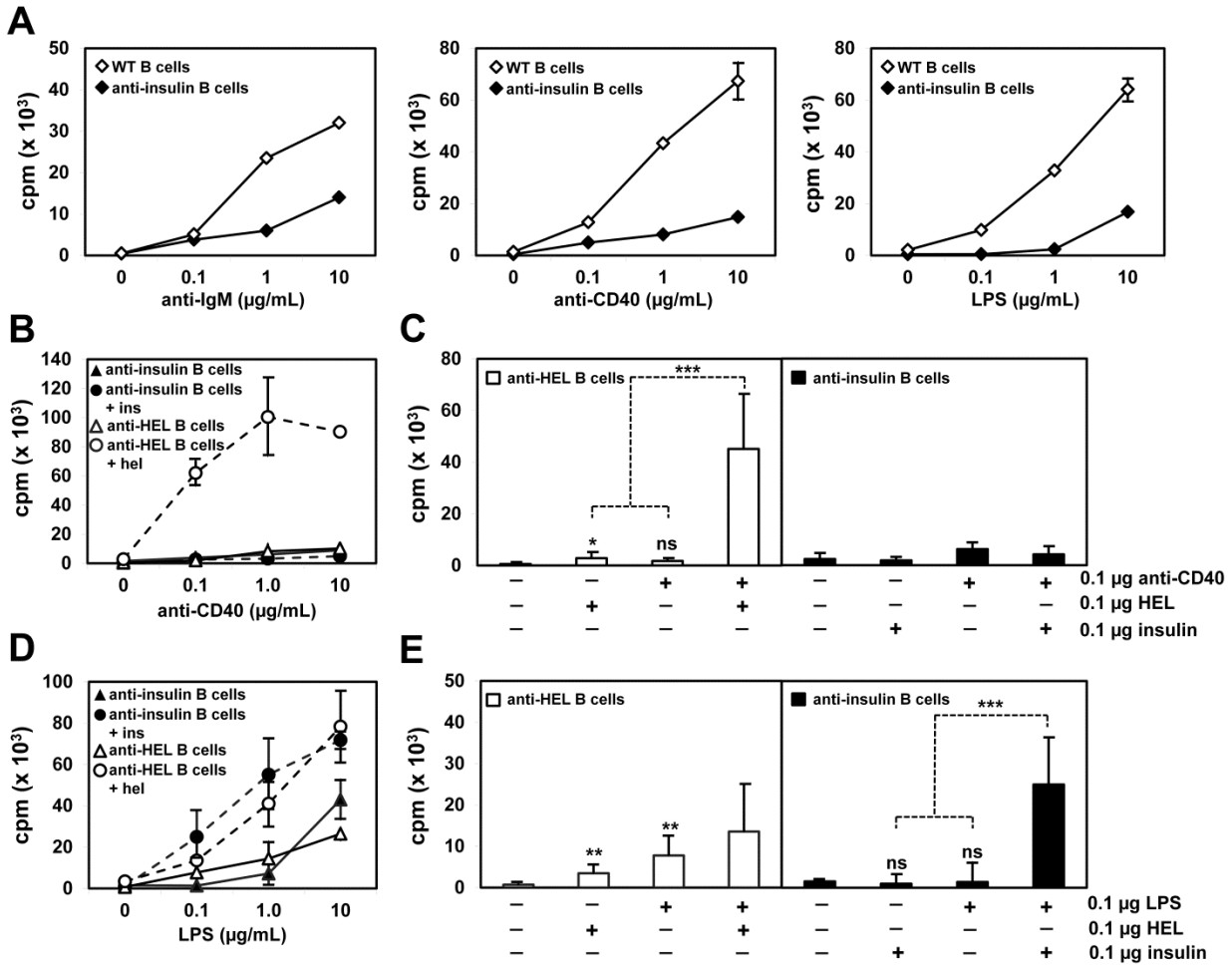

FIGURE II-4. Anergy in anti-insulin B cells is reversed by TLR4 but not CD40 co-stimulation *in vitro*. B cells were CD43$^-$ MACS purified from either V_H125^{SD}/Vκ125Tg, or control MD4 anti-HEL Tg or wild-type (WT) B6 mice. **(A)** B cells from WT and V_H125^{SD}/Vκ125Tg mice were cultured for 72 h to a dose response of anti-IgM, anti-CD40, or LPS. B cells from V_H125^{SD}/Vκ125Tg and MD4 anti-HEL Tg mice were cultured to a dose response of anti-CD40 **(B)** or LPS **(D)** with or without 0.1 µg/mL insulin or HEL Ag. The proliferative response at the combined suboptimal dose of 0.1 µg/mL is shown for Ag plus either an anti-CD40 **(C)** or LPS **(E)** stimulus. B cells received a 1 µCi pulse of tritiated thymidine after 48 h in culture before harvest at 72 h. For anti-CD40 studies, n = 6 for both V_H125^{SD}/Vκ125Tg and MD4 anti-HEL Tg mice. For LPS studies, n = 9 for V_H125^{SD}/Vκ125Tg and n = 8 for MD4 anti-HEL Tg mice. Data represent at least three independent experiments. * $p < 0.05$, ** $p < 0.01$, *** $p < 0.001$, two-tailed t test. ns, not significant.

Not all TLR agonists synergize with insulin to reverse anergy in anti-insulin B cells

The ability for LPS to synergize with insulin to reverse anergy and drive proliferation for anti-insulin B cells *in vitro* is profound. I repeated these experiments using other TLR agonists to determine whether some other innate stimulus besides LPS/TLR4 could synergize with insulin to drive proliferation of anti-insulin B cells. This would also clarify whether there is some transducing molecule/protein in the TLR4 signaling pathway that is uniquely responsible for synergizing with the BCR to deliver the signal to reverse anergy in anti-insulin B cells. Alternatively, there may be multiple TLR pathways that, when activated by the appropriate ligand, can combine with insulin/BCR signaling to reverse anergy in these autoreactive cells.

Anti-insulin B cells or naïve control anti-HEL B cells were stimulated for 72 h with media, antigen alone (insulin or HEL), TLR agonist alone, or co-stimulated with TLR agonist plus antigen. Cells were pulsed with tritiated thymidine at 48 h, and incorporation of tritiated thymidine was measured at 72 h as readout for proliferation. The TLR agonists used were as follows: triacylated lipopeptide Pam3CSK4 (TLR1/2), diacylated lipopeptide FSL-1 (TLR6/2), poly(I:C) dsRNA (TLR3), or unmethylated CpG DNA (TLR9). B cells do not express TLR5 (101). Synergy was observed when anti-insulin B cells were stimulated with LPS plus insulin at the suboptimal concentration of 0.1 μg/mL (Fig. II-4E), so synergy values were determined for each TLR agonist's co-stimulation effect (TLR agonist plus BCR antigen) for both anti-insulin and anti-HEL B cells at the suboptimal dose (Table II-1).

Synergy was very mild or not observed in naïve anti-HEL B cells when co-stimulated with HEL plus TLR1/2 (1.2x), TLR6/2 (0.8x), or TLR3 (1.8x) agonists. In other words, the effect of co-stimulation was additive. Co-stimulation of anti-HEL B cells with HEL plus TLR9 agonist, however, yielded good synergy (6.8x), indicating that TLR9 signaling is important for

naïve B cells and may augment their activation and proliferation in the presence of cognate antigen. In contrast, anti-insulin B cells failed to demonstrate synergy when stimulated with insulin plus any of the TLR agonists used in the experiment, except LPS. This does not indicate the cells failed to respond to the specific TLR agonist, but rather that the addition of insulin reduced the ability to proliferate in all cases. Thus, TLR4 is the only TLR tested that demonstrated synergy with BCR/insulin stimulation to break tolerance in anti-insulin B cells to drive proliferation *in vitro*. Synergy was the most prolific at the lowest stimulating concentration used for both insulin and LPS (100 ng/mL), suggesting that only small amounts of innate stimulus and antigen may be required in combination to reverse anergy.

TLR	Agonist	Synergy value	
		Anti-HEL B cells	*Anti-insulin B cells*
TLR4	LPS	1.2	10
TLR1/2	Pam3CSK4 (triacylated lipopeptide)	1.2	0.3
TLR6/2	FSL-1 (diacylated lipopeptide)	0.8	0.4
TLR3	poly(I:C) dsRNA	1.8	0.9
TLR9	Unmethylated CpG DNA	6.8	0.9

$$\text{Synergy} = \frac{(\text{Antigen} + \text{Agonist})}{(\text{Antigen}) + (\text{Agonist})}$$

TABLE II-1. Not all TLR agonists synergize with insulin to drive anti-insulin B cell proliferation. Anti-insulin or anti-HEL B cells were CD43- purified using MACS from either V_H125^{SD}/Vκ125Tg or MD4 anti-HEL Tg B6 mice and stimulated for 72 h to antigen alone (insulin or HEL), TLR agonist alone, or antigen plus TLR agonist in combination. B cells received a 1 µCi pulse of tritiated thymidine after 48 h in culture before harvest at 72 h. Synergy values for anti-insulin and anti-HEL B cells are listed on the right, with synergy defined as the mathematical value representing the effect of B cell co-stimulation relative to the effect of the sum of each individual stimulus. The concentration used for calculating synergy values was 0.1 µg/mL for all stimuli.

Impaired BCR-mediated Ca^{2+} mobilization in anti-insulin B cells is not restored following TLR4 co-stimulation

Anti-insulin B cell proliferation was observed when LPS and insulin were combined at low stimulating concentration. LPS alone elicited mild responses, while insulin alone enforced anergy and even blunted proliferation (Fig. II-4). Non-tolerant BCRs flux Ca^{2+} when engaged by their antigen, so I determined whether the observed reversal of anergy in anti-insulin B cells led to a concomitant restoration of Ca^{2+} flux. Accordingly, anti-insulin and anti-HEL B cells were examined for their ability to flux Ca^{2+} in response to LPS alone, cognate antigen, or the two combined in a standard 340/380 nm bound/free excitation assay. Briefly, when intracellular Ca^{2+} is released from stores in a PLCγ2- and inositol trisphosphate-dependent manner, such as through BCR signaling, the free Ca^{2+} in the cytosol may diffuse across the plasma membrane and promote influx of extracellular Ca^{2+} that may be pumped back into the endoplasmic reticulum with the help of an ATPase. Anti-insulin or anti-HEL B cells were cultured in media supplemented with Ca^{2+} to ensure availability of extracellular Ca^{2+} at the time of stimulation. One hour prior to stimulation, the cells were loaded with a Fura-2 ratiometric dye that internalizes and binds free intracellular Ca^{2+}. Excitation of Fura-2 at 340 nm (bound) and 380 nm (free) is expressed as a ratio and directly correlates with the amount of newly available intracellular Ca^{2+} that is internalized as a result of initial Ca^{2+} release from the endoplasmic reticulum. Thus, whether loss of tolerance in anti-insulin B cells driven by simultaneous insulin and LPS stimulation extends to restoration of impaired BCR-dependent Ca^{2+} mobilization was determined.

It was previously observed in a different model that anti-insulin B cells exhibit impaired Ca^{2+} mobilization when stimulated with insulin (102). This phenotype was shown to be the

consequence of tolerance, as bone marrow-derived, naïve anti-insulin B cells demonstrated normal Ca^{2+} flux in response to insulin. This observation was validated using anti-insulin B cells in the new site-directed V_H125^{SD}/Vκ125Tg B6 model, with naïve anti-HEL B cells as control. Ca^{2+} flux was observed in anti-HEL B cells to a dose response of HEL antigen, as expected for a naïve B cell seeing cognate antigen for the first time (Fig. II-5, n = 3). In contrast, Ca^{2+} flux did not occur in anti-insulin B cells in response to insulin (n = 3), a finding that is consistent with prior studies and indicates anergy is an ongoing, active tolerance program in the cell.

Ionomycin diffuses across plasma membranes in B cells independently of the BCR and is a potent inducer of intracellular Ca^{2+} release (103). It served as positive control for the assay. Stimulation with ionomycin led to robust Ca^{2+} release in both control, anti-HEL B cells and in anergic anti-insulin B cells (Fig. II-5), demonstrating that the impaired Ca^{2+} release normally observed in anti-insulin B cells is not due to some inherent flaw in the ability of tolerant B cells to either store or release intracellular Ca^{2+}.

TLR4 signaling results in either MyD88-dependent NF-κB activation that originates from the plasma membrane, or TRIF-mediated interferon regulatory factor 3 (IRF) activation that depends on TLR4 translocation to endosomes. Studies have demonstrated that LPS-induced Ca^{2+} mobilization occurs in a PLCγ2-dependent manner in some myeloid cell populations, including macrophages and dendritic cells (104). Mice deficient in PLCγ2 exhibit reduced IRF3 but enhanced NF-κB activation in macrophages in response to LPS stimulation, demonstrating that only IRF3 depends on intracellular Ca^{2+} release (105). LPS alone did not elicit Ca^{2+} mobilization in anti-HEL (data not shown) or anti-insulin B cells (Fig. II-6, top left), suggesting that TLR4 stimulation in B cells does not require TRIF-dependent intracellular Ca^{2+} release.

Neither LPS nor insulin alone induced Ca^{2+} mobilization in anti-insulin B cells, yet the two stimuli in combination drove robust proliferation. This suggests that LPS combines with insulin to promote proliferation in a Ca^{2+}-independent manner, or that some unique signaling event arises when both BCR and TLR4 are engaged on anti-insulin B cells that breaks tolerance and permits BCR-mediated Ca^{2+} mobilization and subsequent proliferation. In contrast to my expectations, LPS plus insulin did not elicit any measurable Ca^{2+} flux in anti-insulin B cells (Fig. II-6, top right). An additional reagent, highlighted in Chapter III, was also used to test the Ca^{2+} independence of BCR/TLR4 co-stimulation of anti-insulin B cells. Insulin was conjugated to a type 1 T cell-independent antigen, the *Brucella abortus* ring test antigen (BRT), which contains non-canonical LPS and thus, TLR4-stimulation. Neither stimulation with BRT alone nor the insulin-BRT conjugate restored Ca^{2+} flux in anti-insulin B cells (Fig. II-6, bottom panels). Thus, the reversal of anergy in anti-insulin B cells as a consequence of BCR/TLR4 co-stimulation is imposed in such a way that does not induce Ca^{2+} mobilization via either TRIF-dependent IRF3 activation or BCR-mediated inositol trisphosphate production.

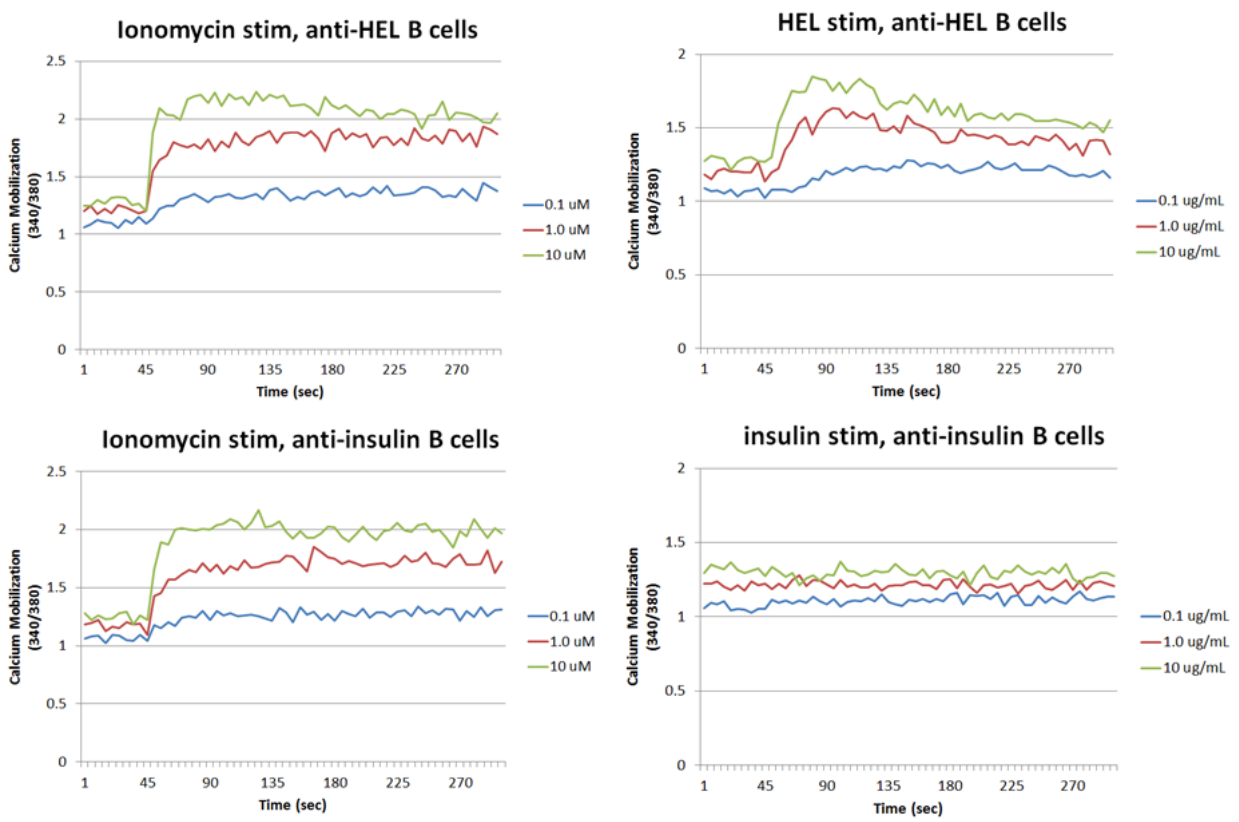

FIGURE II-5. Stimulation with insulin does not induce detectable Ca^{2+} mobilization in anti-insulin B cells. Anti-insulin or anti-HEL B cells were CD43- MACS purified from either V_H125^{SD}/Vκ125Tg or MD4 anti-HEL Tg B6 mice and stimulated with either antigen (insulin or HEL) or ionomycin as a positive control for intracellular Ca^{2+} release. Before stimulation, cells were loaded with a fluorescent dye that binds intracellular Ca^{2+}. Cells were stimulated in Ca^{2+}-rich media for five minutes, and Ca^{2+} mobilization was measured as the bound/free excitation ratio at 340 nm and 380 nm of the fluorescent dye (detailed in Materials and Methods).

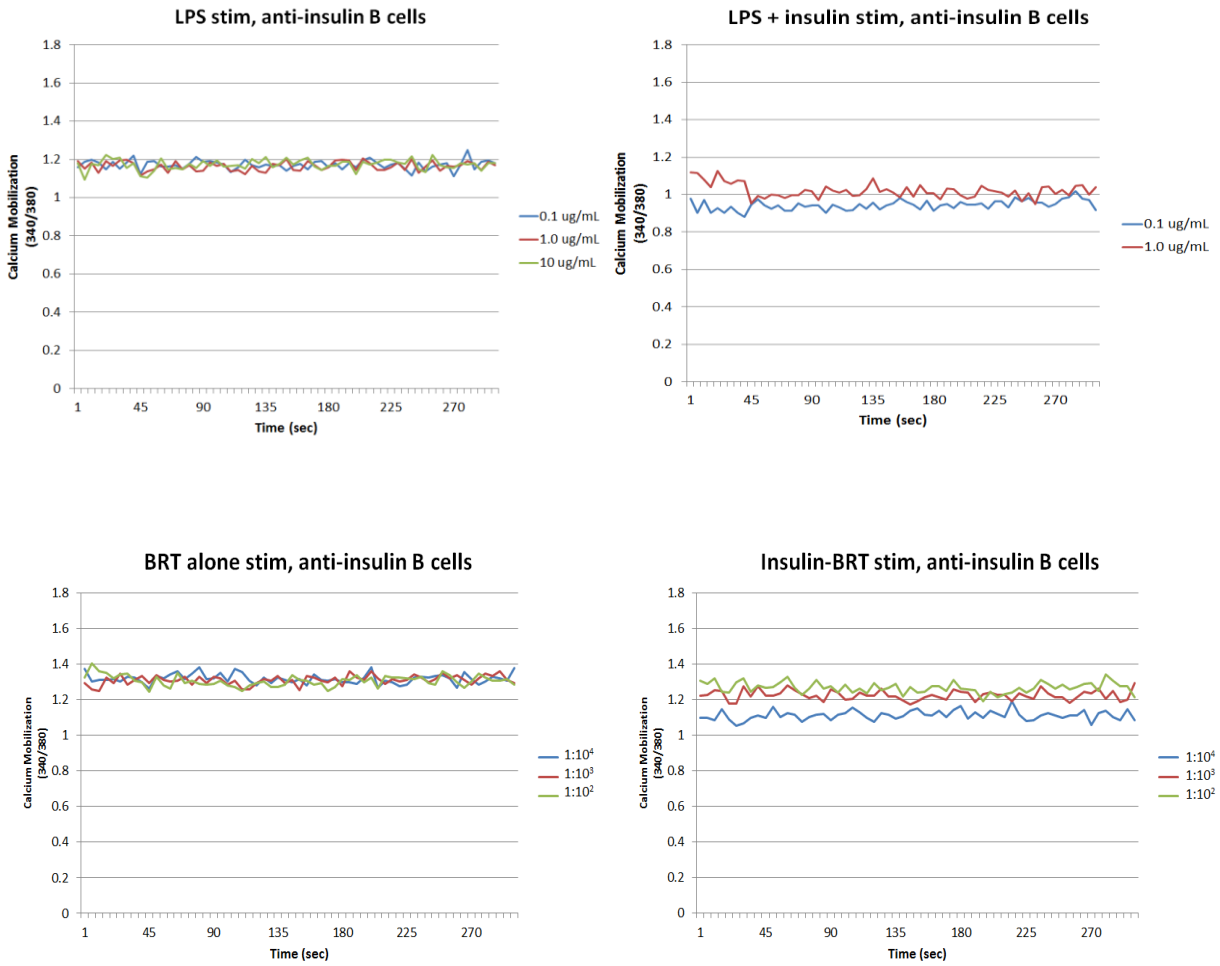

FIGURE II-6. Impaired BCR-mediated Ca^{2+} mobilization in anti-insulin B cells is not restored following TLR4 co-stimulation. Anti-insulin were CD43- MACS purified from V_H125^{SD}/Vκ125Tg B6 mice and stimulated with LPS or LPS plus insulin (top two panels) or with BRT alone or insulin-BRT conjugate (bottom two panels) to determine whether BCR/TLR4 co-stimulation promoted a restoration in Ca^{2+} mobilization. Before stimulation, cells were loaded with a fluorescent dye that binds intracellular Ca^{2+}. Cells were stimulated in Ca^{2+}-rich media for five minutes, and Ca^{2+} mobilization was measured as the bound/free excitation ratio at 340 nm and 380 nm of the fluorescent dye (detailed in Materials and Methods).

Discussion

I first wished to understand the function of anti-insulin B cells in the new BCR Tg mouse model. V_H125^{SD}/Vκ125Tg B6 mice possess a nearly monoclonal population of anti-insulin B cells whose anti-insulin H chain was site-directed to the endogenous locus. Thus, the new model represents the most functionally relevant BCR Tg model to date in studies of self-tolerance to insulin. Stimulation through the BCR, CD40, or LPS alone resulted in blunted proliferation of anti-insulin B cells compared to WT B cells (Fig. II-4A). This confirms that CSR-competent anti-insulin B cells are anergic, similar to CSR-incompetent IgM-restricted anti-insulin B cells in earlier models. Naïve anti-HEL B cells robustly responded to combined stimulation of HEL plus anti-CD40, as expected for naïve B cells receiving "T cell help" and seeing their antigen for the first time. Anti-insulin B cells stimulated with anti-CD40 plus insulin, however, remained profoundly anergic (Fig. II-4C), suggesting that CD40 signaling in these cells does not reverse but rather enforces tolerance. This observation was later validated through TD immunization experiments (Chapter III).

Surprisingly, LPS plus insulin synergized to promote robust proliferation in anti-insulin B cells (Fig. II-4E). LPS is a potent BCR-independent mitogen and polyclonal activator, yet at low stimulating concentration (0.1 μg/mL), it only reversed anergy in tolerant anti-insulin B cells when combined with insulin. This finding is very peculiar, as stimulation with insulin alone *in vitro* enforces anergy in these cells. Somehow, simultaneous engagement of BCR and TLR4 mediates tolerance reversal in anti-insulin B cells. This likely results from some unique signaling event that is present only when both receptors are engaged at the same time. While signaling experiments were not a major part of my studies, the logical next step/future direction would be to identify the phospho-proteins in the BCR signaling cascade that are activated in

response to insulin alone, and insulin plus LPS. This should point to the transducing molecule(s) responsible for interpreting the anti-insulin BCR signal as a positive signal rather than a tolerance-enforcing signal in these normally quiescent B cells. A possible signaling mechanism is discussed in further detail in Chapter IV, and a proposed model is illustrated in Fig. IV-1.

The capacity of various TLR agonists, like ssRNA and CpG DNA, to synergize with insulin *in vitro* to reverse anergy in anti-insulin B cells was examined, and LPS was the only TLR agonist that enhanced proliferation (Table II-1). This implicates TLR4 in the reversal of anergy in anti-insulin B cells. The fact that this phenotype occurred at very low stimulating concentrations suggests that signaling thresholds for autoreactive B cells are quite low, and that loss of anergy may arise more quickly and easily than previously thought.

The importance of BCR/TLR4 synergy in reversing anergy may not be unique only for anti-insulin B cells. Crosstalk between BCR and TLR4 has been shown to unlock alternate signaling pathways for ERK phosphorylation in B cells independent of the conventional BCR-mediated signaling mediators (66). This event could be critical in reversing tolerance in anti-insulin B cells. While I did not observe synergy between BCR and any other TLRs, there is data to suggest other TLRs are important for tolerance to different autoAgs. Notably, TLR9 has been implicated in reversing tolerance in anti-DNA B cells through the activation of both the BCR and TLR9 by DNA autoAg. Each stimulus by itself might be sub-threshold, yet co-stimulation of both receptors breaks tolerance. This highlights the importance of TLR/BCR synergy in anti-insulin B cells but also the biological relevance of synergy in autoreactive B cells as a whole.

Anti-insulin B cells in the monoclonal repertoire of V_H125^{SD}/Vκ125Tg B6 mice are anergic, yet they do not fail to compete for residence in the periphery and readily occupy the major splenic compartments. Anti-HEL B cells from site-directed SW_{HEL} x soluble HEL double

Tg mice are also anergic, but they compete poorly for residence in the periphery with non-HEL-binding B cells (96). This is not due to an inherent inability to undergo maturation but rather is the consequence of V_H gene replacement that occurs in these mice and thus generates an appreciable frequency of non-anergic, non-HEL-binding B cells that out-compete the tolerant anti-HEL B cells for peripheral residence. This phenomenon either does not occur in V_H125^{SD}/Vκ125Tg B6 mice or occurs at a very low frequency, as greater than 95% of the B cells in these mice are $IgMa^+$. Even if low levels of H chain replacement did arise in these mice, the frequency of non-insulin-binding B cells is not enough to restrict access of anti-insulin B cells to peripheral niches in the spleen.

Normally, anergy is enforced in anti-insulin B cells stimulated with insulin alone, yet the addition of LPS breaks tolerance (Fig. II-4E), a finding that was also observed in the original CSR-incompetent 125Tg B6 mice (unpublished data). Surprisingly, this reversal of anergy administered through BCR/TLR4 co-stimulation does not restore BCR-mediated Ca^{2+} mobilization. This was unexpected considering the fact that non-tolerant B cells should be able to mobilize Ca^{2+} in response to antigen stimulation through the BCR. However, there are instances when B cells can proliferate in the absence of Ca^{2+} mobilization, such as through anti-CD40 plus IL-4 stimulation that is known to drive proliferation of tolerant anti-insulin B cells as efficiently as normal WT B cells (78) and, more generally, protect B cells against Fas-mediated apoptosis (106). The primary outcome of Ca^{2+} mobilization in B cells is the activation of the phosphatase, calcineurin, which activates nuclear factor of activated T cells (NFAT), also expressed in B cells, through a dephosphorylation event and promotes its translocation to the nucleus for gene transcription. NFAT complexes with AP-1 and drives cellular proliferation. NF-κB transcription also drives proliferation independently of Ca^{2+} flux, indicating that reversal

of anergy in anti-insulin B cells may be accomplished via NF-κB without restoring the cell's ability to mobilize Ca^{2+}. In addition, different NFATs have different functions, illustrated by the restoration of proliferation in anti-insulin B cells in NFAT1-/- (NFATc2) mice (107). BCR/TLR co-stimulation may alter anergy in anti-insulin B cells imposed by the NFAT1 pathway independent of Ca^{2+} mobilization.

The monoclonal B cell repertoire in V_H125^{SD}/Vκ125Tg mice is useful for understanding the function of CSR-competent anti-insulin B cells, yet it does not represent a physiologically relevant population of such cells. Thus, a different model ("H chain only" V_H125^{SD}) will be employed in the next chapter to assess how tolerance applies to a more relevant frequency of autoreactive insulin-binding B cells, and how these cells participate in both TD and TI immune responses. Anti-insulin B cells in V_H125^{SD} B6 mice are only generated when the anti-insulin H chain pairs with an endogenous L chain that also possesses specificity for insulin. Thus, important biological processes that occur during an immune response, like BCR selection in GCs, can be addressed with the H chain only model. Production of IgG anti-insulin antibodies during both TD and TI immune responses will also be studied.

CHAPTER III

REVERSING TOLERANCE IN ISOTYPE SWITCH-COMPETENT ANTI-INSULIN B LYMPHOCYTES

Introduction

B lymphocytes that escape central tolerance and mature in the periphery are a liability for developing autoimmunity. IgG insulin autoAbs that predict type 1 diabetes and complicate insulin therapies indicate that mechanisms for tolerance to insulin are flawed. Prior anti-insulin BCR Tg mouse models were conventional μ-only transgenic, IgM-restricted (V_H125Tg), and could not undergo CSR (77). While these models provided great information regarding anti-insulin B cell tolerance, the studies ultimately were limited by the fact that the B cell population studied was not truly physiologically-relevant.

To examine peripheral tolerance in anti-insulin B cells, we generated C57BL/6 mice that harbor anti-insulin VDJ_H-125 site-directed to the native Ig H chain locus (V_H125^{SD}). The importance of cognate T cells for anergic B cells through CD40 signaling paired with the role T cells play in supporting IgG antibody responses led me to originally hypothesize that anti-insulin B cells from V_H125^{SD} B6 mice would be able to mount an IgG anti-insulin antibody response following TD immunization with heterologous bovine insulin. This insulin was chosen for TD immunization because the I-A^b MHC-II in B6 mice is genetically a strong responder to bovine but not to other species of insulin. Therefore, bovine insulin should induce a strong T cell response. In contrast to my expectations, CSR-competent anti-insulin B cells failed to produce IgG anti-insulin antibodies following TD immunization of V_H125^{SD} mice. This finding was

supported by *in vitro* studies using anti-insulin B cells from V_H125^{SD}/Vκ125Tg B6 mice stimulated with anti-CD40 plus insulin (Fig. II-4C).

The observation that LPS plus insulin reversed anergy and drove proliferation of anti-insulin B cells *in vitro* prompted an examination of this BCR/TLR co-stimulation effect *in vivo*. Immunization of V_H125^{SD} B6 mice with human insulin conjugated to type 1 T cell-independent (TI) *Brucella abortus* ring test antigen (BRT) elicited IgM and IgG2a anti-insulin antibodies by day 4, and BRT alone failed to yield a response. Human insulin was chosen for this immunization to avoid introduction of T cell epitopes via $I\text{-}A^b$. BRT contains a form of LPS that is TLR4-stimulating (108, 109), thus, the observation that LPS plus insulin but not LPS alone can promote anti-insulin B cell proliferation *in vitro* is supported by this immunization model that utilizes an antigen that is historically recognized to be TI (95, 110).

The spontaneous generation of IgG insulin autoAbs in humans and NOD mice points to a role for the germinal center (GC) in supporting loss of anti-insulin B cell tolerance. GC induction is largely accepted to be a TD phenomenon; however, there is evidence to suggest that GCs can form in the absence of cognate T cell help (111, 112). It was determined whether anti-insulin B cells participate in GC reactions following both immunization strategies, including evidence for somatic hypermutation. The results demonstrate that class switch-competent anti-insulin B cells ultimately remain functionally silent in TD immune responses, yet these B cells are vulnerable to reversal of anergy following combined BCR/TLR engagement that drives antigen-specific GC responses and IgM and IgG anti-insulin antibody production.

Results

Anti-insulin B cells undergo peripheral maturation in V_H125^{SD} B6 mice

It is important to understand how the features of tolerance observed in a monoclonal population of anti-insulin B cells apply to a polyclonal repertoire that contains relatively few anti-insulin B cells (V_H125^{SD}). Factors that govern anergy for autoreactive B lymphocytes in a polyclonal repertoire include competition for survival and entry into mature compartmental niches (49, 55, 78, 113). To assess whether CSR-competent anti-insulin B cells in the polyclonal repertoire of V_H125^{SD} B6 mice enter mature subsets, flow cytometry was used to identify B cells ($B220^+$ IgM^{a+} live lymphocytes) that distributed into transitional 1 (T1, $CD21^-$ $CD23^-$), follicular (FO, $CD21^{int}$ $CD23^{high}$), and marginal zone (MZ, $CD21^{high}$ $CD23^{low}$) compartments of the spleen (Fig. III-1). In contrast to WT B6 mice, a small population of anti-insulin B cells is observed in V_H125^{SD} B6 mice (0.42 ± 0.05%, n = 9), and their specificity is confirmed by inhibition with unlabeled competitive insulin (Fig. III-1A, left panels). Rare insulin-binding B cells in WT B6 mice (0.03 ± 0.01%, n = 3) are not inhibited by excess insulin (Fig. III-1A, right panels).

The ability of B cells to enter T1, FO, and MZ subsets was compared for non-insulin binding (ins^-) or insulin-binding B cells (ins^+) in V_H125^{SD} B6 mice, or for WT B cells (Fig. III-1B). As represented in Fig. III-1C, ins^+ B cells predominantly populate the FO subset in V_H125^{SD} B6 mice, whereas fewer ins^+ B cells are found in other subsets (8.1 ± 3.2% T1, 78.9 ± 5.5% FO, 2.7 ± 1.9% MZ, n = 7). The reduced representation of ins^+ B cells in the MZ contrasts ins^- B cells (12.25 ± 2.6% T1, 57.7 ± 3.5% FO, 16.5 ± 1.7% MZ) in V_H125^{SD} B6 mice and normal B cells (8.4 ± 1.7% T1, 78.3 ± 3.7% FO, 6.0 ± 0.9% MZ, n = 6) in WT B6 mice. These data suggest that anti-insulin B cells in the peripheral repertoire of V_H125^{SD} B6 mice are principally mature follicular B cells and do not undergo developmental arrest.

To determine whether anti-insulin B cells are clonally ignorant or if their BCRs have encountered endogenous rodent insulin *in vivo*, a second anti-insulin monoclonal antibody (mAb123) was used. MAb123 recognizes a different insulin epitope and binds insulin-occupied BCRs (77, 114). Flow cytometry labeling with mAb123 confirms that BCRs are occupied by endogenous insulin in V_H125^{SD} B6 mice (0.4 ± 0.1%, Fig. III-1D). These data demonstrate that CSR-competent anti-insulin B cells in V_H125^{SD} B6 mice successfully compete in a polyclonal repertoire and populate follicular compartments despite encounter with physiologic autoAg during development and early peripheral maturation.

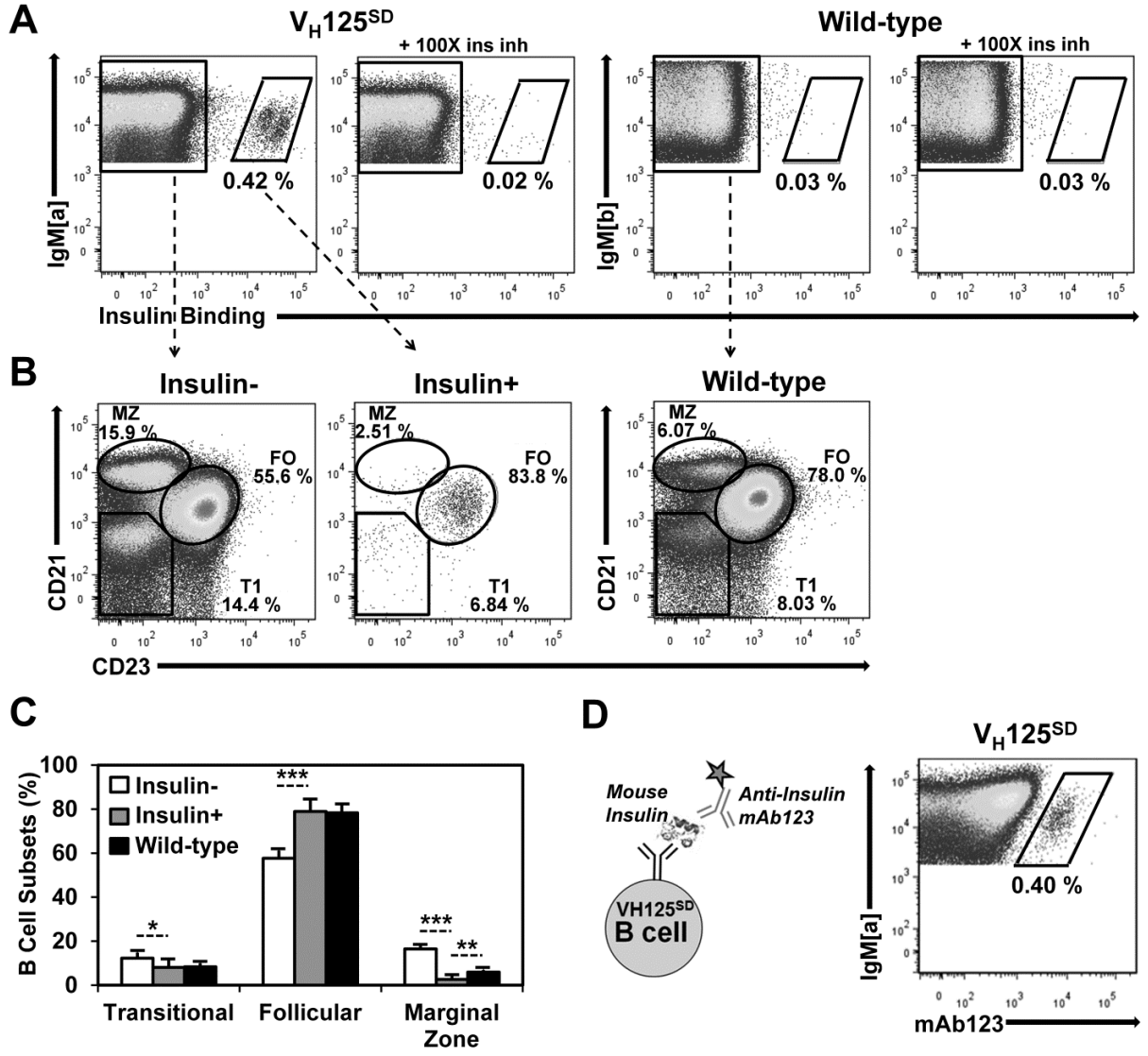

FIGURE III-1. Anti-insulin B cells in V_H125^{SD} B6 mice undergo peripheral maturation. **(A)** Splenocytes were gated on $B220^+$ IgM^+ live lymphocytes. Splenocytes were harvested from V_H125^{SD} (left) or WT (right) B6 mice and were incubated with 17 nM biotinylated human insulin with or without 100X free insulin to detect insulin-specific B cells using flow cytometry. Anti-IgM^a detects transgenic B cells; anti-IgM^b detects WT B cells **(B)** CD21 and CD23 expression were used to define Transitional 1 (T1), Follicular (FO), or Marginal Zone (MZ) B cell subset distribution of $insulin^-$ (left), $insulin^+$ (middle), or WT (right) B cells, quantified in **(C)** as subset percentage of IgM^+ B cells. **(D)** Biotinylated anti-insulin mAb123, depicted in the schematic (left), was used to detect V_H125^{SD} B cells that bind endogenous rodent insulin (right). * $p < 0.05$, ** $p < 0.01$, *** $p < 0.001$, two-tailed t test.

Anti-insulin B cells in the polyclonal repertoire of V_H125^{SD} B6 mice do not upregulate activation markers when stimulated with antigen

Stimulation of antigen-specific B cells with their cognate antigen mediates B cell activation and initiates immune responses. To determine whether anti-insulin B cells in the polyclonal repertoire of V_H125^{SD} B6 mice are anergic, their ability to upregulate two activation markers, CD86 and MHC-II, upon stimulation with insulin was assessed (Fig. III-2). CD86 (B7.2) is a costimulatory marker that is expressed on activated APCs, including B cells, and it binds CD28 on naïve cognate T cells to promote T cell activation and downstream immune function (115, 116). MHC-II is also upregulated in activated APCs, and protein antigens that have been internalized get processed into peptide fragments, loaded onto MHC-II, and shuttled to the surface for interaction with CD4 on helper T cells.

Tolerance serves to restrict B cell function, and one of the features of an anergic B cell is the impaired ability to be activated by antigen. Using naïve anti-HEL B cells as control, stimulation with HEL antigen significantly augmented CD86 expression (Fig. III-2, top panel) and mildly increased MHC-II expression (Fig. III-2, bottom panel). In contrast, anti-insulin B cells from both V_H125^{SD} and V_H125^{SD}/Vκ125Tg B6 mice exhibited marked decrease in CD86 expression, as well as MHC-II to a lesser degree. This downregulation of activation markers was antigen-specific, as non-insulin-binding B cells from V_H125^{SD} B6 mice did not respond to insulin. Data are expressed as fold-change stimulation over unstimulated wells for each group. Raw MFIs of the unstimulated wells are indicated in the figure legend. These data suggest that anergy in anti-insulin B cells extends to impaired antigen-specific activation.

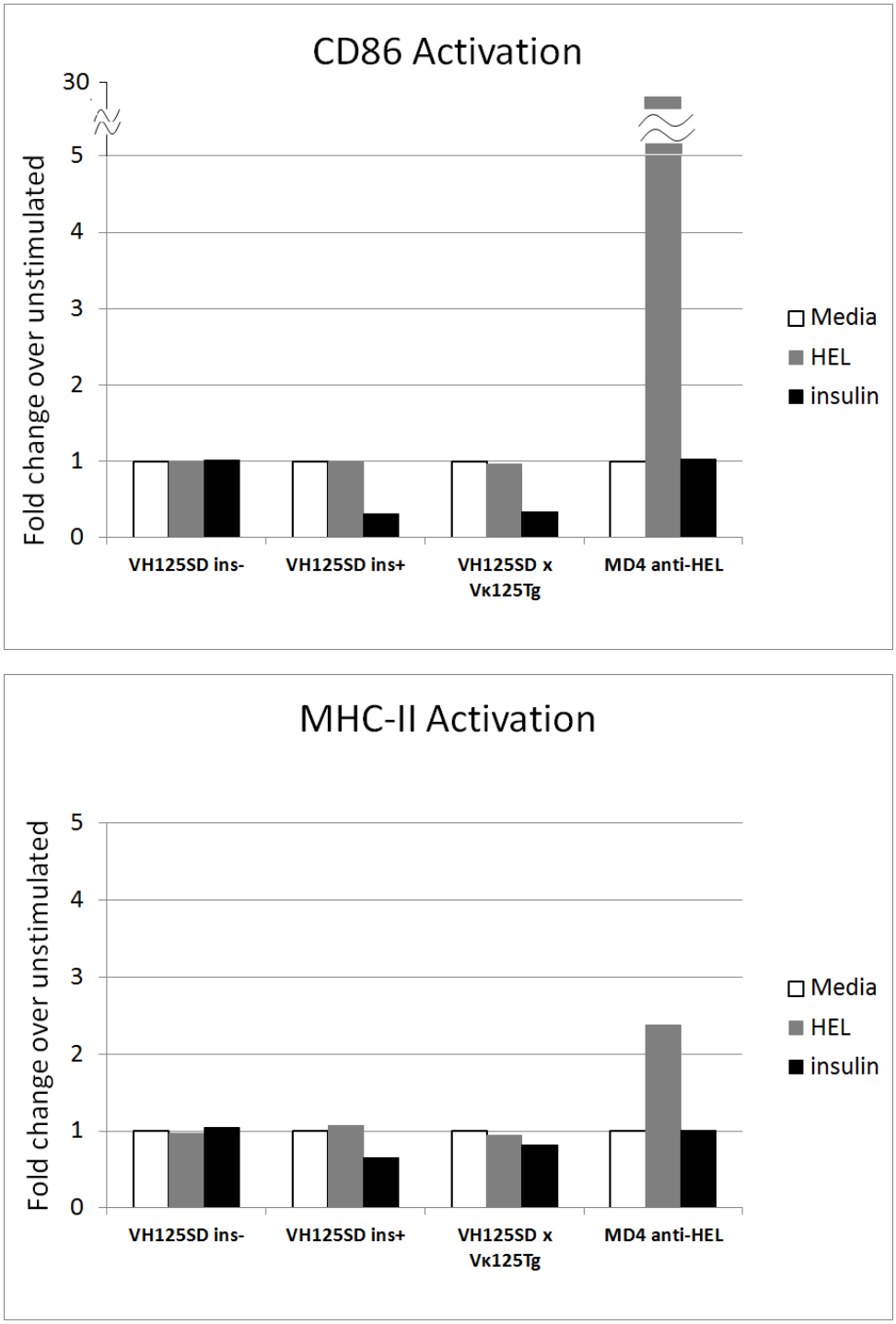

FIGURE III-2. Anti-insulin B cells fail to upregulate CD86 and MHC-II upon antigen stimulation. B cells from either V_H125^{SD} or MD4 anti-HEL B6 mice were placed in culture overnight, either unstimulated (media) or stimulated with HEL (gray) or insulin (black). CD86 (top panel) and MHC-II (bottom panel) activation markers were assessed by flow cytometry and expressed as fold change over the unstimulated wells. Raw MFIs for each unstimulated group: 190 (ins^-), 858 (ins^+), 1251 (H + L chain), 254 (MD4) for CD86; 2635 (ins^-), 6523 (ins^+), 8005 (H + L chain), 6526 (MD4).

IgM and IgG anti-insulin antibodies are produced in V_H125^{SD} B6 mice following TI but not TD immunization

Prior studies in mice harboring IgM^a-restricted anti-insulin B cells demonstrated failure to respond to TD immunization (77). To dissect the functional status of CSR-competent IgM^{a+} IgD^{a+} anti-insulin B cells in V_H125^{SD} B6 mice, antibody responses were assessed following two different immunization strategies. IgM and IgG anti-insulin antibodies in sera were measured by ELISA (Fig. III-3). For TD responses, mice were immunized with bovine insulin emulsified in complete Freund's adjuvant (CFA). Bovine insulin was chosen for TD immunization because the MHC-II of B6 mice ($I\text{-}A^b$) is genetically a strong responder to bovine but not to other insulins, notably human (90). Conventional WT B6 mice generated a strong $IgG1^b$ anti-insulin response following insulin/CFA immunization, whereas CSR-competent anti-insulin B cells in V_H125^{SD} B6 mice failed to produce $IgG1^a$ anti-insulin antibodies (Fig. III-3A). To ensure that the absence of response to insulin/CFA immunization in these mice is not attributed to lack of bovine insulin processing by anti-insulin BCRs, we used competitive inhibition in flow cytometry to confirm that bovine insulin at concentrations well below that used in immunization fully competes with human insulin for binding to anti-insulin B cells in V_H125^{SD} B6 mice (Fig. III-4). IgG1 was the predominant isotype observed following insulin/CFA immunization, a finding that agrees with previous work that examined the Ig response to insulin in B6 mice (90).

To test whether TLR signaling provided by *Mycobacteria* in CFA is necessary for the antibody response, mice were also immunized with bovine insulin emulsified in incomplete Freund's adjuvant (IFA). While the $IgG1^a$ anti-insulin response remained absent in V_H125^{SD} B6 mice, WT B6 mice generated $IgG1^b$ anti-insulin antibodies following insulin/IFA immunization (data not shown). This agrees with prior studies demonstrating that B cells deficient in both

MyD88 and TRIF were able to mount antibody responses to multiple antigens administered in a variety of adjuvants, including both CFA and IFA (117). These data validate that tolerance for anti-insulin B cells is maintained for TD immune responses to heterologous insulin, in either the presence or absence of mycobacterial adjuvant.

To assess anti-insulin B cell competence to produce antibodies in the absence of cognate T cell help, V_H125^{SD} B6 mice were immunized with human insulin conjugated to *Brucella abortus* ring test antigen (insulin-BRT), or BRT alone. Human insulin was chosen for BRT conjugates to avoid introduction of T cell epitopes. Prior studies showed that insulin-BRT behaves as a typical type 1 TI antigen, including response kinetics, expected antibody isotypes, and responses observed in both athymic and X-linked immunodeficient mice (95, 110). Following immunization with insulin-BRT, B cells from WT B6 mice and CSR-competent anti-insulin B cells from V_H125^{SD} B6 mice produced IgM^b and $IgG2c^b$ or IgM^a and $IgG2a^a$ anti-insulin antibodies, respectively (Fig. III-3B). Immunization with BRT alone, however, failed to induce any detectable IgG anti-insulin antibodies in either V_H125^{SD} or WT B6 mice (Fig. III-3B). Similarly, immunization with physically mixed BRT and insulin failed to induce any response (data not shown). Insulin-BRT immunization elicited IgM and IgG2a/c but not IgG1 antibodies, consistent with the expected isotypes associated with BRT conjugates administered to B6 mice (95, 110). These data suggest that insulin-BRT promotes loss of tolerance for CSR-competent anti-insulin B cells *in vivo* through a combination of BCR and TLR signaling that drives production of IgM and IgG anti-insulin antibodies. Experimental design and time course for both immunization strategies is shown in Fig. III-3C.

The proportion of IgM and IgG anti-insulin antibodies secreted from B cell clones at the cellular level was analyzed through the generation of monoclonal anti-insulin hybridomas four

days following insulin-BRT immunization. Splenocytes from immunized V_H125^{SD} B6 mice were fused with an NSO myeloma cell line and plated at limiting dilution to select rare clones that secreted anti-insulin antibodies. The small proportion of wells that demonstrated initial growth (less than 2%) were expanded, and the hybridoma supernatants were screened for IgM and IgG anti-insulin antibodies by ELISA (Fig. III-5). Ten IgM^+ and six IgG^+ anti-insulin hybridomas were recovered, validating the proportion of IgM:IgG expected at this early time point in the insulin-BRT immune response.

To determine the pathological consequences of the breach in tolerance observed in V_H125^{SD} B6 mice following insulin-BRT immunization, pancreata were examined for insulitis and the presence of IgG anti-insulin antibodies at day 12 of the response. A 0-4 scoring system was used to assess insulitis by H&E staining in pancreata sections from unimmunized or insulin-BRT immunized mice (outlined in Methods). NOD mouse pancreata sections served as a positive control for islet infiltration. No insulitis was detected in 60 islets examined in two unimmunized V_H125^{SD} B6 mice or in 82 islets examined in four immunized mice, such that 100% of islets examined received a score of 0. In contrast, 64 islets were scored in two 16-20 week old female, non-diabetic NOD mice, with 53% islets scoring 0, 14% islets scoring 1, 9% islets scoring 2, 8% islets scoring 3, and 16% islets scoring 4. Endogenous Ig deposition in the islets was assessed by direct immunofluorescence. Ig deposition was not detected in pancreata of either unimmunized or insulin-BRT immunized mice (data not shown). Ig was observed by indirect immunofluorescence, confirming that antibodies produced following insulin-BRT immunization are autoreactive. These data indicate that the breach in B cell tolerance driven by insulin-BRT does not elicit a detectable organ-specific autoimmune attack.

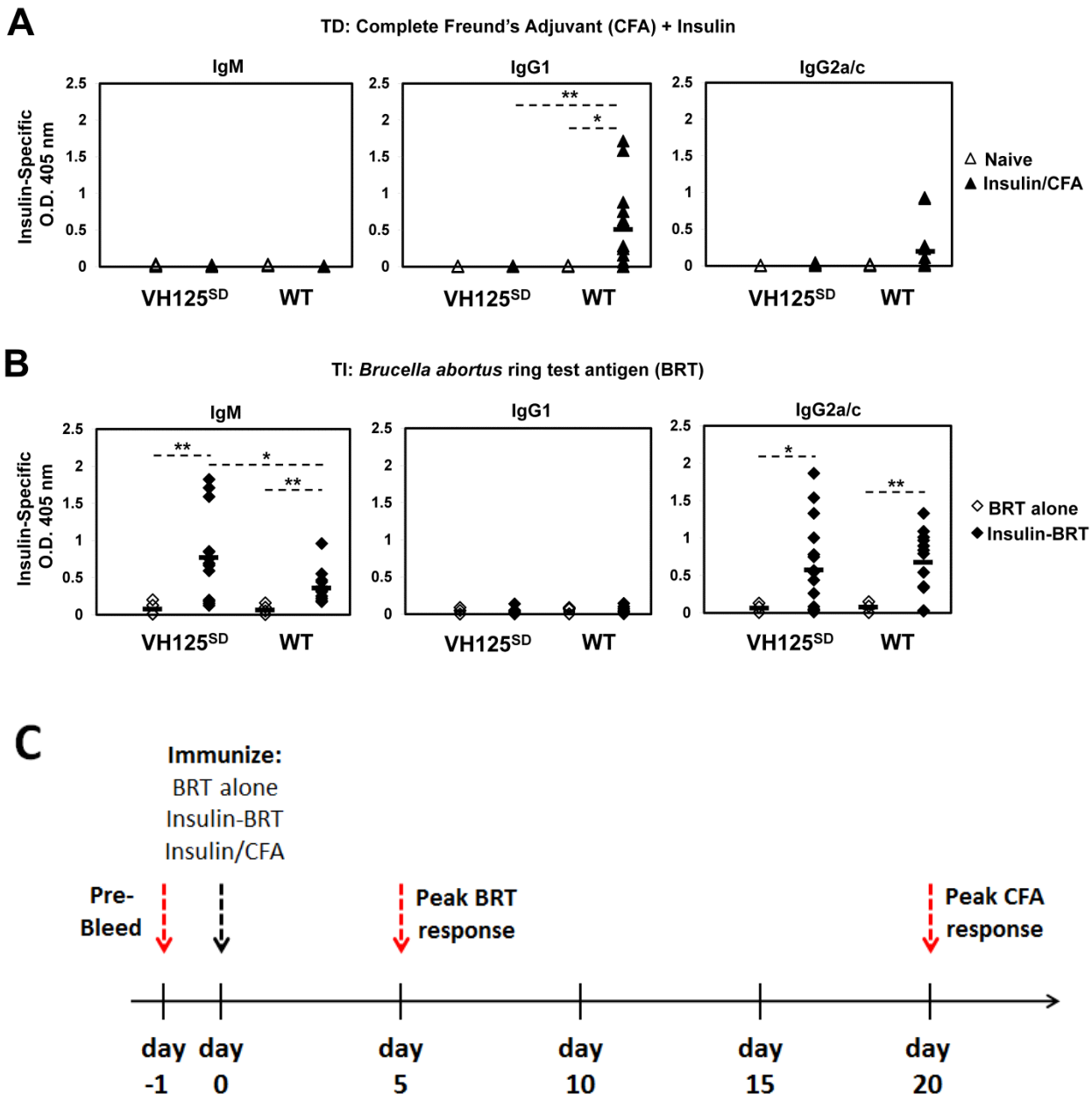

FIGURE III-3. IgM and IgG anti-insulin antibodies are produced in V_H125^{SD} B6 mice following TI but not TD immunization. V_H125^{SD} and WT B6 mice were immunized with either bovine insulin in 1X PBS emulsified in CFA (insulin/CFA) s.c. base of the tail, or *Brucella abortus* ring test Ag (BRT) alone, or human insulin conjugated to BRT (insulin-BRT) i.p. in 1X PBS. **(A)** Insulin-specific IgM^a, $IgG1^a$, and $IgG2a^a$ (V_H125^{SD}) or IgM^b, $IgG1^b$, and $IgG2c^b$ (WT) in sera were measured by ELISA before (open) and 2-3 weeks following TD immunization with insulin/CFA (closed). **(B)** Insulin-specific IgM, IgG1, and IgG2a/c in sera were measured by ELISA 5 days following immunization with BRT alone (open) or insulin-BRT (closed). **(C)** Time course for the immunizations. For insulin/CFA, n = 12 for both V_H125^{SD} and WT. For insulin-BRT, n = 12 V_H125^{SD} and n = 10 WT. For BRT alone, n = 6 mice per group. Data represent at least three independent experiments. * $p < 0.05$, ** $p < 0.01$, *** $p < 0.001$, two-tailed t test.

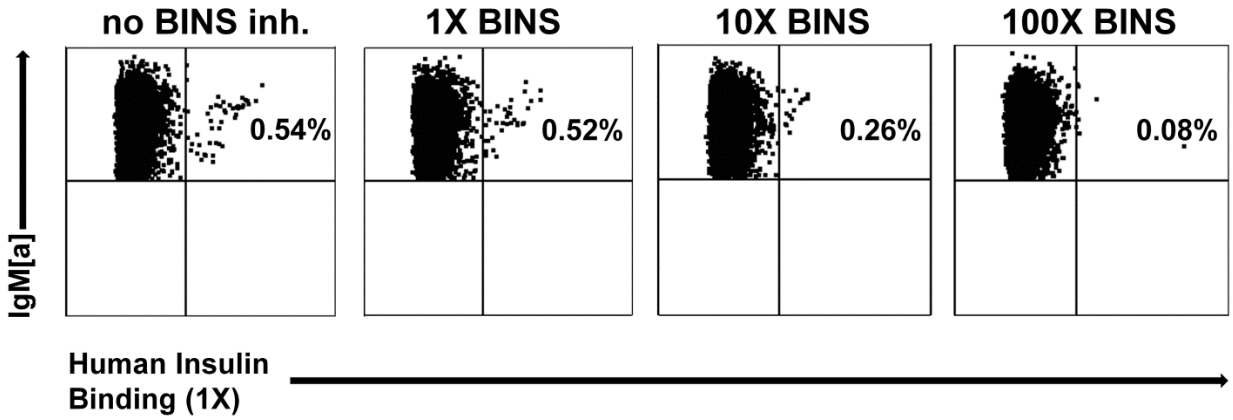

FIGURE III-4. Bovine insulin successfully competes with human insulin for binding to anti-insulin BCRs. Using flow cytometry, B cells ($B220^{+}$ IgM^{a+} live lymphocytes) from unimmunized V_H125^{SD} B6 mice were incubated with 17 nM (1X) biotinylated human insulin in the presence of increasing concentrations of bovine insulin (BINS) in a classic competitive inhibition assay. 10 µg/mL BINS, or 1.7 µM (100X), completely inhibits human insulin binding by anti-insulin BCRs.

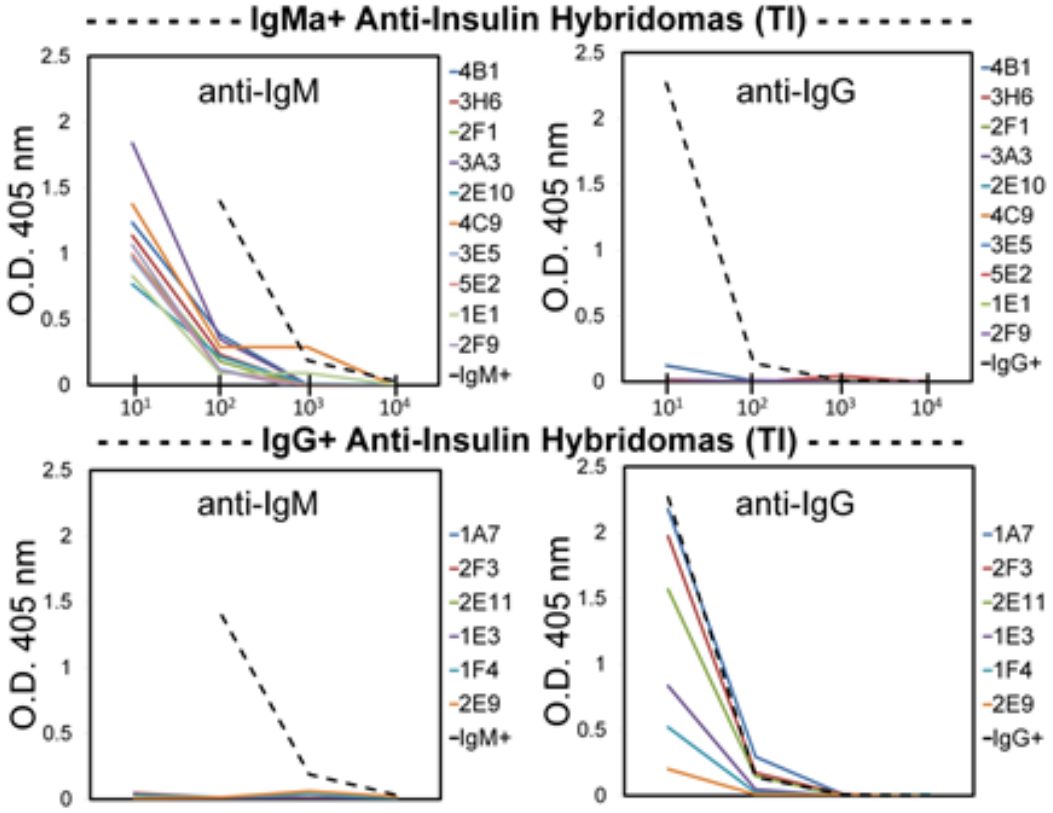

FIGURE III-5. $IgMa^+$ and IgG^+ anti-insulin hybridomas following immunization of V_H125^{SD} B6 mice with insulin-BRT. Splenocytes from V_H125^{SD} B6 mice four days following insulin-BRT immunization were fused with an NSO myeloma cell line and plated at limiting dilution to select rare clones that secreted anti-insulin antibodies. The small proportion of wells that demonstrated initial growth were expanded (less than 2%), and the hybridoma supernatants were screened for IgM and IgG anti-insulin antibodies by ELISA. See Methods for full experimental detail.

Anti-insulin B cells do not form memory IgG antibody responses following primary or secondary TD immunizations

Immunization of V_H125^{SD} B6 mice with insulin/CFA failed to elicit IgG anti-insulin antibodies (Fig. III-3A). To determine if this functional block extends to impaired formation of memory IgG antibody responses, V_H125^{SD} B6 mice were boosted with insulin/IFA 10 weeks after primary immunization with insulin/CFA. It is possible that antibody responses may be absent in the primary phase yet arise in the memory/recall phase, as frequently occurs with vaccination. One week after boost, bones were removed from the mice, and the marrow was placed in culture with or without IL-6, a cytokine that supports differentiated plasma cell production. Supernatant was collected every 24 h for four days, and then IgG anti-insulin antibodies were measured by ELISA (Fig. III-6). WT B6 mice served as positive control for the formation of long-lived IgG responses.

IgG anti-insulin antibodies were detected in bone marrow cultures from boosted WT B6 mice (Fig. III-6, right). The addition of IL-6 enhanced the response, indicating that the source of the IgG anti-insulin was indeed bone marrow plasma cells. Anti-insulin B cells from immunized and boosted V_H125^{SD} B6 mice did not exhibit long-lived IgG antibody responses, providing further evidence for a profound block in the ability for anti-insulin B cells to mount TD antibody responses. The frequency of anti-insulin B cells in WT B6 mice is below the level of detection by flow cytometry (Fig. III-1A), but the presence of IgG anti-insulin antibodies in these mice following insulin/CFA immunization and insulin/IFA boost suggests that the very low frequency of anti-insulin B cells in WT mice are not tolerant. However, tolerance imposed on anti-insulin B cells in V_H125^{SD} B6 mice completely restricts their ability to participate in TD immune responses. This is likely due to impaired CD40 signaling in anti-insulin B cells as a consequence

of the anergy program in place in these cells. Normally, stimulation through CD40 serves to activate B cells and rescue them from Fas-mediated cell death. However, the ability to respond to CD40 stimulation may be altered in tolerant anti-insulin B cells, an observation validated by the *in vitro* proliferative response to anti-CD40 plus insulin stimulation (Fig. II-4C).

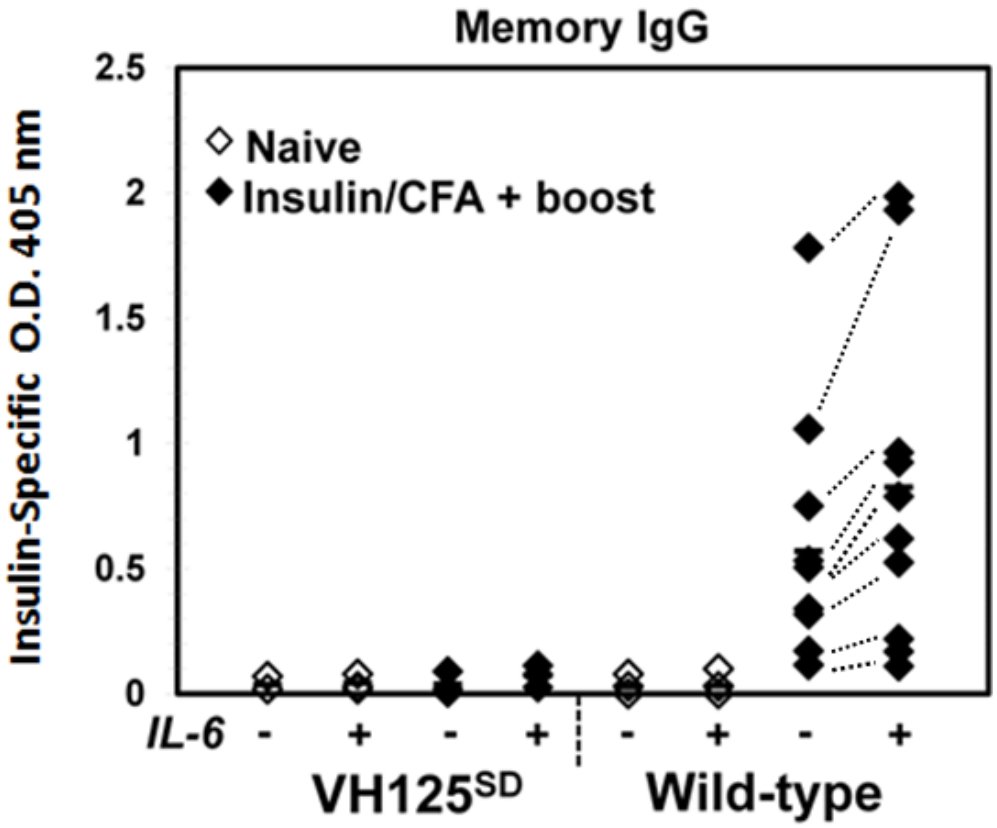

FIGURE III-6. Memory IgG antibody responses to TD immunization and boost are absent in V_H125^{SD} B6 mice. V_H125^{SD} and WT B6 mice were immunized with insulin/CFA and then boosted with insulin/IFA 8 weeks later. One week later, bone marrow cultures were established with and without IL-6, and IgG anti-insulin antibodies in culture supernatants were measured by ELISA in the presence of excess soluble insulin to measure insulin-specific IgG antibodies.

Insulin-BRT immunization promotes clonal expansion and restoration of surface IgM for anti-insulin B cells

To assess the fate of anti-insulin B cells undergoing an active breach of tolerance, clonal expansion and proliferation were measured *in vivo* following immunization with insulin-BRT (Fig. III-7). IgM^+ insulin-binding B cells (IgM^{a+} ins^+) in V_H125^{SD} B6 mice immunized with BRT alone (0.33% ± 0.07, n = 7) were not increased compared to unimmunized mice (0.34% ± 0.08, n = 6). In contrast, IgM^+ insulin-binding B cells were expanded in mice immunized with insulin-BRT (2.97% ± 1.28, n = 9) (Fig. III-7A). A small population of IgM^- insulin-binding B cells (IgM^{a-} ins^+), that have likely undergone CSR, were detected in V_H125^{SD} mice immunized with insulin-BRT (0.79% ± 0.46, n = 9) but not in unimmunized mice or in mice immunized with BRT alone.

Bromodeoxyuridine (BrdU) is a synthetic analog of thymidine and is incorporated into newly-synthesized DNA of proliferating cells during S phase of cell cycle. BrdU incorporation was used concomitantly to demonstrate that the increase in anti-insulin B cells represented antigen-specific expansion (Fig. III-7B). Insulin-binding B cells in V_H125^{SD} mice immunized with BRT alone did not incorporate BrdU and were similar in frequency to that in unimmunized mice. In contrast, both IgM^+ and IgM^- insulin-binding B cell populations in mice immunized with insulin-BRT incorporated BrdU (39.8% ± 7.2 for IgM^+ and 40.5% ± 14.1 for IgM^-, n = 5). These findings correlate with the antibody responses observed in V_H125^{SD} mice following immunization and show that the insulin-BRT conjugate drives clonal expansion and proliferation of anti-insulin B cells *in vivo*.

One hallmark of anergy is reduced surface IgM expression (49, 50, 53). Surface IgM for insulin-binding B cells (ins^+) in unimmunized V_H125^{SD} mice is reduced relative to non-insulin

binders (ins^-), expressed as a ratio of mean fluorescence intensity (MFI) of ins^+ to ins^- (0.58 ± 0.12, n = 6). To test whether insulin-BRT immunization promotes restoration of normal surface IgM expression, the MFI of surface IgM was compared for ins^+ and ins^- B cells following immunization (Fig. III-7C). Surface IgM for ins^+ B cells was not restored in V_H125^{SD} mice immunized with BRT alone (0.64 ± 0.08, n = 5). In contrast, surface IgM for ins^+ B cells was completely restored following insulin-BRT immunization (1.04 ± 0.09, n = 6). Surface IgM restoration is consistent with reversal of anergy in CSR-competent anti-insulin B cells.

Even though anti-insulin B cells in V_H125^{SD} B6 mice completely failed to produce IgG anti-insulin antibodies following TD immunization with insulin/CFA, I wished to determine where and when this block occurred during the TD immune response. The lack of antibody production could result from the lack of differentiation into antibody-producing plasmablasts and plasma cells that arise from GC reactions. Alternatively, anti-insulin B cells may never initiate the immune response and fail to expand or proliferate *in vivo* or participate in GCs. In contrast to expectations, IgM^+ insulin-binding B cells in V_H125^{SD} B6 mice immunized with insulin/CFA underwent clonal expansion (1.22% ± 0.38, n = 6) (Fig. III-7A). A small population of IgM^- insulin-binding B cells also emerged (0.33% ± 0.36, n = 6), and both IgM^+ and IgM^- insulin-binding B cell populations incorporated BrdU (13.2% ± 6.1 for IgM^+ and 25.2% ± 7.2 for IgM^-, n = 3) (Fig. III-7B), though not as robustly as when mice were immunized with insulin-BRT. Surface IgM expression, however, was not restored on ins^+ B cells relative to ins^- B cells following TD immunization (0.57 ± 0.05, n = 6) compared to ins^+ B cells from unimmunized mice (0.58 ± 0.12, n = 6) (Fig. III-7C).

Taken together, these data suggest that anti-insulin B cells undergo clonal expansion and proliferation *in vivo* following both immunization strategies, though the phenotype was more

robust following insulin-BRT immunization. The ability to respond to stimulation through CD40 may be reprogrammed in anti-insulin B cells as a consequence of the anergy imposed on these cells. IL-4 produced by T_H2 cells in the TD response may stimulate anti-insulin B cells together with CD40, a combination known to reverse tolerance in anergic B cells. While it is plausible that IL-4 plus CD40 stimulation may temporarily reverse anergy in anti-insulin B cells, the total lack of antibody production following TD immunization suggests that tolerance is ultimately enforced in this response. Generation of T cell epitopes takes some time, so it is possible the CD40 signaling that comes from a T cell will ultimately be ineffective and not serve to promote anti-insulin B cell differentiation. These cognate T cells, and presumably CD40 signaling, are likely not involved in the insulin-BRT response, hence why anti-insulin B cells are competent to produce anti-insulin antibodies following this immunization.

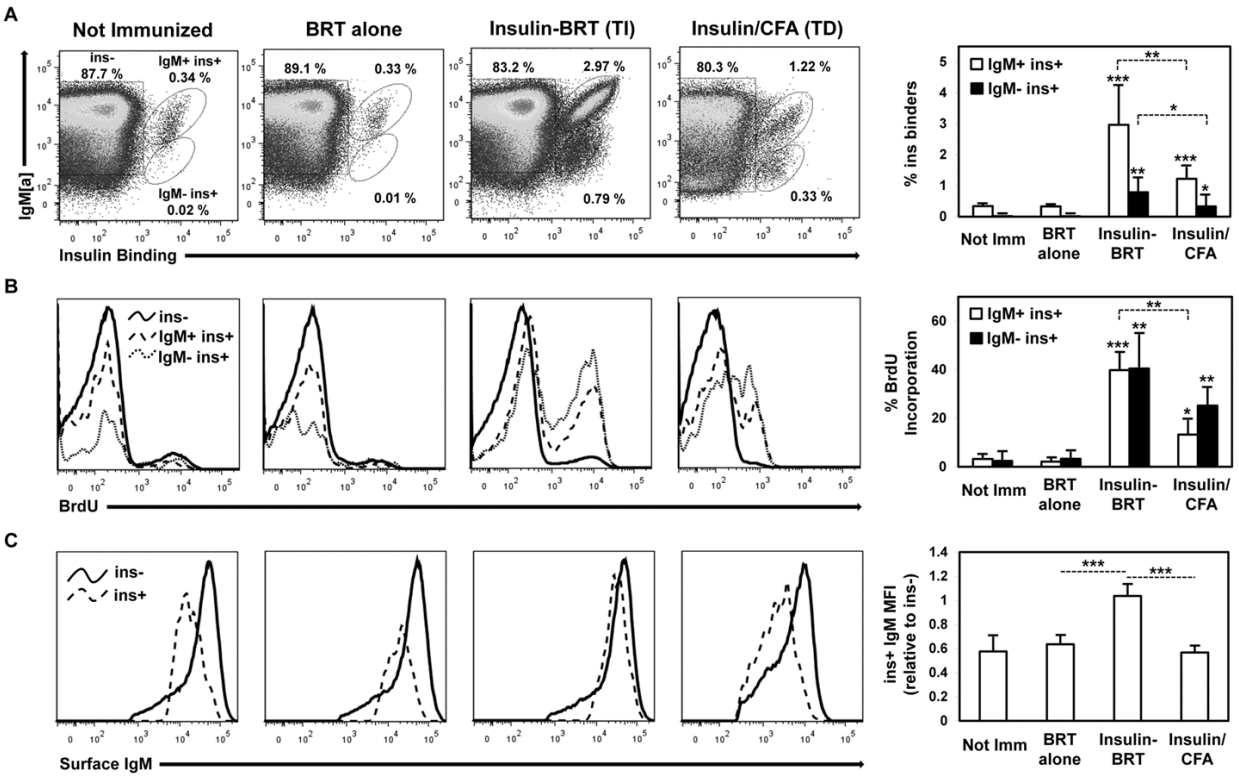

FIGURE III-7. Insulin-BRT promotes clonal expansion and restoration of surface IgM for anti-insulin B cells. V_H125^{SD} B6 mice were not immunized (n = 6) or immunized with either BRT alone (n = 7) or insulin-BRT (n = 9) i.p. in 1X PBS, or insulin/CFA (n = 6). **(A)** Insulin-binding B cells ($B220^+$ live lymphocytes) in the spleen were quantified 5 d following immunization by flow cytometry. Representative plots (left) and averages (right) are shown. **(B)** Mice were injected twice with BrdU i.p. 48h and 24h before sacrifice, and intracellular BrdU incorporation was measured in non-insulin binders (ins^-, solid black line), IgM^+ insulin binders (IgM^+ ins^+, dashed line), and IgM^- insulin binders (IgM^- ins^+, fine dashed line). Representative histograms (left) and averages (right) are shown. **(C)** The mean fluorescence intensity (MFI) of surface IgM for ins^- and ins^+ B cells is shown in representative histograms (left) and is also expressed as a ratio of ins^+/ins^- IgM MFI average ± SD (right). Data represent at least three independent experiments. Unless otherwise indicated, statistical comparisons are to unimmunized mice. * $p < 0.05$, ** $p < 0.01$, *** $p < 0.001$, two-tailed t test.

Insulin-specific germinal centers arise in V_H125^{SD} B6 mice

Ig isotype switch in B cells is principally recognized to occur in GC reactions that arise in the follicle following cognate interactions between $CD4^+$ T helper cells and antigen-specific B cells (118-120). Most rapid TI B cell responses are expected to occur in the extrafollicular spaces of the spleen (121); however, it has been demonstrated that some TI B cell responses can promote the unconventional formation of GCs in the absence of T cell help (111, 112). Accordingly, I assessed whether the observed breach in peripheral tolerance for anti-insulin B cells in the insulin-BRT response extended to the formation of GCs (Fig. III-8). Additionally, I determined whether the mild proliferative response in anti-insulin B cells induced by TD immunization with insulin/CFA also prompted a GC response, despite the lack of anti-insulin antibody production.

Flow cytometry was used to assess expression of the GC markers, GL7 and Fas, on anti-insulin B cells in V_H125^{SD} B6 mice 5 days following insulin-BRT immunization or 12 days following TD immunization with insulin/CFA. IgM^+ insulin-binding B cells (IgM^{a+} ins^+) in unimmunized mice established the background for the GC phenotype in the spleen (0.01% $GL7^+$ Fas^+, n = 5), and immunization with BRT alone did not increase this response (0.03% $GL7^+$ Fas^+, n = 7) (Fig. III-8A). In striking contrast, the GC phenotype was acquired in both IgM^+ insulin-binding B cells in mice immunized with insulin-BRT (24.4% ± 19.0 $GL7^+$ Fas^+, n = 9), as well as IgM^+ insulin-binders in mice immunized with insulin/CFA (24.4% ± 19.1 $GL7^+$ Fas^+, n = 6) (Fig. III-8A). An increased proportion of IgM^- insulin-binding B cells (IgM^{a-} ins^+) acquired the GC phenotype following insulin-BRT immunization (34.2% ± 27.6 $GL7^+$ Fas^+, n = 9) and insulin/CFA immunization (57.4% ± 18.2 $GL7^+$ Fas^+, n = 6), demonstrating that a portion of ins^+ B cells participating in GC reactions have undergone CSR, a finding consistent with eventual

production of IgG anti-insulin antibodies. However, antibody production is absent in mice immunized with insulin/CFA.

Notably, non-insulin-binding B cells (IgM^{a+} ins^{-}) in V_H125^{SD} B6 mice did not upregulate GC markers following insulin-BRT immunization (0.39% ± 0.19 $GL7^{+}$ Fas^{+}) when compared to unimmunized mice (0.36% ± 0.46 $GL7^{+}$ Fas^{+}) (Fig. III-8A, top row), suggesting that acquisition of the insulin-specific GC B cell phenotype is limited to cognate anti-insulin B cells and not merely a consequence of global B cell activation from BRT-mediated TLR stimulation. Flow cytometry labeling confirmed that $GL7^{+}$ Fas^{+} GC B cells were IgD^{-} (Fig. III-8B), consistent with induction of a GC B cell phenotype.

To confirm formation of anatomical GCs following insulin-BRT, immunofluorescence analysis was performed on spleen sections from both unimmunized and immunized V_H125^{SD} B6 mice. IgM, IgD, and CD3 were used to define follicular architecture, and GCs were identified as IgD^{-} and $GL7^{+}$. Whereas some $GL7^{+}$ IgD^{-} GCs were observed in unimmunized mice and in mice immunized with BRT alone, they were small by microscopy and non-insulin-specific by flow cytometry (Fig. III-8A, C). In contrast, large $GL7^{+}$ IgD^{-} GCs were readily detected in spleen sections from mice immunized with insulin-BRT (Fig. III-8C). Unfortunately, only a couple of spleen sections from insulin/CFA-immunized mice were available for immunolabeling, and only one was successfully labeled for GC detection. That image is displayed in the bottom right of the figure. These preliminary data reveal that anti-insulin B cells acquire a GC phenotype and localize to GC structures in the spleen following immunization with insulin-BRT. There is an impressive antigen-specific GC response in V_H125^{SD} mice following insulin/CFA immunization that correlates with the clonal expansion and proliferation observed in Fig. III-7A-B, yet

peripheral tolerance is ultimately effective at restricting any sort of anti-insulin antibody response (Fig. III-3A).

Examination of GC reactions at a later time point in the insulin-BRT response (day 12) revealed a sporadic yet significantly reduced population of ins^+ GC B cells. Three of eight mice examined at day 12 had detectable ins^+ GC B cells (5.22 ± 0.08%), while the other five mice did not have a detectable population of the same B cells (0.20 ± 0.13%) (Fig. III-9). Rapid decline in insulin-specific GC B cells and antibody production at day 12 following insulin-BRT (data not shown) is consistent with previous work in other models describing the fate of antigen-specific GCs in the absence of cognate T cell help (112). These data support the concept that the insulin-BRT conjugate drives IgG anti-insulin antibody production largely through the generation of antigen-specific GCs that are short-lived.

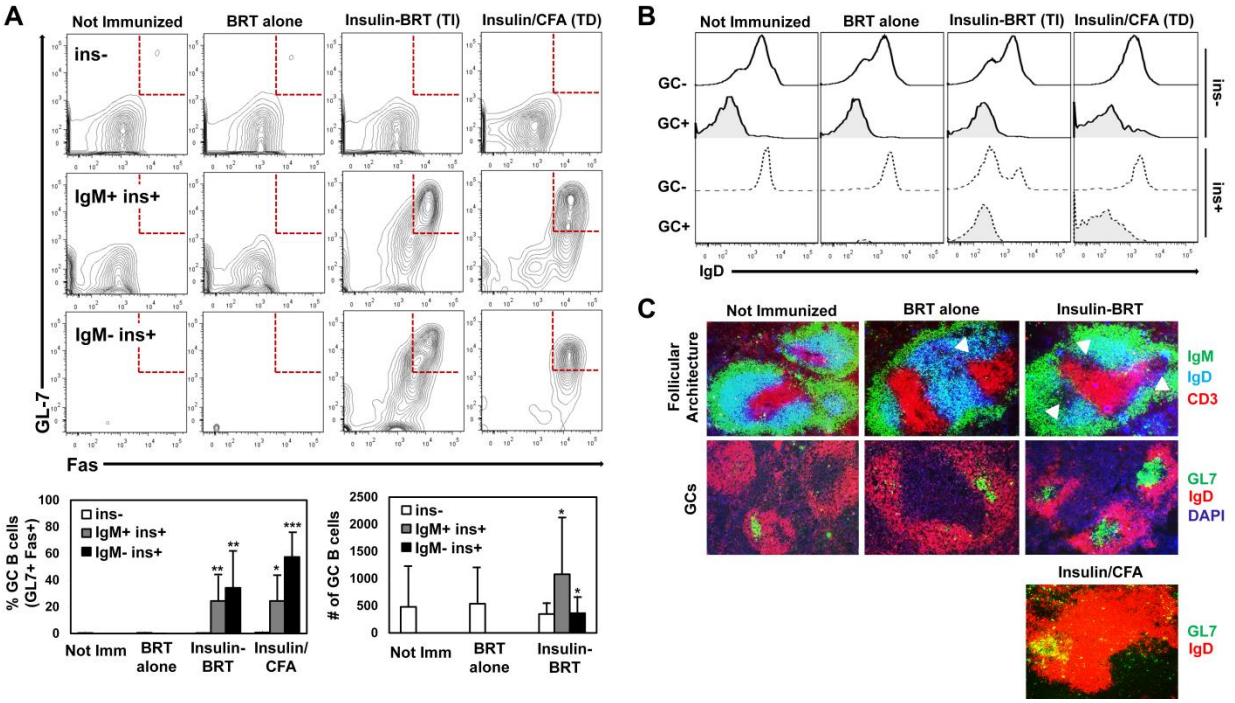

FIGURE III-8. Insulin-specific germinal centers arise in V_H125^{SD} B6 mice. V_H125^{SD} B6 mice were immunized with either BRT alone or insulin-BRT i.p. in 1X PBS or with insulin/CFA. **(A)** Flow cytometry was used to assess GC B cell phenotype by GL7 and Fas expression on B cells ($B220^+$ live lymphocytes) separated into non-insulin binders (ins^-, white), IgM^+ insulin binders (IgM^+ ins^+, gray), and IgM^- insulin binders (IgM^- ins^+, black). Representative plots (top) and GC B cell subset percent and cell number averages (bottom) are shown. **(B)** IgD expression was measured for ins^- (solid black line) and ins^+ B cells (dashed line) following immunization, and representative histograms are shown. **(C)** Immunofluorescence microscopy detected follicular architecture (top, IgD^- $CD3^-$, GCs indicated by arrows) and GC structures (bottom, $GL7^+$ IgD^-) in spleens from V_H125^{SD} B6 mice (n = 4). Follicles counted: n = 21 not immunized, n = 12 BRT alone, and n = 17 insulin-BRT. Data represent at least three independent experiments. Unless otherwise indicated, statistical comparisons are to unimmunized mice. * $p < 0.05$, ** $p < 0.01$, *** $p < 0.001$, two-tailed t test.

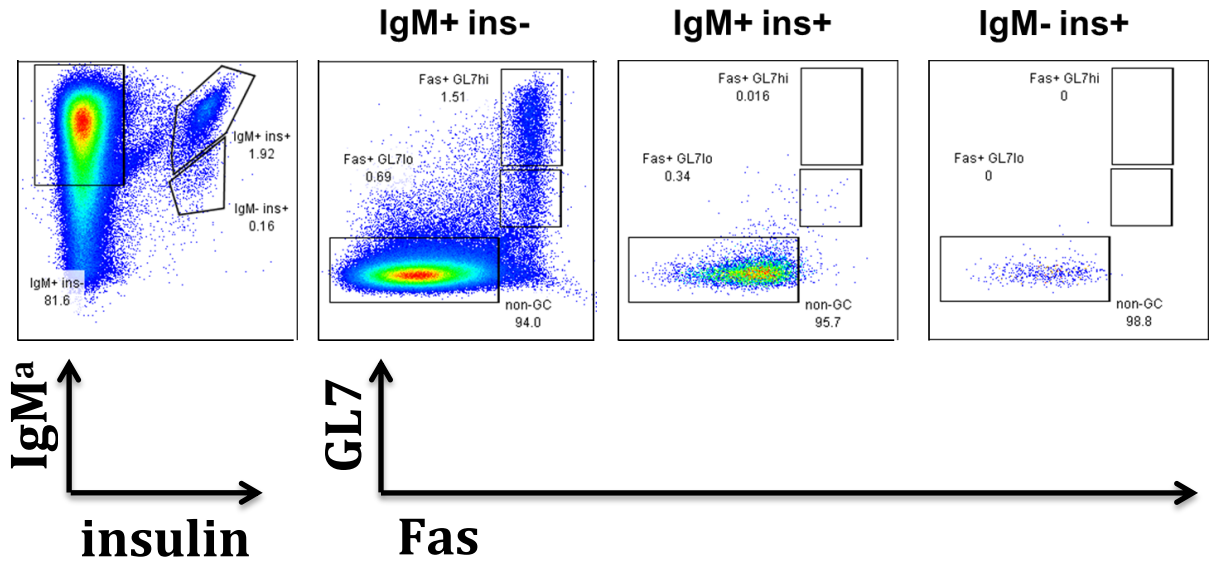

FIGURE III-9. Anti-insulin germinal centers are not readily detected in V_H125^{SD} B6 mice 12 days following insulin-BRT immunization. Germinal center B cell markers, GL7 and Fas, were analyzed on non-insulin-binding B cells (IgM+ ins-), non-switched insulin-binding B cells (IgM+ ins+), and Ig switched insulin-binding B cells (IgM- ins+) 12 days following immunization with insulin-BRT.

Anti-insulin B cells can acquire a GC phenotype in the absence of T cells in vitro

Issues have been raised regarding the "T-independence" of the insulin-BRT conjugate. Historically, BRT is defined as a type 1 TI antigen, as athymic mice and immunologically defective CBA/N mice are still able to mount antibody responses against it (110). The kinetics of the antibody response following insulin-BRT immunization in V_H125^{SD} B6 mice (four days), the predominant isotype of the antibody response (IgG2a), and the presence of TLR4-stimulating ligands in BRT all support the concept of insulin-BRT as a TI antigen. However, the presence of antigen-specific GCs has raised concern over whether this molecule truly is TI.

In the current study, *in vivo* T cell depletion was not performed prior to insulin-BRT immunization, but the capacity of the insulin-BRT conjugate to elicit a GC B cell phenotype *in vitro* in anti-insulin B cells was examined in the absence of T cell help (Fig. III-10). Accordingly, MACS was used to purify $CD43^-$ B cells from either 125^{SD} (H + L chain) or WT B6 mice, and then the cells were stimulated for 72 h with either BRT alone or insulin-BRT. Flow cytometry was used to examine acquisition of the $GL7^+$ Fas^+ GC B cell phenotype, and the supernatants were screened for IgM and IgG anti-insulin antibodies by ELISA.

Unstimulated B cells from 125^{SD} mice and control WT mice established the background for GL7 expression (1.12% and 1.23%, respectively). WT B cells, which have a polyclonal BCR repertoire, activated and became $GL7^{int}$ following BRT (74.8%) or insulin-BRT stimulation (66.2%), yet neither stimulating condition elicited Fas expression on $GL7^+$ cells from WT mice (Fig. III-10, bottom right panel). GL7 was upregulated in anti-insulin B cells from 125^{SD} mice following BRT (89%) or insulin-BRT stimulation (83.9%), although GL7 expression appeared the highest on anti-insulin B cells stimulated with insulin-BRT. GL7 expression was also higher on anti-insulin B cells compared to WT B cells. Furthermore, insulin-BRT but not BRT alone

promoted increased Fas expression on $GL7^+$ anti-insulin B cells (Fig. III-10, top right panel), indicating that anti-insulin B cells have the capacity to acquire a GC phenotype *in vitro* in the relative absence of T cells.

Supernatant from anti-insulin B cells stimulated with insulin-BRT contained specific IgM anti-insulin antibodies that were inhibitable by excess insulin in ELISA (data not shown). High concentrations of insulin-BRT actually yielded less of an antibody response, likely explained by absorption of anti-insulin antibodies by insulin present in the well. Anti-insulin B cells stimulated with BRT alone also produced IgM anti-insulin antibodies, a finding that differs from the relative absence of this response observed in V_H125^{SD} B6 mice immunized with BRT alone (Fig. III-3B). One explanation for this is that a monoclonal population of anti-insulin B cells *in vitro* may receive a TLR signal from BRT strong enough to elicit an IgM antibody response. IgG anti-insulin antibodies were not detected in any stimulating condition (data not shown), either the result of total absorption of the IgG antibodies in the well or, more likely, the result of a lack of necessary cytokines that promote CSR to specific isotypes.

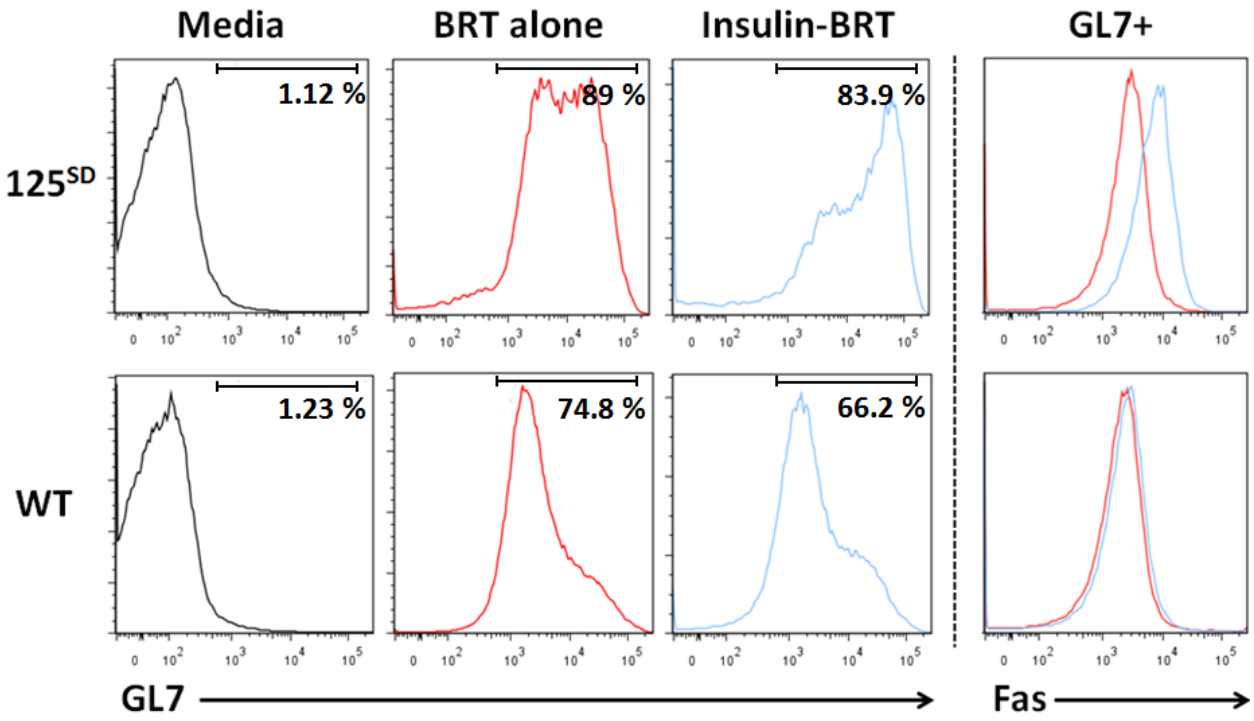

FIGURE III-10. Anti-insulin B cells can acquire a GC phenotype in the absence of T cells *in vitro*. B cells from either 125^{SD} (H + L chain) or WT B6 mice were $CD43^-$ MACS purified and stimulated for 72 h to a dose response of BRT alone or insulin-BRT. Germinal center B cell markers, GL7 and Fas, were analyzed by flow cytometry after 72 h and are displayed here as histograms of GL7 ($B220^+$ $7AAD^-$, left panels) and Fas ($GL7^+$, right panels).

Anti-insulin L chains are selected from the pre-immune repertoire to enter germinal center reactions

Anti-insulin B cells are detected in GCs following insulin-BRT immunization (Fig. III-8). These GC B cells may reflect expansion of insulin-binding B cells that were present in the pre-immune repertoire (Fig. III-1D). Alternatively, the unique environment of GC reactions may select rare anti-insulin B cells that are clonally ignorant or below the level of detection. Accordingly, we investigated selection of anti-insulin Igκ from the pre-immune repertoire by insulin-binding GC B cells (Fig. III-11). Spleens were harvested from unimmunized V_H125^{SD} B6 mice or from mice immunized with insulin-BRT. Non-GC (IgM^+ $GL7^-$ Fas^-), IgM^+ GC (IgM^+ $GL7^+$ Fas^+), or IgM^- GC (IgM^- $GL7^+$ Fas^+) insulin-binding B cells were purified by flow cytometry sorting as identified in Fig. III-7A and III-8A. RNA was purified, and cDNA was used as template for Igκ amplification. The Ig BLAST tool was used to identify Vκ and Jκ gene segment usage (using IMGT nomenclature) as well as any nucleotide mutations (see Methods).

The Vκ125Tg in the previously published anti-insulin 125Tg (H + L chain) mouse model is a Vκ4-74 (77, 122). This L chain is associated with anti-insulin B cells loaded with endogenous rodent insulin detected by mAb123 in V_H125^{SD} B6 mice (Fig. III-1D), confirming this Vκ is autoreactive when combined with V_H125. Insulin-binding B cells sorted in unimmunized V_H125^{SD} mice exclusively used Vκ4-74 (Fig. III-11A). Vκ4-74 was also the main Vκ used by insulin-binding B cells following insulin-BRT immunization, including 11/12 non-GC (Fig. III-11B), 8/9 IgM^+ GC, and 5/6 IgM^- GC clones (Fig. III-11C-D). Vκ4-74 clones were paired with all Jκ, forming different CDR3 amino acid junctions associated with previously recognized low/moderate (P-L) and high (P-P) affinity for rodent insulin, as deduced from sequences identified in studies of anti-insulin hybridomas (114). The 5' degenerate primer

sequence was removed, and L chain sequences were deposited into GenBank (http://www.ncbi.nlm.nih.gov/genbank/) with the following accession numbers: unimmunized (KP790058-KP790071), non-GC (KP790072-KP790083), IgM^+ GC (KP790084-KP790092), and IgM^- GC (KP790093-KP790098).

The majority (5/9) of IgM^+ GC anti-insulin B cell clones sorted from V_H125^{SD} B6 mice on day 5 following insulin-BRT retained nucleotide sequences in germline Igκ configuration with CDRs identical to those found in unimmunized mice (Fig. III-11G). However, an increased frequency of both IgM^+ and IgM^- GC anti-insulin B cell clones sorted from immunized mice possessed one or more nucleotide mutations relative to non-GC anti-insulin B cells from immunized mice or anti-insulin B cells isolated from unimmunized mice (Fig. III-11E-H). Mutations were randomly yet equally distributed in framework regions and CDRs, though no amino acid changes were observed (data not shown). Taken together, these data suggest that anti-insulin B cells enter GCs from the pre-immune repertoire following immunization with the insulin-BRT conjugate, and a proportion of B cells undergo somatic hypermutation.

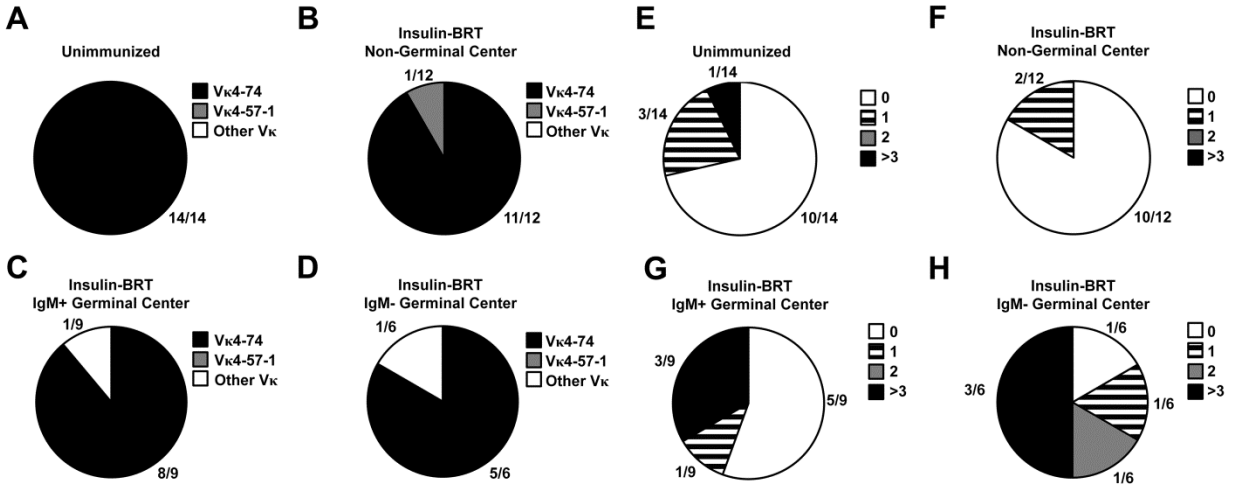

FIGURE III-11. Anti-insulin L chains are selected from the pre-immune repertoire to enter germinal center reactions. Spleens were harvested from unimmunized V_H125^{SD} B6 mice, or from mice 4 days following immunization with insulin-BRT. Flow cytometry sorting was using to purify insulin-binding B cells ($B220^+$ live lymphocytes), that were further gated in immunized mice as IgM^+ non-GC ($GL7^-$ Fas^-), IgM^+ GC ($GL7^+$ Fas^+), or IgM^- GC populations. Isolated RNA was transcribed to cDNA, and Igκ genes were amplified by PCR. Sequences were analyzed using the Ig BLAST database (see Methods). **(A-D)** The number of clones identified by the indicated Vκ is divided by the total number of clones analyzed for each immunization group. Vκ4-74 (black), Vκ4-57-1 (gray), all other Vκ (white). **(E-H)** Igκ clone sequences were compared to germline sequences, excluding the 5' region that correlated with degenerate primers used for amplification. The number of sequences that possess the indicated number of nucleotide changes, 0 (white), 1 (striped), 2 (gray), or > 3 (black), is shown for each immunization group.

Anti-insulin plasmablasts arise in V_H125^{SD} B6 mice following insulin-BRT immunization

Antibody-secretion is performed by short-lived plasmablasts and long-lived plasma cells that have undergone B cell differentiation. To confirm the cellular origin of IgM and IgG anti-insulin antibodies that arise in V_H125^{SD} B6 mice following immunization with the insulin-BRT conjugate, the formation of plasmablasts at the corresponding time point was assessed using flow cytometry (Fig. III-12). B cells from V_H125^{SD} B6 mice immunized with BRT alone or insulin-BRT were incubated with biotinylated insulin to label surface BCRs and FITC-conjugated insulin to label intracellular/internalized BCRs. Plasmablast and plasma cell differentiation is concomitant with loss of B220 expression, so both $B220^+$ and $B220^-$ populations were analyzed.

V_H125^{SD} B6 mice immunized with BRT alone possessed only the requisite $surface^+$ anti-insulin B cells (Fig. III-12, top left), and this population was absent on $B220^-$ cells (top right). V_H125^{SD} B6 mice immunized with insulin-BRT, however, possessed clonally expanded $surface^+$ anti-insulin B cells and $surface^+$ $intracellular^+$ plasmablasts in both $B220^+$ and $B220^-$ populations. This indicates that the IgM and IgG anti-insulin antibodies that arise following immunization of V_H125^{SD} B6 mice with insulin-BRT originate from actively-differentiating plasmablasts. Fully differentiated plasma cells have completely lost surface BCR expression, and it appears that the $B220^-$ plasmablast population is beginning to lose surface positivity (Fig. III-12, bottom right). However, these populations were not examined at later time points in the insulin-BRT response, so it is unclear whether anti-insulin B cells undergo full plasma cell differentiation or merely rely upon shorter-lived plasmablasts for IgM and IgG antibody-secretion. Plasmablast and plasma cell formation in V_H125^{SD} B6 mice following insulin/CFA immunization was not assessed, as there is a complete lack of IgM and IgG anti-insulin antibody production in these mice in the insulin/CFA response.

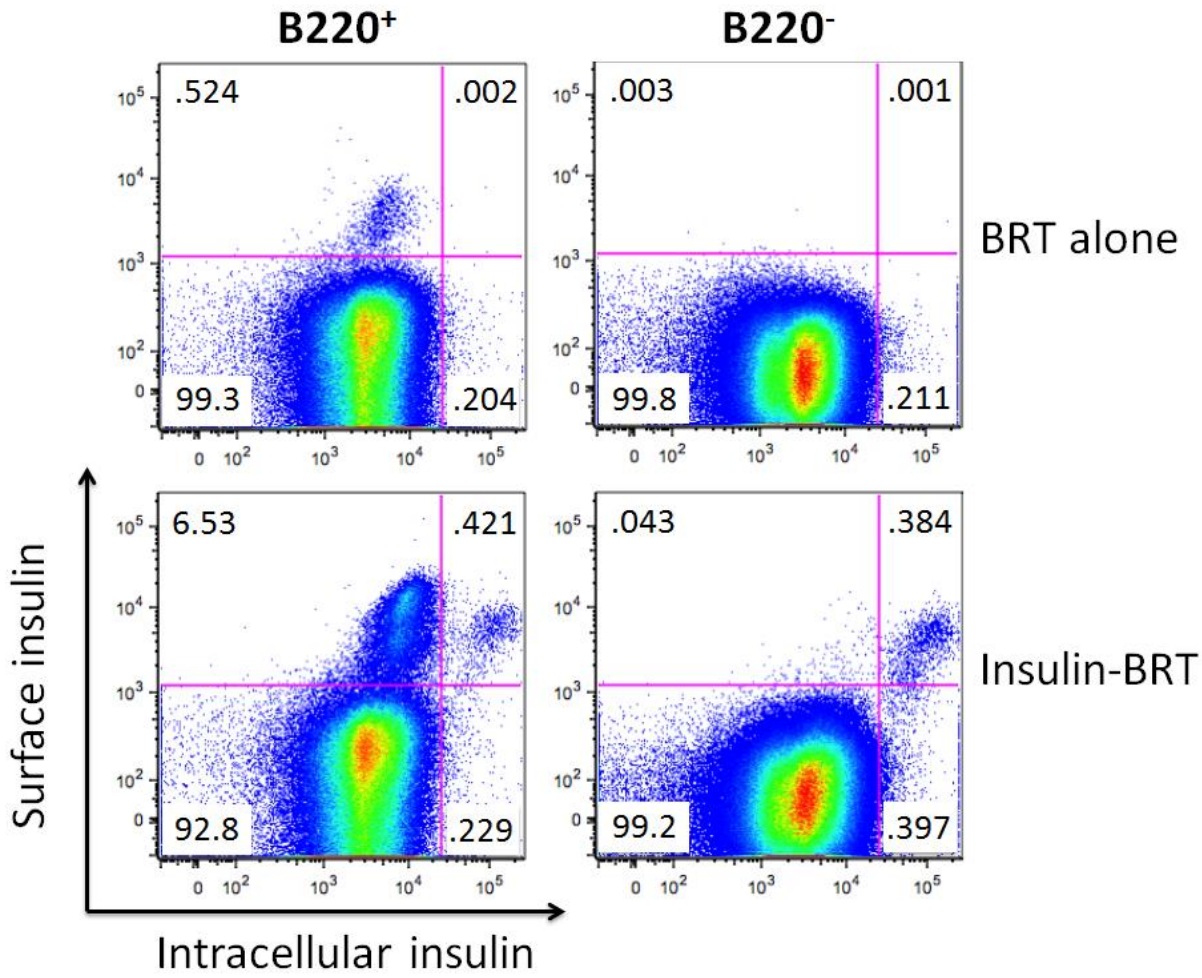

FIGURE III-12. Anti-insulin plasmablasts arise in V_H125^{SD} B6 mice following insulin-BRT immunization. $B220^+$ (left) and $B220^-$ (right) populations are shown five days following immunization with BRT alone (top row) or insulin-BRT (bottom row). Cells were incubated with biotinylated human insulin (surface) and Alexa 488-conjugated pork insulin (intracellular) using flow cytometry.

Discussion

Autoreactive B lymphocytes are recognized to enter the peripheral repertoire of normal individuals, and their presence is considered a liability for developing autoimmune disease (123). The association of IgG autoAbs with pathological processes suggests that self-reactive B cells are recruited into immune responses. How this occurs is not clear, though a general assumption is that T cell-mediated help is required to reverse tolerance in such B cells. The present studies identify an alternative mechanism by which autoreactive B cells may escape peripheral tolerance without cognate T cell help. I describe the V_H125^{SD} B6 mouse, a new site-directed transgenic model that has a polyclonal B cell repertoire with a detectable population of IgM^+ IgD^+ anti-insulin B cells that have the ability to undergo isotype switch. Anti-insulin B cells in V_H125^{SD} B6 mice are not eliminated but rather rendered clonally anergic in the periphery, unlike other models where high-affinity antigen-specific B cells are eliminated because they fail to compete in the repertoire for residence in mature compartments (76, 124, 125). Tolerance is maintained in CSR-competent anti-insulin B cells following TD immunization, as immunized V_H125^{SD} B6 mice do not produce IgG anti-insulin antibodies despite undergoing proliferation *in vivo* and differentiation into GCs. Immunization of V_H125^{SD} B6 mice with insulin conjugated to a type 1 TI antigen (insulin-BRT), however, provides BCR/TLR co-stimulation that reverses anergy in anti-insulin B cells and promotes proliferation, differentiation into GCs, somatic hypermutation, and production of IgG autoAbs. An overall summary figure is provided, depicting both the anergic state of anti-insulin B cells (Fig. III-13A) and how this anergy is lifted following BCR/TLR co-stimulation (Fig. III-13B).

Insulin-BRT was previously used to uncover rare anti-insulin B cells in the repertoires of normal mice independently of T cell help (95). As originally observed, conjugation of insulin

and BRT was necessary to drive antibody production (95). As such, immunization of V_H125^{SD} B6 mice with insulin-BRT elicits IgM and IgG2a anti-insulin antibodies, whereas neither BRT alone (Fig. III-3B) nor BRT physically mixed with insulin (data not shown) elicits antibody production. The kinetics of the insulin-BRT response (3-5 d) and antibody isotypes observed following immunization agree with those seen in response to classic type 1 TI antigens. BRT contains non-canonical LPS (108, 109, 126), thus I hypothesize that the proliferation induced by insulin-BRT *in vivo* (Fig. III-7B) occurs in part by TLR4 stimulation.

Insulin-BRT responses have been shown to occur in the absence of T cells (95, 110), a finding I validated with an *in vitro* approach using purified anti-insulin B cells. However, they are likely influenced by bystander effects or other non-specific T cell factors, as demonstrated for other TI antigens (127). Indeed, historically, experiments involving insulin-BRT always demonstrated better responses in the presence of T cells. This does not, however, prove that cognate T cells are required to initiate anti-insulin B cell differentiation into GCs.

Other examples of B cell tolerance reversal independent of T cell help have been described. B cells specific for MHC-I in 3-83 transgenic mice develop normally in the bone marrow but undergo clonal deletion in the periphery when they encounter liver-expressed $H\text{-}2^k$ (74, 75). However, administration of a bacteriophage containing a 15 amino acid mimotope that is recognized by 3-83 B cells reverses tolerance and drives robust Ig production (74). Thus, tolerant B cells that are normally deleted in the periphery are actually rescued when self-antigen is presented to the B cell in a TI fashion. Similarly, anergy in anti-insulin B cells is reversed by BCR/TLR co-stimulation in the insulin-BRT response that is relatively TI. Immunization of V_H125^{SD} B6 mice with insulin-BRT does not promote type 1 diabetes, indicating that loss of tolerance in these mice is restricted to the B cell compartment. While the antibodies produced in

the response are short-lived and non-pathogenic, anti-insulin B cells that regain their function are pernicious for the development of autoimmunity.

Insulin-specific GCs are found in V_H125^{SD} B6 mice at day 5 of the insulin-BRT response (Fig. III-8), consistent with previous studies demonstrating that B cells specific for the hapten nitrophenol (NP) can enter GCs without T cell help following immunization with the type 2 TI immunogen NP-Ficoll (112). NP-Ficoll immunization only elicited GCs in QM transgenic mice, which have ~ 60% B cells specific for NP, but not in non-transgenic (WT) littermates. Vinuesa et al. used transfer experiments to confirm that TI GCs only arose when the NP-specific B cell precursor frequency was 1 in 1000 or higher (112). V_H125^{SD} B6 mice possess ~ 0.4% anti-insulin B cells in the periphery (1 in 250), whereas the frequency in WT B6 is closer to 1 in 100,000. As such, we did not observe any detectable insulin-specific GCs in WT mice following insulin-BRT immunization (data not shown), despite IgM and IgG anti-insulin antibody production in the same mice. The increased frequency of anti-insulin B cell precursors in V_H125^{SD} B6 mice supports the generation of insulin-specific GCs by day 5 and could explain the increased IgM anti-insulin antibody production observed in V_H125^{SD} compared to WT B6 mice. Insulin-specific GCs are found in V_H125^{SD} B6 mice at day 12 but at a much lower frequency, as expected for GCs over time in the absence of T cell help. We are currently introducing V_H125^{SD} into NOD mice to determine how these unconventional GC reactions are controlled in a strain of mice predisposed to develop autoimmunity and type 1 diabetes.

Surface IgM is not restored in anti-insulin B cells following TD immunization with insulin/CFA, a finding that correlates with an anergy program in place in these cells. This may cause a genetic reprogramming in anti-insulin B cells that impairs their ability to respond to T cell-mediated CD40 signaling. The emergence of insulin-binding B cells into GCs following TD

immunization is surprising, paired with the observation that these cells undergo clonal expansion and proliferation. Ultimately, peripheral tolerance is effective in the TD immune response, as there is a complete lack of IgM or IgG anti-insulin antibodies following both primary immunization and secondary boost. This indicates that GCs behave as sites of negative selection for anti-insulin B cells that have had their anergy temporarily reversed upstream of GC differentiation. This phenotype early in the TD response (clonal expansion and proliferation) could be the result of CD40 and IL-4 signaling, a combination known to reverse tolerance in B cells. IL-4 is secreted by T_H2 cells and promotes B cells to switch to the IgG1 isotype. WT mice exhibit $IgG1^b$ anti-insulin antibody production following insulin/CFA immunization, indicating that IL-4 is likely induced during this TD response.

Igκ genes from the pre-immune repertoire do not undergo negative selection in GCs, as evidenced by exclusive anti-insulin Vκ4-74 usage by BCRs in anti-insulin B cells from unimmunized V_H125^{SD} B6 mice and in IgM^+ and IgM^- insulin-binding GC B cells from mice immunized with insulin-BRT (Fig. III-11). Prior studies show that Vκ4-74 pairs with several Jκ to form autoreactive insulin-binding BCRs when combined with V_H125 (114). Thus, insulin-binding B cells from the pre-immune repertoire, and not obscure clonally ignorant B cells, are selected for GC entry during the insulin-BRT response. The presence of nucleotide mutations in Vκ4-74 clones indicates somatic hypermutation occurs in these GC reactions. Approximately half of the mutations observed in both IgM^+ and IgM^- insulin-binding GC clones were found in CDRs, yet no amino acid replacements were observed. However, the presence of ongoing mutations suggests that antigen binding could be altered in these GC reactions. Igκ analysis on GC B cells from mice following TD immunization was not performed in the current study.

While insulin-BRT may not mimic any natural molecule, loss of B cell tolerance via similar pathways may be possible in circumstances where the levels of autoAg and innate stimulus are high, such as on the surface of APCs. This could occur in association with islet inflammation in T1D where APCs are found in close contact with insulin-producing beta cells (128) or following uptake of insulin injected through contaminated skin by epidermal and dermal APCs (129). This may be the case for patients with type 2 or gestational diabetes who receive temporary insulin treatment. Recently, TLR7 signaling was implicated in the development of spontaneous GCs and autoAbs in a lupus model (130), in addition to the previously recognized role of TLR9 in autoimmune disease (131). Further, BCR/TLR synergy has been shown to induce TI CSR through the non-canonical NF-κB pathway (132). Thus, there is growing evidence to support a unique role for TLRs in the generation of antigen-specific GCs and production of IgG autoAbs.

IgG anti-insulin antibodies that arise in the insulin-BRT response were confirmed to be autoreactive by indirect immunofluorescence, as they bound mouse insulin on pancreata sections from both unimmunized and immunized mice. These same autoAbs were not detected endogenously on the tissue using direct immunofluorescence, suggesting that a lack of access of autoAbs to their tissue targets may limit their autoimmune potential. For example, anti-H-2^k antibodies generated by phage-mimotope immunization were found on surfaces of hepatocytes in 3-83 Tg mice (74), reflecting the ubiquitous surface expression of MHC-I in the target organ. Access to insulin epitopes may be more restricted in the islets. Experiments in V_H125^{SD} NOD mice will determine if reversal of anergy in anti-insulin B cells driven by BCR/TLR co-stimulation accelerates immunopathology.

Type 1 diabetes in mice and humans is a multigenic autoimmune disorder in which detection of IgG insulin autoAbs indicates that loss of tolerance in anti-insulin B cells is an early event in disease pathogenesis. We show evidence that a breach in anti-insulin B cells may arise in the absence of conventional T cell help. Common environmental triggers resulting from infection and inflammation that are prevalent in children could combine with endogenous insulin to break anti-insulin B cell tolerance. BCR/TLR co-stimulation of autoreactive B lymphocytes could represent an early event in the induction of autoimmunity.

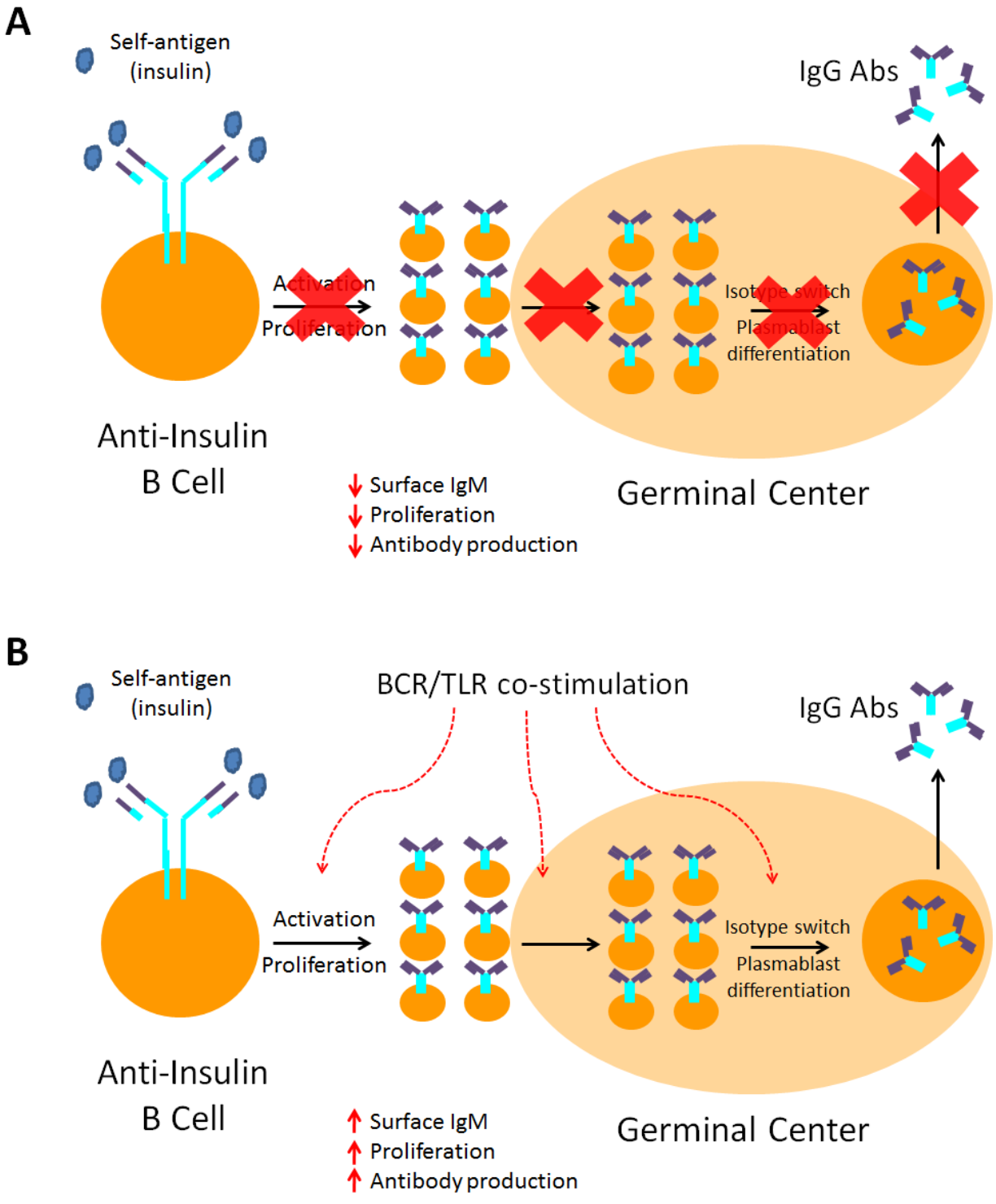

FIGURE III-13. BCR/TLR co-stimulation reverses anergy **(A)** in anti-insulin B cells and promotes their proliferation, differentiation into GCs, and production of IgG anti-insulin antibodies **(B)**.

CHAPTER IV

CONCLUSIONS AND FUTURE DIRECTIONS

Thesis Summary

Overall, these studies examine how peripheral tolerance is governed for autoreactive B lymphocytes that bind the relevant autoAg, insulin. CSR-competent anti-insulin B cells enter mature compartments but are anergic, demonstrated by impaired proliferation to stimulation by a panel of B cell mitogens *in vitro* and total lack of IgG anti-insulin antibody production following TD immunization of V_H125^{SD} B6 mice. Reversal of anti-insulin B cell anergy is demonstrated by proliferation to insulin plus LPS *in vitro* and IgG2a antibody production following immunization of V_H125^{SD} B6 mice with insulin conjugated to a type 1 TI antigen (90, 95). This combined BCR/TLR co-stimulation effect *in vivo* is accompanied by entry of insulin-binding B cells into GCs, in contrast to expectations that such TI-mediated responses would arise in extrafollicular sites. In GCs, anti-insulin L chains are not discarded but rather selected from the pre-immune repertoire. These studies reveal a new pathway to drive loss of tolerance for CSR-competent anti-insulin B cells.

Implications of the Research

Tolerance to self-antigens must be maintained to protect from autoimmunity. However, the incidence of autoimmune disease in this country and around the world remains shockingly high, indicating that mechanisms of immune tolerance are imperfect and often fail. The main contributing factor that drives loss of tolerance is likely a combination of a genetic predisposition

to develop autoimmunity plus some environmental trigger that acts as a catalyst in the initiation of the autoimmune response. The fact IgG insulin autoAbs spontaneously arise in patients with type 1 diabetes paired with the observation that cognate, autoreactive B and T cells are found in the pancreatic islets indicate that a breach in self-tolerance in anti-insulin B cells is foundational in the pathogenesis of type 1 diabetes. The success of B cell-targeted therapies like Rituximab (anti-CD20) in offering disease protection is promising, but there are obvious disadvantages to not having a B cell repertoire. Thus, antigen-specific B cell therapies offer a newfound hope, with the thought being that one could specifically target the harmful anti-insulin B cells for elimination while leaving the protective polyclonal B cell repertoire intact. These efforts will only be successful with as much of a thorough and complete understanding as possible of how tolerance is imposed on anti-insulin B cells and how tolerance ultimately fails. In my studies, I uncovered a new pathway to reversing tolerance in anti-insulin B cells competent to undergo isotype switch. My data provide a nice foundation for future studies, but the implications of my research offer some outstanding questions that must be addressed.

The original mAb125 contains two amino acid mutations away from germline that are absolutely essential for autoreactivity (122, 133). This is a fascinating observation considering that the germline sequence is completely not insulin-reactive. Perhaps having only one of those mutations is enough to avoid tolerance induction by altering BCR specificity or affinity. The affinity of the original mAb125 for human insulin is 3×10^8, and its affinity for rodent insulin is 8×10^6 (77, 86, 122). Maybe these affinities are a product of the BCR Tg, and natural anti-insulin BCR affinity is actually lower than what has been reported for mAb125. While tolerance is quite good in the V_H125^{SD} B6 model, insulin autoAbs do arise under the right circumstances, suggesting that BCR affinity may be altered in GC reactions that give rise to IgG autoAbs.

For years, it was assumed that insulin's small size and low circulating concentration were such that anti-insulin B cells were clonally ignorant to insulin and that tolerance was not imposed on such B cells. We know now this is not the case. My finding that anti-insulin B cells are competent to participate in antigen-specific GC reactions and that anti-insulin L chains in the GC undergo somatic hypermutation indicates that the difference in generation of a non-insulin-reactive BCR and an autoreactive insulin-specific BCR may be minimal. It is possible that a non-insulin-reactive BCR could acquire the mutations necessary to gain autoreactivity, although this "gain-of-function" autoreactive mutation would likely be disallowed through negative selection of the B cell clone in the GC environment by Fas-mediated cell death, a process critical for T and B cell homeostasis within the GC (32). Several studies have demonstrated that administration of soluble self-antigen at the peak of the GC B cell response induces rapid apoptosis, indicating negative selection (134, 135). The fact that anti-insulin B cells develop with autoreactive BCRs might make the process of circumventing negative selection in the GC much easier, as long as the B cells undergo tolerance reversal prior to entering the GC. BCR/TLR co-stimulation appears to deliver a strong enough signal to ensure anergy is reversed throughout the GC reaction, at least to the point of antibody production. These insulin-specific GC reactions do wane quite dramatically by day 12 of the insulin-BRT response, indicating their short-lived nature.

Interestingly, TD immunization of V_H125^{SD} B6 mice with insulin/CFA promoted an insulin-specific GC response despite the complete lack of IgG anti-insulin antibody production, suggesting that tolerance ultimately wins in a TD immune response. Analysis of Igκ genes in V_H125^{SD} mice immunized with insulin-BRT, however, reveals that anti-insulin Vκ from the pre-immune repertoire are positively selected in GCs. Thus, whether anti-insulin B cells undergo

positive or negative selection in GCs and produce autoAbs is likely determined by the presence or absence of CD40 signaling that may be impaired in anergic anti-insulin B cells. My *in vitro* proliferation data validate this hypothesis, as stimulation with anti-CD40 plus insulin did not reverse anti-insulin B cell anergy while LPS plus insulin drove robust proliferation. It is clear that anti-insulin B cells in V_H125^{SD} B6 mice immunized with insulin/CFA do undergo some proliferation, potentially the result of some TLR stimulation in CFA that combines with insulin to mildly reverse anergy, but not to the point of antibody production. Surface IgM expression remains profoundly impaired in anti-insulin B cells following TD immunization but is completely restored after insulin-BRT immunization. Signal transduction in B cells starts with antigen-mediated activation of the IgM^+ BCR, so the impaired surface IgM expression in anti-insulin B cells may serve to restrict their function during a TD immune response, but the restoration of surface IgM following insulin-BRT immunization may reflect beginning stages of functional restoration.

Maybe low levels of autoreactivity in the B and T cell repertoires actually provide a benefit to the host. Otherwise, microbes might be able to mask their presence through molecular mimicry, a phenomenon where foreign antigens share structural or sequence similarities with self-antigens. The induction of tolerance in autoreactive B and T cells might serve the purpose of ensuring that this does not take place and allow harmful pathogens to disguise themselves in the repertoire and remain undetected. Not all tolerance is useful, however, as self-like epitopes can inappropriately induce tolerance to a foreign antigen. This occurs in HIV infection with the membrane-proximal region of gp41, an epitope that erroneously induces self-tolerance (136).

Generation of TI GCs is a controversial idea. There is not much in the literature that suggests this phenomenon is even possible, although GCs without T cells have been shown to

arise in a separate BCR Tg model following immunization with NP-Ficoll, a TI type 2 antigen. In these experiments, NP-specific B cells from QM Tg mice enter GCs and produce anti-NP antibodies, whereas non-Tg (WT) littermates did not demonstrate a GC response (112). The authors implicated the frequency of NP-specific B cell precursors as the predominant factor in whether NP-specific GCs arose or not. Serial dilutions of QM spleen cells were adoptively transferred into irradiated congenic mice to determine the minimum B cell precursor frequency required to induce a GC response, and the authors found that a frequency no less than 1 in 1,000 NP-specific B cells was necessary. V_H125^{SD} B6 mice possess an anti-insulin B cell frequency in the spleen of 1 in 250, which is in agreement with the observations of de Vinuesa et al.

WT mice have B cells specific for insulin but at a much lower frequency, which explains why insulin-BRT immunization failed to elicit an antigen-specific GC response in WT mice. This begs the question of whether the rare TI GC induction in QM Tg and V_H125^{SD} B6 mice is merely a product of having a BCR Tg, versus an actual biologically relevant phenomenon. NP-specific GCs dramatically aborted by day 6 following NP-Ficoll immunization, right about the time high-affinity GC B cells are selected by T cells, indicating a "fail-safe mechanism" against autoreactivity (112). The observation that insulin-specific GCs are either not detected or detected at very low frequency at day 12 of the insulin-BRT response might support the notion that this fail-safe mechanism also exists for insulin-specific GCs. Maybe this abortion is the result of a lack of T cell selection within the GC. IgG autoAbs are detected by day 4 of the insulin-BRT response, so it is plausible that the window of time necessary for autoimmunity to initiate via GC reactions is shorter than the time necessary to cull such insulin-specific GCs. This would suggest that TI GCs are a very real biological event and can be quite pernicious for the development of autoAbs. GCs were observed in the spleens of V_H125^{SD} B6 mice; however,

the high concentration of insulin autoAg in the pancreatic islets may offer a more fertile setting for autoreactivity than what is force-fed during immunization.

There is recent evidence that shows that TLR4-mediated B cell proliferation is actually BCR-dependent. This was illustrated using a mouse model whose B cell repertoire contained B cells that lacked BCRs (BCR^{null}). LPS did not induce proliferation in BCR^{null} B cells, yet if the same B cells possessed a Tg that constitutively expressed PI3K, they regained response to LPS (137). While anergic anti-insulin B cells express BCRs, it is possible the basal signals delivered through the BCR are interpreted in the B cell in a similar fashion as one that is lacking a BCR. In other words, downstream signal transduction through PI3K may be significantly impaired in anti-insulin B cells. PI3K promotes NF-κB activation and FoxO1 repression via glycogen synthase kinase 3β, important events for B cell proliferation. TLR4 signaling via MyD88 also elicits PI3K activity, yet anti-insulin B cells are anergic and fail to proliferate *in vitro* to either LPS or insulin alone, and they do not produce anti-insulin antibodies following immunization with BRT alone. The gain-of-function achieved in anti-insulin B cells through BCR/TLR co-stimulation could be the result of enhanced/additional PI3K activity as a consequence of two separate pathways feeding into this pathway. This may improve NF-κB translocation to the nucleus and repression of FoxO1, ultimately driving cellular proliferation. A proposed model of the signaling events that occur in anti-insulin B cells stimulated with insulin alone (Fig. IV-1A), which enforces anergy, and with LPS plus insulin (Fig. IV-1B), which lifts anergy, is provided.

Taken together, my studies reveal a new pathway to reverse tolerance in anti-insulin B cells that are competent to undergo isotype switch. Using both *in vitro* and *in vivo* experimental approaches, I showed that insulin plus anti-CD40 signaling, which mimics T cell help, enforces the anergy program already in place in anti-insulin B cells and completely impairs their ability to

produce IgG anti-insulin antibodies. Combined stimulation through the BCR and TLR4 with insulin plus LPS or insulin-BRT immunization reverses anergy in anti-insulin B cells, promoting the restoration of surface IgM, robust proliferation, entry into antigen-specific GCs, and IgM and IgG anti-insulin antibody production. These findings emphasize how both innate and adaptive components of BCR signaling are important in the peripheral tolerance of anti-insulin B cells. Environmental factors that lead to infection and inflammation could play a critical yet under-appreciated role in driving loss of tolerance and promoting autoimmune disease.

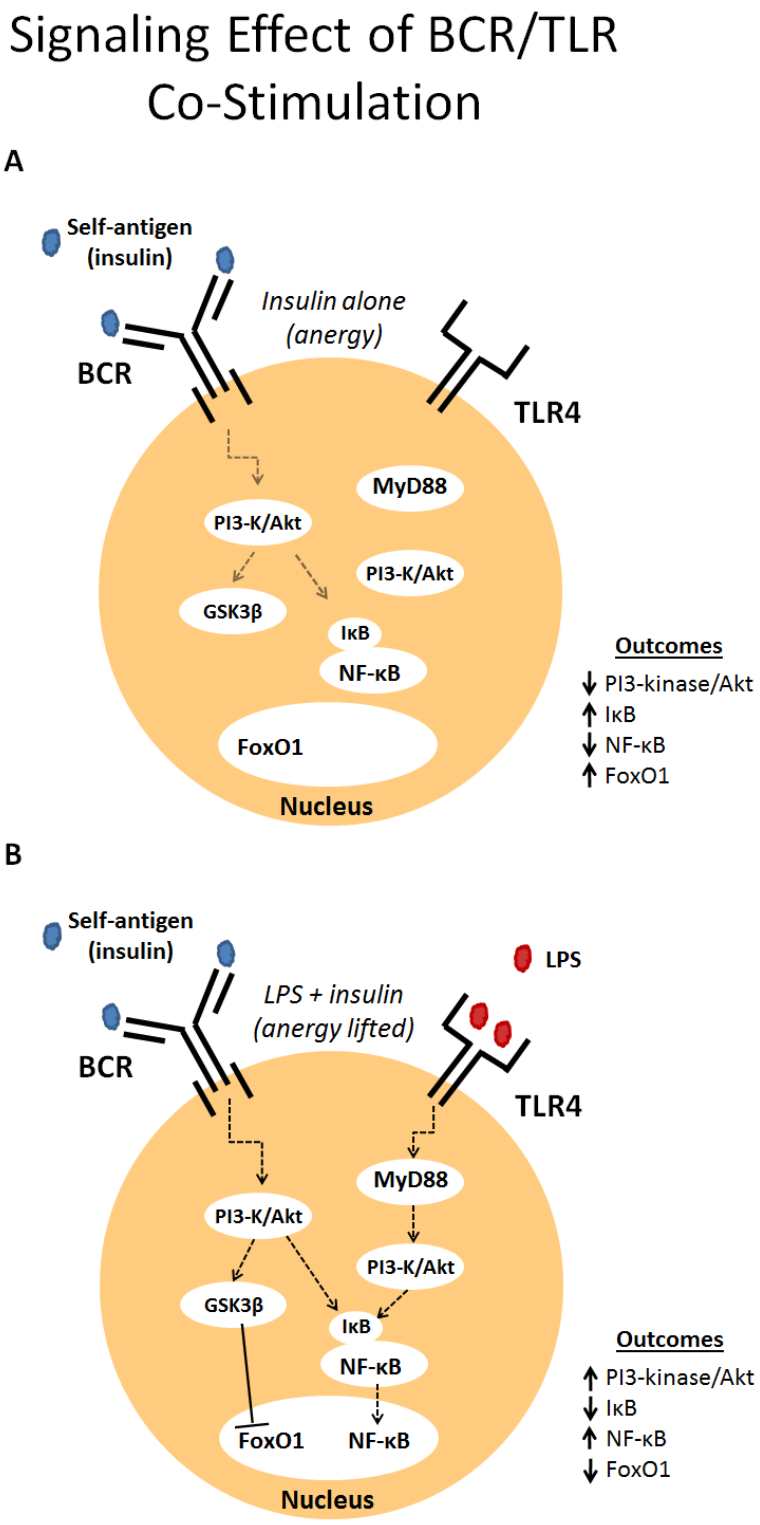

FIGURE IV-1. Signaling effect of BCR/TLR co-stimulation in anti-insulin B cells. Stimulation of anti-insulin B cells with insulin alone enforces anergy **(A)** while BCR/TLR co-stimulation provides a signal that may reverse anergy through a combination of NF-κB activation and FoxO1 repression **(B)**.

Future Directions

I am preparing to transition into the next stage of my career, but there are several new experiments and future directions I think would be very relevant for this project and would serve to strengthen the data already in place. I highlight a few of these proposed experiments below.

Is insulin-BRT truly T-independent?

Insulin-BRT is a conjugate of insulin to an antigen that contains non-canonical LPS and thus TLR4 stimulation potential. It has been largely characterized as a type 1 TI antigen, and my data support this concept. Immunization of V_H125^{SD} B6 mice with insulin-BRT results in clonal expansion of anti-insulin B cells and promotes their entry into antigen-specific GCs and production of IgM and IgG anti-insulin antibodies. These results have raised questions as to whether the synthesized insulin-BRT molecule is truly a TI antigen. Accordingly, I think it would be worthwhile to repeat these immunizations in V_H125^{SD} B6 mice whose T cell repertoire is either eliminated or restricted.

Injection of mice with anti-CD3 (2C11) depletes the T cells, so this would be a viable approach to assess the contribution of T cells to the insulin-BRT response in V_H125^{SD} B6 mice. I could also attempt an adoptive transfer of anti-insulin B cells into irradiated RAG-/- mice, an approach that also would assess the insulin-BRT response in the absence of T cells. The latter is a cleaner approach, however, as anti-CD3 treatment does not guarantee T cell depletion over longer periods of time. Perhaps the simplest approach would be to immunize V_H125^{SD} B6 mice that lack a thymus, as these mice would be completely unable to generate any T cells. I would hypothesize that immunization of V_H125^{SD} B6 mice that were athymic, RAG-deficient, or injected with anti-CD3 would be able to mount an insulin-specific GC response and produce IgM

and IgG antibodies following insulin-BRT immunization. I definitely would not expect the response to be as great as one in a T cell-replete mouse, but that could indicate some bystander T cell effects like cytokine secretion rather than a requirement for cognate anti-insulin T cells to initiate the response.

An entirely different approach is one where the T cell repertoire is not eliminated but rather its specificity is altered. I obtained OT-II TCR Tg mice (Jax) and bred them with my V_H125^{SD} B6 mice to generate V_H125^{SD} x OT-II mice. The T cell repertoire in these mice is specific for ovalbumin, an antigen that is not expressed in mice or humans. Thus, the frequency of cognate anti-insulin T cells in these mice should be very low if not absent. I immunized V_H125^{SD} x OT-II and V_H125^{SD} mice with insulin-BRT and examined whether anti-insulin B cells that lack cognate T cell help *in vivo* were able to mount an insulin-specific GC response and production of IgG anti-insulin antibodies. My hypothesis was that V_H125^{SD} x OT-II mice would still be able to form GCs and produce IgG antibodies; however, the results were not conclusive. I was able to see insulin-specific GCs in V_H125^{SD} x OT-II mice albeit at much lower frequency than in V_H125^{SD} mice following insulin-BRT immunization (data not shown). Surprisingly, IgG anti-insulin antibodies were not detected in either OT-II or V_H125^{SD} x OT-II mice.

This result opposed my theory of insulin-BRT as a TI antigen, and I was perplexed until I discovered in the literature that OT-II mice also completely fail to mount an IgG anti-OVA antibody response to intranasal immunization with OVA-cholera toxin (CT), a TI antigen (138). There is evidence for a defect in OT-II mice to produce antigen-specific IgG antibodies under certain challenges, thus, my results were inconclusive as there was no way to determine whether the lack of anti-insulin antibodies in insulin-BRT-immunized V_H125^{SD} x OT-II mice was due to the lack of cognate T cell help versus an impairment in OT-II mice to produce IgG antibodies.

OT-II mice have been reported to make DNA-specific IgG antibodies following normal i.p. or i.v. immunization, thus, it is not entirely clear why V_H125^{SD} x OT-II mice have a diminished GC response and lack of IgG anti-insulin antibody production. T cell depletion studies would be more advantageous.

Can insulin-BRT-primed anti-insulin B cells respond to TD immunization or T cell help in vitro?

Stimulation with anti-CD40 and insulin *in vitro* enforces tolerance and restricts anti-insulin B cell proliferation. The lack of IgM or IgG anti-insulin antibody response in V_H125^{SD} B6 mice following TD immunization with insulin/CFA validates this concept. It is thought that CD40 signaling is required to rescue anergic B cells, though I have only ever seen the opposite. I think it would be worthwhile to determine whether loss of tolerance in anti-insulin B cells driven by BCR/TLR co-stimulation provided by insulin-BRT immunization can rescue the B cell's ability to respond to anti-CD40. I would take anti-insulin B cells out of freshly immunized insulin-BRT mice and stimulate them with anti-CD40 plus or minus insulin in cell culture to see which "direction" tolerance takes the cell. My hypothesis is that anergy would be enforced upon CD40 stimulation, and all gain-of-function phenotypes in anti-insulin B cells would be lost. My readout would be proliferation and the production of IgG1 anti-insulin antibodies, which are known to arise in WT mice immunized with insulin/CFA. Anti-insulin B cells taken out of a mouse immunized with insulin-BRT will be proliferating, but I should be able to see quantitative differences after anti-CD40 stimulation.

I could also immunize V_H125^{SD} B6 mice with insulin/CFA after initial insulin-BRT immunization and look for IgG1 anti-insulin antibody production. This *in vivo* correlate to the experiment outlined above raises the question of when the necessary T cell epitopes will be

generated. A better approach using an immunization model might be to first immunize with insulin/CFA, and then several days later follow up with insulin-BRT. This experiment asks a slightly different question and probes whether enforcement of anergy upon TD immunization and CD40 signaling can be lifted by BCR/TLR co-stimulation provided by insulin-BRT. Surface IgM expression remains blunted following TD immunization yet is restored with insulin-BRT immunization, so this experiment would determine whether anti-insulin B cells go the direction of an immune response or remain tolerant.

Experiments in V_H125^{SD} NOD mice

All of my experiments were performed in non-autoimmune B6 mice. Thus, while my data has informed a great deal regarding B cell tolerance to insulin, there is ultimately still not a functional consequence to the mice for having an anti-insulin B cell repertoire that is competent to undergo CSR and participate in antigen-specific GC reactions. Disease studies that have been performed to date in V_H125^{SD} NOD mice reveal that these mice get accelerated disease compared to WT NOD mice, similar to what was originally observed in V_H125Tg NOD mice (79). So while the incidence of diabetes may not be different in V_H125^{SD} NOD compared to V_H125Tg NOD mice, it is possible the immunopathology in the former is accelerated *in vivo*. The loss of anergy delivered by BCR/TLR co-stimulation drives clonal expansion of anti-insulin B cells. This may provide a pernicious army of newly capable antigen-presenting cells.

Role of SAP in anti-insulin B cell response to insulin-BRT

Signaling lymphocyte activation molecule-associated protein (SAP) is essential for TD GC reactions (120). SAP-deficient mice exhibit dramatically decreased GC responses and IgG

antibody production, though a role for SAP has only ever been investigated in the context of a TD immune response. I see insulin-specific GCs in V_H125^{SD} B6 mice following insulin-BRT immunization, thus, I wish to determine whether loss of SAP leads to a reduction in the GC response I observe. If SAP is indispensable for GC formation, I would expect a block or reduction in the induction of insulin-specific GCs following insulin-BRT immunization. If SAP-deficient V_H125^{SD} B6 mice still formed GCs, I would conclude that SAP's role in GC formation lies predominantly on the T cell side, and that there is no intrinsic B cell requirement for SAP to engage in a GC reaction that is cognate TI.

Phosphotyrosine Western Blot in Anti-Insulin B Cells

The reversal of anergy observed in anti-insulin B cells upon simultaneous engagement of BCR and TLR4 with insulin and LPS, respectively, must be the result of altered signal transduction in the tolerant cell. Functionally speaking, when anti-insulin B cells are stimulated with antigen alone there is a blunting effect that does not promote gain-of-function, demonstrated by impaired proliferation and Ca^{2+} mobilization in response to insulin *in vitro*. Additionally, treatment with LPS alone induces only a moderate proliferative response. These studies were corroborated *in vivo* using an immunization model, as V_H125^{SD} B6 mice immunized with BRT alone (a TLR4 agonist) did not demonstrate a phenotype, whereas anti-insulin B cells in mice immunized with insulin-BRT produced IgG anti-insulin antibodies and short-lived GC reactions.

Impaired or blunted signal transduction in autoreactive B cells is a hallmark of peripheral tolerance, or anergy. Loss of tolerance in anti-insulin B cells from BCR/TLR4 co-stimulation must alter or re-program BCR signaling in some capacity; otherwise functional BCR-mediated responses to autoAg (insulin) should not occur. Tyrosine phosphorylation is associated with

activation of BCR signal transduction proteins, and Western blotting is commonly used to identify phosphotyrosine residues on these proteins. Therefore, a potentially very informative experiment would be attempting to identify if there is a protein or multiple proteins whose tyrosine phosphorylation profile points to a step in the BCR signaling cascade that is altered upon stimulation of anti-insulin B cells with LPS and insulin. Stimulation with insulin alone should establish the baseline signaling prolife in the tolerant B cells. Naïve MD4 anti-HEL B cells could be used as control to determine the phospho proteins in the BCR signaling cascade that should activate upon stimulation with antigen. If the PI3K/Akt pathway is involved in the reversal of anergy in anti-insulin B cells, as proposed in Fig. IV-1, then differences in phospho Akt should be observed under conditions of BCR/TLR co-stimulation compared to stimulation with insulin or LPS alone.

CHAPTER V

MATERIALS AND METHODS

Targeting Vector and Generation of V_H125^{SD} Mice

$pIV_HL2neoR$ is a vector designed for targeted insertion of a rearranged V_H gene replacing J_H loci, and was a kind gift from Dr. Klaus Rajewsky (139). We first modified $pIV_HL2neoR$ by cloning in two regions of short arm homology (SAH) at *Cla1* and *Not1* sites. This was necessary after initial efforts of homologous recombination were poor. Anti-insulin VDJ_H-125 from our original H chain plus L chain 125Tg mice (77) was sub-cloned into the pGEM-5Z vector and then cloned into modified $pIV_HL2neoR$-SAH at *Sal1* and *Cla1* sites to generate our targeting vector, pIV_H-SAH-125-VDJ_H. All sequences were verified throughout the cloning process. pIV_H-SAH-125-VDJ_H was linearized through digestion with *Not1* and electroporated into 129/Ola ES cells. The electroporated cells were selected for neomycin resistance. ES clone DNA was digested with *Hin*dIII, and Southern blot hybridization using a cDNA probe against an *Xba1* enhancer located upstream of V_H125^{SD} detected the proper 6.1kb fragment size of the construct in the targeted locus. Clones were confirmed by PCR using H chain primers FWD 5'-CAG ATC CAG TTG GTG CAG TC-3' and REV 5'-CCA GAC ATC GAA GTA CCC CT-3'. Positive ES clones were injected into blastocysts and transplanted into pseudopregnant female mice. Tail DNA from founder chimeric pups and their progeny were screened for V_H125^{SD}. Southern blot was used to confirm the presence of the targeted allele. These founder mice were backcrossed onto the C57BL/6 background.

Animals

B6 mice and MD4 anti-HEL mice (B6-Tg [IghelMD4]4Ccg/J) were purchased from Jackson Laboratory, Bar Harbor, ME. EIIA-Cre B6 mice, kindly provided by Dr. Richard Breyer, Vanderbilt University, were intercrossed with V_H125^{SD} mice to permanently remove the neomycin resistance cassette. Transgene transmission was monitored in subsequent generations of site-directed V_H125^{SD} B6 mice using PCR, and flow cytometry confirmed the presence of transgenic IgM^{a+} B cells (> 95%). Male and female mice aged 7-14 weeks were used in these studies and backcrossed > 10 times to B6. All animals were housed in specific pathogen free conditions, and all studies were approved by the AAALAC certified Vanderbilt Institute of Animal Care and Use Committee.

Proliferation Assays

B cells were purified from whole spleens using negative selection with anti-CD43 magnetic beads (MACS, Miltenyi Biotec). Average B cell purity across all experiments performed: V_H125^{SD}/Vκ125Tg – 91.4%, n = 9; MD4 anti-HEL – 91%, n = 8; Wild-type – 92.5%, n = 3. Cells were plated at $2x10^5$ per well in complete RPMI (10% FBS, 1% HEPES, 1% L-Glutamine, 1% gentamycin), and cultured for 72h in a 37°C 5% CO_2 incubator. Cells were pulsed with tritiated thymidine deoxyribose ([^{3}H]-TdR) on d2 and harvested using a semi-automated cell harvester (Skatron) on d3. [^{3}H]-TdR incorporation was measured by scintillation counting, and results are expressed as the mean cpm ± SD for the indicated number of mice in each experimental group. For *in vivo* proliferation experiments, mice were injected i.p. with BrdU per the manufacturer's instructions (BD Pharmingen) 48h and 24h before sacrifice, in both

unimmunized and insulin-BRT immunized mice. FITC-conjugated anti-BrdU (BD Pharmingen) was used to detect intracellular incorporation of BrdU.

Ca^{2+} Mobilization

For Ca^{2+} mobilization assays, anti-insulin B cells were purified as described above using anti-CD43 MACS beads. Cells were washed in Ca^{2+}-free, Mg^{2+}-free media and pre-loaded with Fura-2 fluorescent dye (company, dissolved in DMSO, brought up in media, pluronic acid added) in black 96-well plates (company) for 1 hour at 37°C 5% CO_2. Fura-2 binds to intracellular Ca^{2+}. Cells were washed and stimulated in media that contained Ca^{2+} to measure BCR-mediated Ca^{2+} release and subsequent mobilization of extracellular Ca^{2+}. Productive BCR signaling should promote release of intracellular Ca^{2+}, and the newly internalized Ca^{2+} from outside the cell will bind the Fura-2 dye. Excitation of the fluorescent dye at 340 nm (bound) and 380 nm (free) is compared over a five minute time course with readings every five seconds. B cell stimulation occurs at 45 seconds of the time course.

Antibodies and Flow Cytometry

Antibodies reactive to murine B220 (RA3-6B2), IgM^a (DS-1), IgM^b (AF6-78), CD21 (7G6), CD23 (B3B4), IgD (11-26), CD86 (GL1), $I\text{-}A^b$ (25-9-17), GL7, or Fas/CD95 (Jo2) (BD Pharmingen), or IgM (μ-chain specific, Invitrogen) were used, along with biotinylated human insulin (114) or anti-insulin mAb 123 (140) with streptavidin-conjugated fluorochrome to detect insulin-binding B cells, and 7-aminoactinomycin D for cell viability. Flow cytometry acquisition was performed after cell suspension in FACS buffer (1X PBS, 10% FBS, 1% sodium azide, 1% EDTA) using an LSR II (BD Biosciences), and sorting experiments were performed using a

FACSAria I or II cell sorter in the Vanderbilt University Shared Resource Facility. Analysis was performed using FlowJo software (Treestar).

Immunization and ELISA

For TD assays, pre-immune sera were collected, and mice were immunized with 40-50 µg bovine insulin in 1X PBS emulsified in either CFA s.c. at the base of the tail or in IFA i.p., and sera were collected 2-3 weeks later. For TI assays, mice were immunized i.p. with human insulin-conjugated *Brucella abortus* ring test antigen (insulin-BRT) (90), BRT alone, or with physically mixed BRT and insulin, and sera were collected at 5-7 days following immunization. Anti-insulin antibodies were measured by ELISA as follows: briefly, 96-well flat-bottom NUNC plates were coated with human insulin in borate buffered saline overnight at 37˚C. Plates were extensively washed with 1X PBS-Tween (0.05%). Diluted sera (1:100) were added to the coated plates with or without 100X soluble human insulin to measure specific, inhibitable anti-insulin antibodies. IgM and IgG anti-insulin antibodies were detected using the following allotype-specific secondary antibodies: IgM^a-biotin (DS-1), $IgG1^a$-biotin (10.9), or $IgG2a^a$-biotin (8.3) for transgenic anti-insulin B cells, or IgM^b-biotin (AF6-78), $IgG1^b$-biotin (B68-2), or $IgG2c^b$-biotin (5.7) (BD Pharmingen) for non-transgenic or WT B cells. Avidin-alkaline phosphatase (AP) (Sigma), or goat anti-mouse IgM-AP or IgG-AP antibodies (Southern Biotech) were added. After washing, p-Nitrophenyl Phosphate substrate (Sigma) was added to the plate and immediately read on a Microplate Autoreader (Bio-Tek Instruments) at O.D. 405 nm. Inhibitable (insulin-specific) binding was determined by the difference in binding in the presence of excess competitive insulin.

Immunohistochemistry

Spleens were removed from unimmunized or insulin-BRT immunized V_H125^{SD} B6 mice and soaked in 30% sucrose (w/v) overnight at 4˚C and snap frozen in OCT medium on dry ice. 8 µM sections were obtained from the Vanderbilt Translational Pathology Shared Resource. Sections were fixed with 4% paraformaldehyde in 0.1M PBS and stained with the following antibody cocktails: IgM Alexa Flour 488 (Life Technologies), IgD^a-biotin (AMS 9.1, BD Pharmingen) plus streptavidin Alexa Flour 350 (Life Technologies), and CD3 PE (17A2, BD Pharmingen) to define follicular architecture, or GL7 FITC, IgD^a-biotin plus streptavidin Texas Red (Molecular Probes), and DAPI (Molecular Probes) to detect GCs. Images were obtained using an Olympus BX60 fluorescent microscope with MagnaFire software. Adobe Photoshop was used to adjust brightness and contrast, and to overlay images.

Pancreata were dissected from unimmunized or insulin-BRT-immunized V_H125^{SD} B6 mice or from 12-16 week old female NOD mice (as a positive control for insulitis assessment) and placed into neutral buffered formalin. After 4-6 h, tissues were transferred to 70% ethanol and incubated overnight. Tissues were subsequently paraffin embedded, 5µm sections were cut, and slides were stained with H&E by the Vanderbilt Translational Pathology Shared Resource. Slides were blind scored for insulitis by light microscopy using the following scale: 0 = no insulitis; 1 = peri-insulitis, < 25% islet infiltration; 2 = 25-50% islet infiltration; 3 = 50-75% islet infiltration; 4 = > 75% islet infiltration. Half of the pancreas was fixed with paraformaldehyde in 0.1M PBS and soaked in 30% sucrose overnight at 4˚C, and then snap frozen in OCT medium on dry ice. 8 µM sections were stained for immunofluorescence with DAPI and biotinylated anti-$IgG2a^a$ plus FITC-conjugated streptavidin.

Light Chain Cloning and Sequencing

Spleens were harvested from unimmunized V_H125^{SD} B6 mice or from mice 4 days following insulin-BRT immunization. Human insulin-binding B cells ($B220^+$ live lymphocytes) were identified by FACS and further gated as IgM^+ non-GC ($GL7^-$ Fas^-), IgM^+ GC ($GL7^+$ Fas^+), or IgM^- GC populations. Cells were sorted directly into RNAqueous lysis buffer, and RNA was isolated using the RNAqueous-Micro Total RNA Isolation Kit per the manufacturer's instructions (Life Technologies). Independent clones were derived from separate tubes of lysate. RNA was reverse transcribed into cDNA using Superscript II RT (Invitrogen) and oligo-dT primer (GE Healthcare) in a standard protocol. Resulting cDNA was used as PCR template to amplify Igκ genes using a murine Vκ primer, 5′−ATT GTK MTS ACM CAR TCT CCA-3′, and murine Cκ primer, 5′−GGA TAC AGT TGG TGC AGC ATC-3′, where K = G or T, M = A or C, S = C or G, and R = A or G with a 44°C annealing temperature. Appropriately sized PCR products were gel purified using the MinElute Gel Extraction Kit (Qiagen) and Igκ were cloned as described previously (141, 142). Vκ and Jκ gene segment identities were assigned using Ig BLAST (http://www.ncbi.nlm.nih.gov/igblast/) with CDR boundaries defined by the KABAT V domain delineation system. Nucleotide mutation analyses were also performed using Ig BLAST.

Generation of Anti-Insulin Hybridomas

Splenocytes from V_H125^{SD} B6 mice four days following insulin-BRT immunization were fused with an NSO myeloma cell line and plated at limiting dilution to select rare clones that secreted anti-insulin antibodies. Approximately 6 x 10^7 spleen cells were fused with 7 x 10^7 NSO cells using polyethylene glycol (Fluka) in Ca^{2+}/Mg^{2+}-free Hank's balanced salt solution and placed in 96 well plates at 2.5 x 10^4 cells/well. Fused cells were selected in hybridoma media

(DMEM containing 10% FCS, 10% NCTC 109, 1% HEPES, 1% L-glutamine, 1% non-essential amino acids, 1% penicillin/streptomycin, and 1% Na^+ pyruvate) with 1X HAT (hypoxanthine, aminopterin, thymidine) (Sigma). The small proportion of wells that demonstrated initial growth (less than 2%) were expanded, and the hybridoma supernatants were screened for IgM and IgG anti-insulin antibodies by ELISA.

REFERENCES

1. Topham, N. J., and E. W. Hewitt. 2009. Natural killer cell cytotoxicity: how do they pull the trigger? *Immunology* 128: 7-15.
2. Vivier, E., E. Tomasello, M. Baratin, T. Walzer, and S. Ugolini. 2008. Functions of natural killer cells. *Nature immunology* 9: 503-510.
3. Mayer, M. M. 1972. Mechanism of cytolysis by complement. *Proceedings of the National Academy of Sciences of the United States of America* 69: 2954-2958.
4. Hammer, C. H., A. Nicholson, and M. M. Mayer. 1975. On the mechanism of cytolysis by complement: evidence on insertion of C5b and C7 subunits of the C5b,6,7 complex into phospholipid bilayers of erythrocyte membranes. *Proceedings of the National Academy of Sciences of the United States of America* 72: 5076-5080.
5. Verbrugh, H. A., P. K. Peterson, B. Y. Nguyen, S. P. Sisson, and Y. Kim. 1982. Opsonization of encapsulated Staphylococcus aureus: the role of specific antibody and complement. *Journal of immunology* 129: 1681-1687.
6. Zanella, A., and W. Barcellini. 2014. Treatment of autoimmune hemolytic anemias. *Haematologica* 99: 1547-1554.
7. Yoshimura, A., E. Lien, R. R. Ingalls, E. Tuomanen, R. Dziarski, and D. Golenbock. 1999. Cutting edge: recognition of Gram-positive bacterial cell wall components by the innate immune system occurs via Toll-like receptor 2. *Journal of immunology* 163: 1-5.
8. Aliprantis, A. O., R. B. Yang, M. R. Mark, S. Suggett, B. Devaux, J. D. Radolf, G. R. Klimpel, P. Godowski, and A. Zychlinsky. 1999. Cell activation and apoptosis by bacterial lipoproteins through toll-like receptor-2. *Science* 285: 736-739.
9. Alexopoulou, L., A. C. Holt, R. Medzhitov, and R. A. Flavell. 2001. Recognition of double-stranded RNA and activation of NF-kappaB by Toll-like receptor 3. *Nature* 413: 732-738.
10. Hemmi, H., T. Kaisho, O. Takeuchi, S. Sato, H. Sanjo, K. Hoshino, T. Horiuchi, H. Tomizawa, K. Takeda, and S. Akira. 2002. Small anti-viral compounds activate immune cells via the TLR7 MyD88-dependent signaling pathway. *Nature immunology* 3: 196-200.
11. Schnare, M., A. C. Holt, K. Takeda, S. Akira, and R. Medzhitov. 2000. Recognition of CpG DNA is mediated by signaling pathways dependent on the adaptor protein MyD88. *Current biology : CB* 10: 1139-1142.
12. Takeuchi, O., K. Hoshino, T. Kawai, H. Sanjo, H. Takada, T. Ogawa, K. Takeda, and S. Akira. 1999. Differential roles of TLR2 and TLR4 in recognition of gram-negative and gram-positive bacterial cell wall components. *Immunity* 11: 443-451.
13. Hoshino, K., O. Takeuchi, T. Kawai, H. Sanjo, T. Ogawa, Y. Takeda, K. Takeda, and S. Akira. 1999. Cutting edge: Toll-like receptor 4 (TLR4)-deficient mice are hyporesponsive to lipopolysaccharide: evidence for TLR4 as the Lps gene product. *Journal of immunology* 162: 3749-3752.
14. Hayashi, F., K. D. Smith, A. Ozinsky, T. R. Hawn, E. C. Yi, D. R. Goodlett, J. K. Eng, S. Akira, D. M. Underhill, and A. Aderem. 2001. The innate immune response to bacterial flagellin is mediated by Toll-like receptor 5. *Nature* 410: 1099-1103.

15. Takeuchi, O., T. Kawai, P. F. Muhlradt, M. Morr, J. D. Radolf, A. Zychlinsky, K. Takeda, and S. Akira. 2001. Discrimination of bacterial lipoproteins by Toll-like receptor 6. *International immunology* 13: 933-940.
16. Wyllie, D. H., E. Kiss-Toth, A. Visintin, S. C. Smith, S. Boussouf, D. M. Segal, G. W. Duff, and S. K. Dower. 2000. Evidence for an accessory protein function for Toll-like receptor 1 in anti-bacterial responses. *Journal of immunology* 165: 7125-7132.
17. Takeuchi, O., S. Sato, T. Horiuchi, K. Hoshino, K. Takeda, Z. Dong, R. L. Modlin, and S. Akira. 2002. Cutting edge: role of Toll-like receptor 1 in mediating immune response to microbial lipoproteins. *Journal of immunology* 169: 10-14.
18. Bekeredjian-Ding, I., and G. Jego. 2009. Toll-like receptors--sentries in the B-cell response. *Immunology* 128: 311-323.
19. Hua, Z., and B. Hou. 2013. TLR signaling in B-cell development and activation. *Cellular & molecular immunology* 10: 103-106.
20. Baeuerle, P. A., and T. Henkel. 1994. Function and activation of NF-kappa B in the immune system. *Annual review of immunology* 12: 141-179.
21. Gerondakis, S., and U. Siebenlist. 2010. Roles of the NF-kappaB pathway in lymphocyte development and function. *Cold Spring Harbor perspectives in biology* 2: a000182.
22. Takeda, K., and S. Akira. 2004. TLR signaling pathways. *Seminars in immunology* 16: 3-9.
23. Bagchi, A., E. A. Herrup, H. S. Warren, J. Trigilio, H. S. Shin, C. Valentine, and J. Hellman. 2007. MyD88-dependent and MyD88-independent pathways in synergy, priming, and tolerance between TLR agonists. *Journal of immunology* 178: 1164-1171.
24. Marshak-Rothstein, A. 2006. Toll-like receptors in systemic autoimmune disease. *Nature reviews. Immunology* 6: 823-835.
25. Kurosaki, T., K. Kometani, and W. Ise. 2015. Memory B cells. *Nature reviews. Immunology* 15: 149-159.
26. MacLeod, M. K., J. W. Kappler, and P. Marrack. 2010. Memory CD4 T cells: generation, reactivation and re-assignment. *Immunology* 130: 10-15.
27. Blattner, F. R., and P. W. Tucker. 1984. The molecular biology of immunoglobulin D. *Nature* 307: 417-422.
28. Stavnezer, J., J. E. Guikema, and C. E. Schrader. 2008. Mechanism and regulation of class switch recombination. *Annual review of immunology* 26: 261-292.
29. Hsu, M. C., K. M. Toellner, C. G. Vinuesa, and I. C. Maclennan. 2006. B cell clones that sustain long-term plasmablast growth in T-independent extrafollicular antibody responses. *Proceedings of the National Academy of Sciences of the United States of America* 103: 5905-5910.
30. Grewal, I. S., and R. A. Flavell. 1996. The role of CD40 ligand in costimulation and T-cell activation. *Immunological reviews* 153: 85-106.
31. Smith, K. G., G. J. Nossal, and D. M. Tarlinton. 1995. FAS is highly expressed in the germinal center but is not required for regulation of the B-cell response to antigen. *Proceedings of the National Academy of Sciences of the United States of America* 92: 11628-11632.
32. Hao, Z., G. S. Duncan, J. Seagal, Y. W. Su, C. Hong, J. Haight, N. J. Chen, A. Elia, A. Wakeham, W. Y. Li, J. Liepa, G. A. Wood, S. Casola, K. Rajewsky, and T. W. Mak. 2008.

Fas receptor expression in germinal-center B cells is essential for T and B lymphocyte homeostasis. *Immunity* 29: 615-627.
33. Di Niro, R., S. J. Lee, J. A. Vander Heiden, R. A. Elsner, N. Trivedi, J. M. Bannock, N. T. Gupta, S. H. Kleinstein, F. Vigneault, T. J. Gilbert, E. Meffre, S. J. McSorley, and M. J. Shlomchik. 2015. Salmonella Infection Drives Promiscuous B Cell Activation Followed by Extrafollicular Affinity Maturation. *Immunity* 43: 120-131.
34. Owen, R. D. 1945. Immunogenetic Consequences of Vascular Anastomoses between Bovine Twins. *Science* 102: 400-401.
35. Wood, K. J., A. R. Bushell, and N. D. Jones. 2010. The discovery of immunological tolerance: now more than just a laboratory solution. *Journal of immunology* 184: 3-4.
36. Billingham, R. E., L. Brent, and P. B. Medawar. 1953. Actively acquired tolerance of foreign cells. *Nature* 172: 603-606.
37. Zhang, M., G. Srivastava, and L. Lu. 2004. The pre-B cell receptor and its function during B cell development. *Cellular & molecular immunology* 1: 89-94.
38. Nemazee, D. A., and K. Burki. 1989. Clonal deletion of B lymphocytes in a transgenic mouse bearing anti-MHC class I antibody genes. *Nature* 337: 562-566.
39. Pelanda, R., and R. M. Torres. 2012. Central B-cell tolerance: where selection begins. *Cold Spring Harbor perspectives in biology* 4: a007146.
40. Casellas, R., T. A. Shih, M. Kleinewietfeld, J. Rakonjac, D. Nemazee, K. Rajewsky, and M. C. Nussenzweig. 2001. Contribution of receptor editing to the antibody repertoire. *Science* 291: 1541-1544.
41. Radic, M. Z., J. Erikson, S. Litwin, and M. Weigert. 1993. B lymphocytes may escape tolerance by revising their antigen receptors. *The Journal of experimental medicine* 177: 1165-1173.
42. Tiegs, S. L., D. M. Russell, and D. Nemazee. 1993. Receptor editing in self-reactive bone marrow B cells. *The Journal of experimental medicine* 177: 1009-1020.
43. Chen, C., Z. Nagy, E. L. Prak, and M. Weigert. 1995. Immunoglobulin heavy chain gene replacement: a mechanism of receptor editing. *Immunity* 3: 747-755.
44. Nemazee, D., and K. Buerki. 1989. Clonal deletion of autoreactive B lymphocytes in bone marrow chimeras. *Proceedings of the National Academy of Sciences of the United States of America* 86: 8039-8043.
45. Liu, S., M. G. Velez, J. Humann, S. Rowland, F. J. Conrad, R. Halverson, R. M. Torres, and R. Pelanda. 2005. Receptor editing can lead to allelic inclusion and development of B cells that retain antibodies reacting with high avidity autoantigens. *Journal of immunology* 175: 5067-5076.
46. Hubert, F. X., S. A. Kinkel, G. M. Davey, B. Phipson, S. N. Mueller, A. Liston, A. I. Proietto, P. Z. Cannon, S. Forehan, G. K. Smyth, L. Wu, C. C. Goodnow, F. R. Carbone, H. S. Scott, and W. R. Heath. 2011. Aire regulates the transfer of antigen from mTECs to dendritic cells for induction of thymic tolerance. *Blood* 118: 2462-2472.
47. Ruan, Q. G., K. Tung, D. Eisenman, Y. Setiady, S. Eckenrode, B. Yi, S. Purohit, W. P. Zheng, Y. Zhang, L. Peltonen, and J. X. She. 2007. The autoimmune regulator directly controls the expression of genes critical for thymic epithelial function. *Journal of immunology* 178: 7173-7180.
48. Vafiadis, P., S. T. Bennett, J. A. Todd, J. Nadeau, R. Grabs, C. G. Goodyer, S. Wickramasinghe, E. Colle, and C. Polychronakos. 1997. Insulin expression in human

thymus is modulated by INS VNTR alleles at the IDDM2 locus. *Nature genetics* 15: 289-292.
49. Cambier, J. C., S. B. Gauld, K. T. Merrell, and B. J. Vilen. 2007. B-cell anergy: from transgenic models to naturally occurring anergic B cells? *Nature reviews. Immunology* 7: 633-643.
50. Yarkoni, Y., A. Getahun, and J. C. Cambier. 2010. Molecular underpinning of B-cell anergy. *Immunological reviews* 237: 249-263.
51. Sakaguchi, S., K. Wing, Y. Onishi, P. Prieto-Martin, and T. Yamaguchi. 2009. Regulatory T cells: how do they suppress immune responses? *International immunology* 21: 1105-1111.
52. Kim, J., K. Lahl, S. Hori, C. Loddenkemper, A. Chaudhry, P. deRoos, A. Rudensky, and T. Sparwasser. 2009. Cutting edge: depletion of Foxp3+ cells leads to induction of autoimmunity by specific ablation of regulatory T cells in genetically targeted mice. *Journal of immunology* 183: 7631-7634.
53. Goodnow, C. C., J. Crosbie, S. Adelstein, T. B. Lavoie, S. J. Smith-Gill, R. A. Brink, H. Pritchard-Briscoe, J. S. Wotherspoon, R. H. Loblay, K. Raphael, and et al. 1988. Altered immunoglobulin expression and functional silencing of self-reactive B lymphocytes in transgenic mice. *Nature* 334: 676-682.
54. Srinivasan, L., Y. Sasaki, D. P. Calado, B. Zhang, J. H. Paik, R. A. DePinho, J. L. Kutok, J. F. Kearney, K. L. Otipoby, and K. Rajewsky. 2009. PI3 kinase signals BCR-dependent mature B cell survival. *Cell* 139: 573-586.
55. Liu, Z., and A. Davidson. 2011. BAFF and selection of autoreactive B cells. *Trends in immunology* 32: 388-394.
56. Jacque, E., E. Schweighoffer, V. L. Tybulewicz, and S. C. Ley. 2015. BAFF activation of the ERK5 MAP kinase pathway regulates B cell survival. *The Journal of experimental medicine* 212: 883-892.
57. Goodnow, C. C., J. Crosbie, H. Jorgensen, R. A. Brink, and A. Basten. 1989. Induction of self-tolerance in mature peripheral B lymphocytes. *Nature* 342: 385-391.
58. Getahun, A., S. K. O'Neill, and J. C. Cambier. 2009. Establishing anergy as a bona fide in vivo mechanism of B cell tolerance. *Journal of immunology* 183: 5439-5441.
59. Merrell, K. T., R. J. Benschop, S. B. Gauld, K. Aviszus, D. Decote-Ricardo, L. J. Wysocki, and J. C. Cambier. 2006. Identification of anergic B cells within a wild-type repertoire. *Immunity* 25: 953-962.
60. Hikida, M., and T. Kurosaki. 2005. Regulation of phospholipase C-gamma2 networks in B lymphocytes. *Advances in immunology* 88: 73-96.
61. Fruman, D. A., and G. Bismuth. 2009. Fine tuning the immune response with PI3K. *Immunological reviews* 228: 253-272.
62. Menard, L., D. Saadoun, I. Isnardi, Y. S. Ng, G. Meyers, C. Massad, C. Price, C. Abraham, R. Motaghedi, J. H. Buckner, P. K. Gregersen, and E. Meffre. 2011. The PTPN22 allele encoding an R620W variant interferes with the removal of developing autoreactive B cells in humans. *The Journal of clinical investigation* 121: 3635-3644.
63. Avalos, A. M., L. Busconi, and A. Marshak-Rothstein. 2010. Regulation of autoreactive B cell responses to endogenous TLR ligands. *Autoimmunity* 43: 76-83.
64. Avalos, A. M., M. B. Uccellini, P. Lenert, G. A. Viglianti, and A. Marshak-Rothstein. 2010. FcgammaRIIB regulation of BCR/TLR-dependent autoreactive B-cell responses. *European journal of immunology* 40: 2692-2698.

65. Maglione, P. J., N. Simchoni, S. Black, L. Radigan, J. R. Overbey, E. Bagiella, J. B. Bussel, X. Bossuyt, J. L. Casanova, I. Meyts, A. Cerutti, C. Picard, and C. Cunningham-Rundles. 2014. IRAK-4 and MyD88 deficiencies impair IgM responses against T-independent bacterial antigens. *Blood* 124: 3561-3571.
66. Dye, J. R., A. Palvanov, B. Guo, and T. L. Rothstein. 2007. B cell receptor cross-talk: exposure to lipopolysaccharide induces an alternate pathway for B cell receptor-induced ERK phosphorylation and NF-kappa B activation. *Journal of immunology* 179: 229-235.
67. Kendall, P. L., G. Yu, E. J. Woodward, and J. W. Thomas. 2007. Tertiary lymphoid structures in the pancreas promote selection of B lymphocytes in autoimmune diabetes. *Journal of immunology* 178: 5643-5651.
68. Kendall, P. L., J. B. Case, A. M. Sullivan, J. S. Holderness, K. S. Wells, E. Liu, and J. W. Thomas. 2013. Tolerant anti-insulin B cells are effective APCs. *Journal of immunology* 190: 2519-2526.
69. Schwartz, R. H. 2003. T cell anergy. *Annual review of immunology* 21: 305-334.
70. Lin, X., M. Chen, Y. Liu, Z. Guo, X. He, D. Brand, and S. G. Zheng. 2013. Advances in distinguishing natural from induced Foxp3(+) regulatory T cells. *International journal of clinical and experimental pathology* 6: 116-123.
71. Fontenot, J. D., M. A. Gavin, and A. Y. Rudensky. 2003. Foxp3 programs the development and function of CD4+CD25+ regulatory T cells. *Nature immunology* 4: 330-336.
72. Feuerer, M., Y. Shen, D. R. Littman, C. Benoist, and D. Mathis. 2009. How punctual ablation of regulatory T cells unleashes an autoimmune lesion within the pancreatic islets. *Immunity* 31: 654-664.
73. Gay, D., T. Saunders, S. Camper, and M. Weigert. 1993. Receptor editing: an approach by autoreactive B cells to escape tolerance. *The Journal of experimental medicine* 177: 999-1008.
74. Kouskoff, V., G. Lacaud, and D. Nemazee. 2000. T cell-independent rescue of B lymphocytes from peripheral immune tolerance. *Science* 287: 2501-2503.
75. Caucheteux, S. M., C. Vernochet, J. Wantyghem, M. C. Gendron, and C. Kanellopoulos-Langevin. 2008. Tolerance induction to self-MHC antigens in fetal and neonatal mouse B cells. *International immunology* 20: 11-20.
76. Hartley, S. B., J. Crosbie, R. Brink, A. B. Kantor, A. Basten, and C. C. Goodnow. 1991. Elimination from peripheral lymphoid tissues of self-reactive B lymphocytes recognizing membrane-bound antigens. *Nature* 353: 765-769.
77. Rojas, M., C. Hulbert, and J. W. Thomas. 2001. Anergy and not clonal ignorance determines the fate of B cells that recognize a physiological autoantigen. *Journal of immunology* 166: 3194-3200.
78. Acevedo-Suarez, C. A., C. Hulbert, E. J. Woodward, and J. W. Thomas. 2005. Uncoupling of anergy from developmental arrest in anti-insulin B cells supports the development of autoimmune diabetes. *Journal of immunology* 174: 827-833.
79. Hulbert, C., B. Riseili, M. Rojas, and J. W. Thomas. 2001. B cell specificity contributes to the outcome of diabetes in nonobese diabetic mice. *Journal of immunology* 167: 5535-5538.

80. Koczwara, K., M. Schenker, S. Schmid, K. Kredel, A. G. Ziegler, and E. Bonifacio. 2003. Characterization of antibody responses to endogenous and exogenous antigen in the nonobese diabetic mouse. *Clinical immunology* 106: 155-162.
81. Boes, M., T. Schmidt, K. Linkemann, B. C. Beaudette, A. Marshak-Rothstein, and J. Chen. 2000. Accelerated development of IgG autoantibodies and autoimmune disease in the absence of secreted IgM. *Proceedings of the National Academy of Sciences of the United States of America* 97: 1184-1189.
82. Hoppu, S., M. S. Ronkainen, T. Kimpimaki, S. Simell, S. Korhonen, J. Ilonen, O. Simell, and M. Knip. 2004. Insulin autoantibody isotypes during the prediabetic process in young children with increased genetic risk of type 1 diabetes. *Pediatric research* 55: 236-242.
83. Hahn, B. H. 1998. Antibodies to DNA. *The New England journal of medicine* 338: 1359-1368.
84. Zhang, L., M. Nakayama, and G. S. Eisenbarth. 2008. Insulin as an autoantigen in NOD/human diabetes. *Current opinion in immunology* 20: 111-118.
85. Nakayama, M. 2011. Insulin as a key autoantigen in the development of type 1 diabetes. *Diabetes/metabolism research and reviews* 27: 773-777.
86. Schroer, J. A., T. Bender, R. J. Feldmann, and K. J. Kim. 1983. Mapping epitopes on the insulin molecule using monoclonal antibodies. *European journal of immunology* 13: 693-700.
87. Mease, P. J. 2008. B cell-targeted therapy in autoimmune disease: rationale, mechanisms, and clinical application. *The Journal of rheumatology* 35: 1245-1255.
88. Bliss, M. 1982. *The discovery of insulin*. University of Chicago Press, Chicago.
89. Yalow, R. S., and S. A. Berson. 1960. Immunoassay of endogenous plasma insulin in man. *The Journal of clinical investigation* 39: 1157-1175.
90. Schroer, J. A., J. K. Inman, J. W. Thomas, and A. S. Rosenthal. 1979. H-2-linked Ir gene control of antibody responses to insulin. I. Anti-insulin plaque-forming cell primary responses. *Journal of immunology* 123: 670-675.
91. Tsirogianni, A., E. Pipi, and K. Soufleros. 2009. Specificity of islet cell autoantibodies and coexistence with other organ specific autoantibodies in type 1 diabetes mellitus. *Autoimmunity reviews* 8: 687-691.
92. Wardemann, H., S. Yurasov, A. Schaefer, J. W. Young, E. Meffre, and M. C. Nussenzweig. 2003. Predominant autoantibody production by early human B cell precursors. *Science* 301: 1374-1377.
93. Chiu, P. P., D. V. Serreze, and J. S. Danska. 2001. Development and function of diabetogenic T-cells in B-cell-deficient nonobese diabetic mice. *Diabetes* 50: 763-770.
94. Berry, G., and H. Waldner. 2013. Accelerated type 1 diabetes induction in mice by adoptive transfer of diabetogenic CD4+ T cells. *Journal of visualized experiments : JoVE*: e50389.
95. Thomas, J. W., R. P. Bucy, and J. A. Kapp. 1982. T cell-independent responses to an Ir gene-controlled antigen. I. Characteristics of the immune response to insulin complexed to Brucella abortus. *Journal of immunology* 129: 6-10.
96. Phan, T. G., M. Amesbury, S. Gardam, J. Crosbie, J. Hasbold, P. D. Hodgkin, A. Basten, and R. Brink. 2003. B cell receptor-independent stimuli trigger immunoglobulin (Ig)

class switch recombination and production of IgG autoantibodies by anergic self-reactive B cells. *The Journal of experimental medicine* 197: 845-860.
97. Stadanlick, J. E., and M. P. Cancro. 2008. BAFF and the plasticity of peripheral B cell tolerance. *Current opinion in immunology* 20: 158-161.
98. Chen, X., F. Martin, K. A. Forbush, R. M. Perlmutter, and J. F. Kearney. 1997. Evidence for selection of a population of multi-reactive B cells into the splenic marginal zone. *International immunology* 9: 27-41.
99. Kanayama, N., M. Cascalho, and H. Ohmori. 2005. Analysis of marginal zone B cell development in the mouse with limited B cell diversity: role of the antigen receptor signals in the recruitment of B cells to the marginal zone. *Journal of immunology* 174: 1438-1445.
100. Duan, B., and L. Morel. 2006. Role of B-1a cells in autoimmunity. *Autoimmunity reviews* 5: 403-408.
101. Gururajan, M., J. Jacob, and B. Pulendran. 2007. Toll-like receptor expression and responsiveness of distinct murine splenic and mucosal B-cell subsets. *PloS one* 2: e863.
102. Acevedo-Suarez, C. A., D. M. Kilkenny, M. B. Reich, and J. W. Thomas. 2006. Impaired intracellular calcium mobilization and NFATc1 availability in tolerant anti-insulin B cells. *Journal of immunology* 177: 2234-2241.
103. Morgan, A. J., and R. Jacob. 1994. Ionomycin enhances Ca2+ influx by stimulating store-regulated cation entry and not by a direct action at the plasma membrane. *The Biochemical journal* 300 (Pt 3): 665-672.
104. Aki, D., Y. Minoda, H. Yoshida, S. Watanabe, R. Yoshida, G. Takaesu, T. Chinen, T. Inaba, M. Hikida, T. Kurosaki, K. Saeki, and A. Yoshimura. 2008. Peptidoglycan and lipopolysaccharide activate PLCgamma2, leading to enhanced cytokine production in macrophages and dendritic cells. *Genes to cells : devoted to molecular & cellular mechanisms* 13: 199-208.
105. Chiang, C. Y., V. Veckman, K. Limmer, and M. David. 2012. Phospholipase Cgamma-2 and intracellular calcium are required for lipopolysaccharide-induced Toll-like receptor 4 (TLR4) endocytosis and interferon regulatory factor 3 (IRF3) activation. *The Journal of biological chemistry* 287: 3704-3709.
106. Nakanishi, K., K. Matsui, S. Kashiwamura, Y. Nishioka, J. Nomura, Y. Nishimura, N. Sakaguchi, S. Yonehara, K. Higashino, and S. Shinka. 1996. IL-4 and anti-CD40 protect against Fas-mediated B cell apoptosis and induce B cell growth and differentiation. *International immunology* 8: 791-798.
107. Bonami, R. H., W. T. Wolfle, J. W. Thomas, and P. L. Kendall. 2014. NFATc2 (NFAT1) assists BCR-mediated anergy in anti-insulin B cells. *Molecular immunology* 62: 321-328.
108. Forestier, C., E. Moreno, S. Meresse, A. Phalipon, D. Olive, P. Sansonetti, and J. P. Gorvel. 1999. Interaction of Brucella abortus lipopolysaccharide with major histocompatibility complex class II molecules in B lymphocytes. *Infection and immunity* 67: 4048-4054.
109. Betts, M., P. Beining, M. Brunswick, J. Inman, R. D. Angus, T. Hoffman, and B. Golding. 1993. Lipopolysaccharide from Brucella abortus behaves as a T-cell-independent type 1 carrier in murine antigen-specific antibody responses. *Infection and immunity* 61: 1722-1729.

110. Mond, J. J., I. Scher, D. E. Mosier, M. Baese, and W. E. Paul. 1978. T-independent responses in B cell-defective CBA/N mice to Brucella abortus and to trinitrophenyl (TNP) conjugates of Brucella abortus. *European journal of immunology* 8: 459-463.
111. Wang, D., S. M. Wells, A. M. Stall, and E. A. Kabat. 1994. Reaction of germinal centers in the T-cell-independent response to the bacterial polysaccharide alpha(1-->6)dextran. *Proceedings of the National Academy of Sciences of the United States of America* 91: 2502-2506.
112. de Vinuesa, C. G., M. C. Cook, J. Ball, M. Drew, Y. Sunners, M. Cascalho, M. Wabl, G. G. Klaus, and I. C. MacLennan. 2000. Germinal centers without T cells. *The Journal of experimental medicine* 191: 485-494.
113. Enzler, T., G. Bonizzi, G. J. Silverman, D. C. Otero, G. F. Widhopf, A. Anzelon-Mills, R. C. Rickert, and M. Karin. 2006. Alternative and classical NF-kappa B signaling retain autoreactive B cells in the splenic marginal zone and result in lupus-like disease. *Immunity* 25: 403-415.
114. Henry-Bonami, R. A., J. M. Williams, A. B. Rachakonda, M. Karamali, P. L. Kendall, and J. W. Thomas. 2013. B lymphocyte "original sin" in the bone marrow enhances islet autoreactivity in type 1 diabetes-prone nonobese diabetic mice. *Journal of immunology* 190: 5992-6003.
115. Thompson, C. B., T. Lindsten, J. A. Ledbetter, S. L. Kunkel, H. A. Young, S. G. Emerson, J. M. Leiden, and C. H. June. 1989. CD28 activation pathway regulates the production of multiple T-cell-derived lymphokines/cytokines. *Proceedings of the National Academy of Sciences of the United States of America* 86: 1333-1337.
116. Howland, K. C., L. J. Ausubel, C. A. London, and A. K. Abbas. 2000. The roles of CD28 and CD40 ligand in T cell activation and tolerance. *Journal of immunology* 164: 4465-4470.
117. Gavin, A. L., K. Hoebe, B. Duong, T. Ota, C. Martin, B. Beutler, and D. Nemazee. 2006. Adjuvant-enhanced antibody responses in the absence of toll-like receptor signaling. *Science* 314: 1936-1938.
118. Gitlin, A. D., Z. Shulman, and M. C. Nussenzweig. 2014. Clonal selection in the germinal centre by regulated proliferation and hypermutation. *Nature* 509: 637-640.
119. Baumjohann, D., S. Preite, A. Reboldi, F. Ronchi, K. M. Ansel, A. Lanzavecchia, and F. Sallusto. 2013. Persistent antigen and germinal center B cells sustain T follicular helper cell responses and phenotype. *Immunity* 38: 596-605.
120. Qi, H., J. L. Cannons, F. Klauschen, P. L. Schwartzberg, and R. N. Germain. 2008. SAP-controlled T-B cell interactions underlie germinal centre formation. *Nature* 455: 764-769.
121. Fagarasan, S., and T. Honjo. 2000. T-Independent immune response: new aspects of B cell biology. *Science* 290: 89-92.
122. Ewulonu, U. K., L. J. Nell, and J. W. Thomas. 1990. VH and VL gene usage by murine IgG antibodies that bind autologous insulin. *Journal of immunology* 144: 3091-3098.
123. Duty, J. A., P. Szodoray, N. Y. Zheng, K. A. Koelsch, Q. Zhang, M. Swiatkowski, M. Mathias, L. Garman, C. Helms, B. Nakken, K. Smith, A. D. Farris, and P. C. Wilson. 2009. Functional anergy in a subpopulation of naive B cells from healthy humans that express autoreactive immunoglobulin receptors. *The Journal of experimental medicine* 206: 139-151.

124. Wang, H., and M. J. Shlomchik. 1997. High affinity rheumatoid factor transgenic B cells are eliminated in normal mice. *Journal of immunology* 159: 1125-1134.
125. Cyster, J. G., S. B. Hartley, and C. C. Goodnow. 1994. Competition for follicular niches excludes self-reactive cells from the recirculating B-cell repertoire. *Nature* 371: 389-395.
126. Weiss, D. S., K. Takeda, S. Akira, A. Zychlinsky, and E. Moreno. 2005. MyD88, but not toll-like receptors 4 and 2, is required for efficient clearance of Brucella abortus. *Infection and immunity* 73: 5137-5143.
127. Endres, R. O., E. Kushnir, J. W. Kappler, P. Marrack, and S. C. Kinsky. 1983. A requirement for nonspecific T cell factors in antibody responses to "T cell independent" antigens. *Journal of immunology* 130: 781-784.
128. Mohan, J. F., M. G. Levisetti, B. Calderon, J. W. Herzog, S. J. Petzold, and E. R. Unanue. 2010. Unique autoreactive T cells recognize insulin peptides generated within the islets of Langerhans in autoimmune diabetes. *Nature immunology* 11: 350-354.
129. Levin, C., H. Perrin, and B. Combadiere. 2014. Tailored immunity by skin antigen-presenting cells. *Human vaccines & immunotherapeutics*: e34299.
130. Soni, C., E. B. Wong, P. P. Domeier, T. N. Khan, T. Satoh, S. Akira, and Z. S. Rahman. 2014. B Cell-Intrinsic TLR7 Signaling Is Essential for the Development of Spontaneous Germinal Centers. *Journal of immunology* 193: 4400-4414.
131. Christensen, S. R., M. Kashgarian, L. Alexopoulou, R. A. Flavell, S. Akira, and M. J. Shlomchik. 2005. Toll-like receptor 9 controls anti-DNA autoantibody production in murine lupus. *The Journal of experimental medicine* 202: 321-331.
132. Pone, E. J., J. Zhang, T. Mai, C. A. White, G. Li, J. K. Sakakura, P. J. Patel, A. Al-Qahtani, H. Zan, Z. Xu, and P. Casali. 2012. BCR-signalling synergizes with TLR-signalling for induction of AID and immunoglobulin class-switching through the non-canonical NF-kappaB pathway. *Nature communications* 3: 767.
133. Thomas, J. W., and C. Hulbert. 1996. Somatically mutated B cell pool provides precursors for insulin antibodies. *Journal of immunology* 157: 763-771.
134. Shokat, K. M., and C. C. Goodnow. 1995. Antigen-induced B-cell death and elimination during germinal-centre immune responses. *Nature* 375: 334-338.
135. Pulendran, B., G. Kannourakis, S. Nouri, K. G. Smith, and G. J. Nossal. 1995. Soluble antigen can cause enhanced apoptosis of germinal-centre B cells. *Nature* 375: 331-334.
136. Kelsoe, G., L. Verkoczy, and B. F. Haynes. 2014. Immune System Regulation in the Induction of Broadly Neutralizing HIV-1 Antibodies. *Vaccines* 2: 1-14.
137. Otipoby, K. L., A. Waisman, E. Derudder, L. Srinivasan, A. Franklin, and K. Rajewsky. 2015. The B-cell antigen receptor integrates adaptive and innate immune signals. *Proceedings of the National Academy of Sciences of the United States of America* 112: 12145-12150.
138. Leung, S., D. Smith, A. Myc, J. Morry, and J. R. Baker, Jr. 2013. OT-II TCR transgenic mice fail to produce anti-ovalbumin antibodies upon vaccination. *Cellular immunology* 282: 79-84.
139. Pewzner-Jung, Y., D. Friedmann, E. Sonoda, S. Jung, K. Rajewsky, and D. Eilat. 1998. B cell deletion, anergy, and receptor editing in "knock in" mice targeted with a germline-encoded or somatically mutated anti-DNA heavy chain. *Journal of immunology* 161: 4634-4645.

140. Thomas, J. W., V. J. Virta, and L. J. Nell. 1986. Idiotypic determinants on human anti-insulin antibodies are cyclically expressed. *Journal of immunology* 137: 1610-1615.
141. Woodward, E. J., and J. W. Thomas. 2005. Multiple germline kappa light chains generate anti-insulin B cells in nonobese diabetic mice. *Journal of immunology* 175: 1073-1079.
142. Henry, R. A., P. L. Kendall, E. J. Woodward, C. Hulbert, and J. W. Thomas. 2010. Vkappa polymorphisms in NOD mice are spread throughout the entire immunoglobulin kappa locus and are shared by other autoimmune strains. *Immunogenetics* 62: 507-520.

Reversing Tolerance in Isotype Switch–Competent Anti-Insulin B Lymphocytes

Jonathan M. Williams,*,† Rachel H. Bonami,† Chrys Hulbert,† and James W. Thomas*,†

Autoreactive B lymphocytes that escape central tolerance and mature in the periphery are a liability for developing autoimmunity. IgG insulin autoantibodies that predict type 1 diabetes and complicate insulin therapies indicate that mechanisms for tolerance to insulin are flawed. To examine peripheral tolerance in anti-insulin B cells, we generated C57BL/6 mice that harbor anti-insulin VDJ_H-125 site directed to the native IgH locus (V_H125^{SD}). Class switch–competent anti-insulin B cells fail to produce IgG Abs following T cell–dependent immunization of V_H125^{SD} mice with heterologous insulin, and they exhibit markedly impaired proliferation to anti-CD40 plus insulin in vitro. In contrast, costimulation with LPS plus insulin drives robust anti-insulin B cell proliferation. Furthermore, V_H125^{SD} mice produce both IgM and IgG2a anti-insulin Abs following immunization with insulin conjugated to type 1 T cell–independent *Brucella abortus* ring test Ag (BRT). Anti-insulin B cells undergo clonal expansion in vivo and emerge as IgM^+ and IgM^- $GL7^+Fas^+$ germinal center (GC) B cells following immunization with insulin-BRT, but not BRT alone. Analysis of Igκ genes in V_H125^{SD} mice immunized with insulin-BRT reveals that anti-insulin Vκ from the preimmune repertoire is selected into GCs. These data demonstrate that class switch–competent anti-insulin B cells remain functionally silent in T cell–dependent immune responses, yet these B cells are vulnerable to reversal of anergy following combined BCR/TLR engagement that promotes Ag-specific GC responses and Ab production. Environmental factors that lead to infection and inflammation could play a critical yet underappreciated role in driving loss of tolerance and promoting autoimmune disease.
***The Journal of Immunology*, 2015, 195: 853–864.**

Tolerance for B lymphocytes in the developing repertoire is maintained first by receptor editing and clonal deletion in the bone marrow (1–3). Not all self-reactive B cells are removed by central tolerance, however, as BCRs with monovalent or weak interactions with autoantigens may avoid elimination or revision (4, 5). Autoreactive B cells that escape central tolerance and mature in the periphery are a liability, and additional mechanisms of tolerance are necessary to guard against autoimmunity (6–9). B cells that continuously encounter self-antigens may be rendered anergic or functionally silent to immune stimuli in the periphery. Tolerant B cells exhibit decreased surface IgM expression, impaired Ca^{2+} mobilization, restricted competition for available survival factors and follicular niches, and impaired responses to both T cell help and B cell mitogens (7, 10). Such anergic B cells are recognized in both normal and autoimmune repertoires (11–13).

The importance of BCR signaling for maintaining peripheral tolerance is emphasized by the reversal of anergy upon removal of chronic cognate Ag (10, 11). Alterations in BCR signaling pathways and mediators such as phosphoinositide 3-kinase, protein kinase Cθ, and the negative regulator protein tyrosine phosphatase non–receptor type 22 have been shown to impact both the induction and maintenance of tolerance (14–16). Innate signaling via TLR and MyD88 reverses anergy in some autoreactive B cells, suggesting that environmental factors that lead to infection and inflammation may also alter tolerance (17, 18). B cells deficient in MyD88 demonstrate impaired IgM responses to bacterial Ags, indicating that innate signaling through TLR pathways is critical for early T cell–independent (TI) immune defense (19). TLR-4 stimulation by LPS unlocks alternate signaling pathways to ERK phosphorylation and NF-κB activation independent of conventional BCR-dependent signaling mediators (20) that may be impaired for anergic B cells. Adaptive interactions with T cells may also drive loss of B cell tolerance and promote somatic hypermutation and Ig class switch recombination (CSR) in germinal center (GC) reactions associated with ongoing autoimmune disorders (21, 22). The fact that most pathogenic autoantibodies are of the IgG isotype further implicates T cells as potential vectors for driving loss of B cell tolerance. Thus, the overall effectiveness of immune tolerance for B lymphocytes depends on the nature of BCR interaction with autoantigens, potential encounter with in-

*Department of Pathology, Microbiology, and Immunology, Vanderbilt University, Nashville, TN 37232; and †Division of Rheumatology and Immunology, Department of Medicine, Vanderbilt University, Nashville, TN 37232

Received for publication December 16, 2014. Accepted for publication May 30, 2015.

This work was supported by National Institutes of Health Grants T32 AR059039, R21 DK091692, and R01 AI051448, Juvenile Diabetes Research Foundation Grants 1-2005-167 and 3-2013-121, and by Vanderbilt Diabetes Research and Training Center Grant DK20593. The Vanderbilt Flow Cytometry Shared Resource Core is supported by Vanderbilt Ingram Cancer Center Grant P30 CA068485 and Vanderbilt Digestive Disease Research Center Grant DK058404. The Vanderbilt Transgenic/Embryonic Stem Cell Shared Resource Core is supported by Cancer Center Support National Institutes of Health Grant CA068485, Vanderbilt Diabetes Research and Training Center Grant DK20593, the Vanderbilt Brain Institute, and by the Center for Stem Cell Biology. The Vanderbilt Technologies for Advanced Genomics Sequencing Facility is supported by Vanderbilt Ingram Cancer Center Grant P30 CA68485, Vanderbilt Vision Center Grant P30 EY08126, and by National Institutes of Health/National Center for Research Resources Grant G20 RR030956. The Vanderbilt Translational Pathology Shared Resource Core is supported by Mouse Metabolic and Phenotyping Center Grant DK059637.

The Igκ sequences presented in this article have been submitted to GenBank (http://www.ncbi.nlm.nih.gov/genbank/) under accession numbers KP790058–KP790071, KP790072–KP790083, KP790084–KP790092, and KP790093-KP790098.

Address correspondence and reprint requests to Dr. James W. Thomas, Vanderbilt University Medical School, 1161 21st Avenue South, Medical Center North T-3113, Nashville, TN 37232. E-mail address: james.w.thomas@vanderbilt.edu

The online version of this article contains supplemental material.

Abbreviations used in this article: B6, C57BL/6; BRT, *Brucella abortus* ring test Ag; CSR, class switch recombination; FO, follicular; GC, germinal center; HEL, hen egg lysozyme; MFI, mean fluorescence intensity; MZ, marginal zone; NP, nitrophenol; SAH, short arm homology; T1, transitional 1; TD, T cell–dependent; TI, T cell–independent; V_H125^{SD}, anti-insulin VDJ_H-125 site directed to the native IgH locus; WT, wild-type.

nate signals in the environment, and availability of epitopes that promote cognate T–B interactions.

Insulin is a protein hormone whose small size and low circulating concentration were previously thought to limit BCR interactions necessary for tolerance (23, 24). Studies using a conventional IgM-restricted anti-insulin BCR transgene revealed that anti-insulin B cells enter the mature repertoire but are anergic and fail to produce anti-insulin Abs following T cell–dependent (TD) immunization (25). Such functionally silenced B cells residing in the periphery retain cellular functions such as Ag presentation that enable them to promote autoimmunity in NOD mice (22, 26). Insulin autoantibodies associated with autoimmune disorders such as type 1 diabetes, as well as Abs that arise in response to insulin therapy and complicate disease management, are predominantly of the IgG isotype (27–32). How the ability to undergo CSR contributes to the maintenance or loss of tolerance for anti-insulin B cells is not known. To assess peripheral tolerance in anti-insulin B cells competent to undergo somatic hypermutation and CSR, we generated C57BL/6 (B6) mice that harbor an anti-insulin H chain site directed to its native locus (V_H125^{SD}). V_H125^{SD} pairs with endogenous L chains to generate a polyclonal B cell repertoire, where physiologically relevant CSR-competent anti-insulin B cells successfully compete and make up a small fraction of the repertoire. V_H125^{SD} B6 mice crossed with anti-insulin Vκ125 transgenic (Tg) mice generates a monoclonal B cell repertoire in which >98% of the B cells bind insulin (V_H125^{SD}/Vκ125Tg), a model used for in vitro experiments. These two models are used to assess the fate and function of anti-insulin B cells that are competent to undergo isotype switch in either a monoclonal or polyclonal repertoire.

In this study, we examine how peripheral tolerance is governed for autoreactive B lymphocytes that bind the relevant autoantigen, insulin. CSR-competent anti-insulin B cells enter mature compartments but are anergic, demonstrated by impaired proliferation to stimulation by a panel of B cell mitogens in vitro and total lack of IgG anti-insulin Ab production following TD immunization of V_H125^{SD} B6 mice. Reversal of anti-insulin B cell anergy is demonstrated by proliferation to insulin plus LPS in vitro and IgG2a Ab production following immunization of V_H125^{SD} B6 mice with insulin conjugated to a type 1 TI Ag (24, 33). This combined BCR/TLR costimulation effect in vivo is accompanied by entry of insulin-binding B cells into GCs, where anti-insulin L chains are not discarded but rather selected from the preimmune repertoire. These studies reveal a new pathway to drive loss of tolerance for CSR-competent anti-insulin B cells.

Materials and Methods

Targeting vector and generation of V_H125^{SD} mice

$pIV_HL2neoR$ is a vector designed for targeted insertion of a rearranged V_H gene replacing J_H loci, and was a gift from Dr. Klaus Rajewsky (34). We first modified $pIV_HL2neoR$ by cloning in two regions of short arm homology (SAH) at ClaI and NotI sites. This was necessary after initial efforts of homologous recombination were poor. Anti-insulin VDJ_H-125 from our original H chain plus L chain 125Tg mice (25) was subcloned into the pGEM-5Z vector and then cloned into modified $pIV_HL2neoR$-SAH at SalI and ClaI sites to generate our targeting vector, pIV_H-SAH-125-VDJ_H. All sequences were verified throughout the cloning process. pIV_H-SAH-125-VDJ_H was linearized through digestion with NotI and electroporated into 129/Ola embryonic stem cells. The electroporated cells were selected for neomycin resistance. Embryonic stem cell clone DNA was digested with HindIII, and Southern blot hybridization using a cDNA probe against an Xba1 enhancer located upstream of V_H125^{SD} detected the proper 6.1-kb fragment size of the construct in the targeted locus. Clones were confirmed by PCR using H chain primers 5′-CAG ATC CAG TTG GTG CAG TC-3′ (forward) and 5′-CCA GAC ATC GAA GTA CCC CT-3′ (reverse). Positive embryonic stem cell clones were injected into blastocysts and transplanted into pseudopregnant female mice. Tail DNA from founder chimeric pups and their progeny were screened for V_H125^{SD}. Southern blot was used to confirm the presence of the targeted allele.

Mice

V_H125^{SD} mice were backcrossed onto the B6 background. B6 mice and MD4 anti–hen egg lysozyme (HEL) mice (B6-Tg[IghelMD4]4Ccg/J) were purchased from The Jackson Laboratory (Bar Harbor, ME). EIIA-Cre B6 mice, provided by Dr. Richard Breyer (Vanderbilt University), were intercrossed with V_H125^{SD} mice to permanently remove the neomycin resistance cassette. Transgene transmission was monitored in subsequent generations of site-directed V_H125^{SD} B6 mice using PCR, and flow cytometry confirmed the presence of >95% transgenic IgM^{a+} B cells. Male and female mice aged 7–14 wk were used in these studies and backcrossed >10 times to B6 mice. All animals were housed in specific pathogen-free conditions, and all studies were approved by the American Association for the Accreditation of Laboratory Animal Care–certified Vanderbilt Institute of Animal Care and Use Committee.

Abs and flow cytometry

Abs reactive to murine B220 (RA3-6B2), IgM^a (DS-1), IgM^b (AF6-78), CD21 (7G6), CD23 (B3B4), IgD (11–26), GL7, or Fas/CD95 (Jo2) (BD Pharmingen), or IgM (μ-chain specific, Invitrogen) were used, along with biotinylated human insulin (35) or biotinylated anti-insulin mAb 123 (36) with streptavidin-conjugated fluorochrome to detect insulin-binding B cells, and 7-aminoactinomycin D for cell viability. Flow cytometry acquisition was performed after cell suspension in FACS buffer (1× PBS, 10% FBS, 1% sodium azide, 1% EDTA) using an LSR II (BD Biosciences), and sorting experiments were performed using a FACSAria I or II cell sorter in the Vanderbilt University Shared Resource Facility. Analysis was performed using FlowJo software (Tree Star).

Proliferation assays

B cells were purified from whole spleens using negative selection with anti-CD43 magnetic beads (MACS, Miltenyi Biotec). Average B cell purity across all experiments performed was: V_H125^{SD}/Vκ125Tg, 91.4%, $n = 9$; MD4 anti-HEL, 91%, $n = 8$; wild-type (WT), 92.5%, $n = 3$. Cells were plated at 2×10^5 per well in complete RPMI (10% FBS, 1% HEPES, 1% L-glutamine, 1% gentamicin) and cultured for 72 h in a 37°C, 5% CO_2 incubator. Cells were pulsed with [^{3}H]thymidine deoxyribose (NEN/PerkinElmer) on day 2 and harvested using a semiautomated cell harvester (Skatron) on day 3. [^{3}H]thymidine deoxyribose incorporation was measured by scintillation counting, and results are expressed as the mean cpm ± SD for the indicated number of mice in each experimental group. For in vivo proliferation experiments, both unimmunized and insulin–*Brucella abortus* ring test Ag (BRT)-immunized mice were injected i.p. with BrdU per the manufacturer's instructions (BD Pharmingen) 48 and 24 h before sacrifice. FITC-conjugated anti-BrdU (BD Pharmingen) was used to detect intracellular incorporation of BrdU.

Immunization and ELISA

For TD assays, preimmune sera were collected and mice were immunized with 40–50 μg bovine insulin in 1× PBS emulsified in either CFA s.c. at the base of the tail or in IFA i.p., and sera were collected 2–3 wk later. For TI assays, mice were immunized i.p. with human insulin–conjugated insulin-BRT (24), with BRT alone, or with physically mixed BRT and insulin, and sera were collected at 5–7 d following immunization. Anti-insulin Abs were measured by ELISA as follows: 96-well flat-bottom Nunc plates were coated with human insulin in borate-buffered saline overnight at 37°C. Plates were extensively washed with 1× PBS-Tween 20 (0.05%). Diluted sera (1:100) were added to the coated plates with or without 100× soluble human insulin to measure specific, inhibitable anti-insulin Abs. IgM and IgG anti-insulin Abs were detected using the following allotype-specific secondary Abs: IgM^a-biotin (DS-1), $IgG1^a$-biotin (10.9), or $IgG2a^a$-biotin (8.3) for transgenic anti-insulin B cells, or IgM^b-biotin (AF6-78), $IgG1^b$-biotin (B68-2), or $IgG2c^b$-biotin (5.7) (BD Pharmingen) for non-transgenic or WT B cells. Avidin–alkaline phosphatase (Sigma-Aldrich) or goat anti-mouse IgM–alkaline phosphatase or IgG–alkaline phosphatase Abs (SouthernBiotech) were added. After washing, *p*-nitrophenyl phosphate substrate (Sigma-Aldrich) was added to the plate and immediately read on a Microplate Autoreader (Bio-Tek Instruments) at an OD of 405 nm. Inhibitable (insulin-specific) binding was determined by the difference in binding in the presence or absence of excess competitive insulin.

Immunohistochemistry

Spleens were removed from unimmunized or insulin-BRT–immunized V_H125^{SD} B6 mice and soaked in 30% sucrose (w/v) overnight at 4°C and

snap frozen in OCT medium on dry ice. Eight-micrometer sections were obtained from the Vanderbilt Translational Pathology Shared Resource. Sections were fixed with 4% paraformaldehyde in 0.1 M PBS and stained with the following Ab cocktails: IgM Alexa Fluor 488 (Life Technologies), IgD^a-biotin (AMS 9.1, BD Pharmingen) plus streptavidin Alexa Fluor 350 (Life Technologies), and CD3 PE (17A2, BD Pharmingen) to define follicular architecture, or GL7 FITC, IgD^a-biotin plus streptavidin Texas Red (Molecular Probes), and DAPI (Molecular Probes) to detect GCs. Images were obtained using an Olympus BX60 fluorescent microscope with MagnaFire software. Adobe Photoshop was used to adjust brightness and contrast and to overlay images.

Pancreata were dissected from unimmunized or insulin-BRT–immunized V_H125^{SD} B6 mice, or from 12- to 16-wk-old female NOD mice (as a positive control for insulitis assessment) and placed into neutral buffered formalin. After 4–6 h, tissues were transferred to 70% ethanol and incubated overnight. Tissues were subsequently paraffin embedded, 5-μm sections were cut, and slides were stained with H&E by the Vanderbilt Translational Pathology Shared Resource. Slides were blind scored for insulitis by light microscopy using the following scale: 0, no insulitis; 1, peri-insulitis, <25% islet infiltration; 2, 25–50% islet infiltration; 3, 50–75% islet infiltration; 4, >75% islet infiltration. Half of the pancreas was fixed with paraformaldehyde in 0.1 M PBS and soaked in 30% sucrose overnight at 4°C, and then snap frozen in OCT medium on dry ice. Eight-micrometer sections were stained for immunofluorescence with DAPI and biotinylated anti-$IgG2a^a$ plus FITC-conjugated streptavidin.

L chain cloning and sequencing

Spleens were harvested from unimmunized V_H125^{SD} B6 mice or from mice 4 d following insulin-BRT immunization. Human insulin-binding B cells ($B220^+$ live lymphocytes) were identified by FACS and further gated as IgM^+ non-GC ($GL7^-Fas^-$), IgM^+ GC ($GL7^+Fas^+$), or IgM^- GC populations. Cells were sorted directly into RNAqueous lysis buffer (Life Technologies), and RNA was isolated using the RNAqueous-micro total RNA isolation kit (Life Technologies) per the manufacturer's instructions. Independent clones were derived from separate tubes of lysate. RNA was reverse transcribed into cDNA using SuperScript II RT (Invitrogen) and oligo(dT) primer (GE Healthcare) in a standard protocol. Resulting cDNA was used as a PCR template to amplify Igκ genes using a murine Vκ primer, 5′-ATT GTK MTS ACM CAR TCT CCA-3′, and murine Cκ primer, 5′-GGA TAC AGT TGG TGC AGC ATC-3′, where K = G or T, M = A or C, S = C or G, and R = A or G with a 44°C annealing temperature for 35 cycles. Appropriately sized PCR products were gel purified using the MinElute gel extraction kit (Qiagen) and Igκ was cloned as described previously (37, 38). Vκ and Jκ gene segment identities were assigned using Ig BLAST (http://www.ncbi.nlm.nih.gov/igblast/) and IMGT nomenclature with CDR boundaries defined by the KABAT V domain delineation system. Nucleotide mutation analyses were also performed using the Ig BLAST tool.

Results

A site-directed BCR transgenic mouse model generates class switch–competent anti-insulin B lymphocytes

Previous μ-only BCR transgenic mouse models do not address how native cellular functions such as CSR impact the state of immune tolerance for anti-insulin B cells. To examine peripheral tolerance for anti-insulin B cells competent to undergo isotype switch, B6 mice that harbor anti-insulin VDJ_H-125 site directed to the IgH locus were developed as described in *Materials and Methods*. Fig. 1A summarizes the strategy for generating the targeting construct used to develop site-directed V_H125^{SD} B6 mice. Southern blot, PCR, and flow cytometry confirmed successful IgH locus targeting, as $B220^+$ splenic B cells from V_H125^{SD} B6 mice coexpress IgM^a and IgD^a whereas those from conventional μ-only V_H125Tg B6 mice express only IgM^a as expected (Fig. 1B).

Flow cytometry with biotinylated insulin was used to investigate the contribution of different anti-insulin transgenes to insulin-binding B cells (Fig. 1C). In Fig. 1C (*left*), mice that possess only an anti-insulin L chain (Vκ125Tg) show low numbers of

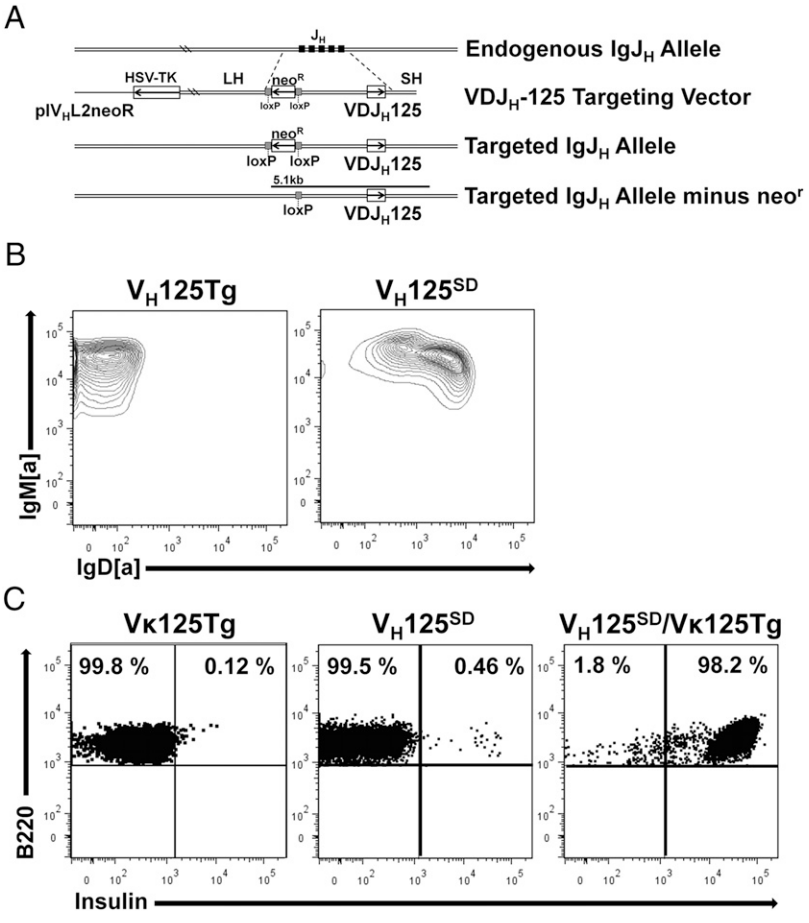

FIGURE 1. A site-directed BCR transgenic mouse model generates class switch–competent anti-insulin B lymphocytes. (**A**) Strategy for targeting anti-insulin VDJ_H-125 to the IgH locus (site-directed V_H125^{SD}). (**B**) Flow cytometry was used to assess IgM and IgD expression on B cells ($B220^+$ live lymphocytes) from spleens of V_H125^{SD} B6 mice (*right*) and conventional IgM-restricted, non–site-directed V_H125Tg B cells (*left*). (**C**) Insulin-binding B cells identified by flow cytometry in Vκ125Tg B6 mice (*left*), site-directed V_H125^{SD} B6 mice (*middle*), and in mice that harbor both V_H125^{SD} and Vκ125Tg (*right*).

insulin-binding B cells in the spleen (0.12 ± 0.01%, $n = 3$), but these weakly binding cells are not specific, as they are not inhibited with excess competitive insulin (not shown). In Fig. 1C (*center*), V_H125^{SD} B6 mice have B cells in which the targeted transgene pairs with endogenous L chains to generate a small population of insulin-binding B cells (0.46 ± 0.05%, $n = 9$). In Fig. 1C (*right*), intercrosses that pair V_H125^{SD} with Vκ125Tg confer insulin-binding specificity to >98% of the B cells. Unlike other site-directed mouse models, such as the SW_{HEL} model (39), V_H gene revision or editing is not prevalent for IgM^+ B cells in V_H125^{SD}, as >95% are [a] allotype and retain their insulin-binding potential. These data demonstrate a novel site-directed BCR transgenic model can be used to assess the fate and function of CSR-competent anti-insulin B lymphocytes within a monoclonal or polyclonal repertoire.

Anergy in anti-insulin B cells is reversed by TLR-4 but not CD40 costimulation in vitro

To determine whether CSR-competent anti-insulin B cells are anergic, B cells were purified from V_H125^{SD}/Vκ125Tg or WT B6 mice using MACS and tritiated thymidine incorporation was used to assess B cell proliferation in vitro to anti-IgM, anti-CD40, or LPS stimulation (Fig. 2). Anti-insulin B cells exhibit impaired proliferative responses to stimulation through BCR, CD40, and TLR-4, compared with B cells from WT B6 mice (Fig. 2A). Thus, anergy is maintained for CSR-competent $IgM^{a+}IgD^{a+}$ anti-insulin B cells in vitro, similar to that reported for anti-insulin B cells in conventional μ-only 125Tg mice (H plus L chain) (26).

Different costimulation pathways were assessed for their impact on proliferation in the context of BCR encounter with autoantigen. B cells were purified from V_H125^{SD}/Vκ125Tg B6 mice or naive anti-HEL MD4-Tg mice (10) and stimulated with anti-CD40 (Fig. 2B) or LPS (Fig. 2D) in the presence or absence of cognate Ag. Using B cells specific for HEL as naive control, stimulation with HEL plus anti-CD40 at low concentration (0.1 μg/ml) synergized to significantly augment proliferation (30-fold increase, Fig. 2C). In contrast, stimulation of anti-insulin B cells with insulin plus anti-CD40 did not enhance their proliferation, but instead blunted the response (0.52-fold, Fig. 2C). Synergy is defined in this study as the mathematical value representing the effect of B cell costimulation relative to the effect of the sum of each individual stimulus. Failure to demonstrate synergy between

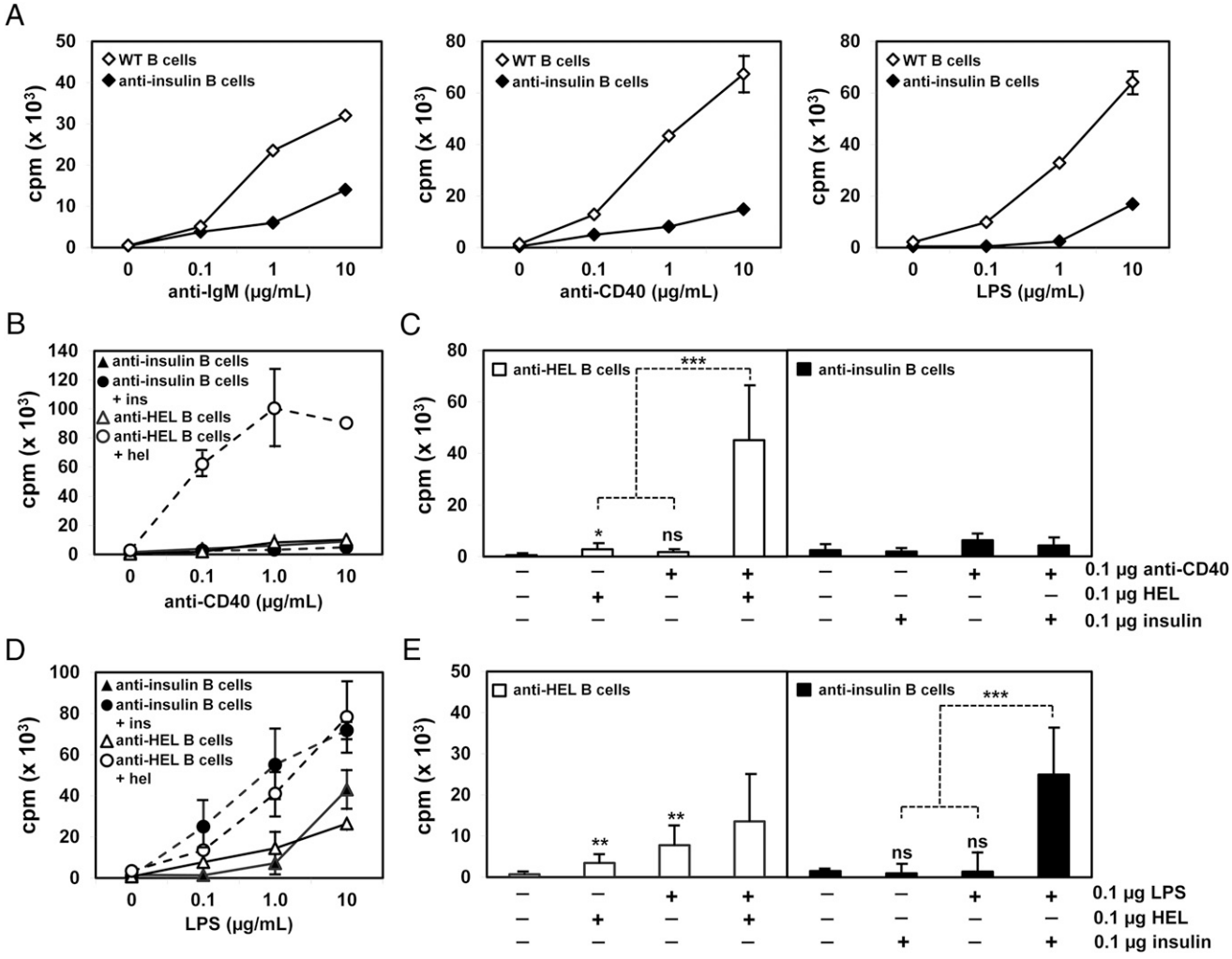

FIGURE 2. Anergy in anti-insulin B cells is reversed by TLR-4 but not CD40 costimulation in vitro. B cells were $CD43^-$ MACS purified from either V_H125^{SD}/Vκ125Tg or control MD4 anti-HEL Tg or WT B6 mice. (**A**) B cells from WT and V_H125^{SD}/Vκ125Tg mice were cultured for 72 h to a dose response of anti-IgM, anti-CD40, or LPS. B cells from V_H125^{SD}/Vκ125Tg and MD4 anti-HEL Tg mice were cultured to a dose response of anti-CD40 (**B**) or LPS (**D**) with or without 0.1 μg/ml insulin or HEL Ag. The proliferative response at the combined suboptimal dose of 0.1 μg/ml is shown for both anti-CD40 (**C**) and LPS (**E**) stimuli plus Ag. B cells received a 1 μCi pulse of tritiated thymidine 48 h into culture before harvest at 72 h. For anti-CD40 studies, $n = 6$ for both V_H125^{SD}/Vκ125Tg and MD4 anti-HEL Tg mice. For LPS studies, $n = 9$ for V_H125^{SD}/Vκ125Tg and $n = 8$ for MD4 anti-HEL Tg mice. Data represent at least three independent experiments. $^*p < 0.05$, $^{**}p < 0.01$, $^{***}p < 0.001$, two-tailed t test.

insulin and anti-CD40 was consistent across a wide range of Ag and Ab concentrations (data not shown). These data suggest that anergy is maintained for CSR-competent anti-insulin B cells costimulated with cognate Ag and anti-CD40, which mimics T cell help.

Using naive anti-HEL B cells as control, costimulation with HEL and LPS at low concentration (0.1 μg/ml) only marginally boosted proliferation, with no evidence of synergy (1.2-fold, Fig. 2E). In striking contrast, costimulation of anti-insulin B cells with insulin and LPS synergized to enhance B cell proliferation (10-fold, Fig. 2E). These data demonstrate that in vitro responses of anti-insulin B cells are altered by prior exposure of the monoclonal repertoire to Ag in vivo. Anti-insulin B cells are anergic, as they fail to proliferate to anti-CD40 with or without Ag. However, this anergy is readily reversed by simultaneous engagement of BCR and TLR-4 in vitro.

Anti-insulin B cells from V_H125^{SD} B6 mice undergo peripheral maturation

We sought to understand how the features of tolerance observed in a nearly monoclonal population of anti-insulin B cells apply to a polyclonal repertoire that contains relatively few anti-insulin B cells (V_H125^{SD}). Factors that govern anergy for autoreactive B lymphocytes in a polyclonal repertoire include competition for survival and entry into mature compartmental niches (6, 26, 40, 41). To assess whether CSR-competent anti-insulin B cells in the polyclonal repertoire of V_H125^{SD} B6 mice enter mature subsets, flow cytometry was used to identify B cells ($B220^+IgM^{a+}$ live lymphocytes) that distributed into transitional 1 (T1, $CD21^-$ $CD23^-$), follicular (FO, $CD21^{int}CD23^{high}$), and marginal zone (MZ, $CD21^{high}CD23^{low}$) compartments of the spleen (Fig. 3). In contrast to WT B6 mice, a small population of anti-insulin B cells is observed in V_H125^{SD} B6 mice (0.42 ± 0.05%, $n = 9$), and their specificity is confirmed by inhibition with unlabeled competitive insulin (Fig. 3A, *left panels*). Rare insulin-binding B cells in WT B6 mice (0.03 ± 0.01%, $n = 3$) are not inhibited by excess insulin (Fig. 3A, *right panels*). The ability of B cells to enter T1, FO, and MZ subsets was compared for non–insulin-binding (ins^-) or insulin-binding B cells (ins^+) in V_H125^{SD} B6 mice, or for WT B cells (Fig. 3B). As represented in Fig. 3C, ins^+ B cells predominantly populate the FO subset in V_H125^{SD} B6 mice, whereas fewer ins^+ B cells are found in other subsets (8.1 ± 3.2% T1, 78.9 ± 5.5% FO, 2.7 ± 1.9% MZ, $n = 7$). The reduced representation of ins^+ B cells in the MZ contrasts ins^- B cells (12.25 ± 2.6% T1, 57.7 ± 3.5% FO, 16.5 ± 1.7% MZ) in V_H125^{SD} B6 mice and normal B cells (8.4 ± 1.7% T1, 78.3 ± 3.7% FO, 6.0 ± 0.9% MZ, $n = 6$) in WT B6 mice. These data suggest that anti-insulin B cells in the peripheral repertoire of V_H125^{SD} B6 mice are principally mature FO B cells.

To determine whether anti-insulin B cells are clonally ignorant or whether their BCRs have encountered endogenous rodent insulin in vivo, a second anti-insulin mAb (mAb123) was used. mAb123

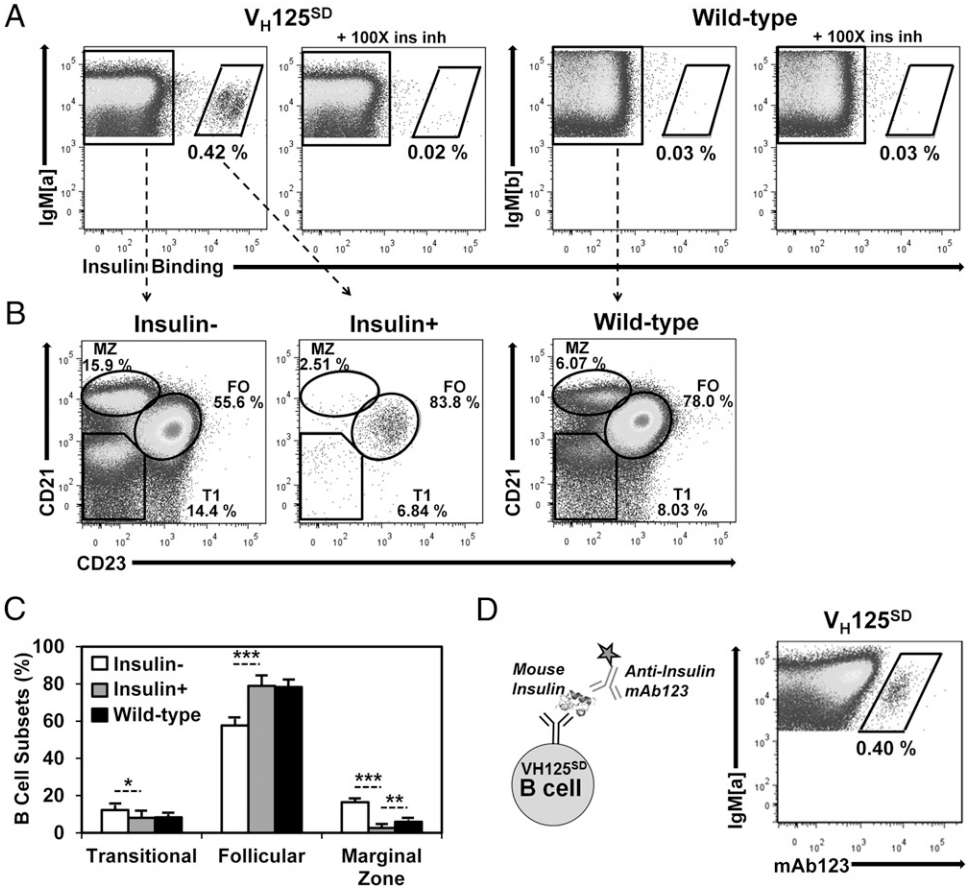

FIGURE 3. Anti-insulin B cells from V_H125^{SD} B6 mice undergo peripheral maturation. (**A**) Splenocytes were gated on $B220^+IgM^+$ live lymphocytes. Splenocytes were harvested from V_H125^{SD} (*left*) or WT (*right*) B6 mice and were incubated with 17 nM biotinylated human insulin with or without 100× free insulin to detect insulin-specific B cells using flow cytometry. Anti-IgM^a detects transgenic B cells; anti-IgM^b detects WT B cells (**B**). Expression of CD21 and CD23 was used to define T1, FO, or MZ B cell subset distribution of ins^- (*left*), ins^+ (*middle*), or WT (*right*) B cells, quantified in (**C**) as subset percentage of IgM^+ B cells. (**D**) Biotinylated anti-insulin mAb123, depicted in the schematic (*left*), was used to detect V_H125^{SD} B cells that bind endogenous rodent insulin (*right*). $^*p < 0.05$, $^{**}p < 0.01$, $^{***}p < 0.001$, two-tailed *t* test.

recognizes a different insulin epitope and binds insulin-occupied BCRs (25, 35). Flow cytometry staining with mAb123 confirms that BCRs are occupied by endogenous insulin in V_H125^{SD} B6 mice (0.4 ± 0.1%, Fig. 3D). These data demonstrate that CSR-competent anti-insulin B cells in V_H125^{SD} B6 mice successfully compete in a polyclonal repertoire and populate FO compartments despite encounter with physiologic autoantigen during development and early peripheral maturation.

IgM and IgG anti-insulin Abs are produced in V_H125^{SD} B6 mice following TI but not TD immunization

Prior studies in mice harboring IgM^a-restricted anti-insulin B cells demonstrated failure to respond to TD immunization (25). To dissect the functional status of CSR-competent $IgM^{a+}IgD^{a+}$ anti-insulin B cells in V_H125^{SD} B6 mice, Ab responses were assessed following two different immunization strategies, and serum IgM and IgG anti-insulin Abs were measured by ELISA (Fig. 4). For TD responses, mice were immunized with bovine insulin emulsified in CFA (insulin/CFA). Bovine insulin was chosen for TD immunization because the MHC class II of B6 mice ($I\text{-}A^b$) is genetically a strong responder to bovine but not to other insulins, notably human (24). Conventional WT B6 mice generated a strong $IgG1^b$ anti-insulin response following insulin/CFA immunization, whereas CSR-competent anti-insulin B cells in V_H125^{SD} B6 mice failed to produce $IgG1^a$ anti-insulin Abs (Fig. 4A). To ensure that the absence of response to insulin/CFA immunization in these mice is not attributed to lack of bovine insulin processing by anti-insulin BCRs, we used competitive inhibition in flow cytometry to confirm that bovine insulin at concentrations well below those used in immunization fully competes with human insulin for binding to anti-insulin B cells in V_H125^{SD} B6 mice (Supplemental Fig. 1). IgG1 was the predominant isotype observed following insulin/CFA immunization, a finding that agrees with previous work that examined the Ig response to insulin in B6 mice (24). To test whether TLR signaling provided by mycobacteria in CFA is necessary, mice were also immunized with bovine insulin emulsified in IFA (insulin/IFA). Whereas the $IgG1^a$ anti-insulin response remained absent in V_H125^{SD} B6 mice, WT B6 mice generated $IgG1^b$ anti-insulin Abs following insulin/IFA immunization (data not shown). This agrees with prior studies that demonstrated B cells deficient in both MyD88 and TRIF were able to mount Ab responses to multiple Ags administered in a variety of adjuvants, including CFA and IFA (42). These data validate that tolerance for anti-insulin B cells is maintained for TD immune responses to heterologous insulin in either the presence or absence of mycobacterial adjuvant.

To assess anti-insulin B cell competence to produce Abs in the absence of cognate T cell help, V_H125^{SD} B6 mice were immunized with human insulin conjugated to BRT or with BRT alone (24). Human insulin is used in BRT conjugates to avoid introduction of T cell epitopes. Prior studies showed that insulin-BRT behaves as a typical type 1 TI Ag, including response kinetics, expected Ab isotypes, and responses observed in both athymic and X-linked immunodeficient mice (33, 43). Following immunization with insulin-BRT, B cells from WT B6 mice and CSR-competent anti-insulin B cells from V_H125^{SD} B6 mice produced IgM^b and $IgG2c^b$ or IgM^a and $IgG2a^a$ anti-insulin Abs, respectively (Fig. 4B). Immunization with BRT alone, however, failed to induce any detectable IgG anti-insulin Abs in either V_H125^{SD} or WT B6 mice (Fig. 4B). Similarly, immunization with physically mixed BRT and insulin failed to induce any response (data not shown). Insulin-BRT immunization did not elicit IgG1 Abs, consistent with the expected isotypes associated with BRT conjugates (33, 43). These data suggest that the insulin-BRT conjugate promotes loss of tolerance for CSR-competent anti-insulin B cells in vivo through a combination of BCR and TLR signaling that drives production of IgM and IgG anti-insulin Abs.

To determine the pathological consequences of the breach in tolerance observed in V_H125^{SD} B6 mice following insulin-BRT

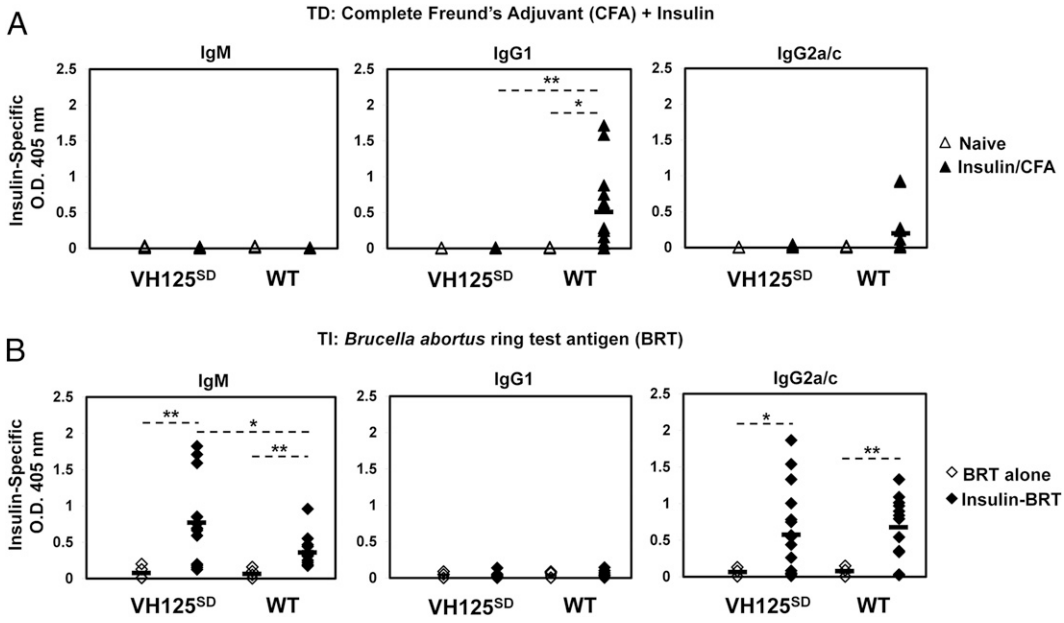

FIGURE 4. IgM and IgG anti-insulin Abs are produced in V_H125^{SD} B6 mice following TI but not TD immunization. V_H125^{SD} and WT B6 mice were immunized with either bovine insulin in 1× PBS emulsified in CFA (insulin/CFA) s.c. in base of the tail, or BRT alone, or human insulin conjugated to BRT (insulin-BRT) i.p. in 1× PBS. (**A**) Insulin-specific IgM^a, $IgG1^a$, and $IgG2a^a$ (V_H125^{SD}) or IgM^b, $IgG1^b$, and $IgG2c^b$ (WT) were measured in sera by ELISA before (△) and 2–3 wk following TD immunization with insulin/CFA (▲). (**B**) Insulin-specific IgM, IgG1, and IgG2a/c were measured in sera by ELISA 5–7 d following immunization with BRT alone (◇) or insulin-BRT (◆). For insulin/CFA, $n = 12$ for both V_H125^{SD} and WT mice. For insulin-BRT, $n = 12$ V_H125^{SD} and $n = 10$ WT mice. For BRT alone, $n = 6$ mice per group. Data represent at least three independent experiments. $^*p < 0.05$, $^{**}p < 0.01$, $^{***}p < 0.001$, two-tailed t test.

immunization, pancreata were examined for insulitis and the presence of IgG anti-insulin Abs at day 12 of the response. A scoring system of 0–4 was used to assess insulitis by H&E staining in pancreata sections from unimmunized or insulin-BRT–immunized mice (outlined in *Materials and Methods*). NOD mouse pancreata sections served as a positive control for islet infiltration. No insulitis was detected in 60 islets examined in two unimmunized V_H125^{SD} B6 mice or in 82 islets examined in four immunized mice, such that 100% of islets examined received a score of 0. In contrast, 64 islets were scored in two 16- to 20-wk-old female, nondiabetic NOD mice, with 53% islets scoring 0, 14% islets scoring 1, 9% islets scoring 2, 8% islets scoring 3, and 16% islets scoring 4. Endogenous Ig deposition in the islets was assessed by direct immunofluorescence. Ig deposition was not detected in pancreata of either unimmunized or insulin-BRT–immunized mice (data not shown). Ig was observed by indirect immunofluorescence, confirming that Abs produced following insulin-BRT immunization are autoreactive. These data indicate that the breach in tolerance driven by insulin-BRT does not elicit a detectable organ-specific autoimmune attack.

Insulin-BRT immunization promotes clonal expansion and restoration of surface IgM for anti-insulin B cells

To assess the fate of anti-insulin B cells undergoing an active breach of tolerance, clonal expansion and proliferation were measured by BrdU incorporation in vivo following insulin-BRT immunization. IgM^+ insulin-binding B cells ($IgM^{a+}ins^+$) in V_H125^{SD} B6 mice immunized with BRT alone (0.33 ± 0.07%, $n = 7$) were not increased compared with unimmunized mice (0.34 ± 0.08%, $n = 6$) (Fig. 5A). In contrast, IgM^+ insulin-binding B cells were expanded in mice immunized with insulin-BRT (2.97 ± 1.28%, $n = 9$) (Fig. 5A). A small population of IgM^- insulin-binding B cells ($IgM^{a-}ins^+$) that have likely undergone CSR were detected in V_H125^{SD} B6 mice immunized with insulin-BRT (0.79 ± 0.46%, $n = 9$) but not in unimmunized mice or in mice immunized with BRT alone. BrdU incorporation was used concomitantly to demonstrate that the increase in anti-insulin B cells represented Ag-specific expansion (Fig. 5B). Insulin-binding B cells in V_H125^{SD} B6 mice immunized with BRT alone did not incorporate BrdU and were similar in frequency to those in unimmunized mice. In contrast, both IgM^+ and IgM^- insulin-binding B cell populations in mice immunized with insulin-BRT incorporated BrdU (39.8 ± 7.2% for IgM^+ and 40.5 ± 14.1% for IgM^-, $n = 5$). These findings correlate with the Ab responses observed in V_H125^{SD} B6 mice following immunization and show that the insulin-BRT conjugate drives clonal expansion and proliferation of anti-insulin B cells in vivo.

One hallmark of anergy is reduced surface IgM expression (6, 7, 10). Surface IgM for insulin-binding B cells (ins^+) in unimmunized V_H125^{SD} B6 mice is reduced relative to non-insulin binders (ins^-), expressed as a ratio of mean fluorescence intensity (MFI) of ins^+ to ins^- (0.58 ± 0.12, $n = 6$) (Fig. 5C). To test whether insulin-BRT immunization promotes restoration of normal surface IgM expression, the MFI of surface IgM was compared for ins^+

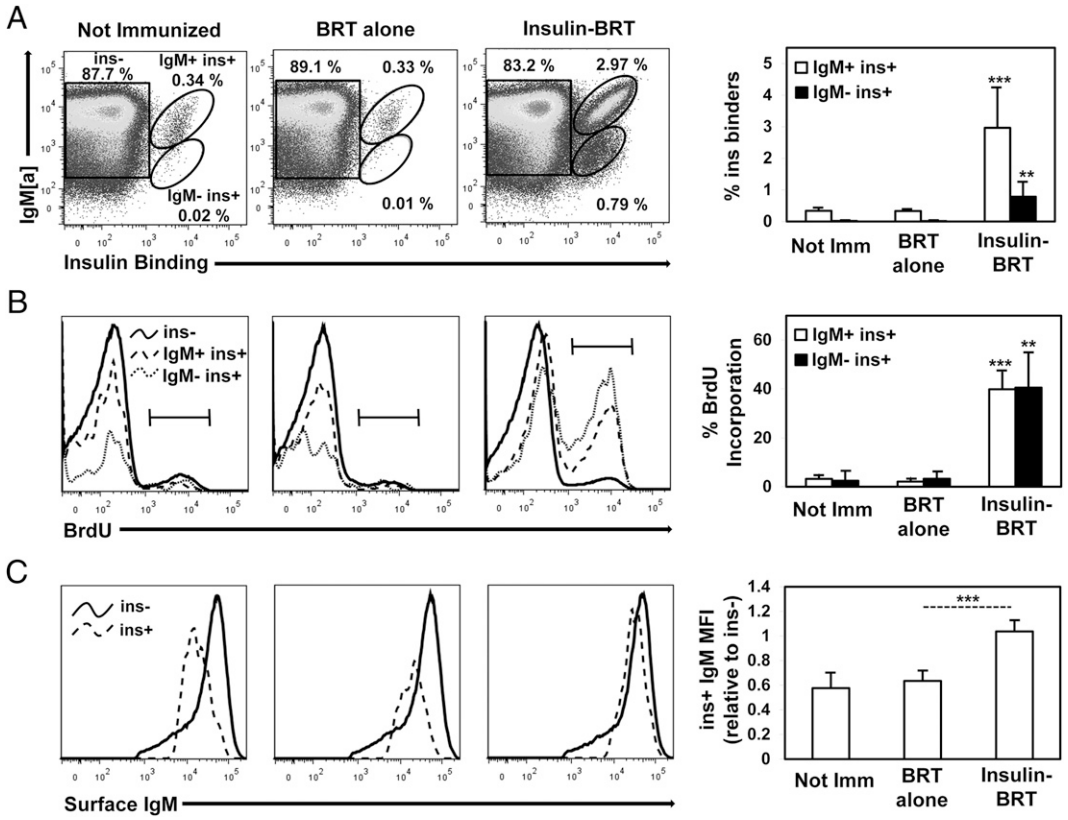

FIGURE 5. Insulin-BRT immunization promotes clonal expansion and restoration of surface IgM for anti-insulin B cells. V_H125^{SD} B6 mice were not immunized ($n = 6$) or immunized with either BRT alone ($n = 7$) or insulin-BRT ($n = 9$) i.p. in 1× PBS. (**A**) Insulin-binding B cells ($B220^+$ live lymphocytes) in the spleen were quantified 5 d following immunization by flow cytometry. Representative plots (*left*) and averages (*right*) are shown. (**B**) Mice were injected twice with BrdU i.p. 48 and 24 h before sacrifice, and intracellular BrdU incorporation was measured in non–insulin binders (ins^-, solid black line), IgM^+ insulin binders (IgM^+ins^+, dashed line), and IgM^- insulin binders (IgM^-ins^+, fine dashed line). Representative histograms (*left*) and averages (*right*) are shown. (**C**) The MFI of surface IgM for ins^- and ins^+ B cells is shown in representative histograms (*left*) and is also expressed as a ratio of ins^+/ins^- IgM MFI average ± SD (*right*). Data represent at least three independent experiments. Unless otherwise indicated, statistical comparisons are to unimmunized mice. $*p < 0.05$, $**p < 0.01$, $***p < 0.001$, two-tailed *t* test.

and ins$^-$ B cells following immunization (Fig. 5C). Surface IgM for ins$^+$ B cells was not restored in V_H125^{SD} B6 mice immunized with BRT alone (0.64 ± 0.08, n = 5). In contrast, surface IgM for ins$^+$ B cells was completely restored following insulin-BRT immunization (1.04 ± 0.09, n = 6). Surface IgM restoration is consistent with reversal of anergy in CSR-competent anti-insulin B cells.

Insulin-specific GCs arise in V_H125^{SD} B6 mice

Ig isotype switch in B cells is principally recognized to occur in GC reactions that arise in the follicle following cognate interactions between CD4$^+$ Th cells and Ag-specific B cells (44–46). Most rapid TI B cell responses are expected to occur in the extrafollicular spaces of the spleen (47); however, it has been demonstrated that some TI B cell responses can promote the unconventional formation of GCs in the absence of T cell help (48, 49). Accordingly, we assessed whether the observed breach in peripheral tolerance for anti-insulin B cells in the insulin-BRT response extends to the formation of GCs. Flow cytometry was used to assess expression of the GC markers, GL7 and Fas, on anti-insulin B cells in V_H125^{SD} B6 mice 5 d following immunization. IgM$^+$ insulin-binding B cells (IgM^{a+}ins$^+$) in unimmunized mice established the background for the GC phenotype in the spleen (0.01% GL7$^+$Fas$^+$, n = 5), and immunization with BRT alone did not increase this response (0.03% GL7$^+$Fas$^+$, n = 7) (Fig. 6A). In striking contrast, IgM$^+$ insulin-binding B cells in mice immunized with insulin-BRT acquired the GC phenotype (24.4 ± 19.0% GL7$^+$Fas$^+$, n = 9) (Fig. 6A). An increased frequency of IgM$^-$ insulin-binding B cells (IgM^{a-}ins$^+$) acquired the GC phenotype following insulin-BRT immunization (34.2 ± 27.6% GL7$^+$Fas$^+$, n = 9), demonstrating that a portion of ins$^+$ B cells participating in GC reactions have undergone CSR, a finding consistent with production of IgG anti-insulin Abs. Examination of these GC reactions at a later time point in the insulin-BRT response (day 12) yielded a sporadic population of ins$^+$ GC B cells. Three of eight mice examined at day 12 had detectable ins$^+$ GC B cells (5.22 ± 0.08%), whereas the other five mice did not have a detectable population of the same B cells (0.20 ± 0.13%). Rapid decline in insulin-specific GC B cells and Ab production at day 12 following insulin-BRT (data not shown) is consistent with previous work in other models describing the fate of Ag-specific GCs in the absence of cognate T cell help (48). These data support the concept that the insulin-BRT conjugate drives IgG anti-insulin Ab production largely through generation of Ag-specific GCs that are short-lived.

Notably, non–insulin-binding B cells (IgM^{a+}ins$^-$) in V_H125^{SD} B6 mice did not upregulate GC markers following insulin-BRT immunization (0.39 ± 0.19% GL7$^+$Fas$^+$) when compared with unimmunized mice (0.36 ± 0.46% GL7$^+$Fas$^+$) (Fig. 6A, *top row*), suggesting that acquisition of the insulin-specific GC B cell phenotype is limited to cognate anti-insulin B cells and not merely a consequence of global B cell activation from BRT-mediated TLR stimulation. Flow cytometry staining confirmed that GL7$^+$ Fas$^+$ GC B cells were IgD$^-$ (Fig. 6B), consistent with induction of a GC B cell phenotype.

To confirm formation of anatomical GCs following insulin-BRT, immunofluorescence staining was performed on spleen sections from both unimmunized and immunized V_H125^{SD} B6 mice. IgM, IgD, and CD3 were used to define FO architecture, and GCs were identified as IgD$^-$ and GL7$^+$. Whereas some GL7$^+$IgD$^-$ GCs were observed in unimmunized mice and in mice immunized with BRT alone, they were small by microscopy and non–insulin-specific by flow cytometry (Fig. 6A, 6C). In contrast, large GL7$^+$IgD$^-$ GCs were readily detected in spleen sections from mice immunized

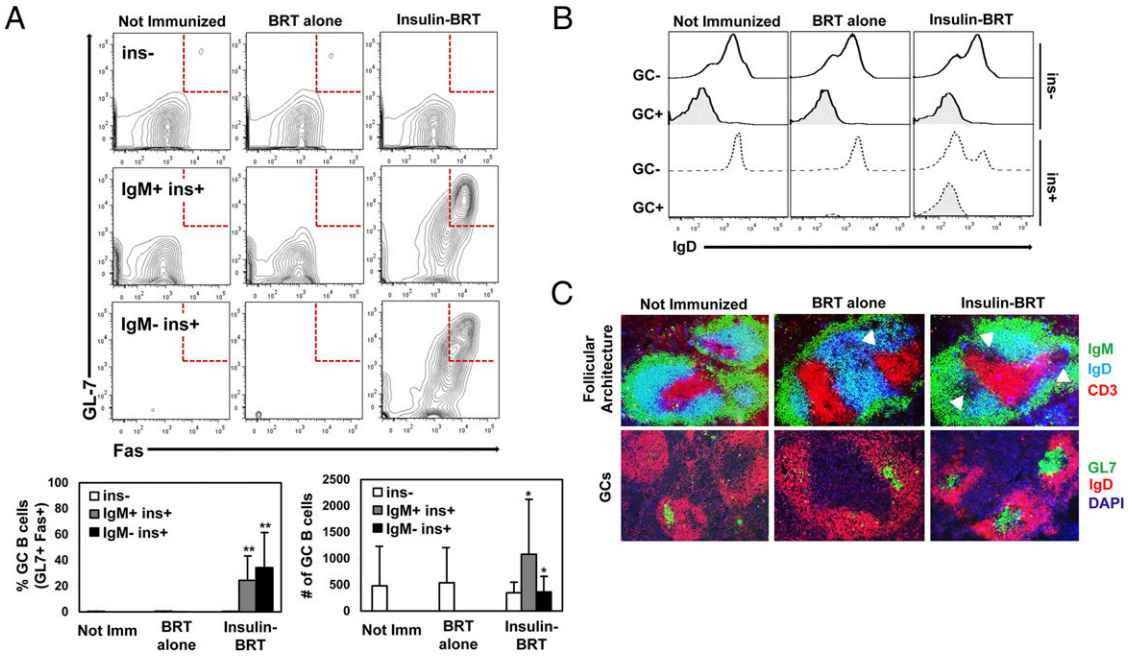

FIGURE 6. Insulin-specific GCs arise in V_H125^{SD} B6 mice. V_H125^{SD} B6 mice were immunized with either BRT alone or insulin-BRT i.p. in 1× PBS. (**A**) Flow cytometry was used to assess GC B cell phenotype by GL7 and Fas expression on B cells (B220$^+$ live lymphocytes) separated into non–insulin binders (ins$^-$, white), IgM$^+$ insulin binders (IgM$^+$ins$^+$, gray), and IgM$^-$ insulin binders (IgM$^-$ins$^+$, black). Representative plots (*top*) and GC B cell subset percentage and cell number averages (*bottom*) are shown. (**B**) IgD expression was measured for ins$^-$ (solid black line) and ins$^+$ B cells (dashed line) following immunization, and representative histograms are shown. (**C**) Immunofluorescence microscopy detected FO architecture (*top*, IgD$^-$CD3$^-$, GCs indicated by arrows) and GC structures (*bottom*, GL7$^+$IgD$^-$) in spleens from V_H125^{SD} B6 mice (n = 4). Follicles counted: n = 21 not immunized, n = 12 BRT alone, and n = 17 insulin-BRT. Data represent at least three independent experiments. Unless otherwise indicated, statistical comparisons are to unimmunized mice. *$p < 0.05$, **$p < 0.01$, ***$p < 0.001$, two-tailed t test.

with insulin-BRT (Fig. 6C). These data show that anti-insulin B cells acquire a GC phenotype and localize to GC structures in the spleen following immunization with insulin-BRT.

Anti-insulin L chains are selected from the preimmune repertoire to enter GC reactions

Anti-insulin B cells are detected in GCs following insulin-BRT immunization (Fig. 6). These GC B cells may reflect expansion of insulin-binding B cells that were present in the preimmune repertoire (Fig. 3D). Alternatively, the unique environment of GC reactions may select rare anti-insulin B cells that are clonally ignorant or below the level of detection. Accordingly, we investigated selection of anti-insulin Igκ from the preimmune repertoire by insulin-binding GC B cells. Spleens were harvested from unimmunized V_H125^{SD} B6 mice or from mice immunized with insulin-BRT. Non-GC ($IgM^+GL7^-Fas^-$), IgM^+ GC ($IgM^+GL7^+Fas^+$), or IgM^- GC ($IgM^-GL7^+Fas^+$) insulin-binding B cells were purified by flow cytometry sorting as identified in Figs. 5A and 6A. RNA was purified, and cDNA was used as template for Igκ amplification. The Ig BLAST tool was used to identify Vκ and Jκ gene segment usage (using IMGT nomenclature) as well as any nucleotide mutations (see *Materials and Methods*).

The Vκ125Tg in the previously published anti-insulin 125Tg (H plus L chain) mouse model is a Vκ4-74 (25, 50). This L chain is associated with anti-insulin B cells loaded with endogenous rodent insulin detected by mAb123 in V_H125^{SD} B6 mice (Fig. 3D and data not shown), confirming that this Vκ is autoreactive when combined with V_H125. Insulin-binding B cells sorted in unimmunized mice exclusively used Vκ4-74 (Fig. 7A). Vκ4-74 was also the dominant Vκ used by insulin-binding B cells following insulin-BRT immunization, including 11 of 12 non-GC (Fig. 7B), 8 of 9 IgM^+ GC, and 5 of 6 IgM^- GC clones (Fig. 7C, 7D). Vκ4-74 clones were paired with all Jκ, forming different CDR3 amino acid junctions associated with previously recognized low/moderate (P-L) and high (P-P) affinity for rodent insulin, as deduced from sequences identified in studies of anti-insulin hybridomas (35). The 5′ degenerate primer sequence was removed, and Igκ sequences were deposited into GenBank (http://www.ncbi.nlm.nih.gov/genbank/) with the following accession numbers: unimmunized (KP790058–KP790071), non-GC (KP790072–KP790083), IgM^+ GC (KP790084–KP790092), and IgM^- GC (KP790093-KP790098).

Most (five of nine) IgM^+ GC anti-insulin B cell clones sorted from V_H125^{SD} B6 mice on day 5 following insulin-BRT retained nucleotide sequences in germline Igκ configuration with CDRs identical to those found in unimmunized mice (Fig. 7G). However, an increased frequency of both IgM^+ and IgM^- GC anti-insulin B cell clones sorted from immunized mice possessed one or more nucleotide mutations relative to non-GC anti-insulin B cells from immunized mice or anti-insulin B cells isolated from unimmunized mice (Fig. 7E–H). Mutations were randomly yet equally distributed in framework regions and CDRs, although no amino acid changes were observed (data not shown). Taken together, these data suggest that anti-insulin B cells enter GCs from the preimmune repertoire following immunization with the insulin-BRT conjugate, and a proportion of B cells undergo somatic hypermutation in these nonconventional GC reactions.

Discussion

Autoreactive B lymphocytes are recognized to enter the peripheral repertoire of normal individuals, and their presence is considered a liability for developing autoimmune disease. The association of IgG autoantibodies with pathological processes suggests that self-reactive B cells are recruited into immune responses. How this occurs is not clear, although a general assumption is that T cell–mediated help is required to reverse tolerance in such B cells. The present studies identify an alternative mechanism by which autoreactive B cells may escape peripheral tolerance without cognate T cell help. We describe the V_H125^{SD} B6 mouse, a new site-directed transgenic model that has a polyclonal B cell repertoire with a detectable population of IgM^+IgD^+ anti-insulin B cells that have the ability to undergo isotype switch. Anti-insulin B cells in V_H125^{SD} B6 mice are not eliminated but rather rendered clonally anergic in the periphery, unlike other models in which high-affinity Ag-specific B cells are eliminated because they fail to compete in the repertoire for residence in mature compartments

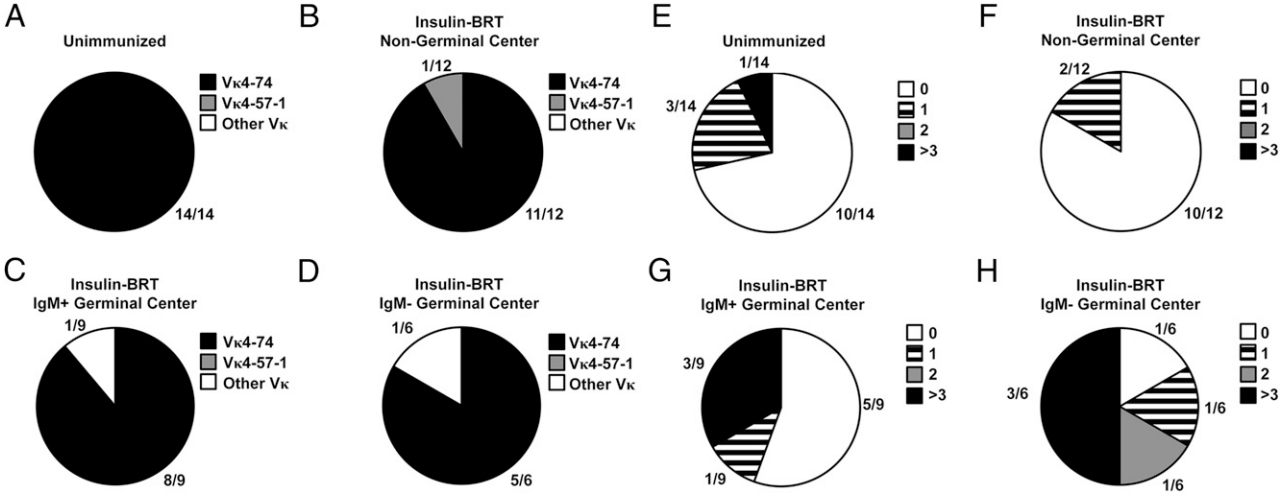

FIGURE 7. Anti-insulin L chains are selected from the preimmune repertoire to enter GC reactions. Spleens were harvested from unimmunized V_H125^{SD} B6 mice, or from mice 4 d following immunization with insulin-BRT. Flow cytometry sorting was used to purify insulin-binding B cells ($B220^+$ live lymphocytes), which were further gated in immunized mice as IgM^+ non-GC ($GL7^-Fas^-$), IgM^+ GC ($GL7^+Fas^+$), or IgM^- GC populations. Isolated RNA was transcribed to cDNA, and Igκ genes were amplified by PCR. Sequences were analyzed using the Ig BLAST database (see *Materials and Methods*). (**A**–**D**) The number of clones identified by the indicated Vκ is divided by the total number of clones analyzed for each immunization group. Vκ4-74 (black), Vκ4-57-1 (gray), all other Vκ (white). (**E**–**H**) Igκ clone sequences were compared with germline sequences, excluding the 5′ region that correlated with degenerate primers used for amplification. The numbers of sequences that possess the indicated number of nucleotide changes are shown for each immunization group: 0 (white), 1 (striped), 2 (gray), or >3 (black).

(51–53). Tolerance is maintained in CSR-competent anti-insulin B cells following TD immunization, as immunized V_H125^{SD} B6 mice do not produce IgG anti-insulin Abs (Fig. 4A). Immunization of V_H125^{SD} B6 mice with insulin conjugated to a type 1 TI Ag (insulin-BRT), however, provides BCR/TLR costimulation that reverses anergy in anti-insulin B cells and promotes proliferation, differentiation into GCs, and IgG autoantibody production.

Insulin-BRT was previously used to uncover rare anti-insulin B cells in the repertoires of normal mice independently of T cell help (33). As originally observed, conjugation of insulin and BRT was necessary to drive Ab production (33). As such, immunization of V_H125^{SD} B6 mice with insulin-BRT elicits IgM and IgG2a anti-insulin Abs, whereas neither BRT alone (Fig. 4B) nor BRT physically mixed with insulin (data not shown) elicits Ab production. The kinetics of the insulin-BRT response (3–5 d) and Ab isotypes observed following immunization are in agreement with those seen in response to classic type 1 TI Ags. Whereas insulin-BRT responses have been shown to occur in the absence of T cells (33, 43), they are likely influenced by bystander effects or other non-specific T cell factors, as demonstrated for other TI Ags (54).

Other examples of B cell tolerance reversal independent of T cell help have been described. B cells specific for MHC class I in 3-83 transgenic mice develop normally in the bone marrow but undergo clonal deletion in the periphery when they encounter liver-expressed H-$2K^b$ (55, 56). However, administration of a bacteriophage containing a 15-aa mimotope that is recognized by 3-83 B cells reverses tolerance and drives robust Ig production (55). Thus, tolerant B cells that are normally deleted in the periphery are actually rescued when self-antigen is presented to the B cell in a TI fashion. Similarly, anergy in anti-insulin B cells is reversed by BCR/TLR costimulation in the insulin-BRT response that is relatively TI.

Insulin-specific GCs are found in V_H125^{SD} B6 mice at day 5 of the insulin-BRT response (Fig. 6), consistent with previous studies that demonstrated B cells specific for the hapten nitrophenol (NP) can enter GCs without T cell help following immunization with the type 2 TI immunogen NP-Ficoll (48). NP-Ficoll immunization only elicited GCs in QM transgenic mice, which have ~60% B cells specific for NP, but not in nontransgenic (WT) littermates. de Vinuesa et al. (48) used transfer experiments to confirm that TI GCs only arose when the NP-specific B cell precursor frequency was 1 in 1000 or higher. V_H125^{SD} B6 mice possess ~0.4% anti-insulin B cells in the periphery (1 in 250), whereas the frequency in WT B6 is closer to 1 in 100,000 (Fig. 3). As such, we did not observe any detectable insulin-specific GCs in WT mice following insulin-BRT immunization (data not shown), despite IgM and IgG anti-insulin Ab production in the same mice (Fig. 4B). The increased frequency of anti-insulin B cell precursors in V_H125^{SD} B6 mice supports the generation of insulin-specific GCs by day 5 and could explain the increased IgM anti-insulin Ab production observed in V_H125^{SD} compared with WT B6 mice. Insulin-specific GCs are found in V_H125^{SD} B6 mice at day 12 but at a much lower frequency, as expected for GCs over time in the absence of T cell help. We are currently introducing V_H125^{SD} into NOD mice to determine how these unconventional GC reactions are controlled in an autoimmune strain of mice predisposed to type 1 diabetes.

Igκ genes from the preimmune repertoire do not undergo negative selection in GCs, as evidenced by exclusive anti-insulin Vκ4-74 usage by BCRs in anti-insulin B cells from unimmunized V_H125^{SD} B6 mice and in IgM^+ and IgM^- insulin-binding GC B cells from mice following insulin-BRT immunization (Fig. 7). Prior studies show that Vκ4-74 pairs with several Jκ to form autoreactive insulin-binding BCRs when combined with V_H125 (35). Thus, insulin-binding B cells from the preimmune repertoire, and not obscure clonally ignorant B cells, are selected for GC entry during the insulin-BRT response.

The presence of nucleotide mutations in Vκ4-74 clones indicates that somatic hypermutation occurs in these TI GCs. Approximately half of the mutations observed in both IgM^+ and IgM^- insulin-binding GC clones were found in CDRs, and although amino acid replacements were not observed, the findings suggest that Ag binding could be altered in these atypical GCs. Our data demonstrate that reversal of anergy in anti-insulin B cells provided by BCR/TLR costimulation in vivo extends to evasion of a tolerance program normally designed to eliminate such autoreactive clones in GCs. Although insulin-BRT may not mimic any natural molecule, loss of B cell tolerance via similar pathways may be possible in circumstances where the levels of autoantigen and innate stimulus are high, such as on the surface of APCs. This could occur in association with islet inflammation in type 1 diabetes where APCs are found in close contact with insulin-producing β cells (57) or following uptake of insulin injected through contaminated skin by epidermal and dermal APCs (58). Recently, TLR-7 signaling was implicated in the development of spontaneous GCs and autoantibodies in a systemic lupus erythematosus model (59), in addition to the previously recognized role of TLR-9 in autoimmune disease (60). Furthermore, BCR/TLR synergy has been shown to induce TI CSR through the noncanonical NF-κB pathway (61). Thus, there is growing evidence to support a unique role for TLRs in the generation of GCs and production of IgG autoantibodies.

We examined the capacity of various TLR mitogens, such as ssRNA and CpG DNA, to synergize with insulin in vitro to reverse anergy in anti-insulin B cells and found that LPS was the only TLR agonist that enhanced proliferation. BRT contains noncanonical LPS (62–64), and thus we expect that the proliferation induced by insulin-BRT in vivo (Fig. 5B) occurs in part by TLR-4 stimulation. These data implicate TLR-4 in the reversal of anergy in anti-insulin B cells, although other TLRs are clearly important for tolerance to different autoantigens. The fact that this phenotype occurred at very low stimulating concentrations (Fig. 2E) suggests that signaling thresholds for autoreactive B cells are quite low, and that loss of anergy may arise more quickly and easily than previously thought.

IgG anti-insulin Abs that arise following insulin-BRT immunization were confirmed to be autoreactive by indirect immunofluorescence, as they bound mouse insulin on pancreata sections from both unimmunized and immunized mice. These same autoantibodies were not detected endogenously on the tissue using direct immunofluorescence, suggesting that a lack of access of autoantibodies to their tissue targets may limit their autoimmune potential. For example, anti–H-$2K^b$ Abs generated by phage-mimotope immunization were found on the surfaces of hepatocytes in 3-83 Tg mice (55), reflecting the ubiquitous surface expression of MHC class I in the target organ. Access to insulin epitopes may be more restricted in the islets. Experiments in V_H125^{SD} NOD mice will determine whether reversal of anergy in anti-insulin B cells driven by BCR/TLR costimulation accelerates immunopathology.

Type 1 diabetes in mice and humans is a multigenic autoimmune disorder in which detection of IgG insulin autoantibodies indicates that loss of tolerance in anti-insulin B cells is a critical event in disease pathogenesis. We show evidence that this breach in the B cell compartment surprisingly does not depend on T cell help. Common environmental triggers resulting from infection and inflammation that are prevalent in children could combine with endogenous insulin to break anti-insulin B cell tolerance. BCR/TLR costimulation of autoreactive B lymphocytes could repre-

sent an early, underappreciated event in the induction of autoimmunity.

Acknowledgments

We thank Dr. Klaus Rajewsky for providing the pIV$_H$L2neoR targeting vector, and we thank Dr. Richard Breyer for EIIA-Cre B6 mice. We thank the Vanderbilt Technologies for Advanced Genomics Sequencing Core, the Transgenic Mouse/Embryonic Stem Cell Shared Resource, the Vanderbilt Flow Cytometry Shared Resource, and the Translational Pathology Shared Resource. We thank the Division of Animal Care for assistance in the maintenance of the mice. We also graciously thank Dr. John Williams, Dr. Daniel Moore, and Dr. Damian Maseda for critical review of the manuscript.

Disclosures

The authors have no financial conflicts of interest.

References

1. Pelanda, R., and R. M. Torres. 2012. Central B-cell tolerance: where selection begins. *Cold Spring Harb. Perspect. Biol.* 4: a007146.
2. Casellas, R., T. A. Shih, M. Kleinewietfeld, J. Rakonjac, D. Nemazee, K. Rajewsky, and M. C. Nussenzweig. 2001. Contribution of receptor editing to the antibody repertoire. *Science* 291: 1541–1544.
3. Radic, M. Z., J. Erikson, S. Litwin, and M. Weigert. 1993. B lymphocytes may escape tolerance by revising their antigen receptors. *J. Exp. Med.* 177: 1165–1173.
4. Nemazee, D., and K. Buerki. 1989. Clonal deletion of autoreactive B lymphocytes in bone marrow chimeras. *Proc. Natl. Acad. Sci. USA* 86: 8039–8043.
5. Chen, C., Z. Nagy, E. L. Prak, and M. Weigert. 1995. Immunoglobulin heavy chain gene replacement: a mechanism of receptor editing. *Immunity* 3: 747–755.
6. Cambier, J. C., S. B. Gauld, K. T. Merrell, and B. J. Vilen. 2007. B-cell anergy: from transgenic models to naturally occurring anergic B cells? *Nat. Rev. Immunol.* 7: 633–643.
7. Yarkoni, Y., A. Getahun, and J. C. Cambier. 2010. Molecular underpinning of B-cell anergy. *Immunol. Rev.* 237: 249–263.
8. Sakaguchi, S., K. Wing, Y. Onishi, P. Prieto-Martin, and T. Yamaguchi. 2009. Regulatory T cells: how do they suppress immune responses? *Int. Immunol.* 21: 1105–1111.
9. Kim, J., K. Lahl, S. Hori, C. Loddenkemper, A. Chaudhry, P. deRoos, A. Rudensky, and T. Sparwasser. 2009. Cutting edge: depletion of Foxp3$^+$ cells leads to induction of autoimmunity by specific ablation of regulatory T cells in genetically targeted mice. *J. Immunol.* 183: 7631–7634.
10. Goodnow, C. C., J. Crosbie, S. Adelstein, T. B. Lavoie, S. J. Smith-Gill, R. A. Brink, H. Pritchard-Briscoe, J. S. Wotherspoon, R. H. Loblay, K. Raphael, et al. 1988. Altered immunoglobulin expression and functional silencing of self-reactive B lymphocytes in transgenic mice. *Nature* 334: 676–682.
11. Goodnow, C. C., J. Crosbie, H. Jorgensen, R. A. Brink, and A. Basten. 1989. Induction of self-tolerance in mature peripheral B lymphocytes. *Nature* 342: 385–391.
12. Getahun, A., S. K. O'Neill, and J. C. Cambier. 2009. Establishing anergy as a bona fide in vivo mechanism of B cell tolerance. *J. Immunol.* 183: 5439–5441.
13. Merrell, K. T., R. J. Benschop, S. B. Gauld, K. Aviszus, D. Decote-Ricardo, L. J. Wysocki, and J. C. Cambier. 2006. Identification of anergic B cells within a wild-type repertoire. *Immunity* 25: 953–962.
14. Hikida, M., and T. Kurosaki. 2005. Regulation of phospholipase C-γ2 networks in B lymphocytes. *Adv. Immunol.* 88: 73–96.
15. Fruman, D. A., and G. Bismuth. 2009. Fine tuning the immune response with PI3K. *Immunol. Rev.* 228: 253–272.
16. Menard, L., D. Saadoun, I. Isnardi, Y. S. Ng, G. Meyers, C. Massad, C. Price, C. Abraham, R. Motaghedi, J. H. Buckner, et al. 2011. The PTPN22 allele encoding an R620W variant interferes with the removal of developing autoreactive B cells in humans. *J. Clin. Invest.* 121: 3635–3644.
17. Avalos, A. M., L. Busconi, and A. Marshak-Rothstein. 2010. Regulation of autoreactive B cell responses to endogenous TLR ligands. *Autoimmunity* 43: 76–83.
18. Avalos, A. M., M. B. Uccellini, P. Lenert, G. A. Viglianti, and A. Marshak-Rothstein. 2010. FcγRIIB regulation of BCR/TLR-dependent autoreactive B-cell responses. *Eur. J. Immunol.* 40: 2692–2698.
19. Maglione, P. J., N. Simchoni, S. Black, L. Radigan, J. R. Overbey, E. Bagiella, J. B. Bussel, X. Bossuyt, J. L. Casanova, I. Meyts, et al. 2014. IRAK-4 and MyD88 deficiencies impair IgM responses against T-independent bacterial antigens. *Blood* 124: 3561–3571.
20. Dye, J. R., A. Palvanov, B. Guo, and T. L. Rothstein. 2007. B cell receptor cross-talk: exposure to lipopolysaccharide induces an alternate pathway for B cell receptor-induced ERK phosphorylation and NF-κB activation. *J. Immunol.* 179: 229–235.
21. Kendall, P. L., G. Yu, E. J. Woodward, and J. W. Thomas. 2007. Tertiary lymphoid structures in the pancreas promote selection of B lymphocytes in autoimmune diabetes. *J. Immunol.* 178: 5643–5651.
22. Kendall, P. L., J. B. Case, A. M. Sullivan, J. S. Holderness, K. S. Wells, E. Liu, and J. W. Thomas. 2013. Tolerant anti-insulin B cells are effective APCs. *J. Immunol.* 190: 2519–2526.
23. Yalow, R. S., and S. A. Berson. 1960. Immunoassay of endogenous plasma insulin in man. *J. Clin. Invest.* 39: 1157–1175.
24. Schroer, J. A., J. K. Inman, J. W. Thomas, and A. S. Rosenthal. 1979. H-2-linked Ir gene control of antibody responses to insulin. I. Anti-insulin plaque-forming cell primary responses. *J. Immunol.* 123: 670–675.
25. Rojas, M., C. Hulbert, and J. W. Thomas. 2001. Anergy and not clonal ignorance determines the fate of B cells that recognize a physiological autoantigen. *J. Immunol.* 166: 3194–3200.
26. Acevedo-Suárez, C. A., C. Hulbert, E. J. Woodward, and J. W. Thomas. 2005. Uncoupling of anergy from developmental arrest in anti-insulin B cells supports the development of autoimmune diabetes. *J. Immunol.* 174: 827–833.
27. Koczwara, K., M. Schenker, S. Schmid, K. Kredel, A. G. Ziegler, and E. Bonifacio. 2003. Characterization of antibody responses to endogenous and exogenous antigen in the nonobese diabetic mouse. *Clin. Immunol.* 106: 155–162.
28. Boes, M., T. Schmidt, K. Linkemann, B. C. Beaudette, A. Marshak-Rothstein, and J. Chen. 2000. Accelerated development of IgG autoantibodies and autoimmune disease in the absence of secreted IgM. *Proc. Natl. Acad. Sci. USA* 97: 1184–1189.
29. Hoppu, S., M. S. Ronkainen, T. Kimpimäki, S. Simell, S. Korhonen, J. Ilonen, O. Simell, and M. Knip. 2004. Insulin autoantibody isotypes during the prediabetic process in young children with increased genetic risk of type 1 diabetes. *Pediatr. Res.* 55: 236–242.
30. Hahn, B. H. 1998. Antibodies to DNA. *N. Engl. J. Med.* 338: 1359–1368.
31. Zhang, L., M. Nakayama, and G. S. Eisenbarth. 2008. Insulin as an autoantigen in NOD/human diabetes. *Curr. Opin. Immunol.* 20: 111–118.
32. Nakayama, M. 2011. Insulin as a key autoantigen in the development of type 1 diabetes. *Diabetes Metab. Res. Rev.* 27: 773–777.
33. Thomas, J. W., R. P. Bucy, and J. A. Kapp. 1982. T cell-independent responses to an Ir gene-controlled antigen. I. Characteristics of the immune response to insulin complexed to *Brucella abortus*. *J. Immunol.* 129: 6–10.
34. Pewzner-Jung, Y., D. Friedmann, E. Sonoda, S. Jung, K. Rajewsky, and D. Eilat. 1998. B cell deletion, anergy, and receptor editing in "knock in" mice targeted with a germline-encoded or somatically mutated anti-DNA heavy chain. *J. Immunol.* 161: 4634–4645.
35. Henry-Bonami, R. A., J. M. Williams, A. B. Rachakonda, M. Karamali, P. L. Kendall, and J. W. Thomas. 2013. B lymphocyte "original sin" in the bone marrow enhances islet autoreactivity in type 1 diabetes-prone nonobese diabetic mice. *J. Immunol.* 190: 5992–6003.
36. Thomas, J. W., V. J. Virta, and L. J. Nell. 1986. Idiotypic determinants on human anti-insulin antibodies are cyclically expressed. *J. Immunol.* 137: 1610–1615.
37. Woodward, E. J., and J. W. Thomas. 2005. Multiple germline κ light chains generate anti-insulin B cells in nonobese diabetic mice. *J. Immunol.* 175: 1073–1079.
38. Henry, R. A., P. L. Kendall, E. J. Woodward, C. Hulbert, and J. W. Thomas. 2010. Vκ polymorphisms in NOD mice are spread throughout the entire immunoglobulin kappa locus and are shared by other autoimmune strains. *Immunogenetics* 62: 507–520.
39. Phan, T. G., M. Amesbury, S. Gardam, J. Crosbie, J. Hasbold, P. D. Hodgkin, A. Basten, and R. Brink. 2003. B cell receptor-independent stimuli trigger immunoglobulin (Ig) class switch recombination and production of IgG autoantibodies by anergic self-reactive B cells. *J. Exp. Med.* 197: 845–860.
40. Liu, Z., and A. Davidson. 2011. BAFF and selection of autoreactive B cells. *Trends Immunol.* 32: 388–394.
41. Enzler, T., G. Bonizzi, G. J. Silverman, D. C. Otero, G. F. Widhopf, A. Anzelon-Mills, R. C. Rickert, and M. Karin. 2006. Alternative and classical NF-κB signaling retain autoreactive B cells in the splenic marginal zone and result in lupus-like disease. *Immunity* 25: 403–415.
42. Gavin, A. L., K. Hoebe, B. Duong, T. Ota, C. Martin, B. Beutler, and D. Nemazee. 2006. Adjuvant-enhanced antibody responses in the absence of Toll-like receptor signaling. *Science* 314: 1936–1938.
43. Mond, J. J., I. Scher, D. E. Mosier, M. Baese, and W. E. Paul. 1978. T-independent responses in B cell-defective CBA/N mice to *Brucella abortus* and to trinitrophenyl (TNP) conjugates of *Brucella abortus*. *Eur. J. Immunol.* 8: 459–463.
44. Gitlin, A. D., Z. Shulman, and M. C. Nussenzweig. 2014. Clonal selection in the germinal centre by regulated proliferation and hypermutation. *Nature* 509: 637–640.
45. Baumjohann, D., S. Preite, A. Reboldi, F. Ronchi, K. M. Ansel, A. Lanzavecchia, and F. Sallusto. 2013. Persistent antigen and germinal center B cells sustain T follicular helper cell responses and phenotype. *Immunity* 38: 596–605.
46. Qi, H., J. L. Cannons, F. Klauschen, P. L. Schwartzberg, and R. N. Germain. 2008. SAP-controlled T-B cell interactions underlie germinal centre formation. *Nature* 455: 764–769.
47. Fagarasan, S., and T. Honjo. 2000. T-Independent immune response: new aspects of B cell biology. *Science* 290: 89–92.
48. de Vinuesa, C. G., M. C. Cook, J. Ball, M. Drew, Y. Sunners, M. Cascalho, M. Wabl, G. G. Klaus, and I. C. MacLennan. 2000. Germinal centers without T cells. *J. Exp. Med.* 191: 485–494.
49. Wang, D., S. M. Wells, A. M. Stall, and E. A. Kabat. 1994. Reaction of germinal centers in the T-cell-independent response to the bacterial polysaccharide alpha (1→6)dextran. *Proc. Natl. Acad. Sci. USA* 91: 2502–2506.

50. Ewulonu, U. K., L. J. Nell, and J. W. Thomas. 1990. V_H and V_L gene usage by murine IgG antibodies that bind autologous insulin. *J. Immunol.* 144: 3091–3098.
51. Hartley, S. B., J. Crosbie, R. Brink, A. B. Kantor, A. Basten, and C. C. Goodnow. 1991. Elimination from peripheral lymphoid tissues of self-reactive B lymphocytes recognizing membrane-bound antigens. *Nature* 353: 765–769.
52. Wang, H., and M. J. Shlomchik. 1997. High affinity rheumatoid factor transgenic B cells are eliminated in normal mice. *J. Immunol.* 159: 1125–1134.
53. Cyster, J. G., S. B. Hartley, and C. C. Goodnow. 1994. Competition for follicular niches excludes self-reactive cells from the recirculating B-cell repertoire. *Nature* 371: 389–395.
54. Endres, R. O., E. Kushnir, J. W. Kappler, P. Marrack, and S. C. Kinsky. 1983. A requirement for nonspecific T cell factors in antibody responses to "T cell independent" antigens. *J. Immunol.* 130: 781–784.
55. Kouskoff, V., G. Lacaud, and D. Nemazee. 2000. T cell-independent rescue of B lymphocytes from peripheral immune tolerance. *Science* 287: 2501–2503.
56. Caucheteux, S. M., C. Vernochet, J. Wantyghem, M. C. Gendron, and C. Kanellopoulos-Langevin. 2008. Tolerance induction to self-MHC antigens in fetal and neonatal mouse B cells. *Int. Immunol.* 20: 11–20.
57. Mohan, J. F., M. G. Levisetti, B. Calderon, J. W. Herzog, S. J. Petzold, and E. R. Unanue. 2010. Unique autoreactive T cells recognize insulin peptides generated within the islets of Langerhans in autoimmune diabetes. *Nat. Immunol.* 11: 350–354.
58. Levin, C., H. Perrin, and B. Combadiere. 2015. Tailored immunity by skin antigen-presenting cells. *Hum. Vaccin. Immunother.* 11: 27–36.
59. Soni, C., E. B. Wong, P. P. Domeier, T. N. Khan, T. Satoh, S. Akira, and Z. S. Rahman. 2014. B cell-intrinsic TLR7 signaling is essential for the development of spontaneous germinal centers. *J. Immunol.* 193: 4400–4414.
60. Christensen, S. R., M. Kashgarian, L. Alexopoulou, R. A. Flavell, S. Akira, and M. J. Shlomchik. 2005. Toll-like receptor 9 controls anti-DNA autoantibody production in murine lupus. *J. Exp. Med.* 202: 321–331.
61. Pone, E. J., J. Zhang, T. Mai, C. A. White, G. Li, J. K. Sakakura, P. J. Patel, A. Al-Qahtani, H. Zan, Z. Xu, and P. Casali. 2012. BCR-signalling synergizes with TLR-signalling for induction of AID and immunoglobulin class-switching through the non-canonical NF-κB pathway. *Nat. Commun.* 3: 767.
62. Forestier, C., E. Moreno, S. Méresse, A. Phalipon, D. Olive, P. Sansonetti, and J. P. Gorvel. 1999. Interaction of *Brucella abortus* lipopolysaccharide with major histocompatibility complex class II molecules in B lymphocytes. *Infect. Immun.* 67: 4048–4054.
63. Betts, M., P. Beining, M. Brunswick, J. Inman, R. D. Angus, T. Hoffman, and B. Golding. 1993. Lipopolysaccharide from *Brucella abortus* behaves as a T-cell-independent type 1 carrier in murine antigen-specific antibody responses. *Infect. Immun.* 61: 1722–1729.
64. Weiss, D. S., K. Takeda, S. Akira, A. Zychlinsky, and E. Moreno. 2005. MyD88, but not Toll-like receptors 4 and 2, is required for efficient clearance of *Brucella abortus*. *Infect. Immun.* 73: 5137–5143.

B Lymphocyte "Original Sin" in the Bone Marrow Enhances Islet Autoreactivity in Type 1 Diabetes–Prone Nonobese Diabetic Mice

Rachel A. Henry-Bonami,* Jonathan M. Williams,† Amita B. Rachakonda,* Mariam Karamali,* Peggy L. Kendall,‡ and James W. Thomas*,†

Effective central tolerance is required to control the large extent of autoreactivity normally present in the developing B cell repertoire. Insulin-reactive B cells are required for type 1 diabetes in the NOD mouse, because engineered mice lacking this population are protected from disease. The Cg-Tg(Igh-6/Igh-V125)2Jwt/JwtJ (VH125Tg) model is used to define this population, which is found with increased frequency in the periphery of NOD mice versus nonautoimmune C57BL/6 VH125Tg mice; however, the ontogeny of this disparity is unknown. To better understand the origins of these pernicious B cells, anti-insulin B cells were tracked during development in the polyclonal repertoire of VH125Tg mice. An increased proportion of insulin-binding B cells is apparent in NOD mice at the earliest point of Ag commitment in the bone marrow. Two predominant L chains were identified in B cells that bind heterologous insulin. Interestingly, Vκ4-57-1 polymorphisms that confer a CDR3 Pro-Pro motif enhance self-reactivity in VH125Tg/NOD mice. Despite binding circulating autoantigen in vivo, anti-insulin B cells transition from the parenchyma to the sinusoids in the bone marrow of NOD mice and enter the periphery unimpeded. Anti-insulin B cells expand at the site of autoimmune attack in the pancreas and correlate with increased numbers of IFN-γ–producing cells in the repertoire. These data identify the failure to cull autoreactive B cells in the bone marrow as the primary source of anti-insulin B cells in NOD mice and suggest that dysregulation of central tolerance permits their escape into the periphery to promote disease. ***The Journal of Immunology*****, 2013, 190: 5992–6003.**

Central tolerance is a critical barrier for the development of autoreactive B lymphocytes. Dangerous self-specificities are seeded into the peripheral B lymphocyte repertoire to promote several autoimmune diseases, suggesting defective central tolerance (1–4). A better understanding of how and why central tolerance fails is necessary to enhance treatment modalities for complex autoimmune disorders. A key goal is to correct the underlying immune defects in these patients, rather than only managing symptoms after the destruction has run its course.

Developmental checkpoints exist in the bone marrow (BM) that revise BCR autoreactivity or limit BM egress and maturational progression. Ag availability and BCR interaction strength control whether and how developing B cells are censored. Receptor editing is the primary mechanism through which autoreactivity is removed from the developing repertoire; if receptor editing fails, deletion may ensue (5). Developing B cells migrate from the BM parenchyma into the BM sinusoids as they mature and prepare for egress into the blood (6). Autoreactive B cells that undergo receptor editing show impaired transition from the BM parenchyma into the sinusoids (7). Furthermore, loss of cannabinoid receptor 2, required for sinusoidal retention, reduces the frequency of λ^+ B cells in the periphery, consistent with the hypothesis that limiting the window of time in the BM reduces receptor editing (6). These data highlight the transition between these anatomical niches as a key central tolerance checkpoint.

The NOD mouse model develops type 1 diabetes (T1D) spontaneously, and it mirrors many aspects of human disease. Insulin autoantibodies are predictive of T1D development in both mice and humans (8–10), suggesting that breaches in B lymphocyte tolerance occur. Insulin is a critical T1D autoantigen; limiting insulin recognition by either the T cell (11) or B cell (12) repertoires is protective against disease development in NOD mice. To better understand how autoreactive B cells are censored differently in the context of autoimmune disease, anti-insulin B cell development was investigated in NOD mice. Despite the clear presence of insulin autoantibodies in wild-type (WT)/NOD mice, anti-insulin B cells are difficult to reliably track in the mature WT/NOD repertoire (13). The Cg-Tg(Igh-6/Igh-V125)2Jwt/JwtJ (VH125Tg) model harbors an anti-insulin H chain that pairs with endogenous L chains. This model permits clear tracking of this important

*Division of Rheumatology and Immunology, Department of Medicine, Vanderbilt University, Nashville TN 37232; †Department of Pathology, Microbiology and Immunology, Vanderbilt University, Nashville, TN 37232; and ‡Division of Allergy, Pulmonary, and Critical Care, Department of Medicine, Vanderbilt University, Nashville TN 37232

Received for publication May 14, 2012. Accepted for publication April 4, 2013.

This work was supported by National Institutes of Health Grants 5T32-HL069765, 5T32-AR059039, R01-AI051448, R01 DK084246, and K08 DK070924 and was supported by the following Vanderbilt University Medical Center core facilities: the Vanderbilt Medical Center Flow Cytometry Shared Resource (supported by the Vanderbilt Ingram Cancer Center [P30 CA68485] and the Vanderbilt Digestive Disease Research Center [DK058404]), the Vanderbilt DNA Sequencing Facility (supported by the Vanderbilt Ingram Cancer Center [P30 CA68485], the Vanderbilt Vision Center [P30 EY08126], and the National Institutes of Health/National Center for Research Resources [G20 RR030956]), and the Vanderbilt Diabetes Research and Training Center (DK20593).

The sequences presented in this article have been submitted to GenBank (http://www/ncbi.nlm.nih.gov/genbank/) under accession numbers JQ915156–JQ915195, JX064462–JX064465, and KC484488–KC484561.

Address correspondence and reprint requests to Dr. James W. Thomas, Vanderbilt University, Medical Center North T3113, 1161 21st Avenue South, Nashville, TN 37232. E-mail address: james.w.thomas@vanderbilt.edu

Abbreviations used in this article: B6, C57BL/6; BM, bone marrow; IMGT, ImMunoGeneTics; MFI, mean fluorescence intensity; RT, room temperature; SHM, somatic hypermutation; T1D, type 1 diabetes; Tg, transgenic; VH, H chain Ig transgenic; VH125Tg, Cg-Tg(Igh-6/Igh-V125)2Jwt/JwtJ; VH281Tg, Tg(Igh-6/Igh-V281)3Jwt/JwtJ; WT, wild-type.

specificity within the context of a polyclonal repertoire (12). Thus, this approach preserves competition of autoreactive B cells with nonautoreactive B cells for survival factors, follicular entry, and other biological aspects known to impact how central tolerance is imposed (14, 15). Previous studies demonstrated that, although anti-insulin B cells are readily observed in the mature repertoire of VH125Tg/NOD mice, this specificity is reduced or absent in the mature repertoire of nonautoimmune VH125Tg/C57BL/6 (B6) mice, despite restricted usage of the same anti-insulin H chain (13, 16). The ontogeny of this disparity is unknown, but it could contain clues about how similar tolerance defects may promote autoimmune disease in humans.

Using the VH125Tg model, we show that anti-insulin B cells form with increased frequency in BM of the autoimmune-prone NOD strain compared with the nonautoimmune B6 strain. This disparity is first evident among immature B cells present in the BM sinusoids, after they have transitioned from the parenchyma. BM culture also enhanced anti-insulin B cell formation in vitro, suggesting that extrinsic factors that might be unique to the autoimmune environment in vivo do not entirely account for this difference. Germline Vκ polymorphisms that confer the potential for generation of a Pro-Pro motif in CDR3 enhance the autoreactivity of the NOD insulin-binding L chain, Vκ4-57-1. In addition, negative selection of anti-insulin BCRs is not evident in VH125Tg/NOD mice, despite insulin encounter at the earliest stages of anti-insulin B cell development. Once this central tolerance defect seeds anti-insulin B cells into the mature repertoire, anti-insulin B cells are further enriched at the site of autoimmune attack in the pancreas. The presence of anti-insulin B cells in the repertoire is associated with an increased frequency of cells that produce IFN-γ, presumably insulin-reactive T cells. These data demonstrate that "original sin" against the insulin autoantigen is traced to enhanced BM production of anti-insulin B cells. The failure of central tolerance to cull this key autoimmune specificity from the developing B cell repertoire ultimately allows critical APCs to facilitate islet autoreactivity.

Materials and Methods

Animals

The anti-insulin VH125Tg [Cg-Tg(Igh-6/Igh-V125)2Jwt/JwtJ] and noninsulin-binding VH281Tg [Tg(Igh-6/Igh-V281)3Jwt/JwtJ] (The Jackson Laboratory) H chain transgenic (Tg) mice used in this study harbor a randomly integrated H chain Ig Tg (VH) on the B6 or NOD background, as described previously (12, 17). Age ranges are indicated in the figure legends. All data are derived from lines that have been backcrossed for >20 generations to B6 or NOD mice, which are hemizygous for all Tg indicated. All mice were housed under sterile conditions, and all studies were approved by the Institutional Animal Care and Use Committee of Vanderbilt University, which is fully accredited by the American Association for the Accreditation of Laboratory Animal Care.

Cell isolation and culture

BM was eluted from femurs, tibias, and humeri with HBSS (Invitrogen) + 10% FBS (HyClone). RBCs were lysed using Tris-NH_4Cl, and cells were used for flow cytometry analysis or resuspended at 2×10^6 cells/ml in complete culture medium (DMEM, 10% FBS, L-glutamine, HEPES, MEM sodium pyruvate, nonessential amino acids, gentamicin, 2×10^5 M 2-ME, and 15 ng/ml human rIL-7 [PeproTech]) and cultured for 5 d in a 37°C CO_2 incubator (all from Invitrogen unless otherwise specified). FBS contains fg/ml amounts of bovine insulin, which is below the threshold necessary to induce any B cell responsiveness in all assays tested. To remove IL-7, 5-d cultures were washed with HBSS + 10% FBS and resuspended at 2×10^6 cells/ml in culture media without IL-7 and grown for an additional 2 d, at which point cells were harvested and stained for flow cytometry analysis. Spleens were harvested and macerated, and RBCs were lysed. Freshly isolated pancreata were digested with 3 ml 1 mg/ml collagenase P diluted in HBSS at 37°C for 30 min and then tissue was disrupted using an 18G needle. HBSS + 10% FBS was added immediately to inhibit collagenase activity. Cells were resuspended and used for flow cytometry analysis.

Flow cytometry

Flow cytometry analysis was performed using an LSR II (BD Biosciences). Ab reagents reactive with B220 (6B2), IgM^a (DS-1), IgM^b (AF6-78), CD4 (RM4-5), CD19 (1D3), CD21 (7G6), CD23 (B3B4) (BD Biosciences), or IgM (μ-chain specific; Invitrogen), or 7-aminoactinomycin D, or DAPI were used for flow cytometry. Human insulin (Sigma-Aldrich) was biotinylated at pH 8 in bicine buffer using biotin N-hydroxysuccinimide ester (Sigma-Aldrich) and detected with fluorochrome-labeled streptavidin (BD Biosciences). Insulin-specific B cells were confirmed among $B220^+$ IgM^+ live lymphocytes by competitive inhibition with 10-fold excess unlabeled insulin, as well as a linear relationship of insulin-binding and IgM^a expression. The percentage of insulin-specific B cells was calculated by subtracting the percentage of insulin-binding B cells in the presence of 10× inhibition with unlabeled insulin competitor (e.g., Fig. 1B, *right panels*) from the percentage of insulin-binding B cells in the absence of unlabeled insulin competitor (e.g., Fig. 1B, *left panels*) to include only Ag-specific B cells in computational analyses. BCR occupancy with endogenous insulin was detected using a second anti-insulin Ab, mAb123 (10–20 μg/ml), which was biotinylated. Preincubation with Fc Block (2.4G2; BD Biosciences) did not impact the frequency of insulin-binding B cells (multiple experiments; data not shown). mAb123 binds a distinct insulin epitope from mAb125 (from which VH125Tg is derived), and it has been used successfully to detect 125Tg BCR occupancy with endogenous insulin (17). These mAbs do not recognize insulin bound to the hormone receptor (18). FlowJo (TreeStar) software was used for analysis.

Hybridoma generation

VH125Tg/NOD or VH125Tg/B6 mice were immunized with human or porcine insulin covalently conjugated to *Brucella abortus* ring test Ag (U.S. Department of Agriculture, Ames, IA) using insulin acylated with *m*-maleimidobenzoyl-N-hydroxysuccinimide ester (Pierce Chemical, Rockville, IL) and *B. abortus* thiolated with methyl-4-mercaptobutyrimidate (Pierce Chemical) (19). This approach was shown to interrogate the germline repertoire for anti-insulin B cells in BALB/c mice (19–22). Splenocytes were harvested after 3–5 d and used in a standard fusion protocol (19) with the mouse myeloma line NSO or to facilitate capture of autoreactive B cells, NSO-BCL2 line (a gift from Dr. Betty Diamond, Feinstein Institute, Manhasset, NY), as fusion partners (23). Hybridomas were selected in hypoxanthine-aminopterin-TdR (Sigma-Aldrich)-supplemented hybridoma medium (DMEM, 10% FBS, L-glutamine, HEPES, MEM sodium pyruvate, penicillin/streptomycin, 2×10^{-5} M 2-ME, and NCTC-109; Invitrogen), and production of anti-insulin Ab was verified through ELISA, as described previously (19). RNA was purified from expanded clones, and Vκ genes were amplified and sequenced as described below.

ELISA and calculation of autoreactivity index

Rows of the same 96-well plate were coated with either 1 μg/ml human (Sigma-Aldrich) or rodent (Novo, Bagsvaerd, Denmark) insulin and then incubated with parallel hybridoma supernatant samples in duplicate. Anti-insulin IgM^a Ab was measured as described previously (19), and wells were monitored for a human insulin with OD ~1.0 to normalize for differences in total Ab levels among hybridoma supernatants. To assess the level of self-reactivity of hybridoma clones with rodent insulin, the "autoreactivity index" was calculated by dividing the average rodent insulin OD by the average human insulin OD read at the same time point on the same plate. A value of 0 indicates no self-reactivity, whereas a value of 1 indicates comparable reactivity for both rodent and human insulin. ELISA duplicates were very precise (data not shown).

Determination of Vκ usage

BM cells were cultured for 5 d with IL-7 (as described above) to enrich for naive developing B cells. Splenocytes were enriched for B cells by $CD43^+$ cell depletion using anti-CD43 magnetic beads through magnetic sorting (Miltenyi). Developing (BM) or peripheral (spleen) B cells from five mice (8–12 wk of age) were incubated with anti-B220, anti-IgM^a, DAPI, and biotinylated insulin/streptavidin, and insulin-binding B cells were purified using a FACSAria I or II cell sorter. RNA was isolated from flow cytometry–sorted insulin-binding B cells using an Ambion RNAqueous-Micro kit or from insulin-binding hybridoma cell lines using an Ambion RNAqueous kit (Applied Biosystems). First-strand cDNA was generated from total RNA using Superscript II RT (Invitrogen) and 0.67 μg oligo-dT primer (GE Healthcare) in a standard protocol. Vκ sequences were amplified from first-strand cDNA using the following primers: murine Cκ primer, 5′−GGA TAC AGT TGG TGC AGC ATC-3′ and murine VκA, 5′−ATT GTK MTS ACM CAR TCT CCA-3′, where K = G or T, M = A or

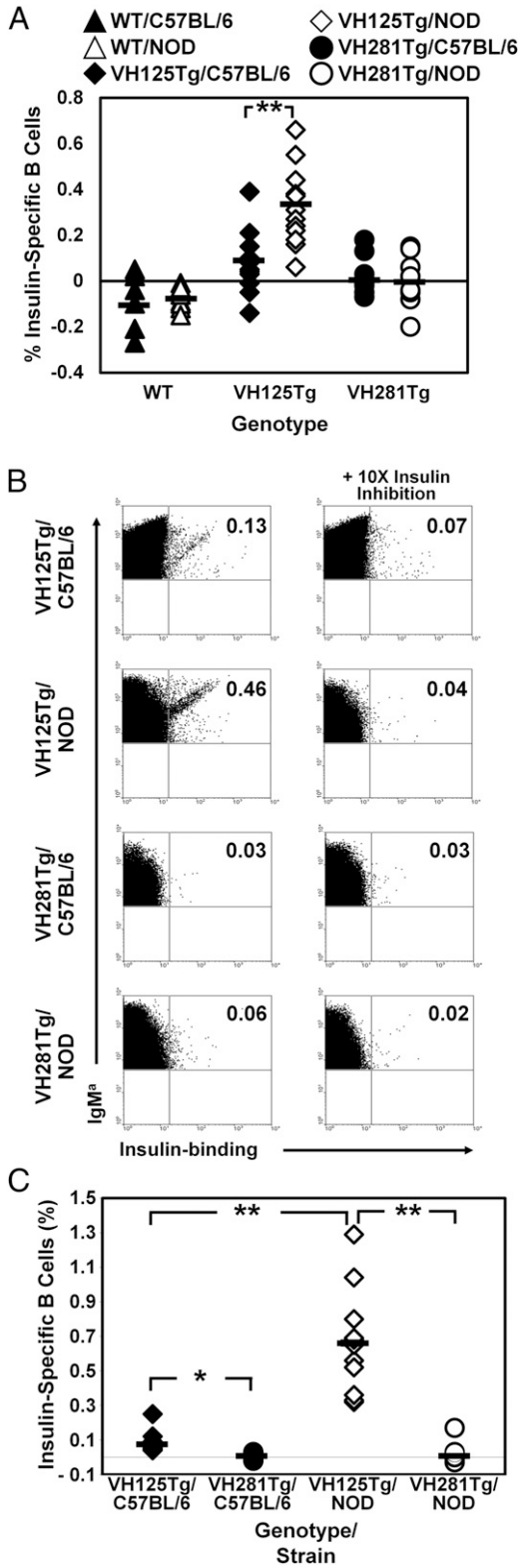

FIGURE 1. Increased formation of anti-insulin B cells initiates in the BM of T1D-prone VH125Tg/NOD mice. (**A**) Freshly isolated BM from B6 or NOD VH Tg (anti-insulin VH125 or noninsulin-binding VH281) or WT mice was phenotyped using high-throughput flow cytometry analysis. Cells were gated on $B220^{mid}$ IgM^{a+} live lymphocytes to show immature B cells. Parallel samples were incubated with 10-fold excess unlabeled insulin to demonstrate a specific interaction of the BCR with insulin; specific insulin binding was calculated as described in *Materials and Methods*. Results for individual 5–19-wk-old mice are plotted ($n \geq 7$ mice, $n \geq 4$ experiments). (**B** and **C**) BM from B6 or NOD VH Tg animals (anti-insulin VH125 or noninsulin-binding VH281) were cultured with IL-7 for 5 d to enrich for Ag-naive B cells. IL-7 was withdrawn, and cells were cultured in the absence of exogenous insulin for an additional 2 d. (B) The frequency of insulin-specific B cells was determined as above; representative flow cytometry plots are shown. (C) Results from individual mice are plotted: B6 (black), NOD (white), VH125Tg (diamonds), and VH281Tg (circles) ($n \geq 6$ 5–19-wk-old mice, $n \geq 4$ experiments). *$p < 0.01$, **$p < 0.001$, two-tailed t test.

C, S = C or G, and R = A or G. Vκ sequences were amplified, cloned, and sequenced as described previously (16, 24). Vκ gene segment sequence alignments (excluding sequence provided by the degenerate 5′ primer) were assigned using the ImMunoGeneTics (IMGT) database (http://www.imgt.cines.fr:8104/) and IgBLAST (http://www.ncbi.nlm.nih.gov/igblast/). Individual clones are each derived from independent pools of RNA, and accession numbers are provided in the legends for Figs. 2, 4, and 5.

In vivo labeling of sinusoidal B cells

Mice were injected i.v. with 1 μg anti–CD19-PE (1D3; BD Biosciences) and sacrificed after 2 min. BM was immediately eluted from femurs, tibias, and humeri, and cells were isolated as above. Cells were stained with Abs reactive with cell surface markers, including anti–CD19-allophycocyanin, to aid in the detection of sinusoidal ($CD19\text{-}PE^{hi}$, $CD19\text{-}allophycocyanin^{low}$) versus parenchymal ($CD19\text{-}PE^{low}$, $CD19\text{-}allophycocyanin^{hi}$) cells using flow cytometry, as described above. Specific labeling of B cells present in these anatomical niches using this method was reported previously (6).

ELISPOT assay to detect IFN-γ production

Ninety-six–well multiscreen filter plates (Millipore) were prewet with 70% methanol, washed with sterile 1× PBS (no Mg^{2+} or Ca^{2+}), coated with 10 μg/ml unlabeled anti-mouse IFN-γ (14-7313-85; eBioscience) in 1× PBS, and incubated overnight at 4°C in the dark. Plates were washed with 1× PBS and blocked with complete RPMI culture medium (RPMI 1640 [Cellgro] containing 10% FBS, 1% L-glutamine, 1% HEPES, 0.2% gentamicin, and 0.1% 2-ME; Life Technologies) for 1 h at room temperature (RT). Splenocytes from VH281Tg/NOD and VH125Tg/NOD female mice were isolated and plated at 5×10^5 cells/well, with or without 100 μg/ml human insulin (Sigma-Aldrich), or with 5 μg/ml anti-mouse CD3 (hybridoma 2C11; American Type Culture Collection) as positive control and incubated for 72–96 h at 37°C in a CO_2 incubator. Plates were washed with 1× PBS and then with wash buffer (1× PBS/1% FBS/0.05% Tween-20), coated with 2 μg/ml biotinylated anti-mouse IFN-γ (13-7312-85; eBioscience) in 1× PBS/0.5% FBS, and rocked for 3 h at RT. Plates were washed with wash buffer, rocked with avidin peroxidase complex (PK-6100; VECTASTAIN) prepared in wash buffer for 1 h at RT, and washed with wash buffer, followed by 1× PBS. Thirty percent H_2O_2 was added immediately before coating the plate with one 3-amino-9-ethyl-carbazole (205-057-7; Sigma-Aldrich) tablet dissolved in 2.5 ml di-methyl formamide and mixed with 0.1 M acetate buffer, which was incubated for 10–15 min at RT. Cold tap water was used to stop the reaction, and dry plates were read on an ImmunoSpot plate reader (Cellular Technology Limited). Data are expressed as the average of technical triplicates of the number of spots/well/10^4 $CD4^+$ T cells (calculated using total cell count and $CD4^+$ live lymphocyte frequency identified using flow cytometry).

Results

The liability for anti-insulin B cell formation arises early during B cell development in the BM of VH125Tg/NOD mice and is independent of autoantigen exposure

An increased frequency of insulin-binding B cells is found in the mature B cell repertoire of NOD mice, despite identical H chain transgenes that provide similar potential to generate anti-insulin B cells in both B6 and NOD strains (13). The small population of anti-insulin B cells present in the mature VH125Tg/NOD B cell repertoire is sufficient to promote T1D (12, 25). To identify the ontogeny of this disparity and uncover where tolerance defects arise, high-throughput flow cytometry was used to investigate these populations in the BM. Insulin autoantibodies are harbingers of disease in WT/NOD mice (9); however, anti-insulin B cells are difficult to detect in the BM (Fig. 1). This issue was circumvented

by the use of the VH125Tg model, in which a small, but reproducible, population of insulin-specific B cells (calculated as described in *Materials and Methods*) was detected among B6 and NOD VH125Tg immature B cells ($B220^{mid}$ IgM^{a+} live lymphocytes) in the BM (Fig. 1A). This population is not observed in VH281Tg mice (12), confirming Ag specificity in VH125Tg mice. Of note, the percentage of insulin-specific immature B cells observed was increased significantly (~3–4-fold) in the BM of VH125Tg/NOD mice (0.32 ± 0.17) compared with VH125Tg/B6 mice (0.08 ± 0.14, $p < 0.001$) (Fig. 1A). Contamination of $CD23^+$ mature recirculating B cells in the $B220^{mid}$ IgM^+ gate is minimal; similar results are observed when immature B cells are defined as $B220^+$ IgM^+ $CD23^-$ (data not shown). These data show that the VH125Tg model can be used to track the otherwise rare population of anti-insulin B cells as they navigate tolerance hurdles during development. Furthermore, these data suggest that the autoimmune strain enhances formation of anti-insulin B cells, despite H chain repertoire restriction.

IL-7–driven BM culture generates Ag-naive immature (IgM^+ $CD23^-$) B cells in vitro (26, 27); thus, it provides a useful tool to eliminate tolerance induced by circulating insulin, as well as other environmental influences present in vivo, which may differentially shape autoreactive B cell development within the two strains. Therefore, B6 or NOD VH125Tg BM was cultured with IL-7 in vitro in the absence of insulin to investigate the generation of anti-insulin immature B cells. Flow cytometry analysis of live $B220^+$ IgM^{a+} VH125Tg/NOD BM cultured with IL-7 showed a nearly 10-fold increased percentage of insulin-binding B cells (0.66 ± 0.29) compared with VH125Tg/B6 BM (0.07 ± 0.06, $p < 0.001$) (Fig. 1B, summarized in Fig. 1C). VH125Tg/B6 mice showed a significantly increased percentage of insulin-binding B cells compared with negative-control VH281Tg/B6 mice ($p < 0.01$). This demonstrates that enhanced formation of insulin-binding B cells in the developing VH125Tg/NOD BM repertoire occurs independently of the in vivo environment, in which circulating insulin exposure occurs.

The increased frequency of anti-insulin B cells is first apparent among immature B cells in the BM sinusoids

Immature B cells migrate from the BM parenchyma into the blood-exposed sinusoids as they mature and prepare for emigration to the periphery; they are subject to tolerance checkpoints at these transitions (6, 28). To investigate the developmental stage at which an increased frequency of anti-insulin B cells is first apparent in the NOD strain, in vivo labeling with anti-CD19, as described in *Materials and Methods*, was used to identify immature B cells ($B220^+$ IgM^+ $CD23^-$ lymphocytes) within the parenchyma and sinusoids in the BM. Insulin-binding immature B cells are present in both parenchyma (0.52 ± 0.11) and sinusoids (0.71 ± 0.13) of VH125Tg/B6 mice, as well as in the parenchyma (0.59 ± 0.10) and sinusoids (1.06 ± 0.21) of VH125Tg/NOD mice (Fig. 2A, 2B). These data suggest that anti-insulin B cells are not counterselected during the transition of immature B cells from the parenchyma into the sinusoids in either VH125Tg/B6 or VH125Tg/NOD mice. Furthermore, the increased frequency of insulin-binding B cells within the NOD strain is first significantly apparent in immature B cells that have reached the sinusoids ($p < 0.001$).

Germline Vκ polymorphisms shape the insulin-binding repertoire of VH125Tg/NOD mice

B6 and NOD VH125Tg mice, which express identical anti-insulin H chains, should possess the same potential to generate insulin-binding B cells; however, the observed frequency is disparate (Figs. 1, 2A, 2B). To identify whether Vκ differences are found in

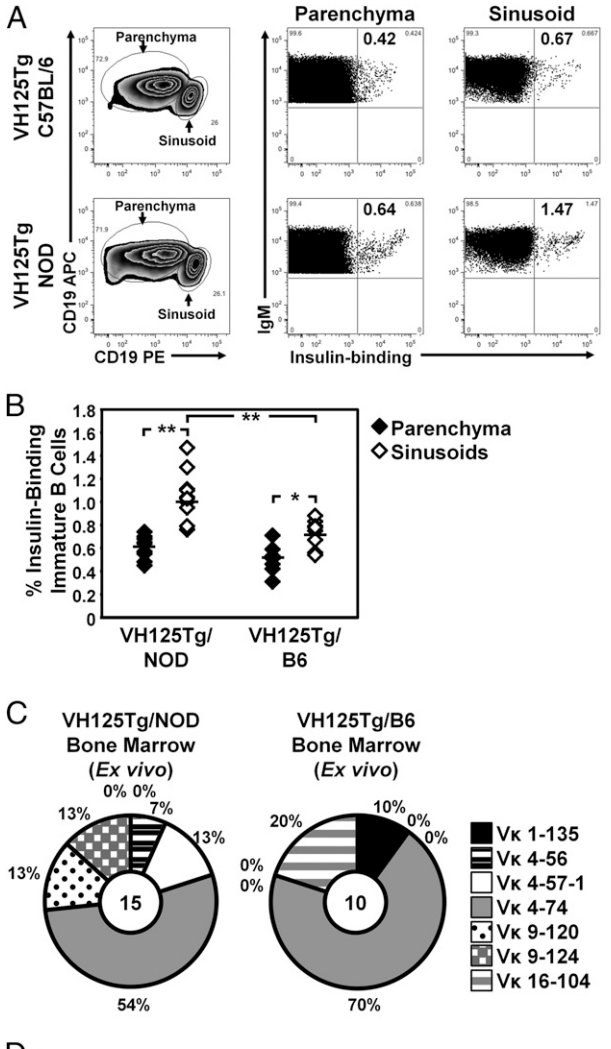

D

Strain	Vκ	CDR1	CDR2	CDR3
C57BL/6	4-57-1	RASSSVSSSYLH	STSNLAS	QQYSGYP
NOD	"4-57-1"	SASSSVSSRYLH	GTSNLAS	QQYHSDP
C57BL/6	4-74	TASSSVSSSYLH	STSNLAS	HQYHRSP
NOD	"4-74"	RASSSVSSSYLH	STSNLAS	QQYDSSP

FIGURE 2. The increase in anti-insulin B cell frequency is first apparent in the BM sinusoids of VH125Tg/NOD mice that harbor polymorphic anti-insulin Vκ4 genes that alter CDR composition. (**A** and **B**) Flow cytometry was used to identify live, $B220^{mid}$ IgM^{a+} lymphocytes (immature B cells) in freshly isolated B6 or NOD VH125Tg BM that had been labeled to detect parenchymal ($CD19\text{-}PE^{low}$) and sinusoidal ($CD19\text{-}PE^{high}$) B cells, as described in *Materials and Methods*. Insulin-binding B cells were detected with biotinylated human insulin. (A) Representative flow cytometry plots depicting the frequency of insulin-binding B cells. (B) Summary graph ($n \geq 9$ 5–13-wk-old mice, $n = 3$ experiments). $^*p < 0.01$, $^{**}p < 0.001$, two-tailed *t* test. (**C**) Flow cytometry sorting was used to isolate insulin-binding immature B cells ($B220^+$ IgM^{a+} $CD23^-$ lymphocytes) identified with biotin-insulin from freshly isolated BM ($n = 6$ VH125Tg/NOD mice, $n = 2$ experiments, $n = 15$ clones, KC484537-KC484551; $n = 15$ VH125Tg/B6 mice, $n = 2$ experiments, $n = 10$ clones, KC484552-KC484561). Mice were 6–17 wk old. Expressed Vκ genes were cloned, sequenced, and identified using IMGT and IgBLAST, as described in *Materials and Methods*. Vκ usage is shown. For each Vκ isolated, the total number of clones is shown within the pie chart; frequency is shown outside the pie chart. Sequences were deposited into GenBank under the accession numbers indicated. (**D**) Comparison of CDR composition of insulin-binding Vκ4 genes identified in (C), amino acid polymorphisms are underlined, relative to B6. Sequences are deposited in Genbank as AC158673, AJ231217, GU179059, and GU179060.

the insulin-binding repertoire of VH125Tg B6 and NOD mice, flow cytometry sorting was used to purify insulin-binding immature B cells from freshly isolated BM. Degenerate PCR primers were used to amplify Vκ genes from cDNA that were cloned, sequenced, and analyzed as described in *Materials and Methods*. Fig. 2C shows that ~70% of the insulin-binding repertoire of VH125Tg B6 and NOD mice consists of two Vκ4 genes, Vκ4-57-1 and Vκ4-74. CDR comparisons between these genes show germline polymorphisms (underlined) present in the NOD strain (Fig. 2D), consistent with previously published data identifying germline polymorphisms in many NOD Vκ sequences (24).

Because of the polymorphic nature of NOD Vκ, a definitive assignment of specific Vκ identity was not previously possible based on sequence homology alone: NOD Vκ4-74 and Vκ4-57-1 each shared similar homology with the corresponding germline sequences (24). The Wellcome Trust Sanger Institute is sequencing the genomes of several strains of mice, including NOD. The Mouse Genomes Project online tool LookSeq was used to compare polymorphisms determined by Wellcome Trust Sanger Institute sequencing of the NOD genome that mapped to the Vκ4-74 region with those experimentally determined for NOD "Vκ4-74" identified in these and prior studies. The current level of coverage is sufficient to show a high degree of agreement between polymorphisms, suggesting that the Vκ4-74 designation is correct and that the nucleotide differences are germline encoded. Sequence coverage in the Vκ4-57-1 region was less robust; however, after ruling out Vκ4-74 as its homolog, it is sufficiently dissimilar to other potential Vκ4 that an alternative identity is unlikely. These data show that two polymorphic Vκ4 genes with altered CDR composition dominate the insulin-binding repertoire in the BM of VH125Tg/NOD mice.

Insulin autoantigen sensing originates in the BM, where a higher frequency of immature B cells is occupied with higher levels of insulin autoantigen in VH125Tg/NOD mice

Polymorphic changes in NOD Vκ CDR might alter autoantigen binding. The anti-insulin Ab, mAb123, recognizes a separate insulin epitope from VH125 and can be used to identify B cells whose BCRs are occupied by endogenous insulin (13, 17). To investigate the anatomical niche in which the insulin autoantigen is first encountered, as well as whether it is differentially recognized by VH125Tg B6 and NOD mice, in vivo labeling with anti-CD19 was used to identify parenchymal and sinusoidal immature B cells in VH125Tg NOD and B6 mice as in Fig. 2. The in vivo labeling was combined with mAb123-biotin staining and flow cytometry to enumerate the frequency of insulin-binding B cells whose BCRs were endogenously occupied with insulin in these anatomical niches. Fig. 3A demonstrates that mAb123 staining is specific; the insulin-binding population identified by mAb123 is not observed with isotype-control staining (*top right panel*) or in VH281Tg mice that harbor a similar H chain but lack insulin-binding B cells (*bottom left panel*) (12). As shown in Fig. 3B and 3C, BM B cells are clearly stained with mAb123-biotin in both parenchyma (0.74 ± 0.22) and sinusoids (1.17 ± 0.21) of VH125Tg/NOD mice, whereas smaller insulin-occupied populations are observed in the parenchyma (0.23 ± 0.03) and sinusoids (0.43 ± 0.10) of VH125Tg/B6 mice. As expected, insulin-occupied B cells are not detected in VH281Tg B6 or NOD mice, confirming mAb123 specificity. The frequencies of mAb123$^+$ B cells detected in VH125Tg mice are significantly higher than are the comparative VH281Tg populations, regardless of strain or anatomical niche ($p < 0.001$). In addition, the frequency of insulin-occupied immature B cells is significantly increased in the sinusoids of VH125Tg mice.

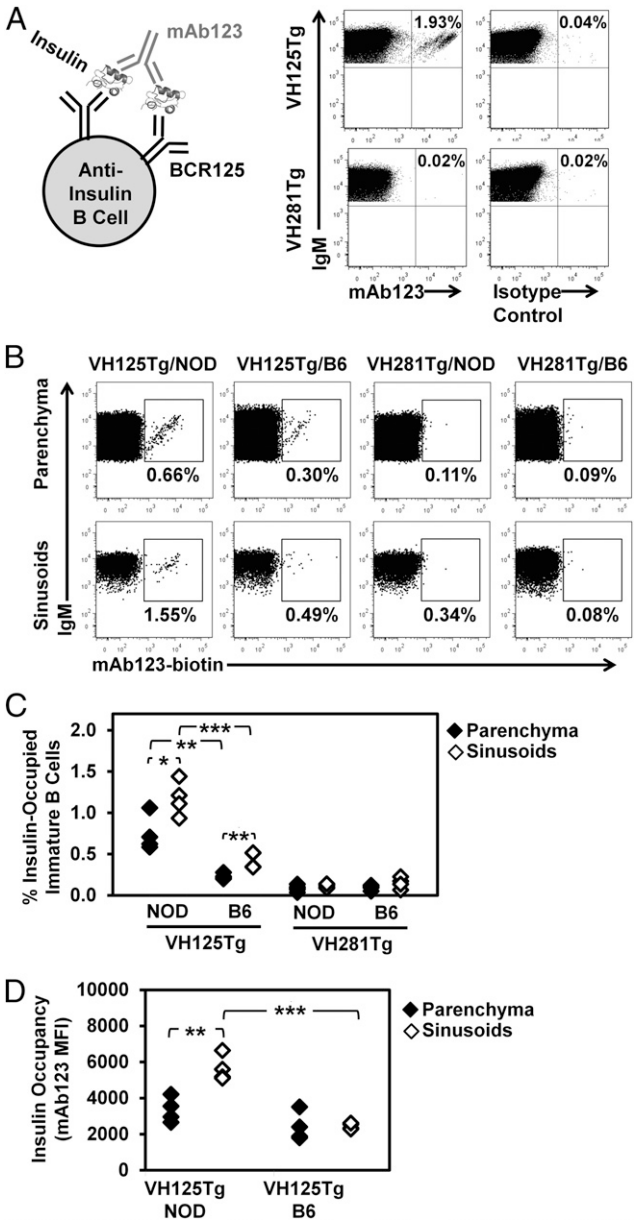

FIGURE 3. The BM parenchyma is the initial site of endogenous insulin encounter, whereas higher insulin occupancy of the BCR occurs in the sinusoids of VH125Tg/NOD mice. (**A**) Schematic diagram of mAb123 recognition of insulin-occupied BCR (*left panel*). Representative flow cytometry plots for insulin-binding (VH125Tg, $n = 6$) or negative-control noninsulin-binding (VH281Tg, $n = 6$) NOD spleens stained with mAb123 or isotype control Ab (*right panel*). B220$^+$ IgM$^+$ live lymphocytes are shown. (**B**–**D**) Parenchymal (CD19-PE^{low}) and sinusoidal (CD19-PE^{high}) immature (CD19$^+$ IgM$^+$ CD23$^-$) live lymphocyte–gated B cells were identified from VH125Tg or VH281Tg NOD and B6 mice using injected CD19-PE, as described in *Materials and Methods*. BM cells were preincubated with Fc Block prior to Ab staining (which did not alter staining profiles or anti-insulin frequencies detected, data not shown) and then stained with mAb123-biotin to detect BCRs occupied with endogenous rodent insulin and other surface marker Ab. (B) Representative plots. (C and D) Summary graphs show at least four individually plotted 10–16-wk-old mice ($n = 2$ experiments). Parenchymal or sinusoidal immature mAb123-stained B cells are identified as above. (C) Percentage of insulin-occupied immature B cells (mAb123$^+$), $p < 0.001$ for all comparisons of VH125Tg with negative-control VH281Tg mice. (D) The mAb123 MFI of mAb123$^+$ immature parenchymal or sinusoidal B cells is plotted to show the level of insulin occupancy on mAb123$^+$ cells. *$p < 0.05$, **$p < 0.01$, ***$p < 0.001$, two-tailed t test.

To investigate whether the degree of insulin occupancy varies with the anatomical niche or with background strain, the mAb123 mean fluorescence intensity (MFI) of mAb123$^+$ B cells identified in Fig. 3B was compared among parenchymal and sinusoidal immature B cells of VH125Tg NOD and B6 mice. Interestingly, Fig. 3D shows that the mAb123 MFI is elevated in the sinusoids of VH125Tg/NOD mice (5630 ± 708) versus the parenchyma (3344 ± 687). In contrast, the mAb123 MFI is unchanged between the parenchyma (2397 ± 787) and sinusoids (2445 ± 161) of VH125Tg/B6 mice. Although there is no significant difference between the mAb123 MFI in the parenchyma of VH125Tg NOD and B6 mice, insulin-occupied BCRs in the sinusoids of NOD mice show a significantly higher mAb123 MFI than in B6 mice. These data show that, despite the low concentration of autoantigen present physiologically (~1–5 ng/ml) (29), insulin occupies the BCR at the earliest detectable stage of Ag-binding commitment of anti-insulin B cells in the BM of VH125Tg mice. The blood-exposed sinusoids of VH125Tg/NOD autoimmune mice are pinpointed as the niche in which insulin-occupied immature B cells are present at higher frequency and with a higher degree of insulin occupancy compared with the nonautoimmune B6 strain.

CDR polymorphisms in NOD Vκ4 genes alter insulin autoantigen recognition

Increased levels of insulin autoantigen occupy a higher frequency of insulin-binding B cells in VH125Tg/NOD mice, compared with the nonautoimmune strain (Fig. 3). To functionally investigate whether CDR polymorphisms identified might provide an explanation for this discrepancy, hybridomas were generated from VH125Tg/NOD or VH125Tg/B6 mice 3 d following immunization with human insulin (the original mAb125 immunogen) or beef insulin that were conjugated to a T cell–independent carrier (*Brucella abortus*). The conjugate was shown to capture a preimmune (unmutated) repertoire for insulin (19). This approach combines potent T cell–independent immunization and enhanced fusion techniques to facilitate the capture of autoreactive B cells (19, 23). ELISA on hybridoma supernatants verified the production of anti-insulin Ab (screened against human insulin), the binding of which was inhibited by the addition of excess human insulin in solution (data not shown).

The large majority of Vκ genes identified among the insulin Ab-secreting NOD hybridoma clones was Vκ4-57-1 or Vκ4-74 and germline encoded (B6 Vκ4-57-1: 9/9; B6 Vκ4-74: 29/34; NOD Vκ4-57-1: 13/15; NOD Vκ4-74: 20/25), based on comparison with published sequences (24). The self-reactive potential of the Abs was determined by measuring reactivity with both human (foreign) and rodent (self) insulin using ELISA, and an autoreactivity index was calculated (*Materials and Methods*). The average autoreactivity index was calculated for each individual Vκ/Jκ species, defined by different CDR amino acid sequences that arise from diverse Vκ/Jκ rearrangement. Thus, error bar variability is due to Vκ/Jκ heterogeneity, rather than assay variability; in the event of multiple identical isolates, the average was used (Fig. 4A). The autoreactivity index is graphed for each individual isolate in Fig. 4B. The autoreactivity index is significantly higher ($p < 0.01$) in NOD Vκ4-57-1 hybridomas compared with B6 hybridomas (Fig. 4A, 4B, *left panel*), but it is unchanged ($p = 0.08$) in NOD versus B6 Vκ4-74 hybridomas (Fig. 4A, 4B, *right panel*). These data show that B6 mice possess at least one endogenous L chain (Vκ4-74) that can pair with VH125 to generate an insulin autoantigen-binding BCR.

Two Jκs (Jκ2 and Jκ4) are polymorphic in the NOD strain (Fig. 4E), clouding interpretation of the specific contribution of Vκ4-57-1 polymorphisms to autoantigen recognition; however, Jκ1 and Jκ5 are the same in the two strains. Fig. 4C shows that, in the presence of identical Jκ5 rearrangements, the autoreactivity index is increased 3-fold by the polymorphic NOD Vκ4-57-1 compared with the B6 Vκ4-57-1. Vκ125Tg (GenBank accession number M34530; http://www.ncbi.nlm.nih.gov/genbank/) is a well-characterized Vκ4-74 insulin-binding L chain that contains a Pro-Pro motif at the Vκ/Jκ join; this motif is found in other insulin-binding L chains (17, 20, 30). This Pro-Pro motif was found in B6 Vκ4-74 and NOD Vκ4-57-1 hybridomas that exhibited significantly higher insulin autoreactivity indices compared with NOD and B6 Vκ4-74 and Vκ4-57-1 Abs that did not contain this motif (Fig. 4D, $p < 0.001$). Pro-Pro was not found in any of the B6 Vκ4-57-1 or NOD Vκ4-74 hybridomas captured, and germline sequence analysis confirms that these L chain sequences cannot encode the Pro-Pro motif, regardless of Jκ join, because the second Pro can only be contributed by the Vκ (Fig. 4E). Of note, the more highly autoreactive NOD Vκ4-74 P-L clones possess the germline sequence, whereas those with lower autoreactivity have framework mutations but identical CDR3. These data suggest that polymorphisms in Vκ4-57-1 confer the potential for a Pro-Pro CDR3 motif that increases insulin autoreactivity in VH125Tg/NOD mice. In contrast, an opposite trend is observed for NOD Vκ4-74, in which the Pro-Pro motif potential is absent.

Anti-insulin Vκ are not counterselected by central tolerance checkpoints present at the developmental transition from BM to spleen

Flow cytometry revealed the presence of insulin-binding B cells in VH125Tg/NOD mice that are occupied by insulin in the developing repertoire of the BM (Fig. 3), as well as the mature repertoire of the spleen (13, 17). Functional studies of Abs captured through hybridoma screens confirm insulin autoantigen binding specificity (Fig. 4). To assess whether these polymorphic anti-insulin Vκ are counterselected by central tolerance mechanisms aimed at developing B cells emigrating from the BM into the spleen, the insulin-binding repertoire of VH125Tg/NOD BM and spleen was compared. To ensure capture of anti-insulin B cells present in the developing repertoire in the absence of counterselection due to autoantigen engagement, VH125Tg/NOD BM cells were cultured with IL-7 in the absence of insulin (as in Fig. 1B, 1C), and anti-insulin B cells were isolated using flow cytometry sorting. Spleen B cells were purified by CD43$^-$ MACS–negative selection of the same mice. Insulin-binding B cells were sorted using FACS, and expressed Igκ genes were amplified, cloned, and sequenced.

As shown in Fig. 5A, preferential usage of Vκ4-57-1 and Vκ4-74 is found in both developing (73%, 11/15 clones) and peripheral (90%, 27/30 clones) VH125Tg/NOD anti-insulin B cells, similar to what was observed in the anti-insulin repertoire of immature B cells derived from BM ex vivo (Fig. 2C). In many instances, the same CDR sequences that were captured in the insulin-binding hybridoma screen were also found among primary isolates: B6 Vκ4-57-1, 0/9; NOD Vκ4-57-1, 10/15; B6 Vκ4-74, 21/34; and NOD Vκ4-74, 23/25 (data not shown). There was no significant difference between the usage of particular insulin-binding L chains in the naive BM culture and peripheral spleen B cells, as determined by a two-sample binomial test to compare the proportions ($p = 0.16$). These data indicate that L chains confirmed to bind autologous insulin when paired with VH125 (Fig. 4) are eluding central tolerance checkpoints to populate the periphery of T1D-prone NOD mice.

Discrete populations (diagonal binding) of anti-insulin B cells are apparent by flow cytometry in the BM and spleens of

A

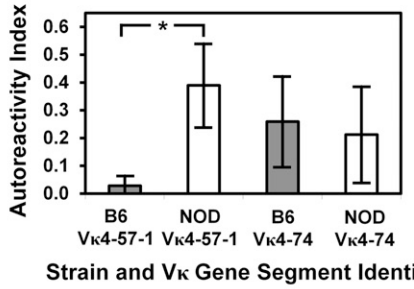

B

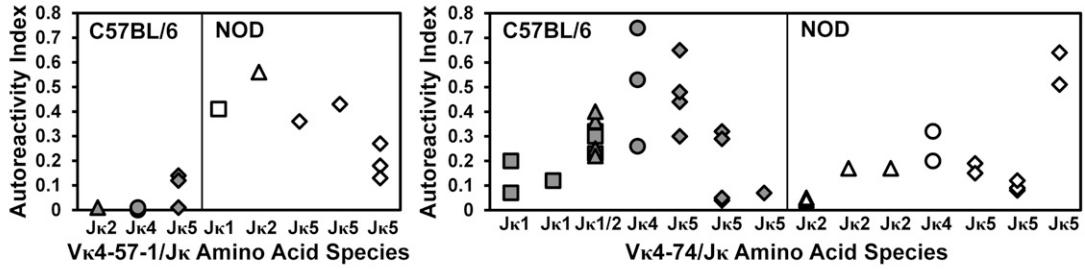

C

Genbank Accession #	Strain	Vκ	Jκ	CDR1	CDR2	CDR3 Vκ (Jκ) FW4	Autoreactivity Index
JQ915158	C57BL/6	4-57-1	5	RASSSVSSSYLH	STSNLAS	QQYSGYP (LT) FGAGTKLELK	0.069
JQ915162	NOD	4-57-1	5	SASSSVSSRYLH	GTSNLAS	QQYHSDP (LT) FGAGTKLELK	0.20
JQ915161	NOD	4-57-1	5	SASSSVSSRYLH	GTSNLAS	QQYHSDP (PT) FGAGTKLELK	0.36

Genbank Accession #	Strain	Vκ	Jκ	CDR1	CDR2	CDR3 Vκ (Jκ) FW4	Autoreactivity Index
JQ915157	C57BL/6	4-57-1	4	RASSSVSSSYLH	STSNLAS	QQYSGYP (LT) FGSGTKLEIK	0.008
JQ915160	NOD	4-57-1	2	SASSSVSSRYLH	GTSNLAS	QQYHSDP (PT) FGSGTKLEIK	0.56

D

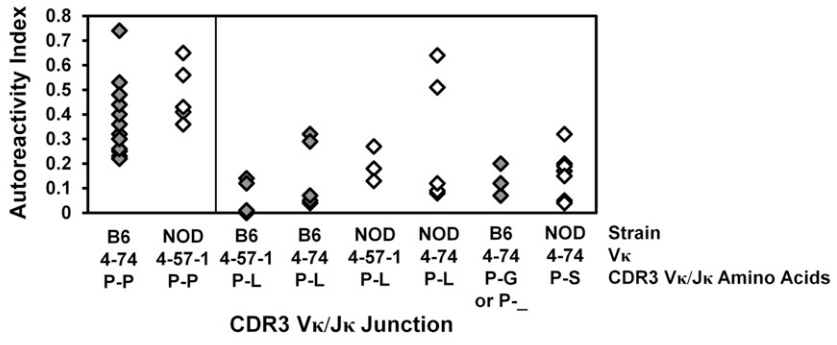

E

Strain	Vκ	Vκ - CDR3	Jκ	Jκ - CDR3/FW4
C57BL/6	4-57-1	Q Q Y S G Y P L CAG CAG TAC AGT GGT TAC CCA CTC	1*01	W T F G G G T K L E I K G TGG ACG TTC GGT GGA GGC ACC AAG CTG GAA ATC AAA C
C57BL/6	4-74	H Q Y H R S P P CAC CAG TAT CAT CGT TCC CCA CCC	2*01	Y T F G G G T K L E I K TG TAC ACG TTC GGA GGG GGG ACC AAG CTG GAA ATA AAA C
C57BL/6			4*01	F T F G S G T K L E I K A TTC ACG TTC GGC TCG GGG ACA AAG TTG GAA ATA AAA C
C57BL/6			5*01	L T F G A G T K L E L K G CTC ACG TTC GGT GCT GGG ACC AAG CTG GAG CTG AAA C
NOD	4-57-1	Q Q Y H S D P P CAG CAG TAT CAT AGT GAC CCA CCN[1]	1*01	W T F G G G T K L E I K G TGG ACG TTC GGT GGA GGC ACC AAG CTG GAA ATC AAA
NOD	4-74	Q Q Y D S S P S CAG CAG TAT GAT AGT TCC CCA TCC	2*03	Y T F G S G T K L E I K TG TAT ACG TTC GGA TCG GGG ACC AAG CTG GAA ATA AAA C
NOD			4*02	F T F G T G T K L E I K A TTC ACG TTC GGC ACG GGG ACA AAA TTG GAA ATA AAA C
NOD			5*01	L T F G A G T K L E L K G CTC ACG TTC GGT GCT GGG ACC AAG CTG GAG CTG AAA C

[1] The codon CCN is most likely CCC based on all Vκ4-57-1 NOD sequences acquired.

FIGURE 4. Vκ polymorphisms enhance insulin autoreactivity in VH125Tg/NOD mice. VH125Tg B6 or NOD mice were immunized in a T-independent manner with heterologous insulin, and hybridomas were generated as described in *Materials and Methods*. Clones producing Ab (*Figure legend continues*)

VH125Tg/NOD mice (Fig. 5B). These populations were sorted separately into low or high MFI populations based on the intensity of staining with biotinylated insulin. Expressed Vκ were isolated, cloned, and identified as above. Among the low MFI population present in BM and spleen, Vκ4-57-1 predominated (57%, 13/23 clones); among the high MFI population, Vκ4-74 was present in the majority of isolates (74%, 20/27 clones, Fig. 5C). Taken together, these data suggest that the majority of anti-insulin B cells isolated from VH125Tg/NOD mice arises from the Vκ4 family, specifically from the Vκ4-57-1 and Vκ4-74 genes, and that BCRs using these L chains are not eliminated from the repertoire through negative selection.

Anti-insulin B cells persist in the repertoire throughout development and are enriched in the pancreas of VH125TgNOD mice

Previous attempts failed to detect insulin-binding B cells in the pancreas of VH125Tg/NOD mice, despite identification of Vκ4-57-1 among pancreatic B cell isolates (31). The finding that VH125Tg/NOD B cells expressing Vκ4-57-1 react with autoantigen (Fig. 4) suggests that insulin-reactive B cells are present in the pancreas but have evaded detection by staining with biotinylated insulin. To assess the frequency of anti-insulin B cells that are present among pancreatic infiltrates, mAb123 was used to identify insulin-binding B cells whose BCRs may be too fully occupied with endogenous insulin to be detected through exogenous staining with biotinylated insulin. Using this method, insulin-binding B cells were detected among $B220^{+}$ IgM^{a+} live lymphocytes in the pancreas (Fig. 6A). This frequency was compared among B cell subsets present at every developmental stage from origination in the BM to pancreas infiltration. The frequency of BCRs occupied by insulin observed in the pancreas was significantly higher than in any other subset compared ($2.66 \pm 0.58\%$, $p < 0.001$ for pancreas versus every other subset, Fig. 6B). These data show that anti-insulin B cells are increased in the pancreas at least ~3–4-fold over the frequency that initially forms in the developing repertoire, suggesting that anti-insulin B cells are positively selected into the organ targeted by autoimmune destruction.

Anti-insulin B cells undergo somatic hypermutation and correlate with an increase in pathogenic anti-insulin T cells

Vκ repertoire analysis of VH125Tg/NOD pancreata identifies Vκ4-57-1 as 7% of the L chain repertoire based on clone frequency (31) (data not shown), a proportion consistent with flow cytometry findings (Fig. 6). CDR amino acid alignment with NOD germline reference sequences (24) shows evidence of somatic hypermutation (SHM) in VH125Tg/NOD spleen and pancreatic Vκ4-57-1 isolates; the mutated CDR amino acids are shown in Fig. 7A. Of the Vκ4-57-1 clones isolated from spleen or pancreata, 28% or 47% of clones show evidence of SHM, respectively (Fig. 7B). These data indicate that a substantial proportion of anti-insulin B cells emerging from the BM ultimately undergoes SHM.

The presence of SHM in anti-insulin Vκ (Fig. 7A) implies autoantigen-specific T–B cell interactions in the disease process and is consistent with our recent data that show anti-insulin B cells can process and present insulin epitopes to T cells (32). We hypothesize that SHM is due to anti-insulin B cell cross-talk with cognate T cells. To investigate whether anti-insulin B cells influence the frequency or function of this important subset, splenocytes were harvested from VH125Tg/NOD or VH281Tg/NOD mice and used in ELISPOT assay to measure Th1 (IFN-γ) and Th2 (IL-4) cytokine production following insulin stimulation. Splenocytes from VH125Tg/NOD mice that harbor anti-insulin B cells show an increase in the number of IFN-γ spots in response to insulin compared with VH281Tg/NOD mice that lack detectable anti-insulin B cells ($p < 0.01$, Fig. 7C). Interestingly, the numbers of spontaneous IFN-γ spots also were increased in VH125Tg/NOD splenocytes at baseline ($p < 0.01$, Fig. 7C). In contrast, IL-4 was undetectable (data not shown). Activated Th1 cells that produce IFN-γ are associated with T1D pathogenesis (33, 34). These findings are consistent with the association of anti-insulin B cells in VH125Tg/NOD mice with acceleration of the disease process (12, 25) and further suggest that flawed central tolerance for anti-insulin B cells generates a pre-T1D environment that promotes expansion of pathogenic anti-insulin T cells.

Discussion

These studies highlight the BM sinusoids as the point of "original sin" for the genesis of anti-insulin B cells in T1D-prone mice. Thomas Francis (35) initially coined the term "original antigenic sin" to describe how early foreign antigenic encounter guides subsequent immune responses. Although the stages of B cell development are different, both processes govern the subsequent focus of B cell/Ab interaction with Ag. In NOD mice, we find a more pernicious source of repertoire bias, in which B lymphocytes display increased insulin autoreactivity from birth in the BM, rather than requiring subsequent affinity maturation to pose an islet threat. In addition to the higher frequency of insulin-binding B cells that form in the autoimmune strain, insulin autoantigen occupancy of cognate BCRs is higher in the BM. Two Vκ4 genes dominate the BM and spleen anti-insulin repertoire of NOD mice and show germline potential for insulin autoreactivity. Polymorphisms in NOD Vκ4-57-1 confer a key CDR3 motif that enhances insulin autoreactivity. The consequence of BM proclivity for insulin autoimmunity is that anti-insulin B cells transit to the periphery and are positively selected into the pancreas, where they show evidence of SHM. The presence of anti-insulin B cells in the

reactive with human insulin were identified by ELISA. Expressed Vκ genes were cloned, sequenced, and identified using IMGT and IgBLAST, as described in *Materials and Methods*. Sequences were deposited into GenBank under accession numbers JQ915156–JQ915175. (**A**) Bar graph summary of autoreactivity index, calculated as described in *Materials and Methods*, of Vκ is shown ($n \geq 7$ independent hybridoma isolates, $^{*}p < 0.01$, as calculated by a two-tailed *t* test). Error bars encompass Vκ/Jκ heterogeneity, rather than assay heterogeneity (see **C**). (**B**) Autoreactivity index values for individual Vκ/Jκ species clones (represented by individual data points). Different Vκ/Jκ species harboring different CDR3 due to combinatorial and junctional diversity are indicated on the *x-axis*. The autoreactivity index of Vκ4-57-1 sequences was compared: B6 (filled symbols, $n = 7$) and NOD (open symbols, $n = 7$) (*left panel*). $p < 0.01$, Mann–Whitney *U* two-tailed test. The autoreactivity index of Vκ4-74 sequences was compared: B6 (filled symbols, $n = 23$) and NOD (open symbols, $n = 13$) (*right panel*). $p = 0.08$, Mann–Whitney *U* two-tailed test. (C) CDR amino acid and autoreactivity index comparison of hybridoma sequences that contain the same (*upper panel*) or similar (*lower panel*) Jκ rearrangements in CDR3 isolated from VH125Tg B6 or NOD hybridomas. (**D**) Vκ/Jκ CDR junction and autoreactivity index comparison of hybridoma sequences isolated from VH125Tg B6 (filled symbols) or NOD (open symbols) mice. The autoreactivity index of P-P–containing sequences (left of vertical line, $n = 19$) was compared with all other sequences (right of vertical line, $n = 31$). $p < 0.001$, Mann–Whitney *U* two-tailed test. (**E**) The nucleotide and amino acid sequences of Vκ4-57-1 and Vκ4-74 CDR3, along with all Jκ to indicate potential CDR3 contributions. B6 sequences are shaded in gray, NOD are not shaded. (C and E) NOD nucleotide polymorphisms and predicted amino acid changes (relative to B6) are underlined.

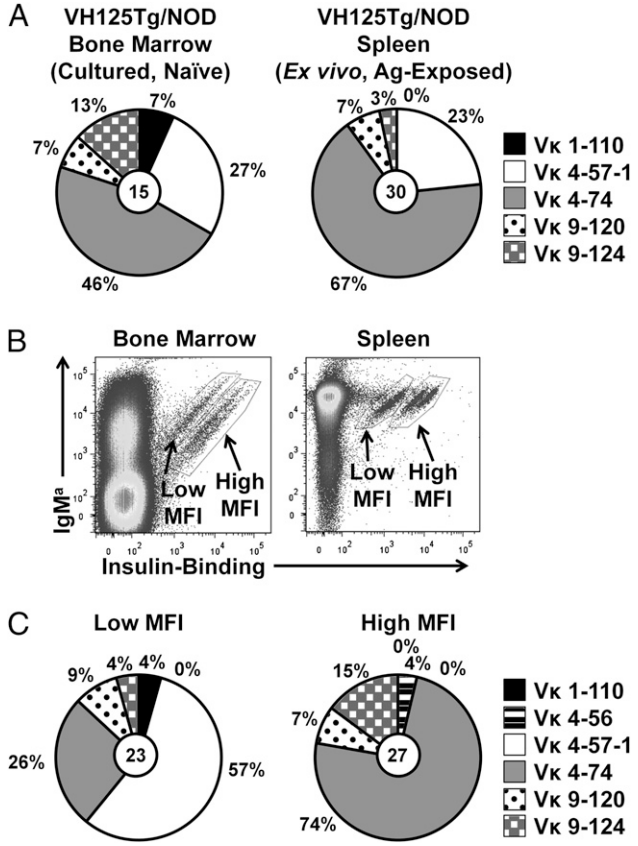

FIGURE 5. Anti-insulin Vκ are not counterselected by central tolerance checkpoints present at the developmental transition from BM to spleen. (**A**) Biotin-insulin was used to identify insulin-binding B cells that were purified using flow cytometry sorting of Ag-naive IL-7–cultured BM immature B cells ($B220^+$ IgM^{a+} $CD23^+$ lymphocytes), generated as described in *Materials and Methods*, or Ag-exposed spleen B cells ($B220^+$ IgM^{a+} lymphocytes) isolated ex vivo. Expressed Vκ genes were cloned, sequenced, and identified using IMGT and IgBLAST, as described in *Materials and Methods*. For each Vκ isolated, the total number of clones is shown within the pie chart; the frequency is shown outside of the pie chart. Sequences were deposited into GenBank under the accession numbers indicated. IL-7–cultured BM (n = 3 VH125Tg/NOD mice, n = 3 experiments, n = 15 clones, GU179059 and KC484488-KC484501) (*left panel*). Ag-experienced ex vivo spleen (n = 5 VH125Tg/NOD mice, n = 4 experiments, n = 27 clones, GU179060, KC484508–KC484536) (*right panel*). Mice were 8–12 wk old. (**B** and **C**) Insulin-binding B cells, sorted using flow cytometry, from VH125Tg/NOD BM and spleen [(A) and Fig. 2)], were separated into low and high insulin-binding MFI populations. (C) Vκ repertoire was identified in low and high MFI populations from (B) and compared as in (A). Genbank accession numbers are as follows: "Low MFI": GU179059, KC484488-491, KC484495, KC484499, KC484510, KC484512, KC484514, KC484515, KC484521, KC484522, KC484525, KC484529, KC484532-534, KC484537-541, and KC484546; "High MFI": KC484494, KC484497-498, KC484500-501, KC484508-509, KC484511, KC484513, KC484516, KC484523-524, KC484526-528, KC484531, KC484536, KC484542-545, and KC484547-551.

repertoire is associated with increased production of the inflammatory cytokine IFN-γ in ELISPOT. These data suggest that the BM "original sin" seeds anti-insulin B cells into the periphery where they likely collaborate with cognate T cells to promote inflammatory attack of the pancreas.

Anti-insulin B cells develop with increased frequency in VH125Tg/NOD BM (Fig. 1A), despite the identical H chain present in NOD and B6 VH125Tg mice. One potential explanation for this difference is that environmental factors in the autoimmune strain may enhance autoreactive B cell development.

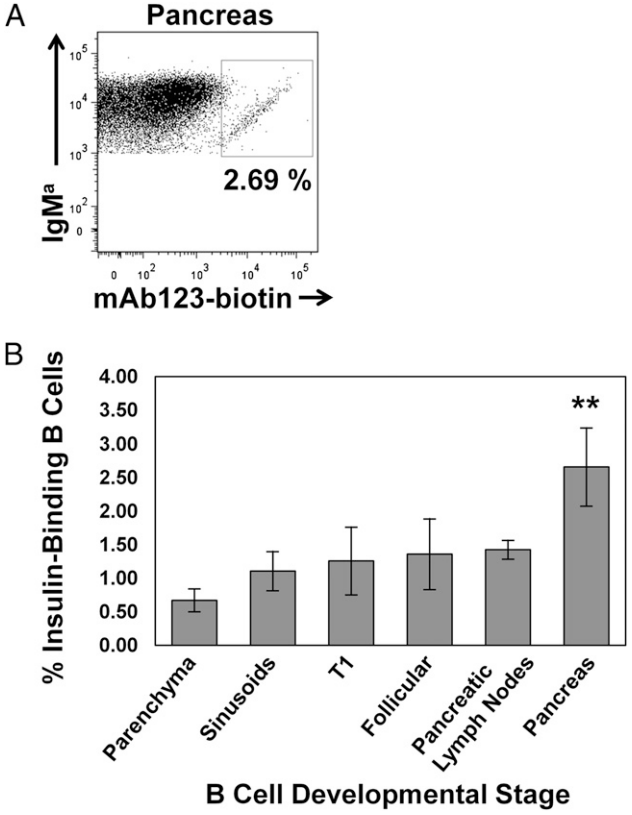

FIGURE 6. Anti-insulin B cells that escape central tolerance are enriched at the site of autoimmune attack. B cells whose BCR were loaded with endogenous insulin were detected by mAb123-biotin staining within $B220^+$ IgM^{a+} live lymphocytes from freshly isolated pancreata of VH125Tg/NOD mice. (**A**) Representative flow cytometry plot. (**B**) Summary bar graph ($n \geq 8$). $^{**}p < 0.001$ versus all other groups, two-tailed t test.

These could include increased survival factor availability or changes in chemokine or homing receptor expression that increase the kinetics of BM exit, limiting the window for central tolerance in the autoimmune strain. Studies on developing B cells that reach mature subsets in WT/NOD mice suggest that negative selection collapses at the transitional stage (36) and are complementary with data suggesting that similar B cell checkpoint defects underlie autoimmunity in patients (2, 3). A receptor-editing defect also was proposed for T1D mice and human patients, based on a lower observed recombining sequence rearrangement frequency (37). The current investigation clearly indicates that receptor editing is failing to eliminate insulin-binding B cells in VH125Tg/NOD mice. Future studies to directly address whether receptor-editing efficiency is altered in autoimmune mice are necessary to outline the role that this key central tolerance mechanism plays in preventing insulin autoimmunity.

IL-7–driven BM culture in vitro limits the influence of environmental factors and eliminates autoantigen exposure to produce naive immature B cells (26, 27). Nonetheless, increased formation of anti-insulin B cells in the NOD strain is still observed in BM cultured in the absence of insulin in vitro (Fig. 1B, 1C). This suggests that, although central tolerance may certainly be a component of the enhanced anti-insulin B cell frequency, it is not the only contributing factor. Vκ polymorphisms alter CDR in the NOD strain (24) and offer one potential explanation for enhanced formation of autoreactive B cells. Two polymorphic Vκ4 family members, Vκ4-57-1 and Vκ4-74, dominate the insulin-binding repertoire in VH125Tg/NOD mice (Figs. 2, 5). The nucleotide

A

Mutated Vκ4-57-1 CDR Identified in VH125Tg/NOD Mice

Isolate	Accession Number	Organ	CDR1	CDR2	CDR3
809	JX064462	Spleen	SASSSVSSRYLH	GTSNLAS	QQ**GWDY**P
817	JX064463	Spleen	SASSSVSSRYLH	GTS**S**LAS	QQYHSDP
756	JX064464	Spleen	SASSSV**N**SRYL**N**	GTSNL**P**S	QQYHSDP
243	JX064465	Spleen	SASS**N**V**H**S**N**YLH	GTSNLAS	QQ**F**HSDP
965	JQ915176	PLN	SASSSVS**F**RYLH	GTSNLAS	QQYHSDP
966	JQ915177	PLN	SASSSVSSRYLH	GTSNL**G**S	QQYHSDP
968	JQ915178	PLN	SASSSVSSRYLH	GTSNLAS	**H**Q**WS**S**Y**P
990	JQ915179	PLN	SASSSV**G**S**S**YLH	GTSNLAS	QQ**GWDY**P
835	JQ915180	PLN	SASSSV**G**S**S**YLH	GTSNLAS	QQY**D**S**S**P
705	JQ915181	Pancreas	SASSSV**N**SRY**F**H	GTSNLAS	QQY**D**S**S**P
787	JQ915182	Pancreas	S**T**SSSVSSRYLH	GTSNLAS	QQYHSDP
703	JQ915183	Pancreas	SASSSV**N**SRYLH	GTSNLAS	QQYHSDP
163	JQ915184	Pancreas	SASSSVSSRYLH	GTSNLAS	Q**HGS**S**LL**
940	JQ915185	Pancreas	SASSSV**G**S**S**YLH	GTSNLAS	QQ**GW**XXP
923	JQ915186	Islet	SASSSV**G**S**S**YLH	GTSNLAS	QQ**GWDY**P
931	JQ915187	Islet	SAXSSVSSRYLH	**D**TSNLAS	QQYHSDP

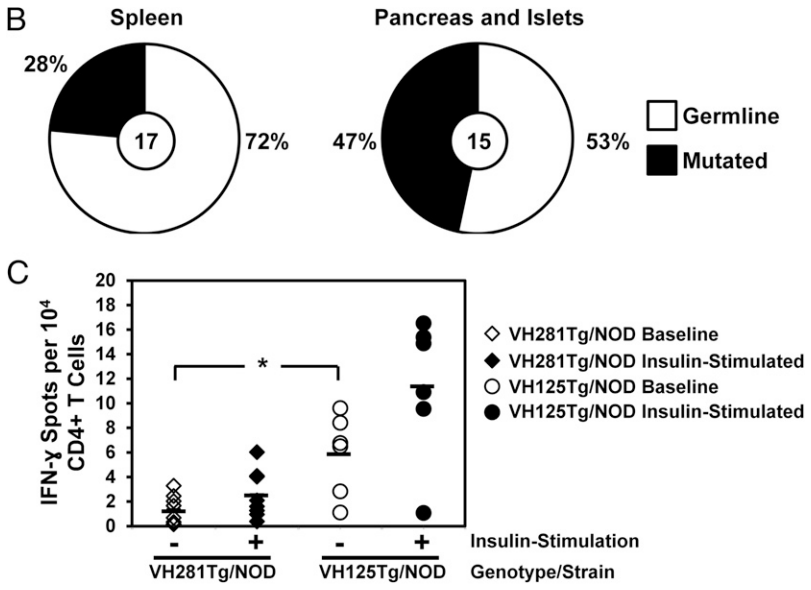

FIGURE 7. Anti-insulin B cells that escape central tolerance undergo SHM and stimulate IFN-γ production. (**A**) The amino acid CDR composition of mutated Vκ4-57-1 isolates from spleen, pancreatic draining lymph nodes (PLN), pancreas, and islets of VH125Tg/NOD mice. Germline amino acids are in gray type; mutated amino acids are in black type and underlined. (**B**) The proportion of VH125Tg/NOD Vκ4-57-1 isolates that shows germline CDR or mutated CDR is indicated for VH125TgNOD spleen (*left panel*) and pancreas/islets (*right panel*). Germline or mutated frequency is shown outside of the pie chart; the total number of clones is shown in the center. Sequences were deposited in GenBank with accession numbers JX064462–JX064465, JQ915176–JQ915195, and KC484502–KC484507. (**C**) Splenocytes from VH281Tg and VH125Tg NOD mice were cultured for 72–96 h in the presence or absence of human insulin, and IFN-γ responses were measured by ELISPOT (see *Materials and Methods*) ($n \geq 6$). $^*p > 0.01$, two-tailed *t* test.

changes in the Vκ sequences are of germline origin and do not arise from SHM, based on comparison with published NOD germline sequences (24). Binding studies confirm that even when the Jκ contribution is the same, Vκ4-57-1 polymorphisms enhance insulin autoantigen recognition in VH125Tg/NOD mice (Fig. 4). A CDR3 Pro-Pro motif was identified in several anti-insulin Vκ (20). These studies show that Vκ4-57-1 polymorphisms in CDR3 confer the potential for generation of this motif, which is shown to enhance insulin autoantigen recognition (Fig. 4).

The serine-rich CDR1 of both Vκ4-57-1 and Vκ4-74 is found among other anti-insulin mAb (20, 38). This motif is reminiscent of that found in the insulin receptor ligand–binding domain and, thus, is a likely contributor to Ag binding. Similar Vκ4 genes are also found in autoreactive Abs derived from insulin immunization in combination with different VH, suggesting that this structure may predispose toward insulin recognition (20, 38, 39). Because the polymorphisms present in NOD Vκ are shared among other systemic lupus erythematosus–prone autoimmune strains (24), and because other anti-insulin autoantibodies characterized from NOD mice showed cross-reactivity with other self-Ags, such as DNA, thyroglobulin, IgG, and cardiolipin (39), we speculate that polymorphic Vκ may also enhance the recognition of other autoantigens. The α-chain of the TCR is the structural correlate to the L chain of the BCR. Interestingly, a polymorphic TCRα-chain also contributes to the formation of TCRs on pathological anti-insulin T cells in NOD mice (40, 41). Polymorphic Vκ are not the only explanation for the higher frequency of insulin-binding B cells generated in the NOD strain, because Vκ4-74 shows potential for autoreactivity in both strains. Differences in regulatory elements that control Vκ usage may also exist between strains. Central and peripheral tolerance may also be differentially applied, in addition to any repertoire bias in the autoimmune strain.

Some anti-insulin mAbs that recognize human insulin do not bind rodent insulin (Fig. 4). This suggests that a fraction of the cells identified by biotinylated human insulin staining may be clonally ignorant. However, it is clear that a proportion of anti-insulin B cells have autoantigen-occupied BCRs when Ag specificity is first acquired in the BM parenchyma (Fig. 3); this frequency is increased in the sinusoids of the NOD strain compared with B6 VH125Tg mice. The increased frequency of insulin-binding B cells observed in the sinusoids compared with the parenchyma suggests that positive selection may be occurring (Figs. 2, 3). An alternative explanation is that receptor editing prolongs the time that anti-insulin B cells spend in the sinusoids, thus in-

creasing the frequency; however, because the anti-insulin B cell percentage in the sinusoids is similar to that observed in transitional and subsequent mature B cell compartments, it is unlikely that receptor editing is culling a major fraction of anti-insulin B cells in VH125Tg/NOD mice.

Naive immature anti-insulin B cells can sense insulin and show signs of anergy induction following autoantigen exposure, supporting the ability of insulin to interact with the BCR in a perceptible way (26). A higher level of BCR occupancy with insulin autoantigen is first observed in this blood-exposed BM niche in VH125Tg/NOD mice (Fig. 3). We speculate that this may be due to a higher average affinity of BCR for endogenous insulin in VH125Tg/NOD mice compared with the nonautoimmune strain. Insulin-occupied BCRs are also clearly observed in VH125Tg/NOD mature peripheral B cell subsets (13); thus, clonal ignorance fails to explain the escape of anti-insulin B cells to the periphery of NOD mice. If anergy is being applied in this model, it certainly does not sufficiently limit the competitive survival of anti-insulin B cells to prevent their infiltration of the pancreas (Fig. 6).

Tracking Vκ usage by anti-insulin B cells in the BM and periphery documents a direct connection between the two compartments (Fig. 5). This identifies BM genesis, rather than peripheral selection of a rare specificity, as the key factor that contributes to autoreactive B cell presence in the mature repertoire. Notably, the Vκ4-57-1 L chain identified in the BM and spleen that was confirmed to be insulin reactive (Fig. 4) is also found among B cells infiltrating the pancreas of VH125Tg/NOD mice (31). Anti-insulin B lymphocytes exit the BM and infiltrate the pancreas with 3–4-fold increased frequency (Fig. 6). Insulin-reactive B cells that escape from the BM can impact the invading repertoire of the pancreas. Vκ1-110, Vκ9-120, and Vκ9-124 were also observed in a minor fraction of insulin-binding B cells isolated from BM and spleen. These L chains also were isolated from other anti-insulin B cell screens (16), as well as from the pancreas, the site of autoimmune destruction (31) (data not shown); however, functional studies are required to confirm their specificity for insulin.

Flow cytometry identifies two distinct insulin-binding populations in the BM and spleen (Fig. 5); however, only one is apparent in the pancreas (Fig. 6). Interestingly, the Vκ4-74 L chain was not observed in the pancreas of VH125Tg/NOD mice (31), despite its ability to bind insulin autoantigen (Fig. 4). One explanation is that Vκ4-57-1 may have higher affinity for autoantigen and, thus, is more heavily selected into the site of autoimmune attack. In support of this, the autoreactivity index is higher, on average, for Vκ4-57-1 than for Vκ4-74, suggesting that Vκ4-57-1 more efficiently binds rodent (self) insulin (Fig. 4). Biotinylated insulin staining is impaired by higher BCR occupancy with endogenous insulin in the pancreas of VH125Tg/NOD mice (31) (Fig. 6). Of the two insulin-binding populations observed in BM and spleens, Vκ4-57-1 is associated primarily with the population that shows lower biotinylated-insulin MFI (Fig. 5). Therefore, we propose that Vκ4-57-1 has higher endogenous Ag affinity (and thus higher occupancy) due to unique polymorphisms, which may lead to its selection into the pancreas.

It is clear that many Vκ4-57-1$^+$ B cells have undergone SHM (Fig. 7A, 7B) (31). Tertiary lymphoid structures with germinal centers are observed to form in the pancreas, and it was proposed that SHM occurs at the site of autoimmune attack (31). Further work is required to determine how SHM impacts the disease process. Regardless of when SHM initiates, productive B lymphocyte collaboration with T cells is also suggested by increased IFN-γ production in the spleens of VH125Tg/NOD, but not VH281Tg/NOD, mice, in which insulin-binding B cells are present or absent, respectively (Fig. 7C). This is further supported by the finding that anti-insulin B cells can present Ag to cognate T cells isolated from NOD mice (32). Therefore, we favor the hypothesis that enhanced IFN-γ production results from Ag-specific T cells activated by anti-insulin B cells in vivo. The production of IFN-γ, but not IL-4, is consistent with Th1 cell activation, which is known to mediate the islet inflammatory process in T1D (33, 34). Therefore, these data serve as indirect evidence that anti-insulin B cells are presenting Ag to insulin-reactive Th1 CD4$^+$ T cells to stimulate their production of IFN-γ within a polyclonal repertoire and suggest inflammatory consequences of anti-insulin B cell escape through tolerance checkpoints.

Based on these findings, we propose the following model. Anti-insulin B cells form with increased frequency in the BM of autoimmune VH125Tg mice, which is first apparent in the BM sinusoids. Polymorphisms that alter CDR composition enhance self-reactivity for insulin in VH125Tg/NOD mice. Despite autoantigen encounter as early as Ag commitment in the BM parenchyma, insulin autoreactive B cells escape into the periphery of the autoimmune strain in the absence of detectable negative selection. Anti-insulin B cells interact with anti-insulin T cells to drive islet-directed inflammation and are enriched in the pancreas, the site of autoimmune attack. Thus, the BM is identified as the point of "original sin," from which dangerous autoimmunity first arises in the B cell repertoire that leads to the peripheral consequence of islet attack.

Acknowledgments

We thank James B. Case, Chrys Hulbert, Allison M. Sullivan, Emily J. Woodward, and Guowu Yu for technical support (Vanderbilt University), as well as the Vanderbilt Medical Center Flow Cytometry Shared Resource and the Vanderbilt Digestive Disease Research Center, the Vanderbilt DNA Sequencing Facility, the Vanderbilt Antibody and Protein Resource, the Vanderbilt Hormone Assay and Analytical Services Core, and the Vanderbilt Diabetes Research and Training Center. We also thank Dr. Betty Diamond for kindly providing the NSO-BCL2 myeloma line.

Disclosures

The authors have no financial conflicts of interest.

References

1. Wardemann, H., S. Yurasov, A. Schaefer, J. W. Young, E. Meffre, and M. C. Nussenzweig. 2003. Predominant autoantibody production by early human B cell precursors. *Science* 301: 1374–1377.
2. Yurasov, S., H. Wardemann, J. Hammersen, M. Tsuiji, E. Meffre, V. Pascual, and M. C. Nussenzweig. 2005. Defective B cell tolerance checkpoints in systemic lupus erythematosus. *J. Exp. Med.* 201: 703–711.
3. Samuels, J., Y. S. Ng, C. Coupillaud, D. Paget, and E. Meffre. 2005. Impaired early B cell tolerance in patients with rheumatoid arthritis. *J. Exp. Med.* 201: 1659–1667.
4. Menard, L., D. Saadoun, I. Isnardi, Y. S. Ng, G. Meyers, C. Massad, C. Price, C. Abraham, R. Motaghedi, J. H. Buckner, et al. 2011. The PTPN22 allele encoding an R620W variant interferes with the removal of developing autoreactive B cells in humans. *J. Clin. Invest.* 121: 3635–3644.
5. Halverson, R., R. M. Torres, and R. Pelanda. 2004. Receptor editing is the main mechanism of B cell tolerance toward membrane antigens. *Nat. Immunol.* 5: 645–650.
6. Pereira, J. P., J. An, Y. Xu, Y. Huang, and J. G. Cyster. 2009. Cannabinoid receptor 2 mediates the retention of immature B cells in bone marrow sinusoids. *Nat. Immunol.* 10: 403–411.
7. Donovan, E. E., R. Pelanda, and R. M. Torres. 2010. S1P3 confers differential S1P-induced migration by autoreactive and non-autoreactive immature B cells and is required for normal B-cell development. *Eur. J. Immunol.* 40: 688–698.
8. Palmer, J. P., C. M. Asplin, P. Clemons, K. Lyen, O. Tatpati, P. K. Raghu, and T. L. Paquette. 1983. Insulin antibodies in insulin-dependent diabetics before insulin treatment. *Science* 222: 1337–1339.
9. Yu, L., D. T. Robles, N. Abiru, P. Kaur, M. Rewers, K. Kelemen, and G. S. Eisenbarth. 2000. Early expression of antiinsulin autoantibodies of humans and the NOD mouse: evidence for early determination of subsequent diabetes. *Proc. Natl. Acad. Sci. USA* 97: 1701–1706.

10. Steck, A. K., K. Johnson, K. J. Barriga, D. Miao, L. Yu, J. C. Hutton, G. S. Eisenbarth, and M. J. Rewers. 2011. Age of islet autoantibody appearance and mean levels of insulin, but not GAD or IA-2 autoantibodies, predict age of diagnosis of type 1 diabetes: diabetes autoimmunity study in the young. *Diabetes Care* 34: 1397–1399.
11. Nakayama, M., N. Abiru, H. Moriyama, N. Babaya, E. Liu, D. Miao, L. Yu, D. R. Wegmann, J. C. Hutton, J. F. Elliott, and G. S. Eisenbarth. 2005. Prime role for an insulin epitope in the development of type 1 diabetes in NOD mice. *Nature* 435: 220–223.
12. Hulbert, C., B. Riseili, M. Rojas, and J. W. Thomas. 2001. B cell specificity contributes to the outcome of diabetes in nonobese diabetic mice. *J. Immunol.* 167: 5535–5538.
13. Henry, R. A., P. L. Kendall, and J. W. Thomas. 2012. Autoantigen-specific B-cell depletion overcomes failed immune tolerance in type 1 diabetes. *Diabetes* 61: 2037–2044.
14. Cyster, J. G., S. B. Hartley, and C. C. Goodnow. 1994. Competition for follicular niches excludes self-reactive cells from the recirculating B-cell repertoire. *Nature* 371: 389–395.
15. Schmidt, K. N., and J. G. Cyster. 1999. Follicular exclusion and rapid elimination of hen egg lysozyme autoantigen-binding B cells are dependent on competitor B cells, but not on T cells. *J. Immunol.* 162: 284–291.
16. Woodward, E. J., and J. W. Thomas. 2005. Multiple germline kappa light chains generate anti-insulin B cells in nonobese diabetic mice. *J. Immunol.* 175: 1073–1079.
17. Rojas, M., C. Hulbert, and J. W. Thomas. 2001. Anergy and not clonal ignorance determines the fate of B cells that recognize a physiological autoantigen. *J. Immunol.* 166: 3194–3200.
18. Taylor, S. I., J. A. Schroer, B. Marcus-Samuels, A. McElduff, and T. P. Bender. 1984. Binding of insulin to its receptor impairs recognition by monoclonal anti-insulin antibodies. *Diabetes* 33: 778–784.
19. Thomas, J. W., P. M. Kralick, and U. K. Ewulonu. 1997. T cell-independent response to *Brucella*-insulin identifies a preimmune repertoire for insulin. *J. Immunol.* 159: 2334–2341.
20. Ewulonu, U. K., L. J. Nell, and J. W. Thomas. 1990. VH and VL gene usage by murine IgG antibodies that bind autologous insulin. *J. Immunol.* 144: 3091–3098.
21. Schroer, J. A., T. Bender, R. J. Feldmann, and K. J. Kim. 1983. Mapping epitopes on the insulin molecule using monoclonal antibodies. *Eur. J. Immunol.* 13: 693–700.
22. Mitchell, H. C., and J. W. Thomas. 1995. VH gene structure predicts a large potential anti-insulin repertoire. *Mol. Immunol.* 32: 311–321.
23. Ray, S. K., C. Putterman, and B. Diamond. 1996. Pathogenic autoantibodies are routinely generated during the response to foreign antigen: a paradigm for autoimmune disease. *Proc. Natl. Acad. Sci. USA* 93: 2019–2024.
24. Henry, R. A., P. L. Kendall, E. J. Woodward, C. Hulbert, and J. W. Thomas. 2010. Vkappa polymorphisms in NOD mice are spread throughout the entire immunoglobulin kappa locus and are shared by other autoimmune strains. *Immunogenetics* 62: 507–520.
25. Kendall, P. L., D. J. Moore, C. Hulbert, K. L. Hoek, W. N. Khan, and J. W. Thomas. 2009. Reduced diabetes in btk-deficient nonobese diabetic mice and restoration of diabetes with provision of an anti-insulin IgH chain transgene. *J. Immunol.* 183: 6403–6412.
26. Henry, R. A., C. A. Acevedo-Suárez, and J. W. Thomas. 2009. Functional silencing is initiated and maintained in immature anti-insulin B cells. *J. Immunol.* 182: 3432–3439.
27. Milne, C. D., H. E. Fleming, and C. J. Paige. 2004. IL-7 does not prevent pro-B/pre-B cell maturation to the immature/sIgM(+) stage. *Eur. J. Immunol.* 34: 2647–2655.
28. Osmond, D. G., and S. J. Batten. 1984. Genesis of B lymphocytes in the bone marrow: extravascular and intravascular localization of surface IgM-bearing cells in mouse bone marrow detected by electron-microscope radioautography after in vivo perfusion of 125I anti-IgM antibody. *Am. J. Anat.* 170: 349–365.
29. Felig, P. 1983. Physiologic action of insulin. In Diabetes Mellitus: Theory and Practice. M. Ellenberg and H. Rifkin, eds. Medical Examination Publishing, New Hyde Park, NY, p. 77–88.
30. Acevedo-Suárez, C. A., C. Hulbert, E. J. Woodward, and J. W. Thomas. 2005. Uncoupling of anergy from developmental arrest in anti-insulin B cells supports the development of autoimmune diabetes. *J. Immunol.* 174: 827–833.
31. Kendall, P. L., G. Yu, E. J. Woodward, and J. W. Thomas. 2007. Tertiary lymphoid structures in the pancreas promote selection of B lymphocytes in autoimmune diabetes. *J. Immunol.* 178: 5643–5651.
32. Kendall, P. L., J. B. Case, A. M. Sullivan, J. S. Holderness, S. K. Wells, E. Liu, and J. W. Thomas. 2013. Tolerant anti-insulin B Cells are effective APCs. *J. Immunol.* 190: 2519–2526.
33. Healey, D., P. Ozegbe, S. Arden, P. Chandler, J. Hutton, and A. Cooke. 1995. In vivo activity and in vitro specificity of CD4+ Th1 and Th2 cells derived from the spleens of diabetic NOD mice. *J. Clin. Invest.* 95: 2979–2985.
34. Huang, X., J. Yuang, A. Goddard, A. Foulis, R. F. James, A. Lernmark, R. Pujol-Borrell, A. Rabinovitch, N. Somoza, and T. A. Stewart. 1995. Interferon expression in the pancreases of patients with type I diabetes. *Diabetes* 44: 658–664.
35. Francis, T., Jr. 1953. Influenza: the new acquayantance. *Ann. Intern. Med.* 39: 203–221.
36. Quinn, W. J., III, N. Noorchashm, J. E. Crowley, A. J. Reed, H. Noorchashm, A. Naji, and M. P. Cancro. 2006. Cutting edge: impaired transitional B cell production and selection in the nonobese diabetic mouse. *J. Immunol.* 176: 7159–7164.
37. Panigrahi, A. K., N. G. Goodman, R. A. Eisenberg, M. R. Rickels, A. Naji, and E. T. Luning Prak. 2008. RS rearrangement frequency as a marker of receptor editing in lupus and type 1 diabetes. *J. Exp. Med.* 205: 2985–2994.
38. Tikhomirov OYu, and J W. Thomas. 1997. Restricted V gene repertoire in the secondary response to insulin in young BALB/c mice. *J. Immunol.* 158: 4292–4300.
39. Thomas, J. W., P. L. Kendall, and H. G. Mitchell. 2002. The natural autoantibody repertoire of nonobese diabetic mice is highly active. *J. Immunol.* 169: 6617–6624.
40. Simone, E., D. Daniel, N. Schloot, P. Gottlieb, S. Babu, E. Kawasaki, D. Wegmann, and G. S. Eisenbarth. 1997. T cell receptor restriction of diabetogenic autoimmune NOD T cells. *Proc. Natl. Acad. Sci. USA* 94: 2518–2521.
41. Simone, E. A., L. Yu, D. R. Wegmann, and G. S. Eisenbarth. 1997. T cell receptor gene polymorphisms associated with anti-insulin, autoimmune T cells in diabetes-prone NOD mice. *J. Autoimmun.* 10: 317–321.